



Warsaw University of Life Sciences
Institute of Environmental Engineering

Mohammadreza Einikarimkandi

Enhancing the accuracy of process-based and data-driven models for predicting drought

Poprawa dokładności predykcji suszy za pomocą modeli opartych na procesach i modeli opartych na danych

Doctoral thesis

Rozprawa doktorska

Doctoral thesis prepared under the supervision of

dr hab. Mikołaj Piniewski, prof. SGGW

Department of Hydrology, Meteorology and Water Management

Warsaw 2024

Statement of the supervisor of the doctoral thesis

I represent that this thesis has been prepared under my supervision and I represent that it fulfils the requirements for submission thereof in the proceedings for the award of the scientific doctoral degree.

Date:

22.07.2024

Signature of the supervisor

Statement of the author of the doctoral thesis

Aware of legal liability, including criminal liability for making a false statement, I hereby represent that the present doctoral thesis has been written by myself and does not contain any content obtained in a manner inconsistent with the applicable laws, in particular the Act of 4 February 1994 on Copyright and Related Rights (consolidated text of 28 October 2022, Polish Journal of Laws of 2022, item 2509, as amended).

I represent that the thesis presented herein has not previously been the basis of any procedure related to the award of the doctoral degree.

I further represent that this version of the thesis is identical to the attached electronic version.

I acknowledge that the doctoral thesis will be subjected to the anti-plagiarism procedure.

Date:

22.04.2024

Signature of the author of the thesis

Table of contents

Abstract	7
1 Introduction	9
1.1 Drought	9
1.2 Modeling approaches in drought assessments	10
1.3 Satellite-based datasets	13
2 Research objectives and hypotheses	14
3 Materials and methods	15
3.1 Study areas	16
3.2 Data	17
3.3 Drought indicators	17
3.4 Modeling tools and approaches	17
4 Results	19
Improvements in agricultural and hydrological drought	
4.1 predictions	19
4.2 Drought detection	24
4.3 Application of satellite-based datasets in hydrological modeling	26
5 Discussion	26
5.1 Improving data-driven simulations via drought indicators	27
5.2 Improving process-based models via satellite-based datasets	28
5.3 Drought detection	29
6 Conclusion	30
7 Other achievements	31
8 References	32
9 Publication 1	39
10 Publication 2	58
11 Publication 3	76
12 Publication 4	94
13 Publication 5	110

Abstract

This thesis explores the use of different agro-hydrological modelling methodologies to understand and predict various types of droughts, as well as river discharge and crop yields. The research hypothesis states that the accuracy of agro-hydrological modelling can be enhanced by utilizing multi-objective calibration approaches and input data from satellite-based datasets. The research underscores the complexity of hydrological phenomena and the need for comprehensive modelling techniques to capture this complexity accurately. The findings suggest that incorporating satellite-based soil moisture data can significantly enhance the accuracy of models such as the Soil and Water Assessment Tool+ (SWAT+). This is particularly evident in the transition from single-objective to multi-objective calibration approach, which not only improved the precision of river discharge simulations but also provided more reliable crop yield estimates. Additionally, this thesis uses a data-driven model (Artificial Neural Networks -ANN) to simulate river discharge, hydrological drought, and crop yields. We found that using drought indicators, such as the Standardized Precipitation Index, as the ANN inputs significantly improved its performance. These advancements in modelling techniques are crucial for regions with limited observed data and are essential for conducting studies on the impacts of climate change and model-based water accounting. The research highlights the challenges associated with satellite-based datasets, such as the PERSIANN products, which have limitations in runoff simulations. Careful dataset selection and calibration are necessary to ensure the reliability of hydrological models. The research also revealed the non-linear relationship between projected changes in climate variables and ANN outputs, which contrasts with process-based model, which suggests that ANNs may respond differently to environmental factors. Overall, the research provides valuable insights into the field of hydrology, and offers innovative methods to improve the accuracy of hydrological models. These methods can help manage water resources, inform agricultural practices, and improve our understanding of hydrological responses to climate variability and change. The findings emphasize the importance of using multiple indices and datasets to capture the complex nature of droughts and their diverse impacts on ecosystems and human societies.

Streszczenie

Celem niniejszej rozprawy jest badanie możliwości wykorzystania różnych technik modelowania agro-hydrologicznego w celu lepszego zrozumienia i prognozowania różnych typów susz, a także przepływów rzecznych i plonów roślin uprawnych. Hipoteza badawcza głosi, że dokładność modelowania agro-hydrologicznego można zwiększyć poprzez wykorzystanie wielokryterialnych podejść kalibracyjnych oraz danych wejściowych pochodzących ze zbiorów danych satelitarnych. Badania podkreślają złożoność zjawisk hydrologicznych i potrzebę kompleksowych technik modelowania w celu dokładnego uchwycenia tej złożoności. Wyniki sugerują, że uwzględnienie danych o wilgotności gleby pochodzących ze zdjęć satelitarnych może znacznie zwiększyć dokładność modeli takich jak Soil and Water Assessment Tool+ (SWAT+). Jest to szczególnie widoczne przy przejściu z jednokryterialnego do wielokryterialnego podejścia kalibracyjnego, które nie tylko poprawiło dokładność symulacji przepływów, ale także zapewniło bardziej wiarygodne szacunki plonów. Ponadto w niniejszej pracy wykorzystano model oparty na danych (sztuczne sieci neuronowe - ANN) do symulacji przepływów, suszy hydrologicznej i plonów. Stwierdzono, że wykorzystanie wskaźników suszy, takich jak znormalizowany wskaźnik opadów (SPI) jako danych wejściowych do modelu ANN w sposób istotny poprawiło dokładność tego modelu. Te postępy w technikach modelowania mają kluczowe znaczenie dla regionów o ograniczonych danych obserwacyjnych i są niezbędne do prowadzenia badań nad wpływem zmiany klimatu. Badania podkreślają wyzwania związane ze zbiorami danych satelitarnych, takimi jak produkty PERSIANN, które mają ograniczenia w symulacjach przepływu. Staranny dobór i kalibracja zbiorów danych są niezbędne do zapewnienia wiarygodności modeli hydrologicznych. Badania ujawniły również istnienie nieliniowego związku między projekcjami zmiennych klimatycznych a wynikami modelu ANN, co sugeruje, że odpowiedź modeli ANN na podobny sygnał zmian środowiskowych może być istotnie różna niż odpowiedź modeli opartych na procesach takich jak SWAT+. Przeprowadzone badania zapewniają cenny wgląd w dziedzinę hydrologii i oferują innowacyjne metody poprawy dokładności modeli hydrologicznych. Metody te mogą pomóc w zarządzaniu zasobami wodnymi, informowaniu o praktykach rolniczych i poprawie zrozumienia odpowiedzi hydrologicznej na zmienność i zmiany klimatu. Wyniki badań podkreślają znaczenie stosowania wielu wskaźników i zbiorów danych w celu uchwycenia złożonego charakteru susz i ich różnorodnego wpływu na ekosystemy i działalność człowieka.

1. Introduction

1.1 Drought

Drought, when intertwined with the effects of climate change, poses a multifaceted environmental challenge that extends its influence to various aspects of global security, food production, inland water bodies, ecosystems, societies, and economies. The interpretation of what constitutes a drought varies across the globe, reflecting the diverse values and significance different societies and regions place on water. In its most severe form, drought has the potential to disrupt daily life; in less extreme cases, it may restrict recreational activities or impede maritime transportation (Hellwig et al., 2017; Langhammer and Bernsteinová, 2020).

In recent years, Central Europe has been subjected to a series of intense and prolonged droughts, which have had far-reaching impacts on sectors such as agriculture, energy production, and water management. Notably, during years like 2015, 2018, and 2019, the region grappled with unusually low water levels and river flows, often in conjunction with exceptionally high water temperatures (Bormann and Pinter, 2017; Ionita et al., 2017; Kubiak-Wójcicka and Machula, 2020; Laaha et al., 2017; Meresa et al., 2016).

The 2018 drought had a more significant impact on land ecosystems than the previously most severe event in 2003, which was considered the most extreme compound heat and drought event in Europe for the past century. In June 2019, over 350 municipalities in Poland were compelled to introduce drinking water usage restrictions. Skierniewice, a town near Warsaw with nearly 50,000 residents, was forced to reduce its municipal water supply in certain districts. An atypical drought in early spring 2020 in Poland led to a wildfire that devastated over 5,000 hectares of Biebrza National Park, a sanctuary for untouched wetlands. This series of events underscores the profound and far-reaching impacts of drought on both natural ecosystems and human societies. Increasing agricultural losses due to extreme weather events, particularly droughts, have been well documented in Poland in recent decades (Bachmair et al., 2015; Piniewski et al., 2022; Piniewski et al., 2018).

Drought is a multifaceted phenomenon that can be classified into various types based on its impacts, such as meteorological, hydrological, agricultural, and socioeconomic droughts (Van Loon, 2015). Each type of drought is characterized by specific indicators and triggers: Meteorological drought is primarily due to a lack of rainfall, which can be immediately noticeable (Prodhan et al., 2022; Wang et al., 2022). It can spread rapidly and end just as quickly. Hydrological drought occurs after extended periods of insufficient rainfall, leading to reduced

runoff, aquifer storage, and lower levels in dams and lakes. Agricultural drought happens when there is a reduction in soil water availability, particularly during the crop farming season, impacting food production and security. Socioeconomic drought arises when the effects of the other drought types influence social and economic activities. While these classifications focus on the human-centric impacts of drought, they may not fully address the environmental aspects (Koohi et al., 2021; Vicente-Serrano et al., 2020).

Drought also serves as an indicator of below-average water availability. The frequency and severity of drought events have increased in many parts of the world due to heightened water demands and climate change. This has made drought a high-priority research topic. The progression of drought typically begins with a significant lack of precipitation, leading to agricultural drought (lack of soil water), and eventually to hydrological drought (decline in river discharges). These droughts threaten food security, farmers' livelihoods, and water availability for both humans and ecosystems. Additionally, drought events have been linked to domestic and international conflicts in some regions, making the projection of drought events crucial, particularly in transboundary river basins (Boxell, 2019; Van Huynh et al., 2019; Van Loon, 2015; von Uexkull, 2014).

To assess drought conditions, several indicators have been developed, including, Standardized Precipitation Evapotranspiration Index (SPEI), Standardized Precipitation Index (SPI), Agricultural Reference Index for Drought (ARID), NOAA Drought Index (NDI), Aggregate Dryness Index (ADI), Standardized Runoff Index (SRI), Combined Drought Indicator (CDI), and Soil Moisture Deficit Index (SMDI) (Prodhan et al., 2022; Raposo et al., 2023; Svoboda and Fuchs, 2016). These indicators employ statistical methods to transform physical variables such as precipitation, runoff, soil moisture, and evaporation into categorized values, facilitating the analysis of water scarcity over time. Drought assessments are usually done in various scales, such as river basins, countries, or even a single observational gauge.

1.2 Modeling approaches in drought assessments

To evaluate the historical patterns and project future occurrences of hydrological and agricultural droughts, it is customary to utilize modeling techniques (Prodhan et al., 2022). These models can be applied across various scales, from national to river basin levels, and can incorporate diverse methodologies to address the multifaceted nature of drought phenomena (Hao and Singh, 2015). Effective modeling requires a comprehensive suite of tools capable of

capturing the intricate interactions within the hydrological cycle and the subsequent impacts on agriculture (Rashid et al., 2020).

River basins are sophisticated networks where a multitude of processes happen continuously. These processes encompass the interplay between groundwater and surface water, fluvial dynamics, agricultural cycles, nutrient cycling, and human influences. Grasping these dynamics at a microscale, such as within a controlled experimental setup or an agricultural plot, might appear manageable. However, the complexity escalates significantly when scaled to real-world conditions. This complexity is due to the high degree of variability encountered in natural settings, which can result in disparate agricultural yields even among farms with similar practices within the same region. Likewise, water conservation strategies may yield divergent results contingent upon regional implementation (Brookfield et al., 2023; Keller et al., 2023).

In response to these complexities, the hydrological community has developed an array of models to serve as decision-support tools. These models are designed to emulate and forecast the outcomes of various hydrological scenarios. Process-based distributed agro-hydrological models such as the Soil and Water Assessment Tool+ (SWAT+) (Bieger et al., 2017) or the Variable Infiltration Capacity model (VIC) (Hamman et al., 2018) in particular, are extensively employed to model the repercussions of anthropogenic actions, such as alterations in land use, as well as natural phenomena, including heatwaves and extreme precipitation events, on the hydrological cycle and agricultural productivity. Nonetheless, a common limitation of these models is their tendency to prioritize runoff during calibration, which can lead to an underrepresentation of other hydrological components, such as the proportion of evapotranspiration within the water balance or the infiltration rates (Delavar et al., 2022). For example, the evaluation of climate change impacts on the water balance or soil moisture within heavily irrigated zones may be skewed if the hydrological model is calibrated predominantly with runoff data. Accurate calibration necessitates a holistic approach that considers all facets of the hydrological cycle to ensure reliable predictions and effective water resource management (Delavar et al., 2022).

In the realm of hydrological modeling, the phenomenon of equifinality — where multiple parameter sets yield comparably satisfactory outcomes for simulated discharge — is a recognized challenge (Beven, 2006). To mitigate this issue, the implementation of multi-objective calibration is advisable. This approach enhances the calibration process by integrating a broader array of temporal and spatial variables, such as crop yields, soil moisture, base flow,

potential and actual evapotranspiration, leaf area index (LAI), infiltration rates, biomass indices, and tile drainage flows (Delavar et al., 2022; Eini et al., 2020).

The quest for precision in hydrological modeling becomes particularly arduous within transboundary basins, where access to comprehensive and reliable measured data may be constrained or non-existent, and where existing datasets may suffer from disparities in precision or granularity. Hydrological evaluations in such basins are imperative not only for an exhaustive analysis of the water balance but also for formulating strategies to manage international conflicts and to promote sustainable management practices across the basin, a necessity that is increasingly pressing in the context of global climate change.

Data-driven approaches like Artificial Intelligence (AI) are beneficial in the field of agro-hydrology, alongside process-based models. Hydrologists have lately shown interest in using artificial intelligence (AI) to model and predict different phenomena (Moghadam et al., 2022; Prodhan et al., 2022). AI-based methodologies rely on statistical and/or mathematical techniques to identify correlations between input data and outcomes. These methods have demonstrated high precision in replicating various processes in hydrology, agriculture, and meteorology, including modeling and forecasts of soil moisture, crop production, wind speed, solar radiation, river flow, drought, and sedimentation (Pektaş and Kerem Cigizoglu, 2013; Piri et al., 2022; Prodhan et al., 2022; Yang et al., 2015).

AI-based models like machine learning and deep learning have significantly influenced drought management and have been utilized as substitutes for process-based hydrological models, as stated by Moghadam et al. (2022). AI-based models can effectively simulate and predict hydrological and meteorological data for detecting droughts due to their ability to self-organize and adapt to non-linear and unstable conditions. Various AI-based models, categorized into unsupervised and supervised learning approaches, have been evaluated in drought simulations. Supervised learning necessitates labeled data during training to allow the model to generate predictions based on known outputs. The model establishes the connection between input and output variables by refining its parameters through the labeled instances. Unsupervised learning involves analyzing unlabeled data to identify patterns and structures without predetermined outputs. The model analyzes the data to detect parallels, differences, or clusters, unveiling hidden linkages. Unsupervised learning is commonly applied in problems such as clustering, anomaly detection, and dimensionality reduction (Alloghani et al., 2020).

1.3 Satellite-based datasets

Global gridded datasets address the shortcomings of incomplete, poorly measured, or unavailable data (Eini et al., 2019). These datasets fall into three categories: ground-based, satellite-based, and a combination of both (Darand and Khandu, 2020; Eini et al., 2021). Remotely sensed datasets have gained traction in hydrology for model calibration and validation, as well as for providing supplementary meteorological data during model setup. Satellite products enhance the consistency of distributed hydrological models by offering spatially comprehensive data. Moreover, the accuracy of hydrological models is often improved by incorporating new processes or refining existing empirical equations, ultimately enhancing water balance simulations at the basin scale.

For hydrological and environmental assessments, including drought monitoring, precipitation data is crucial. Traditional in situ measurements, while highly accurate, suffer from limitations such as sparse spatial distribution, expensive maintenance, delays in data dissemination by regional authorities, and lack of global reach. These shortcomings can compromise the effectiveness of drought monitoring, especially in large transboundary river basins or in developing countries.

Current methods provide a uniform network for precipitation time series, encompassing reanalysis, gauge-interpolated, non-gauge-corrected satellite-based, and gauge-corrected satellite-based precipitation estimates. Satellite-based precipitation estimates, in particular, offer high-resolution, near real-time, and sub-daily data on a global scale, making them invaluable for drought monitoring, hydrological modeling, water resource analysis, and climate studies. Despite their widespread use as a substitute for ground-based data, the reliability of these satellite-derived products varies regionally, and their precision in some areas is yet to be determined (Brocca et al., 2014; Darand and Khandu, 2020).

Soil moisture (SM) is a key variable that bridges the energy and water cycles, playing a strategic role in runoff generation and crop development. It affects runoff, land-atmosphere carbon fluxes, vegetation, and evapotranspiration processes across the basin. Soil moisture exhibits temporal, spatial, and vertical variability, influenced by meteorological parameters, soil texture, land cover and use, groundwater levels, and topography. Consequently, ground-based measurement of soil moisture necessitates an extensive network. Additionally, models often rely on parameterizations of soil, land cover, and climate forcing, which may not always be precise. Therefore, access to spatially distributed soil moisture data is essential for enhancing

model accuracy and developing robust hydrological systems (Azimi et al., 2020; Brocca et al., 2011; Brocca et al., 2020; Brocca et al., 2010).

2. Research objectives and hypotheses

The following three objectives have been formulated in this thesis:

- a) Improving the accuracy of agro-hydrological process-based and data-driven models for predicting drought
- b) Assessing the changes in different types of drought in Poland
- c) Evaluating satellite-based datasets in agro-hydrological applications

The hypothesis of this thesis states that the accuracy of agro-hydrological modeling can be enhanced by utilizing multi-objective calibration approaches and input data from satellite-based datasets. It suggests that by integrating different modeling techniques and homogeneous datasets, one can potentially improve the precision of models that predict agricultural and hydrological processes. This approach acknowledges the complexity of environmental systems and the value of multi-source data integration in capturing this complexity more effectively.

The outputs of this study were published in five publications, which can be found as attachment of the thesis. The links between objectives and outputs are shown in Figure 1.

- 1- Eini, M. R., Ziveh, A. R., Salmani, H., Mujahid, S., Ghezelayagh, P., & Piniewski, M. (2023). Detecting drought events over a region in Central Europe using a regional and two satellite-based precipitation datasets. *Agricultural and Forest Meteorology*, 342, 109733. <https://doi.org/10.1016/j.agrformet.2023.109733>
Impact factor: 6.2 – MeiN: 200
- 2- Eini, M. R., Rahmati, A., & Piniewski, M. (2022). Hydrological application and accuracy evaluation of PERSIANN satellite-based precipitation estimates over a humid continental climate catchment. *Journal of Hydrology: Regional Studies*, 41, 101109. <https://doi.org/10.1016/j.ejrh.2022.101109>
Impact factor: 4.7 – MeiN: 100
- 3- Eini, M. R., Salmani, H., & Piniewski, M. (2023). Comparison of process-based and statistical approaches for simulation and projections of rainfed crop yields. *Agricultural Water Management*, 277, 108107. <https://doi.org/10.1016/j.agwat.2022.108107>
Impact factor: 6.7 – MeiN: 140

- 4- Eini, M. R., Massari, C., & Piniewski, M. (2023). Satellite-based soil moisture enhances the reliability of agro-hydrological modeling in large transboundary river basins. *Science of the Total Environment*, 873, 162396. <https://doi.org/10.1016/j.scitotenv.2023.162396>
Impact factor: 9.8 – MeiN: 200
- 5- Eini, M. R., Najminejad, F., & Piniewski, M. (2023). Direct and indirect simulating and projecting hydrological drought using a supervised machine learning method. *Science of The Total Environment*, 898, 165523. <https://doi.org/10.1016/j.scitotenv.2023.165523>
Impact factor: 9.8 – MeiN: 200

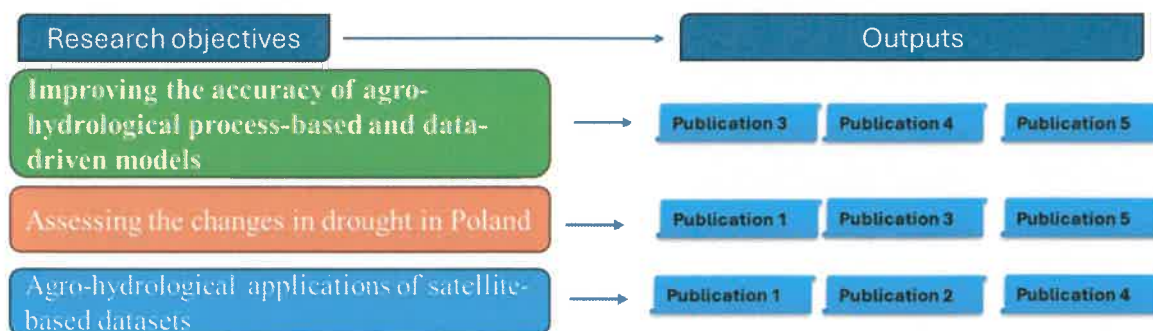


Figure 1- Relationships between research objectives and outputs.

3. Materials and methods

In this research, various types of datasets and models were utilized. Figure 2 shows the connections between data, models and outputs. The models used in this study are SWAT+ and a data-driven method (ANNs), which represent two distinct types of models. The former is an agro-hydrological process-based model, while the latter is a data-driven model. Additionally, satellite-based datasets were selected as inputs for this study and were employed for different purposes. A brief explanation of their applications is described below:

- a) The satellite-based soil moisture dataset was utilized in hydrological modeling to enhance the accuracy of streamflow and crop yield simulations.
- b) Precipitation datasets from various sources were employed to detect droughts and for integration into hydrological modeling.

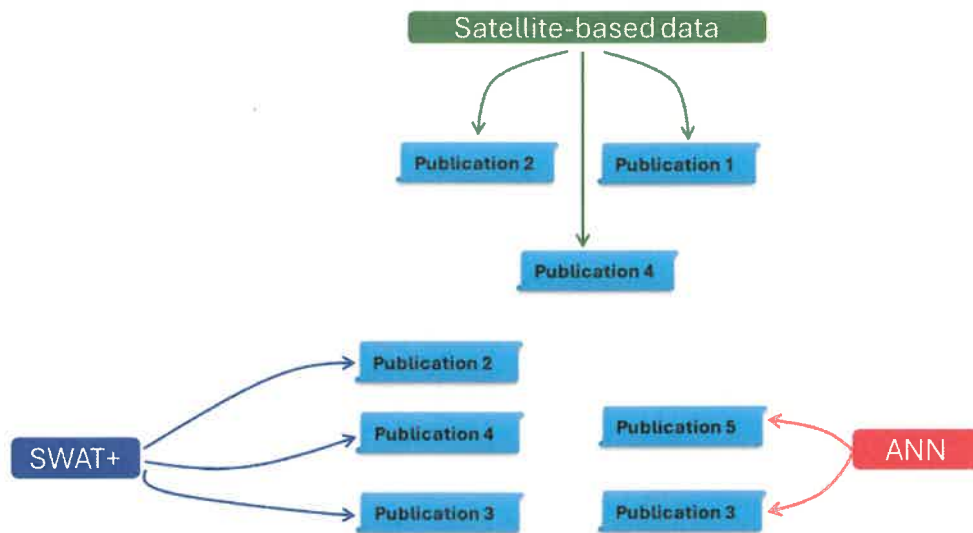


Figure 2- The connections between data, models, and outputs.

3.1 Study areas

In this thesis, the focus was on two different scales and three different study areas, a meso-scale watershed (Wełna catchment), and two macro-scale areas: a large-transboundary river basin (Odra River Basin - ORB), and the union of Odra and Vistula river basins and Poland territory (hereafter denoted as 'Poland+'). Figure 3 illustrates the study areas. Complete descriptions of the selected study areas are included in attached publications.

These study areas were selected due to the below reasons:

- An assessment of drought conditions and using global datasets over a large region in Central Europe (Poland+)
- Assessing climate change effects on meso-scale and large scale transboundary basin



Figure 3- Study areas: Wełna River catchment, Odra River Basin (ORB), and Poland+.

3.2 Data

In this study different types of datasets were used. For precipitation, as a reference dataset, we employed a gridded daily climate dataset (G2DC-PL+) (Piniewski et al., 2021). As satellite-based precipitation datasets, PERSIANN family products and SM2RAIN-ASCAT were used in the hydrological modeling (Brocca et al., 2019; Nguyen et al., 2019). In addition, we employed ESA (European Space Agency) CCI (Climate Change Initiative) Soil Moisture (SM) dataset (version 07.1) to calibrate SWAT+ model (Gruber et al., 2019). River discharge were provided by the Institute of Meteorology and Water Management - National Research Institute (IMGW-PIB) of Poland. The details of the datasets are mentioned in attached publications extensively.

3.3 Drought indicators

In the first step of this research (Publication 1), understanding the spatio-temporal variability of droughts in Poland was crucial. In this regard, different types of precipitation datasets were employed as inputs for calculating SPI drought indicator for the Poland+ area. SPI is a widely used metric for quantifying drought severity and evaluating environmental variations based on precipitation, as introduced by McKee et al. (1993). Its value lies in its straightforward calculation and temporal flexibility, allowing for the identification of different drought types, including meteorological, agricultural, and hydrological. For instance, Xu et al. (2015) employed SPI-3 to represent meteorological drought, while Koohi et al. (2021) utilized SPI-6 and SPI-12 as proxies for agricultural and hydrological droughts, respectively. In this thesis, SPI was employed as input of the ANN model developed for simulations and projections of crop yields, river discharges, and hydrological droughts.

In publication 5, the Standardized Runoff Index (SRI), similar to SPI in its computational approach, serves as a metric for hydrological drought. It leverages river discharge data to evaluate drought severity. The SRI is computed over different time spans to represent the varying durations of droughts: SRI-3 for short-term droughts, SRI-6 and SRI-9 for mid-term droughts, and SRI-12 for long-term drought conditions. This allows for an accurate understanding of drought impacts over time.

3.4 Modeling tools and approaches

The second step of research conducted within this thesis involved modeling agro-hydrological processes using two distinct modeling approaches (publication 2, 3, and 4). The first is the SWAT+ model, an advanced iteration of the SWAT model that is currently in

development (Bieger et al., 2017). The second approach employs a data-driven method (ANNs), which is increasingly popular in Earth sciences (publication 3 and 5). Figure 4 displays the connections between topics and outputs.

The initial application of the SWAT+ model was conducted on the Welna watershed, a meso-scale catchment area (publication 2 and 3). This preliminary phase aimed to evaluate the available data and the feasibility of implementing SWAT+. At the study's inception in 2020, SWAT+ was a novel and somewhat unstable model, necessitating a trial run on a smaller scale to ascertain its strengths and weaknesses. Additionally, the SWAT+ model was utilized to simulate and project crop yields within the Welna watershed.

Subsequently, a second SWAT+ configuration was developed for the Odra River Basin (publication 4). This model underwent calibration and validation processes using river discharge data, soil moisture, and crop yield figures. For these procedures, both multi-objective and single-objective methods were employed to ensure the model's accuracy and reliability.

In this thesis, Artificial Neural Networks (ANNs) were employed to simulate crop yields, river discharges, and hydrological droughts. A variety of input data was incorporated into the ANN to enhance the model's precision. This data-driven approach allows for the refinement of simulations, making them more representative of the complex interactions in agro-hydrological systems.

In the Welna watershed, crop yield simulations using ANN were conducted by incorporating SPI-1 to SPI-12 as input data beside the other meteorological datasets. SPI also were used for simulating and projecting river discharges and hydrological drought over Odra River Basin, via direct and indirect methods. The direct method involves simulating and projecting the SRI from the specified predictors. Conversely, the indirect method produces river discharge outputs via an ANN, which are then used to calculate the SRI. Following the completion of training, validation, and testing phases, two ANN models are prepared to estimate river discharge projections using the indirect method and SRI projections using the direct method.

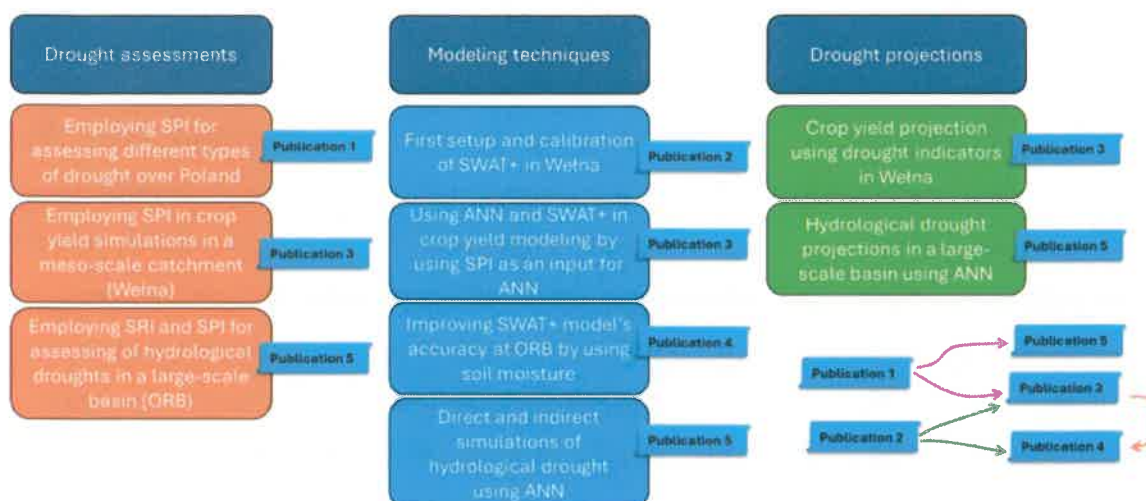


Figure 4- Connections between main topics and outputs.

4. Results

In this section, we briefly summarize the key findings pertinent to the current study, as derived from the published publications. While some publications, notably publication 3, delve into a broader range of sub-topics and introduce multiple novel concepts, we have chosen to streamline the content presented in this thesis. This ensures a focused and cohesive narrative that aligns closely with the core research objectives, facilitating a clear and comprehensive understanding for the reader.

4.1 Improvements in agricultural and hydrological drought predictions

The main objective of this thesis was to improve the accuracy of agro-hydrological models for predicting drought using different techniques. We used drought indicators ranging from SPI-1 to SPI-12 as inputs for Artificial Neural Network (ANN) models to simulate and predict river discharge, hydrological drought indicator (SRI), and crop yields. The accuracy of the ANN model can be greatly enhanced by incorporating drought indicators as inputs, as suggested by our research. For instance, incorporating drought variables into crop yield simulations substantially improved the model's precision (see Table 7 in publication 3). The variables include SPI (1 to 12 scales), precipitation, maximum and minimum temperatures, and solar radiation. The Root Mean Square Error (RMSE) was significantly decreased from approximately 0.49 to 0.07 in the test phase by including these components. The coefficient of determination (R-square) increased from 0.34 to 0.98, suggesting a strong correlation between the observed and estimated values. Each SPI (1 to 12) retains important data for crop yield modeling.

In the next assessment, we used SPI as input for hydrological drought simulations and projections (SRI indicator) using direct and indirect approaches. Direct method involves simulating and projecting SRI directly from inputs, while indirect method bases SRI calculations on simulated river discharge. Our findings indicate that indirect simulations of hydrological drought are more accurate than the direct approach for all accumulation periods of the SRI (Figure 5). Higher precision in runoff simulations results in higher accuracy in hydrological drought simulations. Employing same predictors (precipitation, temperature, and SPI) in both methods did not result in similar accuracy in hydrological drought simulations, with the indirect method demonstrating superior performance. Figure 5 shows results for the last gauging station on the Odra river (Gozdowice), but the same conclusions can be drawn for three other gauges used in the analysis (see Fig. 5 of publication 3).

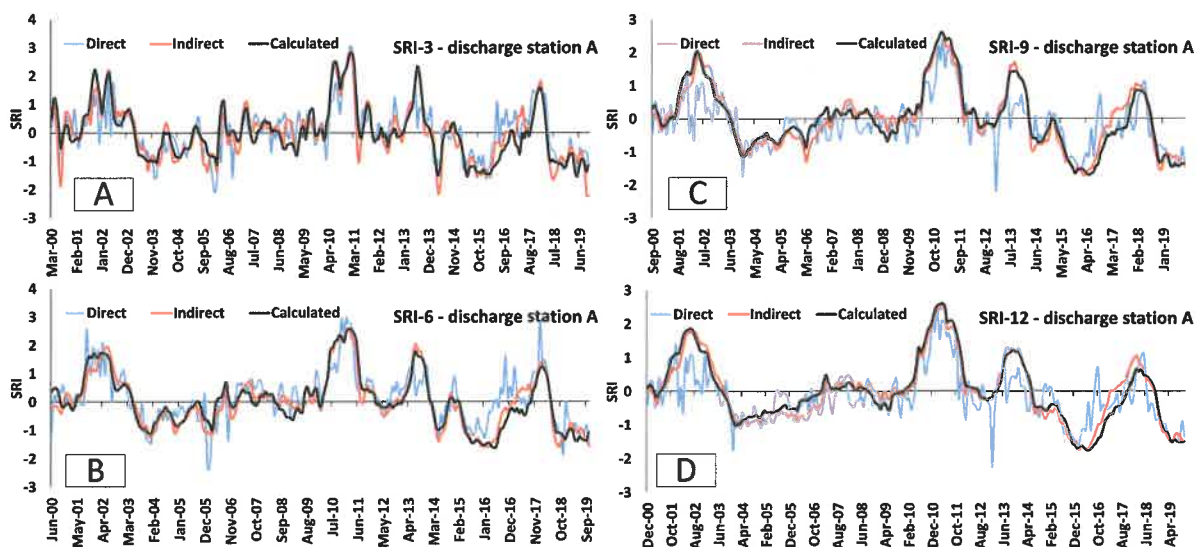


Figure 5- SRI time series estimation based on observed data, direct, and indirect approaches for the Odra river at Gozdowice gauging station. Different panels present different SRI accumulation periods (A – SRI-3, B- SRI-6, C- SRI-9, D - SRI-12).

For future projections, four CMIP5-based General Circulation Models (GCMs) were downscaled using the LARS-WG downscaling tool to estimate precipitation and temperature for two future timeframes: the near future (2021–2040) and the far future (2041–2060), under the most severe CO₂ concentration scenario (RCP8.5). The corresponding climate scenarios were labelled: "moderate", "warm and dry", and "warm and wet" in the analyses.

The research results suggest that estimates derived from indirect simulations are more reliable and also indicate differences in projections between the two methodologies. On the other hand, the direct method indicates substantial alterations in hydrological drought projections when compared to the historical period. A subset of results for the Odra river main

outlet and two accumulation periods (SRI-3 and SRI-6) is presented in Table 1, while a more comprehensive analysis involving other gauges and accumulation periods can be found in Figures 8 and 9 of the publication 5.

Another example of enhancing agro-hydrological modelling is included in publication 4, in which we used a soil moisture satellite-based dataset, in addition to discharge, for a multi-objective SWAT+ model calibration.

Table 1- Projected SRI-3 and SRI-6 against historical SRIs for the outlet of ORB using the direct and indirect approaches- according to run theory with threshold level -1.

Scenario	SRI-3				SRI-6			
	Minimum (most severe drought)	Number of severe droughts (months)	Severity (sum if SRI ≤ -1)	Intensity (Severity /Duration)	Minimum (most severe drought)	Number of severe droughts (months)	Severity (sum if SRI ≤ -1)	Intensity (Severity /Duration)
Indirect approach - Discharge station A								
Historical	-1.56	34	-42.32	-1.24	-1.64	34	-44.12	-1.3
Moderate (NF)	-2.99	36	-61.33	-1.7	-2.94	26	-44.62	-1.72
Warm and dry (NF)	-3.03	32	-56.94	-1.78	-2.9	27	-45.87	-1.7
Warm and wet (NF)	-2.97	32	-56.52	-1.77	-2.98	31	-50.33	-1.62
Moderate (FF)	-2.84	36	-59.35	-1.65	-2.98	31	-50.34	-1.62
Warm and dry (FF)	-2.98	32	-56.92	-1.78	-3.11	32	-51.56	-1.61
Warm and wet (FF)	-3.28	31	-54.97	-1.77	-3.07	32	-50.2	-1.57
Direct approach - Discharge station A								
Historical	-1.56	34	-42.32	-1.24	-1.64	34	-44.12	-1.3
Moderate (NF)	-2.03	73	-92.32	-1.26	-1.81	45	-57.26	-1.27
Warm and dry (NF)	-2	61	-77.23	-1.27	-1.81	43	-54.22	-1.26
Warm and wet (NF)	-1.93	63	-79.77	-1.27	-1.86	43	-54.74	-1.27
Moderate (FF)	-1.74	49	-60.38	-1.23	-1.72	37	-45.89	-1.24
Warm and dry (FF)	-1.92	54	-68.21	-1.26	-1.8	42	-53.07	-1.26
Warm and wet (FF)	-1.89	49	-62.52	-1.28	-1.82	41	-52.61	-1.28

In the single-objective calibration approach, which focused solely on discharge, the SWAT+ model demonstrated commendable accuracy in runoff simulations. The average Kling-Gupta Efficiency (KGE) was above 0.60 and 0.63 in the calibration and validation periods, respectively. In this approach, we adjusted the satellite-based soil moisture with the SWI index and incorporated it as the second variable in the calibration step, thus transitioning to a multi-objective approach.

In the multi-objective approach, which considered both discharge and soil moisture, the accuracy of simulations at river discharge stations saw a substantial increase (KGE = 0.67 in the calibration and 0.69 in the validation periods) compared to the single-objective approach.

In the simulations of daily discharge, soil moisture emerged as a crucial factor that substantially improved the results (Figure 6). This underscores the importance of incorporating relevant environmental factors into modeling efforts to ensure more accurate and reliable outcomes. Indeed, the calibration of soil moisture proved to be a pivotal factor in enhancing the accuracy of our model. Not only did it lead to an improvement in the simulations of discharge, but it also enhanced the results of crop yield simulations. This dual improvement underscores the interconnected nature of these agro-hydrological variables.

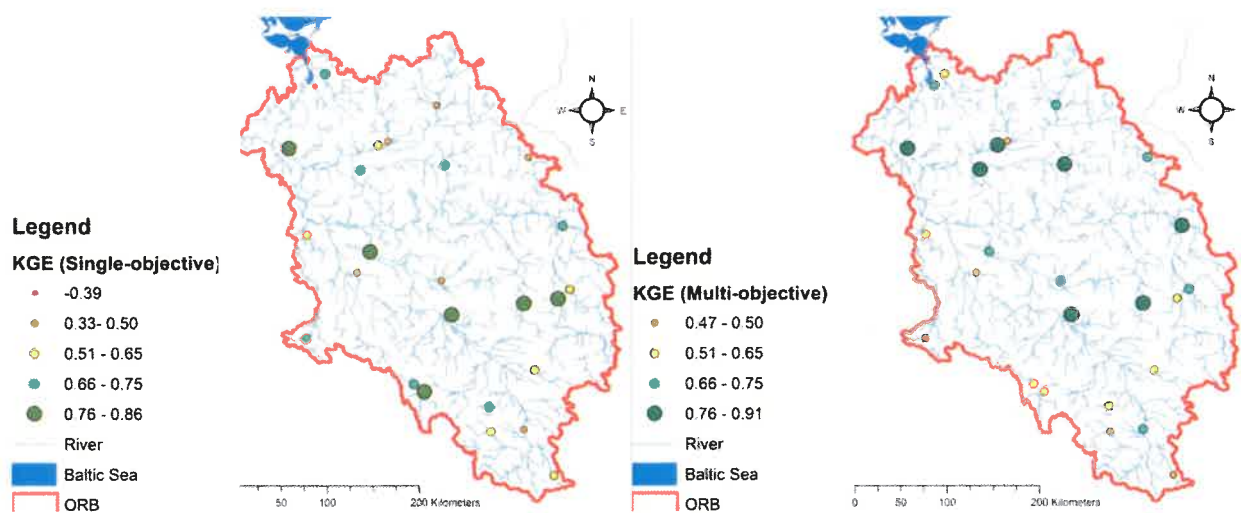


Figure 6- Comparison of the SWAT+ model performance in river discharge simulations in the ORB using KGE metrics between single- and multi- objective calibration approaches.

Furthermore, multi-objective method offered useful information about the distribution of soil moisture within the basin as seen in Figure 7. By matching our model's results with satellite-based SM data, we could validate and gain a deeper insight into the spatial and temporal patterns of soil moisture in the basin. This enhances the understanding of the basin's hydrological dynamics and specifically drought conditions. The results emphasize the significance of calibrating soil moisture in hydrological modeling to enhance the precision of agricultural and hydrological predictions.

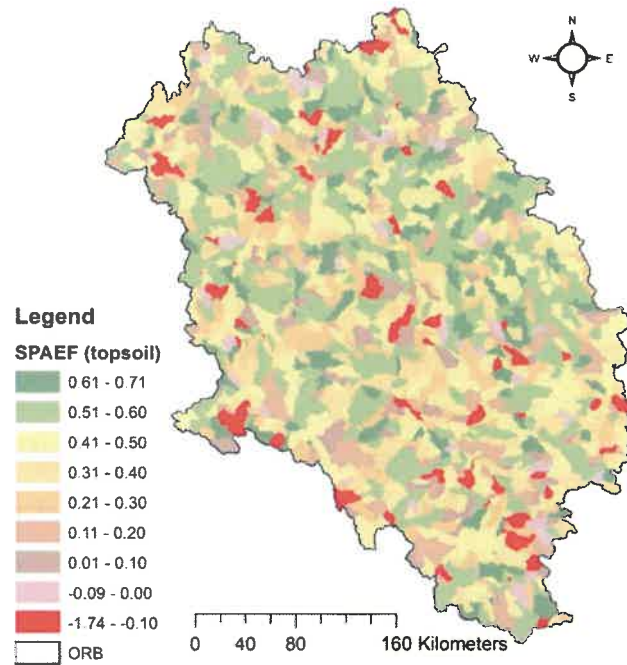


Figure 7- Distribution of the SWAT+ model accuracy in soil moisture (top soil) simulations according to SPAEF metrics in the ORB against satellite-based SM dataset.

Finally, the multi-objective approach also improved process-based crop yield simulations for two most important grain crops: winter wheat and spring barley (Fig. 8). The multi-objective approach led to more variation in simulated yield, which is closer to observed records. The model performance in corn and rapeseed yield simulation was poorer and less dependent on the calibration approach than for grain crops.

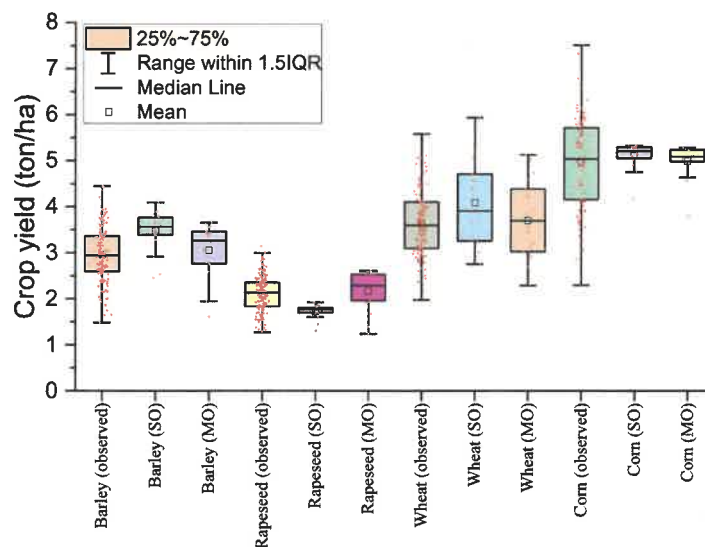


Figure 8- Comparison of multi-annual distribution of simulated crop yields using single- and multi-objective approaches (SO and MO) with the observed data.

4.2 Drought detection

According to the selected methodology in publication 1, our results show that, based on reference dataset, over a period of 154 months, the study area (Poland+) experienced 15 severe meteorological droughts ($SPI-3 < -1$) and was in a state of meteorological drought for over 80 months ($SPI-3 < 0$), affecting more than half of the observed months. Agricultural droughts were also prevalent, with the reference dataset identifying 12 severe instances using SPI-6 and 16 with SPI-9. In comparison, our analysis, based on the PERSIANN-CDR dataset, shows 24 severe agricultural droughts using SPI-6 and 20 using SPI-9. Also, 11 severe agricultural droughts were found across both SPI-6 and SPI-9, based on SM2RAIN-ASCAT dataset. For hydrological droughts, the reference dataset recorded 15 severe events ($SPI-12 < -1$) and 75 occurrences of hydrological drought ($SPI-12 < 0$). The PERSIANN-CDR dataset detected fewer overall hydrological droughts (67 events) but identified 20 severe ones. Meanwhile, the SM2RAIN-ASCAT dataset noted 84 hydrological droughts between 2007 and 2019, with 11 classified as severe. Figure 9 shows different types of drought for the reference and PERSIANN-CDR datasets, in general it can be seen that PERSIANN-CDR match well in estimating SPIs.

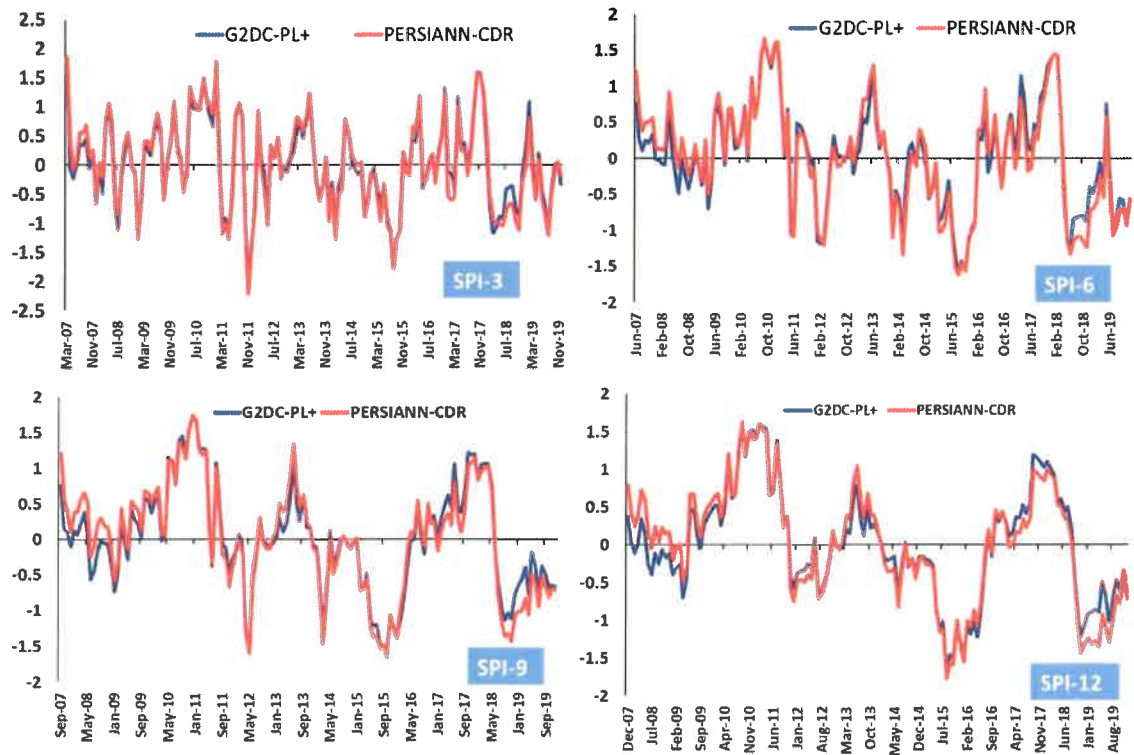


Figure 9- Different types of drought based on SPI, reference dataset against PERSIANN-CDR

Our research indicates that meteorological droughts (SPI-3) have distinct geographical distributions compared to agricultural (SPI-6 and SPI-9) and hydrological droughts (SPI-12), suggesting that each form of drought displays distinctive spatial features and patterns in the study region (Figure 10). This emphasizes the need of utilizing several indicators and datasets to precisely depict the intricate characteristics of droughts.

Enlarging the SPI window shows that the western part of the research area has faced more intense droughts according to the reference dataset. PERSIANN-CDR shows a pattern like the reference dataset, especially when using SPI-6 (see Figure 7 in publication 1). Severe meteorological droughts were detected mostly in the eastern region, whereas agricultural and hydrological droughts were more common in the western region. The satellite datasets were unable to detect the regional variations among the different types of droughts.

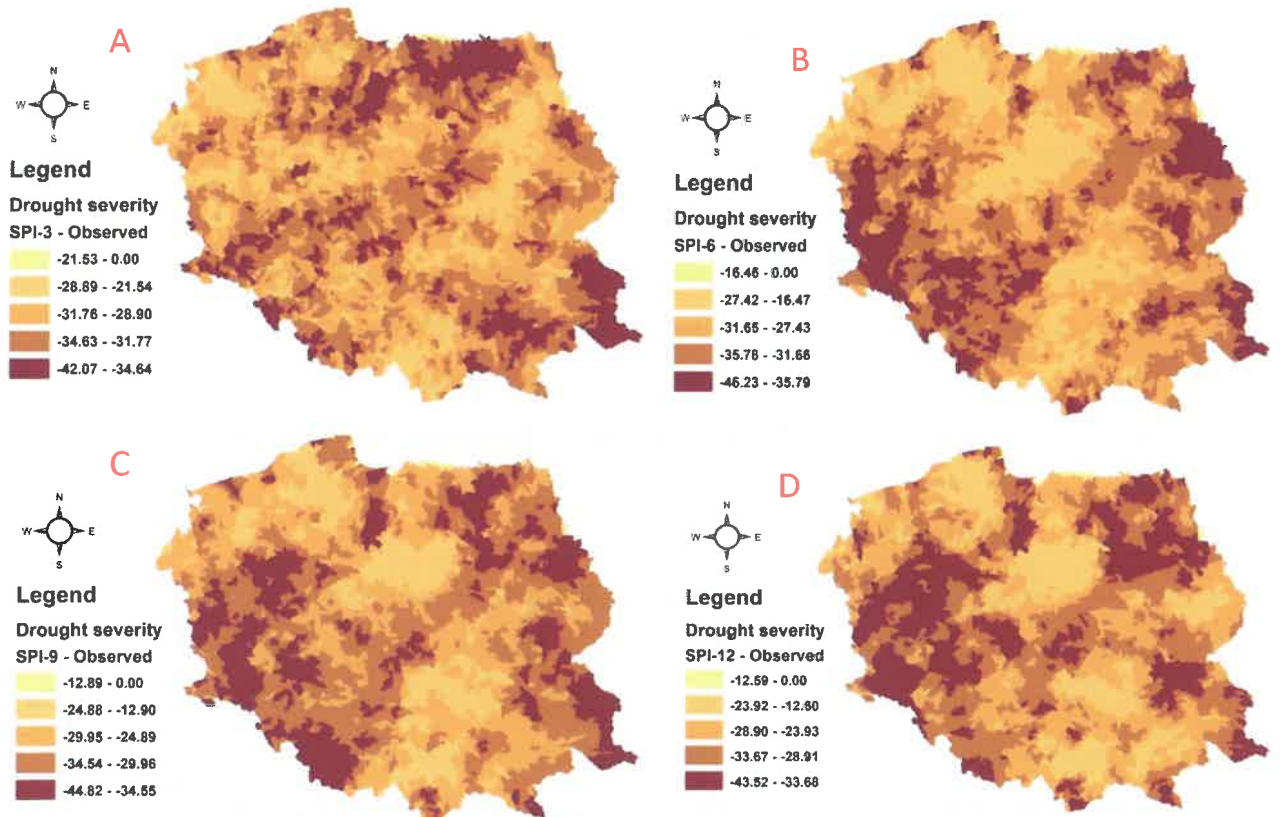


Figure 10- Spatial distribution of drought severity (SPI < -1) based on reference dataset over the study region (2007-2019) for different SPI accumulation periods (A – SPI-3; B – SPI-6; C – SPI-9; D- SPI-12).

4.3 Application of satellite-based datasets in hydrological modeling

While the usefulness of the satellite-based soil moisture dataset was already discussed in section 4.1, here we focus on our experience with using precipitation datasets for agro-hydrological modelling. An additional aim of this research was to delve into the utilization of satellite-based datasets in the realm of hydrological modeling (Figure 2). This was specifically addressed in the second and fourth publications, where satellite-based datasets were employed for hydrological modeling purposes.

The second publication undertook a comprehensive evaluation of the PERSIANN family products, applying them to a meso-scale catchment and comparing the results against a reference dataset. Following the calibration of each dataset, it was found that the PERSIANN products did not produce satisfactory results for runoff simulations in our analysis. The Kling-Gupta Efficiency (KGE) values for these datasets, which ranged from -11 to 0.34, indicated subpar model performance. Furthermore, the Percent Bias (PBIAS) values were significantly higher, suggesting the presence of substantial errors in the runoff simulations. This underscores the challenges and limitations associated with the use of these products in hydrological modeling.

In hydrological modeling, the configuration of the model, the calibration of its parameters, and the quality of the input data are critical factors that introduce uncertainty into the simulation results. Specifically, inaccuracies in the rainfall data used as input can lead to significant errors in the modeled runoff, affecting the reliability of the simulations. It's essential to address these sources of uncertainty to improve the model's predictive capability.

5. Discussion

Discussion of results achieved in this thesis can be categorized into three sections based on the objectives. The main objective was to improve the precision of drought simulations and predictions through the utilization of process-based and data-driven techniques. The second objective was to comprehend the variability of droughts in Poland. The last objective was to evaluate the hydrological use of satellite-based information in hydrological models. Various techniques can help achieve these aims and may provide varied outcomes, as indicated in the literature.

5.1 Improving data-driven simulations via drought indicators

We used drought indicators (SPI-1 to SPI-12) and meteorological datasets in a data-driven method (ANN) to investigate the effectiveness of drought indicators in simulating crop yield, hydrological drought, and river discharge. Similar to our approach, other research has demonstrated great accuracy in river discharge models using data-driven approaches. Ikram et al. (2022) utilized five various data-driven techniques to model monthly river discharge in mountainous regions of Pakistan, finding that these methods exhibit great precision in predicting discharge. In a research conducted in Iran, ANN was shown to be less effective in runoff simulations compared to SWAT and IHACRES (Moghadam et al., 2022). Kisi et al. (2013) conducted a study in Turkey and found that data-driven approaches such as ANN, ANFIS, and GEP are effective and precise tools for runoff simulations, which aligns with our findings. These approaches may not effectively detect human-induced changes in a basin and are more likely to work well in natural basins without agricultural activity or man-made buildings. These strategies are not dependable in complex and controlled basins. The study demonstrated that ANN outperformed in simulating discharge in a lowland catchment when compared to a mountainous catchment. This discovery contributes a novel perspective to the current understanding of the efficacy of ANN in hydrological modeling and emphasizes the impact of catchment features on model accuracy.

Like our study, data-driven approaches used in hydrological drought simulations have shown good accuracy levels. Shamshirband et al. (2020) utilized three data-driven approaches (SVR, GEP, and MT) to simulate several drought indicators directly in an Iranian basin. The present study shows results that align with their previous research in terms of correlation and RMSE performance metrics. Nabipour et al. (2020) used ANN to directly predict hydrological drought in an Iranian basin. Their study, like ours, utilized the SPI as a predictor of the Standardized Hydrological Drought Index (SHDI) over several time scales, and ANN yielded comparable outcomes to our study. Other investigations, as detailed in Prodhan et al. (2022), show that data-driven strategies yield similar performance indicators to those of the current research. The direct technique has been utilized in all the investigations listed.

Our research suggests that using indirect methods for simulating hydrological droughts is more precise than using direct methods. The accuracy of hydrological drought models using the indirect approach relies on the precision of river discharge simulations. Improved precision in river discharge simulations leads to enhanced precision in hydrological drought simulations. Utilizing the same variables (precipitation, temperature, and SPI) in both approaches did not

yield comparable accuracy in hydrological drought simulations, with the indirect strategy demonstrating higher performance.

Utilizing climatic data like precipitation, maximum and minimum temperature, and solar radiation directly in statistical models is a prevalent method for simulating crop yields. Our findings indicate that using a metrological drought index as an input enhances the dependability of the statistical method in crop yield modeling. Research conducted in Germany and India found that deviations in soil moisture levels may accurately forecast silage maize yield, aligning with our findings (Modanesi et al., 2020; Peichl et al., 2018).

Various studies have demonstrated that utilizing different models and climatic scenarios can result in varied crop yield projections when employing machine learning methods. These projections may indicate both increases and decreases under similar conditions (Johnson, 2013; Knox et al., 2016; Kolberg et al., 2019).

5.2 Improving process-based models via satellite-based datasets

The multi-objective calibration improved the accuracy of the SWAT+ model (an process-based agro-hydrological model) in simulating river flow and crop yields in our study over the Odra River Basin. Previous research have found enhancements in river discharge simulations and water balance components through multi-objective calibration in the SWAT model. Delavar et al. (2022) used runoff, aquifer water table, infiltration rate, crop yields, and ET to enhance the model's consistency. Furthermore, Ma et al. (2019) demonstrated that utilizing MODIS-based Leaf Area Index (LAI) greatly improved the model's adaptability and the geographical spread of plant cover in subtropical areas.

Rajib and Merwade (2016) used a time-dependent Soil Moisture Accounting approach to calibrate the SWAT model and assess soil moisture at various levels in two watersheds in Indiana. They found that using SM in the calibration process enhances the accuracy of simulations and observed datasets, as well as improves efficiency metrics, which aligns with the results of our work. Furthermore, it is noted that calibrating soil moisture based on in-situ root zone soil moisture significantly enhances the performance of the SWAT model (Rajib et al., 2016). Azimi et al. (2020) demonstrated that integrating satellite-derived soil moisture data from SMAP and Sentinel-1 into the SWAT model enhanced the precision of river flow predictions.

Multi-objective calibrated models are valuable for conducting water balance and water accounting evaluations. These models are particularly beneficial for conducting national and

international studies in transboundary basins (De Lannoy et al., 2022). Additionally, we want to highlight that our study was limited by the challenge of capturing the variability in crop yields across a wide range of collected data in this extensive basin. In future projects, this limitation can be overcome by utilizing satellite-based datasets like LAI or canopy height estimations.

It is advisable to assess how root zone soil moisture datasets, such the one from Grillakis et al. (2021) or Copernicus Global Land service, might enhance the precision of the SWAT+ model. Satellite-based soil moisture data can be validated with in-situ observations to reduce uncertainty in hydrological modeling. However, in large river basins, only short time series of in-situ soil moisture may be accessible. Assessing the impact of multi-objective calibration on crop production, evapotranspiration (ET), and infiltration rate might reduce the uncertainty in comprehensive hydrological modeling.

5.3 Drought detection

This study assessed the spatial spread of various types of drought by utilizing one regional and two gridded satellite-based precipitation datasets. Several research have utilized satellite-derived information to estimate drought conditions in various regions worldwide and compared these datasets with a trustworthy reference. Satellite-derived precipitation estimates are recommended for drought evaluations and practical applications due to their ability to accurately estimate small amounts of precipitation, reduce overestimations, and offer a reliable assessment of the spatial distribution of low precipitation levels and events (Degefu et al., 2022).

SPI is the most frequently employed drought indicator among several options available. Koohi et al. (2021) said that the SM2RAIN-ASCAT data accurately identifies drought episodes, particularly in agricultural and meteorological contexts, across a wide area. Their study chose SPI-1, SPI-3, SPI-6, and SPI-12 to identify various types of droughts. The PERSIANN-CDR data in Ethiopia accurately detected drought using the SPI as reported by Degefu et al. (2022).

6. Conclusion

In this thesis, a series of publications has been provided that delve into the improving the accuracy of drought simulations via process-based agro-hydrological modeling and data-driven methods and the use of satellite-based datasets, drought indicators, and modeling techniques for understanding and predicting droughts, river discharge, and crop yields.

- Drought indicators (SPI-1 to SPI-12) retain information from prior months and are useful for crop yield and hydrological drought predictions using data-driven techniques.
- The integration of satellite-based soil moisture data can significantly improve the accuracy of process-based agro-hydrological models like SWAT+ in river discharge and crop yield simulations.
- Shifting from single-objective to multi-objective calibration methods and including using Artificial Intelligence methods have been demonstrated to improve the simulation of drought indicators, river discharge and crop yields.
- Direct simulations of hydrological droughts are less reliable than indirect simulations.
- The research also highlights the challenges with precipitation satellite-based datasets and the need for careful dataset selection and calibration.
- The study shows that meteorological, agricultural, and hydrological droughts have different spatial distributions, indicating distinctive spatial features for each form of drought in the region.

According to the outputs and our methodology, we would like to continue our exploration in the realm of satellite based datasets. There are several useful agro-hydrological datasets, such as, amount of irrigation, snow cover, altimetry datasets for the height of water in rivers and lakes, actual evapotranspiration, and precipitation datasets, which their accuracy is still unknown and can be useful in agro-hydrological modeling. In addition, multi-aspect calibration facilitates more investigations in transboundary river basins or other important rivers. Additionally, due to the fact that there are several AI-based models, it is recommended that it should be helpful to the hydrologists to test and try other methods in drought simulations.

Our results can be used in different governmental sectors such as agriculture and water management. These sections can have assessments along with other sources of information to have more robust and reliable decision.

7. Other achievements

During my PhD studies at Warsaw University of Life Sciences – SGGW, I had opportunity to present my results in many outstanding international conferences such as EGU (2023 and 2024), SWAT international conferences (2022, 2023, and 2024), IUGG 2023, and other local conferences.

My work and focus was on agro-hydrological modeling and drought, but during my PhD, I used this unique opportunity at SGGW and delved into several topics such as water accounting, groundwater management and modeling, water saving plans in basin level, and extreme events. The list of other publications are listed below.

Beyond my academic pursuits and research, I was fortunate to participate in three enriching internships. In 2022, I interned at IRPI-CNR in Italy under the supervision of Dr. Luca Brocca and Dr. Christian Massari. The following year, in 2023, I had the opportunity to intern at PIK in Potsdam guided by Dr. Tobias Condrat and UFZ in Leipzig, supervised by Dr. Martin Volk Germany. These internships were funded by SGGW, Helmholtz Association (HIDA, Germany), and NAWA (Poland). Hereby, I would like to acknowledge all of mentioned organizations, and National Science Centre – NCN, Poland. This research was made possible by the support of the National Science Centre (Narodowe Centrum Nauki), Warsaw, Poland (PRELUDIUM BIS-1 project, UMO-2019/35/O/ST10/04392).

The list of articles published during my doctoral studies at SGGW, which are not included in my thesis:

- Delavar, M., Raeisi, L., Eini, M. R., Morid S., Zaghiyan, M. R., (2024). Assessing the effectiveness of water-saving plans from the farm level to the basin level using agro-hydrological modeling approach and water accounting. *Journal of Irrigation and Drainage Engineering*.
- Szyga-Pluta, K., Tomczyk, A. M., Piniewski, M., & Eini, M. R. (2023). Past and future changes in the start, end, and duration of the growing season in Poland. *Acta Geophysica*, 1-15.
- Salmani, H., Javadi, S., Eini M.R., & Golmohammadi, G. (2023). Compilation simulation of surface water & groundwater resources using the SWAT-MODFLOW model for karstic basin. *Hydrogeology Journal*.
- Eini, M. R., Motehayeri, S. M. S., Rahmati, A., & Piniewski, M. (2023). Evaluation of the accuracy of satellite-based rainfed wheat yield dataset over an area with complex geography. *Journal of Arid Environments*, 212, 104963.
- Piniewski, M., Eini, M.R., Chattopadhyay, S., Okruszko, T. and Kundzewicz, Z.W., (2022). Is there a coherence in observed and projected changes in riverine low flow indices across Central Europe?. *Earth-Science Reviews*, p.104187.

- Eini, M. R., Rahmati, A., Salmani, H., Brocca L., and Piniewski, M. (2022). Detecting characteristics of extreme precipitation events using regional and satellite-based precipitation gridded datasets over a region in Central Europe. *Science of The Total Environment*:158497.
- Delavar, M., Eini, M. R., Kuchak, V. S., Zaghiyan, M. R., Shahbazi, A., Nourmohammadi, F., and Motamedi, A. (2022). Model-based water accounting for integrated assessment of water resources systems at the basin scale. *Science of the Total Environment*, 830, 154810.
- Tomczyk, A. M., Piniewski, M., Eini, M. R., and Bednorz, E. (2022). Projections of changes in maximum air temperature and hot days in Poland. *International Journal of Climatology*, 42(10), 5242– 5254.
- Eini, M.R., Olyaei, M.A., Kamyab, T., Teymoori, J., Brocca, L. and Piniewski, M., (2021). Evaluating three non-gauge-corrected satellite precipitation estimates by a regional gauge interpolated dataset over Iran. *Journal of Hydrology: Regional Studies*, 38, p.100942.

8. References

Alloghani, M., Al-Jumeily, D., Mustafina, J., Hussain, A., Aljaaf, A.J., 2020. A Systematic Review on Supervised and Unsupervised Machine Learning Algorithms for Data Science, in: Berry, M.W., Mohamed, A., Yap, B.W. (Eds.), *Supervised and Unsupervised Learning for Data Science*. Springer International Publishing, Cham, pp. 3-21. https://doi.org/10.1007/978-3-030-22475-2_1

Azimi, S., Dariane, A.B., Modanesi, S., Bauer-Marschallinger, B., Bindlish, R., Wagner, W., Massari, C., 2020. Assimilation of Sentinel 1 and SMAP – based satellite soil moisture retrievals into SWAT hydrological model: the impact of satellite revisit time and product spatial resolution on flood simulations in small basins. *J. Hydrol.* 581, 124367. <https://doi.org/https://doi.org/10.1016/j.jhydrol.2019.124367>

Bachmair, S., Kohn, I., Stahl, K., 2015. Exploring the link between drought indicators and impacts. *Nat. Hazards Earth Syst. Sci.* 15, 1381-1397. <https://doi.org/10.5194/nhess-15-1381-2015>

Beven, K., 2006. A manifesto for the equifinality thesis. *Journal of Hydrology* 320, 18-36. <https://doi.org/https://doi.org/10.1016/j.jhydrol.2005.07.007>

Bieger, K., Arnold, J.G., Rathjens, H., White, M.J., Bosch, D.D., Allen, P.M., Volk, M., Srinivasan, R., 2017. Introduction to SWAT plus , A Completely Restructured Version of the Soil and Water Assessment Tool. *Journal of the American Water Resources Association* 53, 115-130. <https://doi.org/10.1111/1752-1688.12482>

Bormann, H., Pinter, N., 2017. Trends in low flows of German rivers since 1950: Comparability of different low-flow indicators and their spatial patterns. *River Res. Appl.* 33, 1191-1204. <https://doi.org/10.1002/rra.3152>

Boxell, L., 2019. Droughts, conflict, and the African slave trade. *Journal of Comparative Economics* 47, 774-791. <https://doi.org/https://doi.org/10.1016/j.jce.2019.06.002>

Brocca, L., Ciabatta, L., Massari, C., Moramarco, T., Hahn, S., Hasenauer, S., Kidd, R., Dorigo, W., Wagner, W., Levizzani, V., 2014. Soil as a natural rain gauge: Estimating global rainfall from satellite soil moisture data. *Journal of Geophysical Research: Atmospheres* 119, 5128-5141. <https://doi.org/10.1002/2014jd021489>

Brocca, L., Filippucci, P., Hahn, S., Ciabatta, L., Massari, C., Camici, S., Schüller, L., Bojkov, B., Wagner, W., 2019. SM2RAIN-ASCAT (2007–2018): global daily satellite rainfall data from ASCAT soil moisture observations. *Earth System Science Data* 11, 1583-1601. <https://doi.org/10.5194/essd-11-1583-2019>

Brocca, L., Hasenauer, S., Lacava, T., Melone, F., Moramarco, T., Wagner, W., Dorigo, W., Matgen, P., Martínez-Fernández, J., Llorens, P., 2011. Soil moisture estimation through ASCAT and AMSR-E sensors: An intercomparison and validation study across Europe. *Remote Sensing of Environment* 115, 3390-3408

Brocca, L., Massari, C., Pellarin, T., Filippucci, P., Ciabatta, L., Camici, S., Kerr, Y.H., Fernández-Prieto, D., 2020. River flow prediction in data scarce regions: soil moisture integrated satellite rainfall products outperform rain gauge observations in West Africa. *Scientific Reports* 10, 12517. <https://doi.org/10.1038/s41598-020-69343-x>

Brocca, L., Melone, F., Moramarco, T., Wagner, W., Naeimi, V., Bartalis, Z., Hasenauer, S., 2010. Improving runoff prediction through the assimilation of the ASCAT soil moisture product. *Hydrol. Earth Syst. Sci.* 14, 1881-1893

Brookfield, A.E., Ajami, H., Carroll, R.W.H., Tague, C., Sullivan, P.L., Condon, L.E., 2023. Recent advances in integrated hydrologic models: Integration of new domains. *Journal of Hydrology* 620, 129515. <https://doi.org/https://doi.org/10.1016/j.jhydrol.2023.129515>

Darand, M., Khandu, K., 2020. Statistical evaluation of gridded precipitation datasets using rain gauge observations over Iran. *Journal of Arid Environments* 178, 104172. <https://doi.org/10.1016/j.jaridenv.2020.104172>

De Lannoy, G.J.M., Bechtold, M., Albergel, C., Brocca, L., Calvet, J.-C., Carrassi, A., Crow, W.T., de Rosnay, P., Durand, M., Forman, B., Geppert, G., Giroto, M., Hendricks Franssen, H.-J., Jonas, T., Kumar, S., Lievens, H., Lu, Y., Massari, C., Pauwels, V.R.N., Reichle, R.H., Steele-Dunne, S., 2022. Perspective on satellite-based land data assimilation to estimate water cycle components in an era of advanced data availability and model sophistication. *Frontiers in Water* 4. <https://doi.org/10.3389/frwa.2022.981745>

Degefu, M.A., Bewket, W., Amha, Y., 2022. Evaluating performance of 20 global and quasi-global precipitation products in representing drought events in Ethiopia I: Visual and correlation analysis. *Weather and Climate Extremes* 35, 100416. <https://doi.org/10.1016/j.wace.2022.100416>

Delavar, M., Eini, M.R., Kuchak, V.S., Zaghiyan, M.R., Shahbazi, A., Nourmohammadi, F., Motamedi, A., 2022. Model-based water accounting for integrated assessment of water resources systems at the basin scale. *Science of the Total Environment* 830, 154810. <https://doi.org/10.1016/j.scitotenv.2022.154810>

Eini, M.R., Javadi, S., Delavar, M., Gassman, P.W., Jarihani, B., 2020. Development of alternative SWAT-based models for simulating water budget components and streamflow for a karstic-influenced watershed. *CATENA* 195, 104801. <https://doi.org/10.1016/j.catena.2020.104801>

Eini, M.R., Javadi, S., Delavar, M., Monteiro, J.A., Darand, M., 2019. High accuracy of precipitation reanalyses resulted in good river discharge simulations in a semi-arid basin. *Ecological engineering* 131, 107-119. <https://doi.org/10.1016/j.ecoleng.2019.03.005>

Eini, M.R., Olyaei, M.A., Kamyab, T., Teymoori, J., Brocca, L., Piniewski, M., 2021. Evaluating three non-gauge-corrected satellite precipitation estimates by a regional gauge interpolated dataset over Iran. *Journal of Hydrology: Regional Studies* 38, 100942. <https://doi.org/10.1016/j.ejrh.2021.100942>

Grillakis, M.G., Koutroulis, A.G., Alexakis, D.D., Polykretis, C., Daliakopoulos, I.N., 2021. Regionalizing Root-Zone Soil Moisture Estimates From ESA CCI Soil Water Index Using Machine Learning and Information on Soil, Vegetation, and Climate. *Water Resources Research* 57, e2020WR029249. <https://doi.org/10.1029/2020WR029249>

Gruber, A., Scanlon, T., van der Schalie, R., Wagner, W., Dorigo, W., 2019. Evolution of the ESA CCI Soil Moisture climate data records and their underlying merging methodology. *Earth Syst. Sci. Data* 11, 717-739. <https://doi.org/10.5194/essd-11-717-2019>

Hamman, J.J., Nijssen, B., Bohn, T.J., Gergel, D.R., Mao, Y., 2018. The Variable Infiltration Capacity model version 5 (VIC-5): infrastructure improvements for new applications and reproducibility. *Geosci. Model Dev.* 11, 3481-3496. <https://doi.org/10.5194/gmd-11-3481-2018>

Hao, Z., Singh, V.P., 2015. Drought characterization from a multivariate perspective: A review. *Journal of Hydrology* 527, 668-678. <https://doi.org/https://doi.org/10.1016/j.jhydrol.2015.05.031>

Hellwig, J., Stahl, K., Lange, J., 2017. Patterns in the linkage of water quantity and quality during low-flows. *Hydrological Processes* 31, 4195-4205. <https://doi.org/10.1002/hyp.11354>

Ikram, R.M.A., Hazarika, B.B., Gupta, D., Heddam, S., Kisi, O., 2022. Streamflow prediction in mountainous region using new machine learning and data preprocessing methods: a case study. *Neural Computing and Applications*. <https://doi.org/10.1007/s00521-022-08163-8>

Ionita, M., Tallaksen, L.M., Kingston, D.G., Stagge, J.H., Laaha, G., Van Lanen, H.A.J., Scholz, P., Chelcea, S.M., Haslinger, K., 2017. The European 2015 drought from a climatological perspective. *Hydrol. Earth Syst. Sci.* 21, 1397-1419. <https://doi.org/10.5194/hess-21-1397-2017>

Johnson, M.D., 2013. Crop yield forecasting on the Canadian Prairies by satellite data and machine learning methods. University of British Columbia

Keller, A.A., Garner, K., Rao, N., Knipping, E., Thomas, J., 2023. Hydrological models for climate-based assessments at the watershed scale: A critical review of existing hydrologic and water quality models. *Science of The Total Environment* 867, 161209. <https://doi.org/https://doi.org/10.1016/j.scitotenv.2022.161209>

Kisi, O., Shiri, J., Tombul, M., 2013. Modeling rainfall-runoff process using soft computing techniques. *Computers & Geosciences* 51, 108-117. <https://doi.org/10.1016/j.cageo.2012.07.001>

Knox, J., Daccache, A., Hess, T., Haro, D., 2016. Meta-analysis of climate impacts and uncertainty on crop yields in Europe. *Environmental Research Letters* 11, 113004. <https://doi.org/Artn11300410.1088/1748-9326/11/11/113004>

Kolberg, D., Persson, T., Mangerud, K., Riley, H., 2019. Impact of projected climate change on workability, attainable yield, profitability and farm mechanization in Norwegian spring cereals. *Soil & Tillage Research* 185, 122-138. <https://doi.org/10.1016/j.still.2018.09.002>

Koohi, S., Azizian, A., Brocca, L., 2021. Spatiotemporal drought monitoring using bottom-up precipitation dataset (SM2RAIN-ASCAT) over different regions of Iran. *Science of The Total Environment* 779, 146535. <https://doi.org/10.1016/j.scitotenv.2021.146535>

Kubiak-Wójcicka, K., Machula, S., 2020. Influence of climate changes on the state of water resources in Poland and their usage. *Geosciences (Switzerland)* 10, 1-21. <https://doi.org/10.3390/geosciences10080312>

Laaha, G., Gauster, T., Tallaksen, L.M., Vidal, J.P., Stahl, K., Prudhomme, C., Heudorfer, B., Vlnas, R., Ionita, M., Van Lanen, H.A.J., Adler, M.J., Caillouet, L., Delus, C., Fendekova, M., Gailliez, S., Hannaford, J., Kingston, D., Van Loon, A.F., Mediero, L., Osuch, M., Romanowicz, R., Sauquet, E., Stagge, J.H., Wong, W.K., 2017. The European 2015 drought from a hydrological perspective. *Hydrol. Earth Syst. Sci.* 21, 3001-3024. <https://doi.org/10.5194/hess-21-3001-2017>

Langhammer, J., Bernsteinová, J., 2020. Which aspects of hydrological regime in mid-latitude montane basins are affected by climate change? *Water (Switzerland)* 12. <https://doi.org/10.3390/w12082279>

Ma, T.X., Duan, Z., Li, R.K., Song, X.F., 2019. Enhancing SWAT with remotely sensed LAI for improved modelling of ecohydrological process in subtropics. *Journal of Hydrology* 570, 802-815. <https://doi.org/10.1016/j.jhydrol.2019.01.024>

McKee, T.B., Doesken, N.J., Kleist, J., 1993. The relationship of drought frequency and duration to time scales, *Proceedings of the 8th Conference on Applied Climatology*. Boston, MA, USA, pp. 179-183

Meresa, H.K., Osuch, M., Romanowicz, R., 2016. Hydro-meteorological drought projections into the 21-st century for selected polish catchments. *Water (Switzerland)* 8. <https://doi.org/10.3390/w8050206>

Modanesi, S., Massari, C., Camici, S., Brocca, L., Amarnath, G., 2020. Do Satellite Surface Soil Moisture Observations Better Retain Information About Crop-Yield Variability in Drought Conditions? *Water Resources Research* 56, e2019WR025855

Moghadam, S.H., Ashofteh, P.-S., Loáiciga, H.A., 2022. Investigating the performance of data mining, lumped, and distributed models in runoff projected under climate change. *Journal of Hydrology*, 128992. <https://doi.org/10.1016/j.jhydrol.2022.128992>

Nabipour, N., Dehghani, M., Mosavi, A., Shamshirband, S., 2020. Short-Term Hydrological Drought Forecasting Based on Different Nature-Inspired Optimization

Algorithms Hybridized With Artificial Neural Networks. *IEEE Access* 8, 15210-15222. <https://doi.org/10.1109/ACCESS.2020.2964584>

Nguyen, P., Shearer, E.J., Tran, H., Ombadi, M., Hayatbini, N., Palacios, T., Huynh, P., Braithwaite, D., Updegraff, G., Hsu, K., 2019. The CHRS Data Portal, an easily accessible public repository for PERSIANN global satellite precipitation data. *Scientific data* 6, 1-10

Peichl, M., Thober, S., Meyer, V., Samaniego, L., 2018. The effect of soil moisture anomalies on maize yield in Germany. *Natural Hazards and Earth System Sciences* 18, 889-906. <https://doi.org/10.5194/nhess-18-889-2018>

Pektaş, A.O., Kerem Cigizoglu, H., 2013. ANN hybrid model versus ARIMA and ARIMAX models of runoff coefficient. *Journal of Hydrology* 500, 21-36. <https://doi.org/10.1016/j.jhydrol.2013.07.020>

Piniewski, M., Eini, M.R., Chattopadhyay, S., Okruszko, T., Kundzewicz, Z.W., 2022. Is there a coherence in observed and projected changes in riverine low flow indices across Central Europe? *Earth-Science Reviews* 233, 104187. <https://doi.org/10.1016/j.earscirev.2022.104187>

Piniewski, M., Marcinkowski, P., Kundzewicz, Z.W., 2018. Trend detection in river flow indices in Poland. *Acta Geophys.* 66, 347-360. <https://doi.org/10.1007/s11600-018-0116-3>

Piniewski, M., Szcześniak, M., Kardel, I., Chattopadhyay, S., Berezowski, T., 2021. G2DC-PL+: a gridded 2 km daily climate dataset for the union of the Polish territory and the Vistula and Odra basins. *Earth Syst. Sci. Data* 13, 1273-1288. <https://doi.org/10.5194/essd-13-1273-2021>

Piri, J., Abdolahipour, M., Keshtegar, B., 2022. Advanced Machine Learning Model for Prediction of Drought Indices using Hybrid SVR-RSM. *Water Resources Management*, 1-30. <https://doi.org/10.1007/s11269-022-03395-8>

Prodhan, F.A., Zhang, J., Hasan, S.S., Pangali Sharma, T.P., Mohana, H.P., 2022. A review of machine learning methods for drought hazard monitoring and forecasting: Current research trends, challenges, and future research directions. *Environmental Modelling & Software* 149, 105327. <https://doi.org/10.1016/j.envsoft.2022.105327>

Rajib, M.A., Merwade, V., 2016. Improving soil moisture accounting and streamflow prediction in SWAT by incorporating a modified time-dependent Curve Number method. *Hydrological Processes* 30, 603-624. <https://doi.org/10.1002/hyp.10639>

Raposo, V.d.M.B., Costa, V.A.F., Rodrigues, A.F., 2023. A review of recent developments on drought characterization, propagation, and influential factors. *Science of The Total Environment* 898, 165550. <https://doi.org/https://doi.org/10.1016/j.scitotenv.2023.165550>

Rashid, M.M., Sharma, A., Johnson, F., 2020. Multi-model drought predictions using temporally aggregated climate indicators. *Journal of Hydrology* 581, 124419. <https://doi.org/https://doi.org/10.1016/j.jhydrol.2019.124419>

Shamshirband, S., Hashemi, S., Salimi, H., Samadianfard, S., Asadi, E., Shadkani, S., Kargar, K., Mosavi, A., Nabipour, N., Chau, K.-W., 2020. Predicting standardized streamflow index for hydrological drought using machine learning models. *Engineering Applications of Computational Fluid Mechanics* 14, 339-350. <https://doi.org/10.1080/19942060.2020.1715844>

Svoboda, M.D., Fuchs, B.A., 2016. Handbook of drought indicators and indices. World Meteorological Organization Geneva, Switzerland

Van Huynh, C., van Scheltinga, C.T., Pham, T.H., Duong, N.Q., Tran, P.T., Nguyen, L.H.K., Pham, T.G., Nguyen, N.B., Timmerman, J., 2019. Drought and conflicts at the local level: Establishing a water sharing mechanism for the summer-autumn rice production in Central Vietnam. *International Soil and Water Conservation Research* 7, 362-375. <https://doi.org/https://doi.org/10.1016/j.iswcr.2019.07.001>

Van Loon, A.F., 2015. Hydrological drought explained. *WIREs Water* 2, 359-392. <https://doi.org/https://doi.org/10.1002/wat2.1085>

Vicente-Serrano, S.M., Quiring, S.M., Pena-Gallardo, M., Yuan, S., Dominguez-Castro, F., 2020. A review of environmental droughts: increased risk under global warming? *Earth-Science Reviews* 201, 102953

von Uexkull, N., 2014. Sustained drought, vulnerability and civil conflict in Sub-Saharan Africa. *Political Geography* 43, 16-26. <https://doi.org/https://doi.org/10.1016/j.polgeo.2014.10.003>

Wang, G.C., Zhang, Q., Band, S.S., Dehghani, M., Chau, K.w., Tho, Q.T., Zhu, S., Samadianfard, S., Mosavi, A., 2022. Monthly and seasonal hydrological drought forecasting using multiple extreme learning machine models. *Engineering Applications of Computational Fluid Mechanics* 16, 1364-1381. <https://doi.org/10.1080/19942060.2022.2089732>

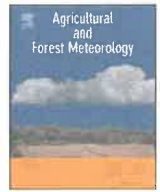
Xu, K., Yang, D., Yang, H., Li, Z., Qin, Y., Shen, Y., 2015. Spatio-temporal variation of drought in China during 1961–2012: A climatic perspective. *Journal of Hydrology* 526, 253-264. <https://doi.org/10.1016/j.jhydrol.2014.09.047>

Yang, T., Zhou, X., Yu, Z., Krysanova, V., Wang, B., 2015. Drought projection based on a hybrid drought index using Artificial Neural Networks. *Hydrological Processes* 29, 2635-2648. <https://doi.org/10.1002/hyp.10394>

9. Publication 1

Eini, M. R., Ziveh, A. R., Salmani, H., Mujahid, S., Ghezelayagh, P., & Piniewski, M. (2023). Detecting drought events over a region in Central Europe using a regional and two satellite-based precipitation datasets. *Agricultural and Forest Meteorology*, 342, 109733. <https://doi.org/10.1016/j.agrformet.2023.109733>

Impact factor: 6.2 – MeiN: 200



Detecting drought events over a region in Central Europe using a regional and two satellite-based precipitation datasets

Mohammad Reza Eini^{a,b,*}, Akbar Rahmati Ziveh^c, Haniyeh Salmani^d, Seemab Mujahid^e, Pouya Ghezelayagh^a, Mikołaj Piniewski^a

^a Department of Hydrology, Meteorology, and Water Management, Institute of Environmental Engineering, Warsaw University of Life Sciences, Warsaw, Poland

^b Potsdam Institute for Climate Impact Research (PIK), Member of the Leibniz Association, Potsdam, Germany

^c Faculty of Environmental Sciences, Czech University of Life Sciences Prague, Kamýcká 129, Praha – Suchbát, 165 00, Czech Republic

^d Department of Economics and Economic History, Universidad de Salamanca, C/Francisco Tomás y Valiente s/n, 37007 Salamanca, Spain

^e Department of Civil Engineering, Architecture, Land, Environment and Mathematics, University of Brescia, Brescia, Italy

ARTICLE INFO

Keywords:

Baltic Sea
Climate change
Satellite products
Drought
Rainfall

ABSTRACT

In this study, the accuracy of two satellite-based datasets is evaluated. The evaluation includes monthly precipitation estimates, spatial detection of precipitation, and drought monitoring against a regional gridded dataset spanning 2007–2019. A study area covering Poland and parts of the neighboring countries in Central Europe was selected for this evaluation. The Standardized Precipitation Index (SPI) at multi-time scales was employed to monitor meteorological (SPI-3), agricultural (SPI-6, SPI-9), and hydrological (SPI-12) droughts over the study region. This study selected PERSIANN-CDR as a top-down precipitation dataset and SM2RAIN-ASCAT as a bottom-up dataset. According to the results, both datasets exhibit good accuracy for precipitation estimations, but PERSIANN-CDR shows higher accuracy based on the R (coefficient of correlation) and KGE (Kling-Gupta Efficiency) performance indicators. However, SM2RAIN-ASCAT has a lower bias according to PBIAS(%) (percent bias). The reference dataset indicates that the study area experienced dry conditions over 50% of the months. Specifically, based on the reference dataset, 12 (SPI-6) and 16 (SPI-9) severe agricultural droughts were detected. Twenty-four severe agricultural drought events were identified via SPI-6, while the longer SPI window (SPI-9) demonstrated that PERSIANN-CDR assessed 20 severe droughts over the study area. SM2RAIN-ASCAT detected 11 severe agricultural droughts via SPI-6 and SPI-9. Furthermore, based on SPI-12, the reference dataset identified 75 hydrological droughts, while the top-down dataset indicated a lower number of hydrological droughts (67 events) than the reference dataset over the studied period. In contrast, the bottom-up dataset detected 84 hydrological droughts. The spatial distribution of severe meteorological droughts showed a clear pattern with predominant occurrence in eastern parts (Vistula River Basin), as shown by the reference dataset, while this pattern changed for agricultural and hydrological droughts (Odra River Basin). Additionally, the results reveal that meteorological drought does not have a similar spatial distribution to agricultural and hydrological droughts.

1. Introduction

Along with climate change, drought is one of the most complex environmental threats, and it can considerably influence world security, food production, inland water bodies, ecosystem, society, and the financial system (Dai et al., 2004; Koohi et al., 2021; Piniewski et al., 2022; Tian et al., 2020; Wilhite, 2000). Drought could have different definitions in different parts of the world due to the different intrinsic values of water in different societies and regions. In the worst case,

drought can have an adverse effect on daily life; at the same time, in other regions, it could limit recreational activities or maritime transportation (Dai et al., 2004; Harisuseno, 2020; Tian et al., 2020). The description of drought can be divided into various types, including meteorological, hydrological, agricultural, and socioeconomic, based on its influence (Crausbay et al., 2017). The foremost type of drought (meteorological drought) is caused by a shortage of rainfall which is quickly tangible. This type of drought can expand rapidly and come to an end abruptly. Prolonged precipitation deficiencies that trigger

* Corresponding author.

E-mail address: mohammad_eini@sggw.edu.pl (M.R. Eini).

<https://doi.org/10.1016/j.agrformet.2023.109733>

Received 15 December 2022; Received in revised form 15 August 2023; Accepted 22 September 2023

Available online 29 September 2023

0168-1923/© 2023 Elsevier B.V. All rights reserved.

declines in the runoff, aquifer storage, dams, and lake levels will cause hydrological drought. Accessible water in soil diminution can cause an agricultural drought then. This type of drought appears throughout the crop farming season and influences food production and security. The effects of the aforementioned types of drought can additionally have an effect on social and financial activities; this describes the socioeconomic drought. However, these droughts do not effectively address drought's environmental aspects and are inclined to be too human-centric (Javed et al., 2021; Tian et al., 2020; Vicente-Serrano et al., 2020; WMO, 2016; Won et al., 2020).

Drought indicators are widely employed for drought monitoring (Ben Abdelmalek and Nouiri, 2020; Javed et al., 2021). Nevertheless, since drought attributes and classifications are complicated, no particular indicator can satisfactorily capture all characteristics of the severity, frequency, and intensity of drought and its influences. According to WMO (2016), there are more than 150 drought indicators in the literature. These indicators are applied to determine different forms of drought, including SPI (Standardized Precipitation Index) (McKee et al., 1993), SPEI (standardized precipitation evapotranspiration index) (Vicente-Serrano et al., 2010), SSI (standardized soil moisture index) (AghaKouchak, 2014), RI (national rainfall index, National Oceanic and Atmospheric), RAI (rainfall anomaly index) (Van Rooy, 1965), DRI (vegetation drought response index) (Tadesse et al., 2005), and DSI (drought severity index) (Bryant et al., 1992). However, according to WMO (World Meteorological Organization), SPI can be used as the leading indicator for global drought monitoring because it is based on only precipitation data, has more transparency, and has less calculation complexity (Eini et al., 2023b, 2023c; Koohi et al., 2021; Mirabbasi et al., 2013; WMO, 2016). Numerous investigations were conducted to evaluate the implementation of SPI in diverse climate regions, and most of them stated that SPI has effectively recognized drought events. In some studies, SPI is used not only as a meteorological drought indicator but also as an indicator of agricultural and hydrological droughts (Abdi et al., 2022; Dikici, 2020; Mirabbasi et al., 2013; Tian et al., 2020; WMO, 2016; Won et al., 2020). For instance, Patel et al. (2007) selected SPI for 3, 6, 9, 12, and 24-month time periods to determine temporal and positional drought risks. In Taiwan, Chen et al. (2009) used SPI-3 for drought analyses and suggested that SPI-3 is a better indicator compared to SPI-1 for analyzing drought duration. Santos et al. (2021) selected different windows of SPI (1, 3, 6, 9, 12, 18, 24, 48) over a basin in India for drought analysis. WMO (2016) also suggests that SPI values for 3 months or less could be useful for basic drought monitoring, values for 6 months for monitoring agricultural impacts and values for 12 months or longer for hydrological impacts.

Precipitation datasets are essential for hydrology and environmental assessments such as drought monitoring (Eini et al., 2019). The traditional and, at the same time, the most accurate method is in situ measurements (ground gage observations) (Eini et al., 2019). Still, there are several limitations, such as low spatial network, pricey maintenance, delay in providing the data by regional authorities, and not being accessible globally (Bakhtar et al., 2022; Beck et al., 2017; Darand and Fathi, 2021; Eini et al., 2019, 2021; Rahmati Ziveh et al., 2022). The mentioned restrictions can decrease the accuracy of drought monitoring, especially over large-scale transboundary river basins or developing countries (Beck et al., 2017; Eini et al., 2019, 2021; Tian et al., 2020). In contrast, some relatively new methods provide a homogeneous network of the precipitation time series. These datasets have different categories: reanalysis, gage interpolated, non-gage-corrected satellite-based precipitation estimates, and gage-corrected satellite-based precipitation estimates (Bakhtar et al., 2022; Darand and Khandu, 2020; Eini et al., 2022a). Between these categories, satellite-based precipitation estimates offer (near) real-time and sub-daily datasets with high resolution over the globe. Hence, satellite-based precipitation products are one of the best options for drought monitoring, hydrological modeling, water resources investigations, and climatic assessments (Brocca, 2007; Eini et al., 2022a). In various studies (Alahacoon and Amarnath, 2022; Chua

et al., 2020; Degefu et al., 2022; Ghizat et al., 2022; Guo et al., 2022; Kazemzadeh et al., 2022; Koohi et al., 2021; Moreno et al., 2022; Rahmati Ziveh et al., 2022; Toté et al., 2015; Wei et al., 2021; Zhong et al., 2019), these products have been used in drought monitoring or hydrological modeling as an alternative to ground-based datasets; however, these datasets are not reliable in some parts of the world, and in some regions, the accuracy of these products is still unidentified (Table 1).

As mentioned earlier, the datasets have different accuracy according to the satellite's sensor type, numbers of included ground-based measurements, resampling methods, and processing algorithms (Brocca et al., 2014; Tang et al., 2015; Tian et al., 2009). Overall, two methods to estimate precipitation using satellites are top-down and bottom-up approaches (Fan et al., 2021; Zhang et al., 2020). In the top-down approach, the characteristics of clouds (derived from remote sensing methods) are of interest, such as the method used to develop the PERSIANN (Precipitation Estimation from Remotely Sensed Information using Artificial Neural Networks) family datasets (<https://chrsdata.eng.uci.edu/>). The second approach (bottom-up) is based on satellite-based soil moisture datasets (Brocca et al., 2013). By using this method, some new datasets are developed, which are relatively new (Brocca et al., 2014), and the accuracy of these types of datasets in daily and monthly precipitation datasets is unknown in some regions (Eini et al., 2022a). In addition, comparing top-down and bottom-up approaches in drought detection is an interesting topic to find the pros and cons of each approach.

Based on the literature, there are no detailed analyses between top-down and bottom-up approaches and their efficiency for drought monitoring over Central Europe. In this study, SM2RAIN-ASCAT (a satellite precipitation product developed by Brocca et al. (2019) and freely available on <http://hydrology.irpi.cnr.it/download-area/sm2rain-data-sets/>) is selected as the representative of the bottom-up approach, and PERSIANN-CDR (Climate Data Record) is employed as the top-down precipitation product. Thus, two main objectives can be considered in this study; first, comparing the accuracy of top-down and bottom-up approaches over two large-scale transboundary basins in Central Europe and Poland; second, monitoring different types of

Table 1

A review of selected recent studies which have used gridded datasets to assess the drought using different drought indicators over different parts of the world.

Study	Region	Datasets	Drought Indicator	Period
Chua et al. (2020)	PAPUA new Guinea	GSMAP and CMORPH	NDVI, VHI, OLR, SPI	2001–2018
Zhong et al. (2019)	China	PERSIANN-CDR, CHIRPS, TRMM, 3B42V7	SPI and PDSI	1983–2015 1998–2015
Ghozat et al. (2022)	Regions of Iran	CHIRPS	SPI	1987–2017
Guo et al. (2022)	North western china	PERSIANN-CDR, CHIRPS, MSWEP	SPI	1983–2013
Toté et al. (2015)	Mozambique	TAMSAT, FEWS NET, CHIRPS	SPI	2001–2012
Alahacoon and Amarnath (2022)	Sri Lanka	MODIS, TRMM, GPM, GLC	VCI, NDVI, PCI, TCI, IDSI	2000–2019
Kazemzadeh et al. (2022)	Iran	TRMM TMPA 3B43 v7, CHIRPS, PERSIANN-CDR	SPI, SPEI, MSPI	1983–2017
Degefu et al. (2022)	Ethiopia	20 products	SPI	1984–2002 2009–2015
Moreno et al. (2022)	Spain	CHIRPS and PERSIANN	SPI	1991–2020
Wei et al. (2021)	China	17 datasets	SPI	2019–2020
Koohi et al. (2021)	Iran	SM2RAIN-ASCAT	SPI	2007–2018

droughts using SPI. Rainfed agriculture is dominant in this region, and SPI for longer accumulation periods can be a reliable indicator of agricultural droughts (Koochi et al., 2021). This research provides the first evaluation of drought monitoring and accuracy evaluation of the top-down and bottom-up approaches over the study region to help find a reliable (near) real-time gridded dataset. In addition, by employing a high-accuracy regional gridded dataset, we have made detailed spatial comparisons between these datasets.

2. Methodology

This section describes the study area in Central Europe, precipitation datasets, drought indicators, and statistical indicators used in this study.

2.1. Study area

Central Europe is a rugged region with colder winters, considerable mountain snowfalls, and warmer summers, particularly in the lowlands. Precipitation is adequate to abundant, with a summer maximum. This study aims to cover the joint territories of Poland and the Vistula and Odra (Oder) river basins, covering approximately 350,000 km² (Eini et al., 2022b; Marcinkowski et al., 2021; Piniewski et al., 2021). Out of

that area, ~37,000 km² (~10.6%) is located beyond the Polish territory. Ukraine (12,694 km², 3.7%), Belarus (9495 km², 2.7%), the Czech Republic (7397 km², 2.1%), Germany (5298 km², 1.5%), Slovakia (1800 km², 0.5%) and Russia (401 km², 0.1%) are located in the study area. The long-term average precipitation over the study area is 661 mm (2007–2019). In addition to Odra and Vistula river basins covering the majority of this area, some minor parts of Baltic coastal, Pregolya, Neman, Danube, Elbe, and Dniester river basins are included in the case study (Fig. 1).

2.2. Precipitation datasets

Three gridded datasets were used in this study: two satellite-based datasets SM2RAIN-ASCAT and PERSIANN-CDR and one reference dataset (G2DC-PL+: a gridded 2 km daily climate dataset for the union of the Polish territory and the Vistula and Odra basins). It is based on observed stations (Piniewski et al., 2021) and developed by a geo-statistical interpolation approach (kriging). This dataset has demonstrated adequate accuracy in various investigations (Berezowski et al., 2016; Eini et al., 2023a, 2022a, 2022b; Marcinkowski et al., 2021; O'Keeffe et al., 2019).

The datasets differed with respect to temporal availability and

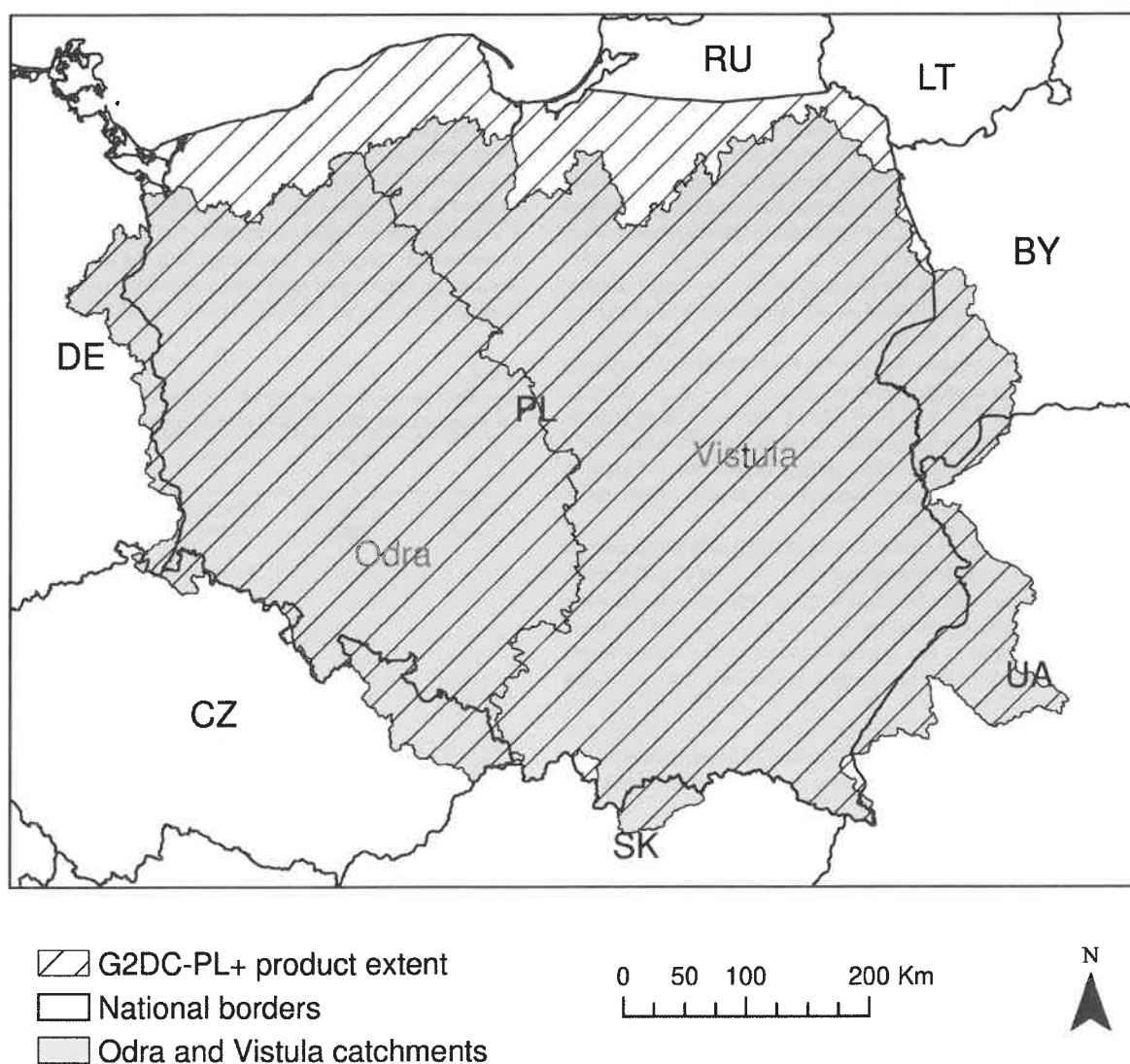


Fig. 1. Selected study area (corresponding to the G2DC-PL+ product extent) in Central Europe - adopted from Piniewski et al. (2021).

temporal/spatial resolution. The bottom-up dataset, SM2RAIN-ASCAT, is a real-time dataset covering the 2007–now period at a daily time step and a regular grid at 0.1-degree sampling (3600×1801) on a global scale. SM2RAIN is a bottom-up process made on methods introduced by Brocca et al. (2014), which can be used for direct rainfall estimation from the station- and satellite-based soil moisture measurements (Brocca et al., 2019; Eini et al., 2021). PERSIANN-CDR (as a top-down dataset) delivers hourly to yearly precipitation data at 0.25° over 60°N – 60°S and covers 2000–Now. PERSIANN-CDR is constructed to meet the demand for a dependable, long-period, high-spatially distributed, and worldwide rainfall dataset for analyzing changes and trends in daily rainfall. G2DC-PL+ was available for the longest period 1951–2019 at daily time step. Table 2 displays key features of the G2DC-PL+ (as the reference) and satellite-based products. We have employed the 2007–2019 period as the joint time window to evaluate the accuracy of satellite datasets and drought detection. All datasets were recalculated to monthly time steps from their native temporal resolution. In addition, G2DC-PL+ and SM2RAIN datasets were regridded to $0.25^\circ \times 0.25^\circ$ resolution (spatial resolution of PERSIANN-CDR) to facilitate grid-by-grid evaluations.

2.3. Drought indicators

The SPI is the commonly applied drought indicator proposed by McKee et al. (1993) to reveal drought intensity and assess areas with various environments based on rainfall. The precious aspect of the SPI is that it is simply calculated and adaptable over time, so it can be used to recognize various forms of droughts and meteorological, agricultural, and hydrological droughts. For example, Xu et al. (2015) used SPI-3 as a proxy of meteorological drought, and in Koohi et al. (2021) study, SPI-6 and SPI-12 were selected as the agricultural drought and hydrological drought proxies.

The SPI computation is based on matching the best probability distribution function to the precipitation dataset, which McKee et al. (1993) suggested as the Gamma function. The drought and wetness definitions used in the current study, based on the SPI, are described in Table 3. According to the definition, the positive values of SPI indicate above the average precipitation (wet conditions), and the negative values of SPI show below the average precipitation (dry conditions). However, these definitions can be changed; for example, in some references $-1 < \text{SPI} < 1$ is considered as near normal conditions (i.e., Xu et al. (2015)). We have employed SPI-3 as the proxy of meteorological drought, SPI-6 and SPI-9 as the proxies of agricultural drought, and SPI-12 as the proxy of hydrological drought (a similar approach is used or suggested in Koohi et al. (2021), Javed et al. (2021), Razei et al. (2009), Dai et al. (2020), and Santos et al. (2011)). Fig. 2 (adopted from Guo et al. (2022)) defines drought events and illustration of drought attributes (run theory), which are discussed in this study. In this research, $\text{SPI} < -1$ is identified as severe drought.

2.4. Evaluation indicators and employed tools

To evaluate the accuracy of SM2RAIN-ASCAT and PERSIANN-CDR datasets in monthly rainfall estimations, Root Mean Square Deviation (RMSD mm, optimum value = 0 mm), Percent bias (PBIAS%, optimum value = 0%), Pearson Correlation Coefficient (R, optimum value = 1),

Table 3

The employed classification of SPI in the current study.

SPI	Classification
$\text{SPI} \geq 0$	Wet conditions
$\text{SPI} < 0$	Dry condition
$\text{SPI} \leq -1$	Severe drought

and Kling-Gupta efficiency (KGE, optimum value = 1). These statistics have been used in several studies, and some thresholds have been proposed; however, different types of statistics have been applied in the assessment of satellite-based precipitation products, but there are no strict guidelines for using specific statistics (Delavar et al., 2022; Duan et al., 2016; Eini et al., 2021; Knoben et al., 2019; Ritter and Munoz-Carpena, 2013).

The calculations were done in the R environment using the "CDT" package (Dinku et al., 2022; Grossi and Dinku, 2022). This package is freely available and can be accessed at <https://iri.columbia.edu/our-expertise/climate/tools/cdt/> and <https://github.com/rija-iri/CDT>. Regridding mentioned in Section 2.2 was carried out in the "CDT" package and also the "Raster" package (<https://cran.r-project.org/web/packages/raster/index.html>) in R. The methodology used is presented in Fig. 3.

3. Results and discussion

In this section, we first present the dataset evaluation results. Next, we quantify meteorological drought using SPI-3. Assessments on agricultural drought were analyzed by employing SPI-6 and SPI-9. Finally, SPI-12 was used as the hydrological drought indicator. We then proceed to evaluate different aspects of the accuracy of SPI estimations based on satellite products.

3.1. Evaluation of satellite-based precipitation products

Using the regridding technique, all the datasets were set on $0.25^\circ \times 0.25^\circ$. This technique helps to have a robust and more reliable evaluation of datasets. The performance of both datasets is evaluated by RMSD (mm), PBIAS (%), R, and KGE statistical indices. Table 4 shows the average and median of each performance indicator over the study region. According to RMSD (mm), both datasets have approximately similar errors, but PBIAS (%) reveals that SM2RAIN-ASCAT has underestimated precipitation ($\sim -3\%$) at monthly scales, and PERSIANN-CDR overestimates precipitation (approximately 20%) against the reference dataset. Correlation (R) shows that PERSIANN-CDR has a higher agreement ($\sim 85\%$) with the reference dataset compared to SM2RAIN-ASCAT ($\sim 75\%$). Finally, KGE again shows that, on average, PERSIANN-CDR performs better relative to SM2RAIN-ASCAT at monthly time steps. Fig. 4 shows the variation of performance indicators. According to Fig. 4, the bias of the SM2RAIN-ASCAT has less variations than PERSIANN-CDR, and the range of RMSD (mm) shows that both have approximately similar variations. The R range shows that PERSIANN-CDR has lower variation and more acceptable results than SM2RAIN-ASCAT against the reference data. Variation of KGE shows that a larger share of this performance indicator is over 0.7 for PERSIANN-CDR than for SM2RAIN-ASCAT. While the range of variation of

Table 2

Selected satellite-based precipitation products and reference dataset.

Product	Time span	Spatial coverage	Temporal resolution	Spatial resolution	Link
G2DC-PL+	1951–2019	Polish territory and the Vistula and Odra basins	Daily	$2 \text{ km} \times 2 \text{ km}$	https://doi.org/10.4121/uuid:a3bed3b8-e22a-4b68-8d75-7b87109c9feb
SM2RAIN-ASCAT	2007–2022	Land	Daily	$0.1^\circ \times 0.1^\circ$	https://zenodo.org/record/3405563
PERSIANN-CDR	1983–Now	60°S to 60°N	Daily to yearly	$0.25^\circ \times 0.25^\circ$	https://chrsdata.eng.uci.edu/

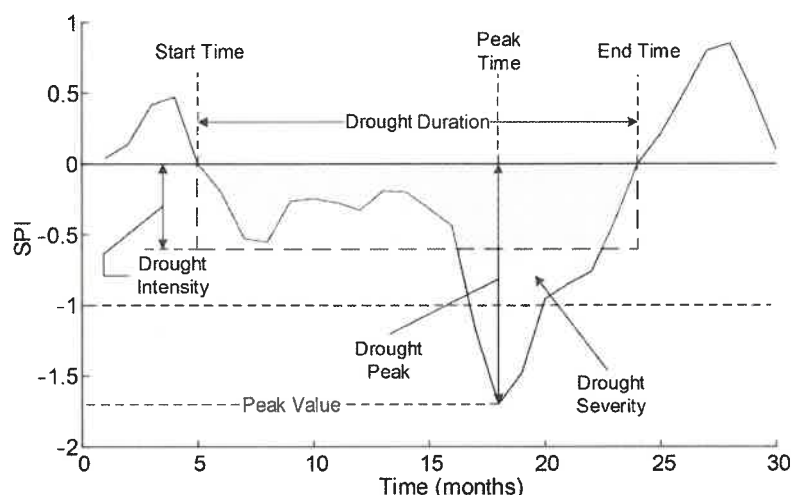


Fig. 2. Schematic description of drought event and illustration of drought attributes according to run theory, adopted from Guo et al. (2022).

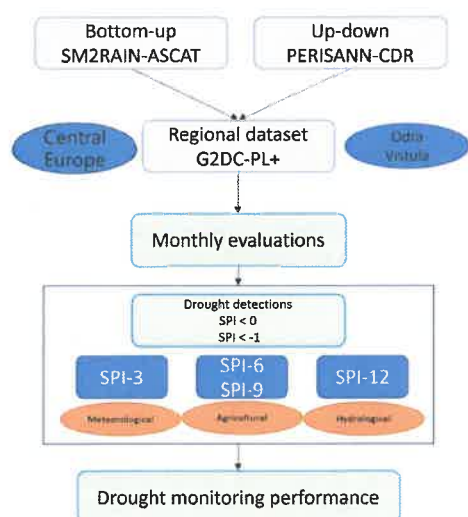


Fig. 3. Flowchart of methods used in the current study.

Table 4

Average and median of performance indicators for monthly time steps (2007–2019).

Performance indicator	Satellite product	Average	Median
RMSD (mm)	PERSIANN-CDR	22.00	21.55
	SM2RAIN-ASCAT	23.86	23.07
PBIAS (%)	PERSIANN-CDR	20.57	21.6
	SM2RAIN-ASCAT	-3.20	-3
R	PERSIANN-CDR	0.87	0.87
	SM2RAIN-ASCAT	0.75	0.75
KGE	PERSIANN-CDR	0.72	0.73
	SM2RAIN-ASCAT	0.65	0.75

KGE for SM2RAIN-ASCAT is similar to PERSIANN-CDR, a significant share of KGE values for SM2RAIN-ASCAT is below 0.7.

The spatial distribution of the accuracy of satellite-based datasets against the reference dataset is presented in Fig. 5. RMSD (mm) shows that both datasets have higher errors over the southern parts of the study area, which is a mountainous area. The minimum error of PERSIANN-CDR (~15.1 – ~19.6 mm, based on RMSD) is detected over the central and eastern parts; in contrast, SM2RAIN-ASCAT shows better

accuracy based on RMSD (mm) over the western parts. Both datasets, based on PBIAS (%), underestimated precipitation over mountainous areas (south of the study area), and the SM2RAIN-ASCAT has a better estimation. PBIAS (%) pattern is almost similar in both datasets over central regions, while SM2RAIN-ASCAT has a lower positive bias in central parts (~2% – ~11%) relative to PERSIANN-CDR. According to the correlation (R) between satellite-based datasets against reference datasets, it is visible that SM2RAIN-ASCAT has a higher correlation over mountains ($R > 0.8$) while having higher errors over this zone. PERSIANN-CDR has a higher correlation ($R > 0.90$) over the central and eastern parts. Finally, KGE shows that the bottom-up approach can provide better estimates over the southern area and lower estimates close to the Baltic Sea (northern parts). The top-down approach can provide a higher accuracy based on KGE for areas close to the Baltic Sea.

In accordance with this research results, based on PBIAS (%), Zhong et al. (2019) have shown that PERSIANN-CDR has a positive bias and high correlation over China at monthly steps. However, Guo et al. (2022) could not detect a high correlation between PERSIANN-CDR and ground-based datasets over northwestern China. Kazemzadeh et al. (2022) show that PERSIANN-CDR has acceptable accuracy over Iran based on PBIAS (%), RMSD (mm), and R . However, at daily time steps, over a catchment in Poland, PERSIANN-CDR did not show acceptable accuracy (Eini et al., 2022a). In addition, Koohi et al. (2021) highlighted that the SM2RAIN-ASCAT is an appropriate dataset for drought detection in most parts of Iran.

3.2. Drought detection

This section describes the results of different types of droughts using the three aforementioned datasets. Meteorological drought via SPI-3, agricultural drought via SPI-6 and SPI-9, and hydrological drought via SPI-12 were assessed.

3.2.1. Meteorological drought detection

By employing SPI-3, which can capture seasonal or short-term droughts, we have tried to assess the meteorological droughts over the study area (2007–2019). First of all, G2DC-PL+ shows that the study area has experienced 15 severe meteorological droughts ($SPI-3 < -1$) in 2011 (five events), 2015 (four events), 2008, 2009, 2014, 2019 (single events), and the worst meteorological drought occurred in November 2011 ($SPI-3 = -1.99$). Also, based on the reference data, the intensity of severe meteorological droughts ($SPI-3 < -1$) was, on average, -1.23, and in 2015, a four-month continuous severe meteorological droughts (Jul. - Oct.) had the longest duration of severe

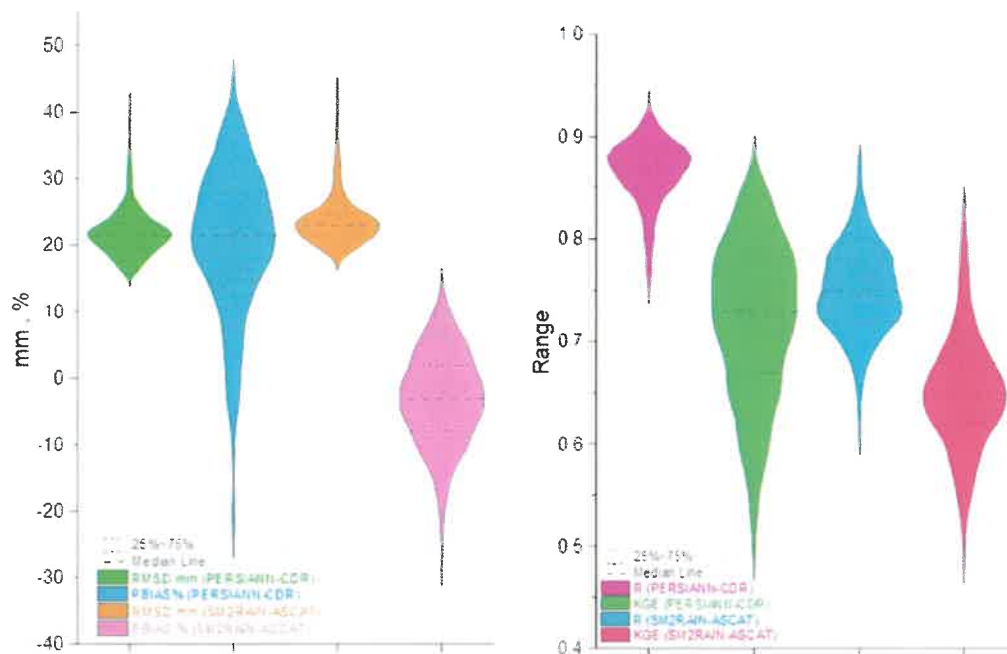


Fig. 4. Variation of performance indicators by employing violin plot (2007–2019).

meteorological droughts over the study area. In total, meteorological dry conditions ($SPI-3 < 0$) happened over 80 months (out of 154). This result shows that in more than 50% of the months, the study area has experienced meteorological dry conditions or below normal (Fig. 6). Our results are also in accordance with the studies of Ionita et al. (2017) and Laaha et al. (2017), which have shown that the 2015 drought events strongly affected Central Europe, and some regions experienced the driest and hottest summer over the 1950–2015. In another study, across Poland, by Somorowska (2022), severe droughts in 2015, 2018, and 2019 were detected. In a transboundary catchment (Lusatian Neisse river catchment) in the southwest of Poland, Otop et al. (2023), also by employing SPI-3 and SPI-12, showed that a shortage of precipitation was noticed from autumn 2017 to spring 2020, which is in line with our findings.

The top-down dataset (PERSIANN—CDR) shows similar fluctuations to the reference dataset in detecting SPI-3 as an indicator of meteorological drought. However, PERSIANN—CDR has estimated more severe meteorological droughts ($SPI-3 < -1$) by 17 events. This dataset also detects November 2011 as the worst condition ($SPI-3 = -2.2$); in 2015, this dataset detected five-month continuous severe meteorological droughts. PERSIANN—CDR also detected 78 dry meteorological conditions ($SPI-3 < 0$), showing that approximately 50% of the period meteorological below normal conditions happened in the study area.

SM2RAIN-ASCAT, a bottom-up dataset, was generally unable to detect SPI-3 accurately (relative to PERSIANN—CDR) and has shown less similarity to the reference dataset. SM2RAIN-ASCAT has shown 13 severe meteorological droughts and 73 meteorological drought events over the study area. According to SM2RAIN-ASCAT, in February 2010, the study area faced the worst situation ($SPI-3 = -1.78$) in the reference dataset, and PERSIANN—CDR this month has a positive value for SPI-3. Based on SM2RAIN-ASCAT, the study area faced a prolonged severe meteorological drought in 2015 with six continuous drought events (May. – Oct.). According to Fig. 6, SM2RAIN-ASCAT has a serious problem in 2013 when it shows drought conditions as opposed to the reference dataset showing wet conditions over several months. This is particularly visible for SPI-6 and SPI-9.

3.2.2. Agricultural drought detection

SPI-6 and SPI-9 were used as representatives of agricultural droughts. SPI-6 can present short- and mid-term effects of lack of precipitation on soil moisture. In other words, soil moisture deficit can be seen after meteorological droughts and extended periods. In addition, because farming activities are based on precipitation (rainfed farming) in the study area, the longer window of SPI can be helpful for crop loss detection. Hence, SPI-9 is also an agricultural drought indicator that can capture all the growing season precipitation deficits. The time series of SPI-6 and SPI-9 are presented in Fig. 6.

According to the reference dataset, 12 severe agricultural droughts based on SPI-6 have occurred over the study area, and half happened continuously in 2015. The worst condition occurred in August 2015 ($SPI-6 = -1.6$). In addition, the region's dry conditions ($SPI-6 < 0$) happened over 75 months. Based on SPI-9, 16 severe agricultural droughts happened. The longest agricultural drought started in May 2015 and finished in February 2016, and the study area faced the worst situation in October 2015 ($SPI-9 = -1.59$). In addition, 78 agricultural drought events happened over the study region based on SPI-9 during 2007–2019. This result reveals that over 2015, massive soil moisture deficits are expected in the study region. This result is in accordance with Laaha et al. (2017) study, which mentioned that in 2015, Central Europe was influenced by drought, and an area across the Czech Republic was most impacted.

The top-down dataset (PERSIANN—CDR) revealed 24 severe agricultural drought events via SPI-6. The longest severe agricultural drought happened in 2015 (Jun – Dec.) and 2018 (May – Nov.), with seven ongoing severe events ($SPI-6 < -1$). The longer SPI window (SPI-9) shows that PERSIANN—CDR has estimated 20 severe agricultural droughts over the study area. This product detected a nine-month ongoing severe agricultural drought that began in May 2015 and ended in January 2016. October 2015 has the lowest SPI-9 (-1.64) in the study period.

SM2RAIN-ASCAT detected 11 severe agricultural droughts via SPI-6 and SPI-9. For both indicators, this dataset showed October 2015 as the month with the harshest ($SPI-6 = -1.74$, $SPI-9 = -1.8$) agricultural drought over the study period. Based on SPI-6 and SPI-9, an ongoing severe agricultural drought from June 2015 to March 2016 was

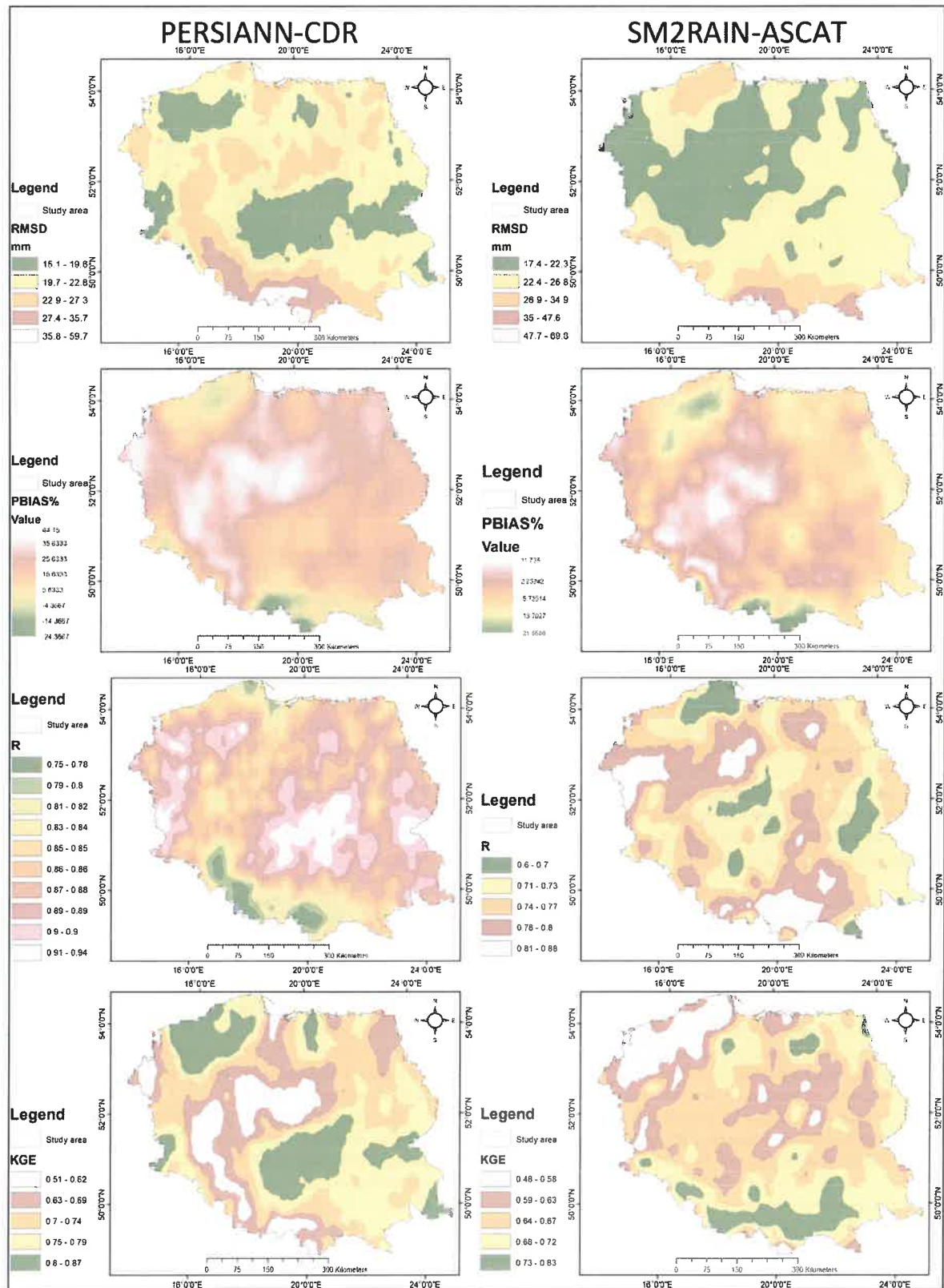


Fig. 5. Spatial distribution of performance indicators over the study area (2007–2019).

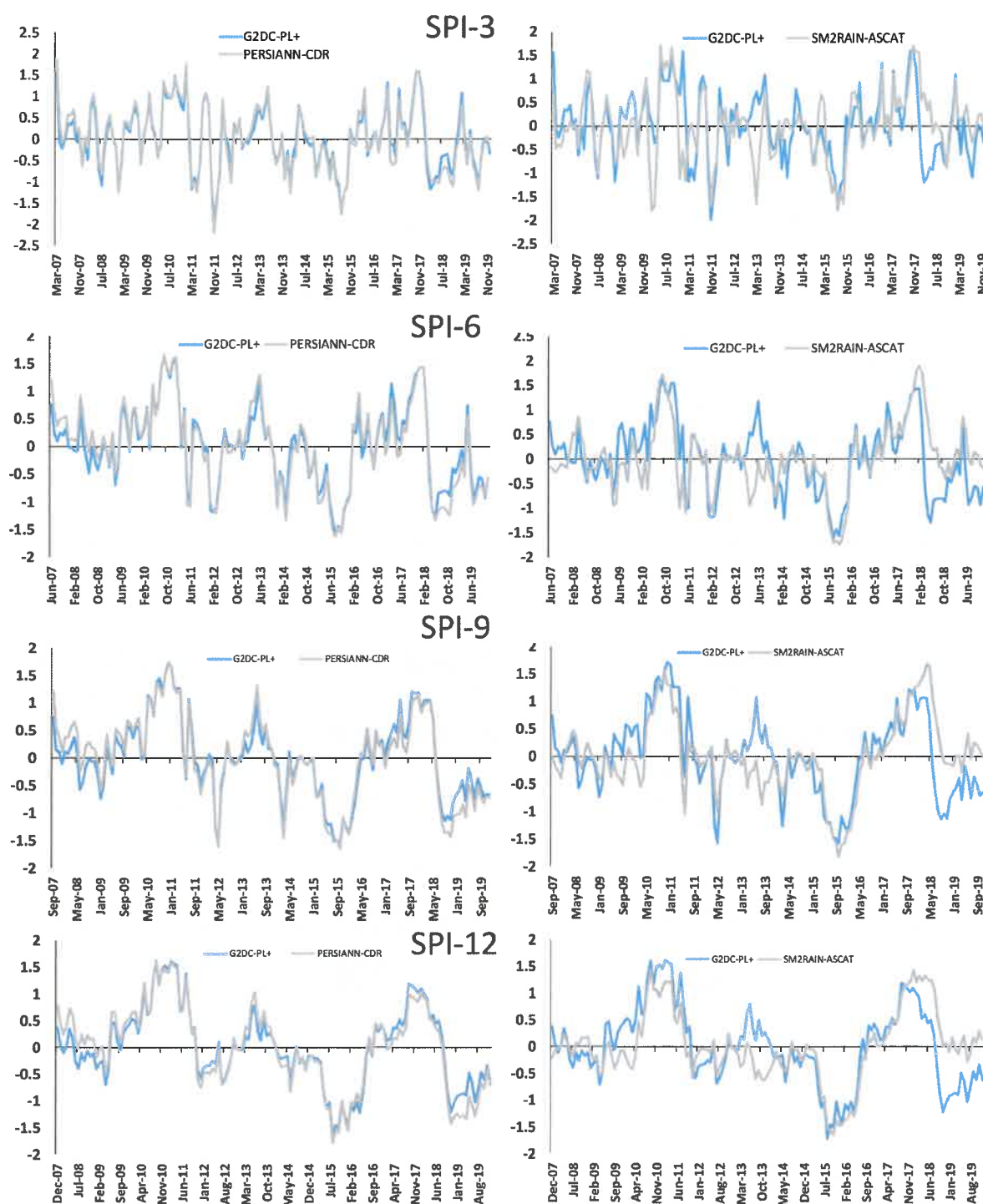


Fig. 6. Evaluation of SPI time series estimated based on reference dataset, PERSIANN—CDR, and SM2RAIN-ASCAT at various time scales over the study area.

identified by SM2RAIN-ASCAT.

3.2.3. Hydrological drought detection

Based on SPI-12, the reference dataset has detected the worst condition in August 2015 ($\text{SPI-12} = -1.72$), and this dataset detected 15 severe hydrological droughts ($\text{SPI-12} < -1$). The longest period of severe hydrological drought started in June 2015 and ended in May 2016. During 2007–2019, 75 hydrological droughts were detected in the reference dataset. In addition, the 2015 drought events are detected in other studies, such as van Lanen et al. (2016), Laaha et al. (2017), and

Ionita et al. (2017), and it is mentioned that in some regions, low flow droughts happened with return period over 100 years. The time series of SPI-12 are presented in Fig. 6.

PERSIANN—CDR shows fewer hydrological droughts over the studied period (67 events, $\text{SPI-12} < 0$) than the reference dataset but detected 20 severe hydrological droughts. The lowest SPI-12 happened in August 2015 (-1.78), similar to the reference dataset. However, PERSIANN—CDR shows that the longest severe hydrological drought occurred from October 2018 to April 2019.

SM2RAIN-ASCAT detected 84 hydrological droughts over

2007–2019 based on $SPI-12 < 0$, and October 2015 was the worst condition ($SPI-12 = -1.66$). Nevertheless, this dataset has detected 11 severe hydrological droughts over the study area from August 2015 to Jun 2016.

3.3. Spatial distribution of severity

The spatial distribution of drought severity ($SPI < -1$, Fig. 2) is presented in Fig. 7. Based on the reference dataset, the severe meteorological droughts were mainly concentrated in the eastern and northern parts of the study area. In the northwest, less intense meteorological droughts occurred, and PERSIANN—CDR does not exhibit a similar pattern, indicating that severity based on SPI-3 happened in the western parts. On the other hand, SM2RAIN-ASCAT shows that the northeast and east experienced more severe droughts than other regions. Additionally, based on this dataset, severe droughts were also detected in the middle of the Odra River basin in the western part.

The datasets, however, exhibit a similar spatial pattern over the central parts of the Odra River basin. This suggests a degree of agreement between the datasets in this region regarding the severity of meteorological droughts.

Considering the information presented in Fig. 7 when interpreting and comparing the spatial distribution of drought severity based on the different datasets is important. The variations in patterns observed in different regions highlight the importance of using multiple datasets to assess drought conditions and impacts in the study area

comprehensively.

Expanding the SPI window provides further insight, revealing that the western part of the study area has experienced more severe droughts based on the reference dataset. PERSIANN—CDR exhibits a pattern similar to the reference dataset, particularly when based on SPI-6. However, it becomes evident that severe meteorological droughts predominantly occur in the eastern parts, whereas agricultural and hydrological droughts have been observed in the western parts. Unfortunately, the satellite datasets could not capture this movement or spatial differentiation between the types of droughts.

The inability of the satellite datasets to detect such spatial variations in drought types emphasizes the limitations and challenges associated with using satellite-based products for drought detection. Different drought types may have distinct characteristics and varying impacts on different regions, making it essential to employ comprehensive and localized assessments when studying drought patterns and their effects. Overall, the expanded SPI window provides a clearer understanding of the distribution of drought severity and highlights the need for cautious interpretation and further investigation when using satellite datasets to monitor and analyze drought conditions across different regions.

3.4. Drought detection performance

By employing the Taylor diagram, the performance of satellite products was evaluated. Fig. 8 shows that PERSIANN—CCS has a higher correlation (0.97, SPI-3) than SM2RAIN-ASCAT, but the standard

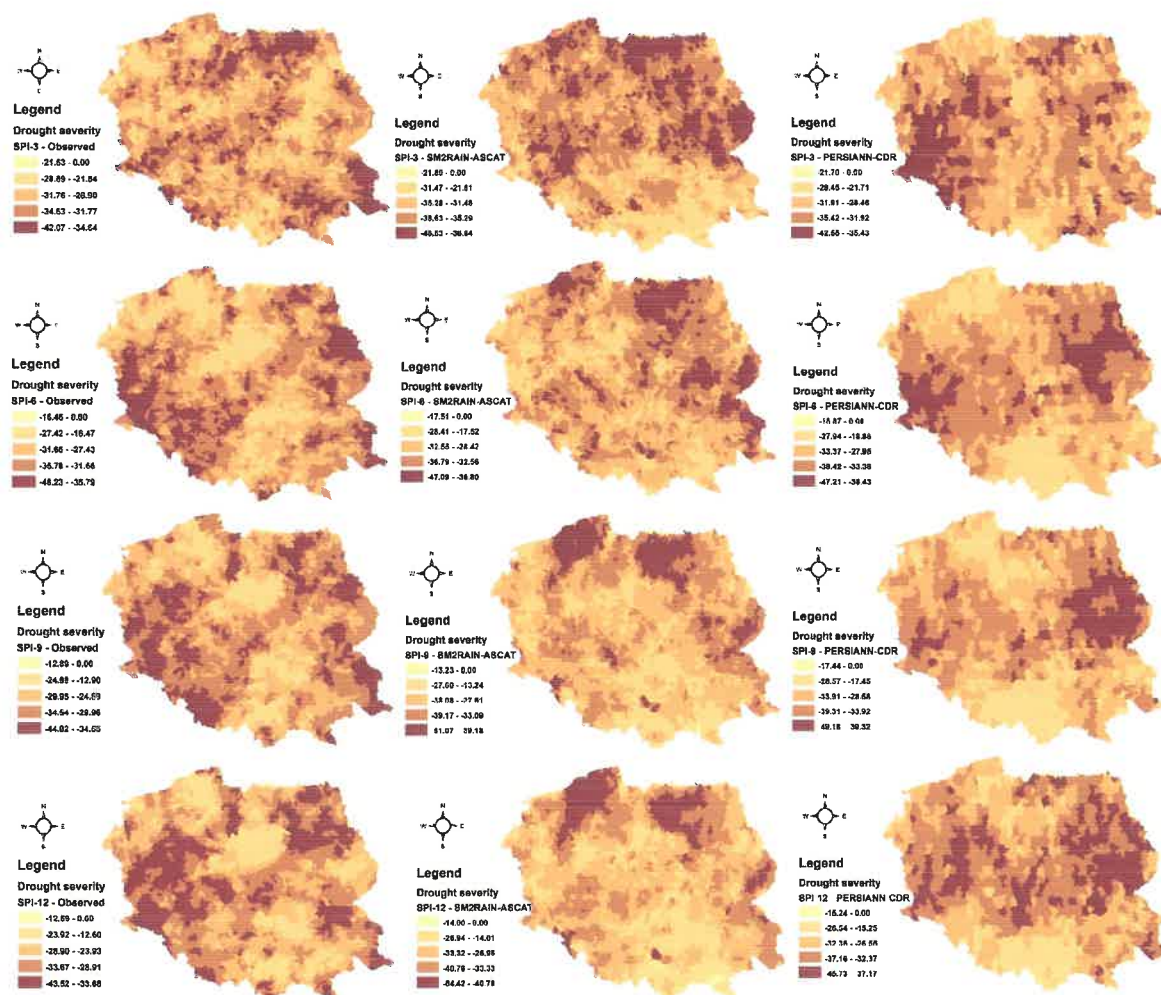


Fig. 7. Spatial distribution of drought severity ($SPI < -1$) over the study region (2007–2019).

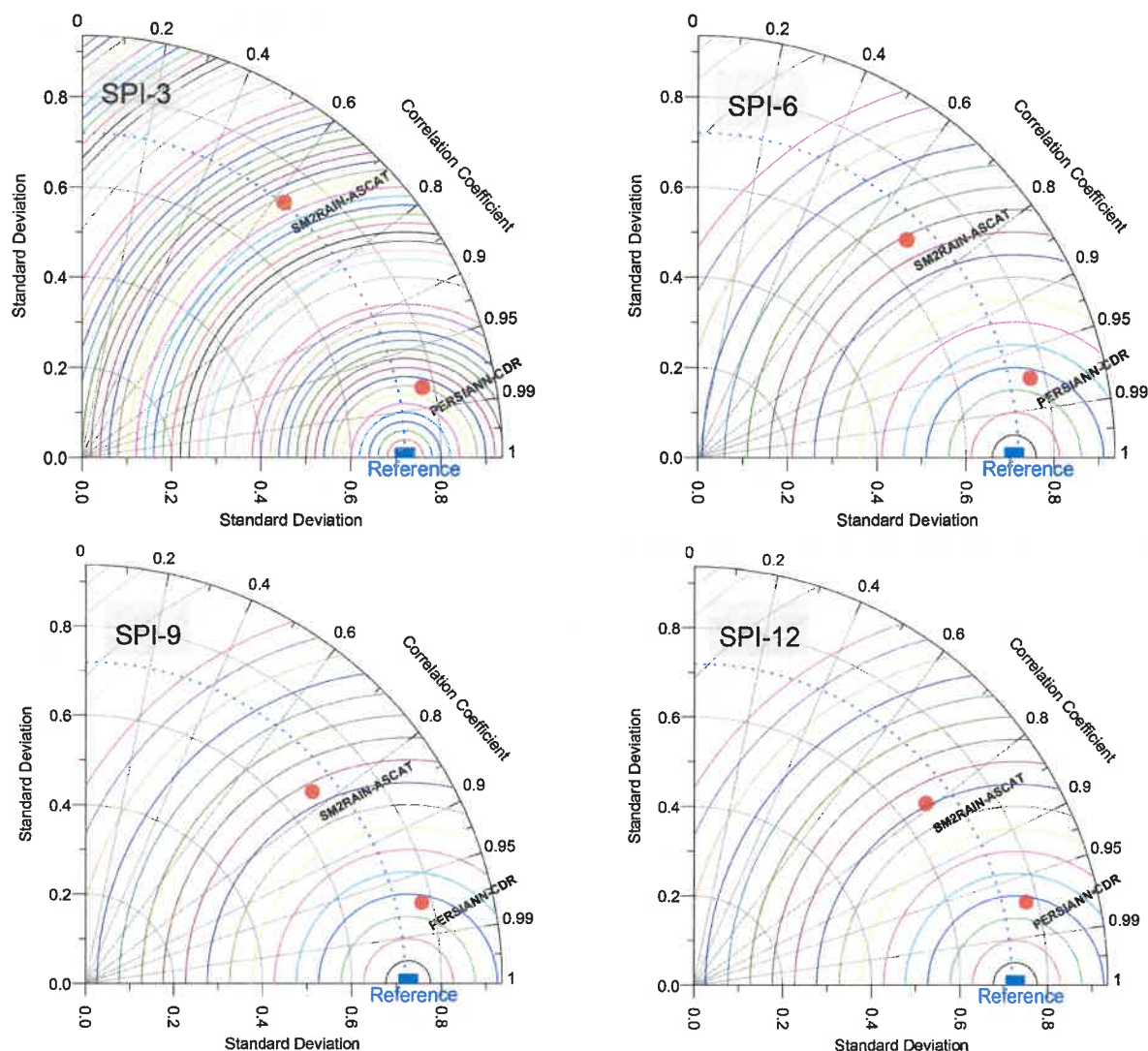


Fig. 8. Performance of each satellite-based dataset in drought detection against the reference dataset.

deviation of SM2RAIN-ASCAT is similar to the reference dataset (0.72, SPI-3). By increasing the window of SPI (agricultural droughts and hydrological droughts), the correlation of SM2RAIN-ASCAT has increased to approximately 0.8. According to Fig. 8, Although SM2RAIN-ASCAT can detect hydrological and agricultural droughts rather than meteorological droughts, PERSIANN—CDR has a better correlation with the reference dataset for all cases.

As mentioned in Table 1, several studies have used satellite-based datasets for drought assessments over different parts of the world and evaluated these datasets against a reliable source. Among the used drought indicators, SPI is the most widespread drought indicator. For example, Koohi et al. (2021) mentioned that the SM2RAIN-ASCAT could precisely detect drought events, predominantly agricultural and meteorological drought assessments, over most parts of the region. Their research selected SPI-1, SPI-3, SPI-6, and SPI-12 to detect different droughts. PERSIANN—CDR in Ethiopia showed accurate results for drought detection based on SPI (Degefu et al., 2022).

Performing satellite-based rainfall estimations in drought assessments is usually defined by their ability to detect the quantity and geographical distribution and to catch high- and low-intensity rainfall events (Degefu et al., 2022; Le Coz and van de Giesen, 2020). Satellite-based precipitation estimates are suggested in drought assessments and real-world actions that adequately estimate tiny precipitation

quantities, have lower overestimations, and provide a fair estimation of the spatial variation of low precipitation quantity and events (Degefu et al., 2022).

In addition to the previous studies, it is important to note that in the current study, PERSIANN—CDR, selected from the PERSIANN family encompassing a wide range of datasets, is a gage-corrected dataset. This implies that the product is not solely based on satellite datasets; some corrections utilizing ground-based datasets have been applied to enhance its accuracy. On the other hand, SM2RAIN-ASCAT is a pure satellite-based dataset without any post-processing. We recommend that other researchers compare SM2RAIN-ASCAT (as the bottom-up precipitation dataset) with other members of satellite-based datasets to facilitate more robust comparisons. This approach will enable a comprehensive evaluation of the datasets and their performances.

One of the uncertainties of this study could arise from the short period of precipitation datasets. It is recommended that a minimum of 30 years of monthly precipitation datasets be needed in SPI evaluations Hinge et al. (2021). However, according to the satellite-based datasets and their limits, we have used 14 years in our evaluations, as Koohi et al. (2021) have used 13 years for the SPI evaluation of SM2RAIN-ASCAT. To have robust assessments, according to Somorowska (2022), soil moisture and evapotranspiration could be considered in drought detections, in addition to meteorological parameters.

4. Conclusion

This study used PERSIANN—CDR as a top-down precipitation dataset and SM2RAIN-ASCAT as a bottom-up precipitation dataset. The accuracy of both datasets for monthly precipitation estimates and drought monitoring was evaluated against a regional gridded dataset covering the period from 2007 to 2019.

According to our results, both datasets demonstrate good accuracy for precipitation estimations. However, PERSIANN—CDR exhibits higher accuracy when evaluated based on the R (coefficient of correlation) and KGE (Kling-Gupta Efficiency) performance indicators. On the other hand, SM2RAIN-ASCAT shows a lower bias according to PBIAS (%), indicating that it tends to have a smaller overall deviation from the observed values. The analysis of RMSD (Root Mean Square Deviation) reveals that both datasets have higher errors over the southern parts of the mountainous region of the study area. Interestingly, PERSIANN—CDR demonstrates the minimum error over the central and eastern parts, whereas SM2RAIN-ASCAT shows better accuracy based on RMSD (mm) over the western parts of the study area.

It is important to note that both datasets tend to underdetermine precipitation over mountainous areas, as indicated by PBIAS (%). The pattern of PBIAS (%) is relatively similar in both datasets over central regions; however, SM2RAIN-ASCAT shows a lower positive bias in these central parts compared to PERSIANN—CDR. Moreover, SM2RAIN-ASCAT displays a higher correlation over mountainous areas, indicating better agreement with observed values and higher errors in this zone. On the other hand, PERSIANN—CDR exhibits a higher correlation over the central and eastern parts of the study area.

Lastly, the evaluation based on KGE suggests that the bottom-up approach (SM2RAIN-ASCAT) provides better precipitation estimates over the southern area, while it tends to provide lower estimates close to the Baltic Sea (northern parts). The top-down approach (PERSIANN—CDR), on the other hand, offers better accuracy based on KGE for areas near the Baltic Sea. Overall, these results indicate that each dataset has its strengths and weaknesses in different regions of the study area, and both approaches contribute valuable insights into the accuracy of precipitation estimates for the given spatial distribution.

To detect drought, we utilized SPI-3 for meteorological drought, SPI-6 and SPI-9 for agricultural drought, and SPI-12 for hydrological drought. According to the reference dataset, the study area experienced 15 severe meteorological droughts ($\text{SPI-3} < -1$) and meteorological drought events ($\text{SPI-3} < 0$) for a total of 80 months out of 154. The results indicate that the study area was affected by meteorological droughts in more than 50% of the months.

Based on the reference dataset, 12 severe agricultural droughts were identified using SPI-6 and 16 severe agricultural droughts using SPI-9 over the study area. On the other hand, the top-down dataset (PERSIANN—CDR) discovered 24 severe agricultural drought events through SPI-6, while the longer SPI window (SPI-9) showed that PERSIANN—CDR assessed 20 severe droughts over the study area. SM2RAIN-ASCAT, on the other hand, detected 11 severe agricultural droughts via SPI-6 and SPI-9.

Regarding hydrological drought, the reference dataset detected 15 severe hydrological droughts ($\text{SPI-12} < -1$) and a total of 75 hydrological droughts ($\text{SPI-12} < 0$). The top-down dataset (PERSIANN—CDR) indicated fewer hydrological droughts over the studied period (67 events, $\text{SPI-12} < 0$) compared to the reference dataset, but it still detected 20 severe hydrological droughts. In contrast, the bottom-up dataset (SM2RAIN-ASCAT) detected 84 hydrological droughts over 2007–2019 based on $\text{SPI-12} < 0$, with 11 being severe hydrological droughts.

Additionally, our results revealed that meteorological drought does not exhibit a similar spatial distribution pattern to agricultural and hydrological droughts. This indicates that different drought types may have distinct spatial characteristics and patterns of occurrence in the study area.

Declaration of Competing Interest

The authors declare that they have no known competing financial interests or personal relationships that could have appeared to influence the work reported in this paper.

Data availability

Data will be made available on request.

Acknowledgement

This research received financial support from the National Science centre (Narodowe Centrum Nauki – NCN, PRELUDIUM BIS-1 project, UMO-2019/35/O/ST10/04392, Poland) and the Polish National Agency for Academic Exchange (NAWA- PPN/STA/2021/1/00054). We also express gratitude to the Potsdam Institute for Climate Impact Research (PIK) in Germany for hosting MRE during an internship that contributed to this research (supported by NAWA).

References

- Abdi, M.J., Raffar, N., Zulkafli, Z., Nurulhuda, K., Rehan, B.M., Muharam, F.M., Khosim, N.A., Tangang, F., 2022. Index-based insurance and hydroclimatic risk management in agriculture: a systematic review of index selection and yield-index modelling methods. *Int. J. Disaster Risk Reduct.* 67, 102653. <https://doi.org/10.1016/j.ijdrr.2021.102653>.
- AghaKouchak, A., 2014. A baseline probabilistic drought forecasting framework using standardized soil moisture index: application to the 2012 United States drought. *Hydrol. Earth Syst. Sci.* 18, 2485–2492. <https://doi.org/10.5194/hess-18-2485-2014>.
- Alahacoon, N., Amarnath, G., 2022. Agricultural drought monitoring in Sri Lanka using multisource satellite data. *Adv. Space Res.* 69, 4078–4097. <https://doi.org/10.1016/j.asr.2022.03.009>.
- Bakhtar, A., Rahmati, A., Shayeghi, A., Teymoori, J., Ghajarnia, N., Saemian, P., 2022. Spatio-temporal evaluation of GPM-IMERGV6.0 final run precipitation product in capturing extreme precipitation events across Iran. *Water (Basel)* 14, 1650. <https://doi.org/10.3390/w14101650>.
- Beck, H.E., Vergopolan, N., Pan, M., Levizzani, V., Van Dijk, A.I., Weedon, G.P., Brocca, L., Pappenberger, F., Huffman, G.J., Wood, E.F., 2017. Global-scale evaluation of 22 precipitation datasets using gauge observations and hydrological modeling. *Hydrol. Earth Syst. Sci.* 21, 6201–6217. <https://doi.org/10.5194/hess-21-6201-2017>.
- Ben Abdelmalek, M., Nouri, I., 2020. Study of trends and mapping of drought events in Tunisia and their impacts on agricultural production. *Sci. Total Environ.* 734, 139311. <https://doi.org/10.1016/j.scitotenv.2020.139311>.
- Berezowski, T., Szczesniak, M., Kardel, I., Michalowski, R., Okruszko, T., Mezghani, A., Piniewski, M., 2016. CPLFD-GDPT5: high-resolution gridded daily precipitation and temperature data set for two largest Polish river basins. *Earth Syst. Sci. Data* 8, 127–139.
- Brocca, L., Ciabatta, L., Massari, C., Moramarco, T., Hahn, S., Hasenauer, S., Kidd, R., Dorigo, W., Wagner, W., Levizzani, V., 2014. Soil as a natural rain gauge: estimating global rainfall from satellite soil moisture data. *J. Geophys. Res.: Atmos.* 119, 5128–5141. <https://doi.org/10.1002/2014jd021489>.
- Brocca, L., Filippucci, P., Hahn, S., Ciabatta, L., Massari, C., Camici, S., Schüller, I., Bojkov, B., Wagner, W., 2019. SM2RAIN-ASCAT (2007–2018): global daily satellite rainfall data from ASCAT soil moisture observations. *Earth Syst. Sci. Data* 11, 1583–1601. <https://doi.org/10.5194/essd-11-1583-2019>.
- Brocca, L., Moramarco, T., Melone, F., Wagner, W., 2013. A new method for rainfall estimation through soil moisture observations. *Geophys. Res. Lett.* 40, 853–858. <https://doi.org/10.1002/grl.50173>.
- Brocca, S.R.A., 2007. Global daily satellite rainfall data from ASCAT soil moisture observations. *Earth Syst. Sci. Data* 1583.
- Bryant, S., Arnell, N., Law, F., 1992. The long-term context for the current hydrological drought. In: *Proceedings of the IWEM Conference on the Management of Scarce Water Resources*.
- Chen, S.-T., Kuo, C.-C., Yu, P.-S., 2009. Historical trends and variability of meteorological droughts in Taiwan /Tendances historiques et variabilité des sécheresses météorologiques à Taiwan. *Hydrol. Sci. J.* 54, 430–441. <https://doi.org/10.1623/hysj.54.3.430>.
- Chua, Z.-W., Kuleshov, Y., Watkins, A.B., 2020. Drought detection over Papua New Guinea using satellite-derived products. *Remote Sens. (Basel)* 12, 3859. <https://doi.org/10.3390/rs12233859>.
- Crausbay, S.D., Ramirez, A.R., Carter, S.L., Cross, M.S., Hall, K.R., Bathke, D.J., Betancourt, J.L., Colt, S., Cravens, A.E., Dalton, M.S., 2017. Defining ecological drought for the twenty-first century. *Bull. Am. Meteorol. Soc.* 98, 2543–2550. <https://doi.org/10.1175/Bams-D-16-0292.1>.

- Dai, A., Trenberth, K.E., Qian, T., 2004. A global dataset of palmer drought severity index for 1870–2002: relationship with soil moisture and effects of surface warming. *J. Hydrometeorol.* 5, 1117–1130. <https://doi.org/10.1175/Jhm-386.1>.
- Dai, M., Huang, S., Huang, Q., Leng, G., Guo, Y., Wang, L., Fang, W., Li, P., Zheng, X., 2020. Assessing agricultural drought risk and its dynamic evolution characteristics. *Agric. Water Manage.* 231, 106003 <https://doi.org/10.1016/j.agwat.2020.106003>.
- Darand, M., Fathi, H., 2021. Evaluation of high resolution global satellite precipitation mapping during meteorological drought over Iran. *Theor. Appl. Climatol.* 145, 1421–1436. <https://doi.org/10.1007/s00704-021-03708-8>.
- Darand, M., Khandu, K., 2020. Statistical evaluation of gridded precipitation datasets using rain gauge observations over Iran. *J. Arid Environ.* 178, 104172 <https://doi.org/10.1016/j.jaridenv.2020.104172>.
- Degefu, M.A., Bewket, W., Amha, Y., 2022. Evaluating performance of 20 global and quasi-global precipitation products in representing drought events in Ethiopia I: visual and correlation analysis. *Weather Climate Extremes* 35, 100416. <https://doi.org/10.1016/j.wace.2022.100416>.
- Delavar, M., Eini, M.R., Kuchak, V.S., Zaghiyan, M.R., Shahbazi, A., Nourmohammadi, F., Motamedi, A., 2022. Model-based water accounting for integrated assessment of water resources systems at the basin scale. *Sci. Total Environ.* 830, 154810 <https://doi.org/10.1016/j.scitotenv.2022.154810>.
- Dikici, M., 2020. Drought analysis with different indices for the Asi Basin (Turkey). *Sci. Rep.* 10, 20739. <https://doi.org/10.1038/s41598-020-77827-z>.
- Dinku, T., Faniriantsoa, R., Islam, S., Sengiyumva, G., Grossi, A., 2022. The climate data tool: enhancing climate services across Africa. *Front. Climate* 3, 185. <https://doi.org/10.3389/fclim.2021.787519>.
- Duan, Z., Liu, J., Tuo, Y., Chiogna, G., Disse, M., 2016. Evaluation of eight high spatial resolution gridded precipitation products in Adige Basin (Italy) at multiple temporal and spatial scales. *Sci. Total Environ.* 573, 1536–1553. <https://doi.org/10.1016/j.scitotenv.2016.08.213>.
- Eini, M.R., Javadi, S., Delavar, M., Monteiro, J.A., Darand, M., 2019. High accuracy of precipitation reanalyses resulted in good river discharge simulations in a semi-arid basin. *Ecol. Eng.* 131, 107–119. <https://doi.org/10.1016/j.ecoleng.2019.03.005>.
- Eini, M.R., Massari, C., Piniewski, M., 2023a. Satellite-based soil moisture enhances the reliability of agro-hydrological modeling in large transboundary river basins. *Sci. Total Environ.* 873, 162396 <https://doi.org/10.1016/j.scitotenv.2023.162396>.
- Eini, M.R., Najminejad, F., Piniewski, M., 2023b. Direct and indirect simulating and projecting hydrological drought using a supervised machine learning method. *Sci. Total Environ.* 898, 165523 <https://doi.org/10.1016/j.scitotenv.2023.165523>.
- Eini, M.R., Olyaei, M.A., Kamyab, T., Teymoori, J., Brocca, L., Piniewski, M., 2021. Evaluating three non-gauge-corrected satellite precipitation estimates by a regional gauge interpolated dataset over Iran. *J. Hydrol.: Region. Stud.* 38, 100942 <https://doi.org/10.1016/j.ejrh.2021.100942>.
- Eini, M.R., Rahmati, A., Piniewski, M., 2022a. Hydrological application and accuracy evaluation of PERSIANN satellite-based precipitation estimates over a humid continental climate catchment. *J. Hydrol.: Region. Stud.* 41, 101109 <https://doi.org/10.1016/j.ejrh.2022.101109>.
- Eini, M.R., Rahmati, A., Salmani, H., Brocca, L., Piniewski, M., 2022b. Detecting characteristics of extreme precipitation events using regional and satellite-based precipitation gridded datasets over a region in Central Europe. *Sci. Total Environ.* 852, 158497 <https://doi.org/10.1016/j.scitotenv.2022.158497>.
- Eini, M.R., Salmani, H., Piniewski, M., 2023c. Comparison of process-based and statistical approaches for simulation and projections of rainfed crop yields. *Agric. Water Manage.* 277, 108107 <https://doi.org/10.1016/j.agwat.2022.108107>.
- Fan, Y., Ma, Z., Ma, Y., Ma, W., Xie, Z., Ding, L., Han, Y., Hu, W., Su, R., 2021. Respective advantages of “Top-Down” based GPM IMERG and “Bottom-Up” based SM2RAIN-ASCAT precipitation products over the tibetan plateau. *J. Geophys. Res.: Atmos.* 126, e2020JD033946 <https://doi.org/10.1029/2020JD033946>.
- Ghozati, A., Sharafati, A., Hosseini, S.A., 2022. Satellite-based monitoring of meteorological drought over different regions of Iran: application of the CHIRPS precipitation product. *Environ. Sci. Pollut. Res.* 29, 36115–36132. <https://doi.org/10.1007/s11356-022-18773-3>.
- Grossi, A., Dinku, T., 2022. Enhancing national climate services: how systems thinking can accelerate locally led adaptation. *One Earth* 5, 74–83. <https://doi.org/10.1016/j.oneear.2021.12.007>.
- Guo, H., Li, M., Nzabarinda, V., Bao, A., Meng, X., Zhu, L., De Maeyer, P., 2022. Assessment of three long-term satellite-based precipitation estimates against ground observations for drought characterization in Northwestern China. *Remote Sens.* (Basel) 14, 828. <https://doi.org/10.3390/rs14040828>.
- Harisuseno, D., 2020. Meteorological drought and its relationship with southern oscillation index (SOI). *Civil Eng. J.* 6, 1864–1875. <https://doi.org/10.28991/cej-2020-03091588>.
- Hinge, G., Mohamed, M.M., Long, D., Hamouda, M.A., 2021. Meta-analysis in using satellite precipitation products for drought monitoring: lessons learnt and way forward. *Remote Sens.* (Basel) 13, 4353. <https://doi.org/10.3390/rs13214353>.
- Ionita, M., Tallaksen, L.M., Kingston, D.G., Stagge, J.H., Laaha, G., Van Lanen, H.A.J., Scholz, P., Chelcea, S.M., Haslinger, K., 2017. The European 2015 drought from a climatological perspective. *Hydrol. Earth Syst. Sci.* 21, 1397–1419. <https://doi.org/10.5194/hess-21-1397-2017>.
- Javed, T., Li, Y., Rashid, S., Li, F., Hu, Q., Feng, H., Chen, X., Ahmad, S., Liu, F., Pulatov, B., 2021. Performance and relationship of four different agricultural drought indices for drought monitoring in China's mainland using remote sensing data. *Sci. Total Environ.* 759, 143530 <https://doi.org/10.1016/j.scitotenv.2020.143530>.
- Kazemzadeh, M., Noori, Z., Alipour, H., Jamali, S., Akbari, J., Ghorbanian, A., Duan, Z., 2022. Detecting drought events over Iran during 1983–2017 using satellite and ground-based precipitation observations. *Atmos. Res.* 269, 106052 <https://doi.org/10.1016/j.atmosres.2022.106052>.
- Knoben, W.J., Freer, J.E., Woods, R.A., 2019. Inherent benchmark or not? Comparing Nash–Sutcliffe and Kling–Gupta efficiency scores. *Hydrol. Earth Syst. Sci.* 23, 4323–4331. <https://doi.org/10.5194/hess-23-4323-2019>.
- Koohi, S., Azizian, A., Brocca, L., 2021. Spatiotemporal drought monitoring using bottom-up precipitation dataset (SM2RAIN-ASCAT) over different regions of Iran. *Sci. Total Environ.* 779, 146535 <https://doi.org/10.1016/j.scitotenv.2021.146535>.
- Laaha, G., Gauster, T., Tallaksen, L.M., Vidal, J.P., Stahl, K., Prudhomme, C., Heudorfer, B., Vlnas, R., Ionita, M., Van Lanen, H.A.J., Adler, M.J., Caillouet, L., Delus, C., Fendekova, M., Gailliez, S., Hannaford, J., Kingston, D., Van Loon, A.F., Mediero, L., Osuch, M., Romanowicz, R., Sauquet, E., Stagge, J.H., Wong, W.K., 2017. The European 2015 drought from a hydrological perspective. *Hydrol. Earth Syst. Sci.* 21, 3001–3024. <https://doi.org/10.5194/hess-21-3001-2017>.
- Le Coz, C., van de Giesen, N., 2020. Comparison of rainfall products over sub-saharan africa. *J. Hydrometeorol.* 21, 553–596.
- Marcinkowski, P., Kardel, I., Placzowska, E., Gielczewski, M., Osuch, P., Okruszko, T., Venegas-Cordero, N., Ignar, S., Piniewski, M., 2021. High-resolution simulated water balance and streamflow data set for 1951–2020 for the territory of Poland. *Geosci. Data J.*
- McKee, T.B., Doesken, N.J., Kleist, J., 1993. The relationship of drought frequency and duration to time scales. In: *Proceedings of the 8th Conference on Applied Climatology*. Boston, MA, USA, pp. 179–183.
- Mirabbasi, R., Anagnostou, E.N., Fakheri-Fard, A., Dinpashoh, Y., Eslamian, S., 2013. Analysis of meteorological drought in northwest Iran using the joint deficit index. *J. Hydrol. (Amst.)* 492, 35–48. <https://doi.org/10.1016/j.jhydrol.2013.04.019>.
- Moreno, M., Bertolín, C., Ortiz, P., Ortiz, P., 2022. Satellite product to map drought and extreme precipitation trend in Andalusia, Spain: a novel method to assess heritage landscapes at risk. *Int. J. Appl. Earth Obs. Geoinf.* 110, 102810 <https://doi.org/10.1016/j.jag.2022.102810>.
- O’Keeffe, J., Piniewski, M., Szczesniak, M., Ogłęcki, P., Parasiewicz, P., Okruszko, T., 2019. Index-based analysis of climate change impact on streamflow conditions important for Northern Pike. Chub and Atlantic salmon. *Fish. Manag. Ecol.* 26, 474–485.
- Otop, I., Adynkiewicz-Piragas, M., Zdralewicz, I., Lejcuś, I., Miszuk, B., 2023. The drought of 2018–2019 in the Lusatian neisse river catchment in relation to the multiannual conditions. *Water (Basel)* 15, 1647. <https://doi.org/10.3390/w15091647>.
- Patel, N., Chopra, P., Dadhwal, V., 2007. Analyzing spatial patterns of meteorological drought using standardized precipitation index. *Meteorol. Appl.: J. Forecast. Practic. Appl. Train. Techn. Modell.* 14, 329–336. <https://doi.org/10.1002/met.33>.
- Piniewski, M., Eini, M.R., Chattopadhyay, S., Okruszko, T., Kundzewicz, Z.W., 2022. Is there a coherence in observed and projected changes in riverine low flow indices across Central Europe? *Earth Sci. Rev.* 233, 104187 <https://doi.org/10.1016/j.earscirev.2022.104187>.
- Piniewski, M., Szczesniak, M., Kardel, I., Chattopadhyay, S., Berezowski, T., 2021. G2DC-PL-1: a gridded 2km daily climate dataset for the union of the Polish territory and the Vistula and Odra basins. *Earth Syst. Sci. Data* 13, 1273–1288.
- Rahmati Ziveh, A., Bakhtar, A., Shayeighi, A., Kalantari, Z., Bavani, A.M., Ghajarnia, N., 2022. Spatio-temporal performance evaluation of 14 global precipitation estimation products across river basins in southwest Iran. *J. Hydrol.: Region. Stud.* 44, 101269 <https://doi.org/10.1016/j.ejrh.2022.101269>.
- Raziel, T., Saghaflani, B., Paulo, A.A., Pereira, L.S., Bordin, I., 2009. Spatial patterns and temporal variability of drought in western Iran. *Water Resour. Manage.* 23, 439–455. <https://doi.org/10.1007/s11269-008-9282-4>.
- Ritter, A., Munoz-Carpena, R., 2013. Performance evaluation of hydrological models: statistical significance for reducing subjectivity in goodness-of-fit assessments. *J. Hydrol. (Amst.)* 480, 33–45. <https://doi.org/10.1016/j.jhydrol.2012.12.004>.
- Santos, C.A.G., Neto, R.M.B., do Nascimento, T.V.M., da Silva, R.M., Mishra, M., Frade, T. G., 2021. Geospatial drought severity analysis based on PERSIANN-CDR-estimated rainfall data for Odisha state in India (1983–2018). *Sci. Total Environ.* 750, 141258 <https://doi.org/10.1016/j.scitotenv.2020.141258>.
- Santos, J., Portela, M., Pulido-Calvo, I., 2011. Regionalization of droughts in Portugal. *WIT Trans. Ecol. Environ* 146, 239–249.
- Somrowska, U., 2022. Amplified signals of soil moisture and evaporative stresses across Poland in the twenty-first century. *Sci. Total Environ.* 812, 151465 <https://doi.org/10.1016/j.scitotenv.2021.151465>.
- Tadesse, T., Brown, J.F., Hayes, M.J., 2005. A new approach for predicting drought-related vegetation stress: integrating satellite, climate, and biophysical data over the US central plains. *ISPRS J. Photogramm. Remote Sens.* 59, 244–253. <https://doi.org/10.1016/j.isprsjprs.2005.02.003>.
- Tang, L., Tian, Y., Yan, F., Habib, E., 2015. An improved procedure for the validation of satellite-based precipitation estimates. *Atmos. Res.* 163, 61–73. <https://doi.org/10.1016/j.atmosres.2014.12.016>.
- Tian, L., Leason, Z.T., Quiring, S.M., 2020. Developing a hybrid drought index: precipitation evapotranspiration difference condition index. *Climate Risk Manag.* 29, 100238 <https://doi.org/10.1016/j.crm.2020.100238>.
- Tian, Y., Peters-Lidard, C.D., Eylander, J.B., Joyce, R.J., Huffman, G.J., Adler, R.F., Hsu, K.-I., Turk, F.J., Garcia, M., Zeng, J., 2009. Component analysis of errors in satellite-based precipitation estimates. *J. Geophys. Res.: Atmos.* 114 <https://doi.org/10.1029/2009JD011949>.
- Tote, C., Patricio, D., Boogaard, H., Van der Wijngaart, R., Tarnavsky, E., Funk, C., 2015. Evaluation of satellite rainfall estimates for drought and flood monitoring in Mozambique. *Remote Sens. (Basel)* 7, 1758–1776.
- van Lanen, H.A.J., Laaha, G., Kingston, D.G., Gauster, T., Ionita, M., Vidal, J.-P., Vlnas, R., Tallaksen, L.M., Stahl, K., Hannaford, J., Delus, C., Fendekova, M.,

- Mediero, L., Prudhomme, C., Rets, E., Romanowicz, R.J., Gailliez, S., Wong, W.K., Adler, M.J., Blauhut, V., Caillouet, L., Chelcea, S., Frolova, N., Gudmundsson, L., Hanel, M., Haslinger, K., Kireeva, M., Osuch, M., Sauquet, E., Stagge, J.H., van Loon, A.F., 2016. Hydrology needed to manage droughts: the 2015 European case. *L'hydrologie est nécessaire pour gérer les sécheresses: l'événement de 2015 en Europe*. *Hydrol. Process.* 30, 3097–3104. <https://doi.org/10.1002/hyp.10838>.
- Van Rooy, M., 1965. A rainfall anomaly index independent of time and space. *Notos*.
- Vicente-Serrano, S.M., Beguería, S., López-Moreno, J.I., Angulo, M., El Kenawy, A., 2010. A new global 0.5 gridded dataset (1901–2006) of a multiscalar drought index: comparison with current drought index datasets based on the palmer drought severity index. *J. Hydrometeorol.* 11, 1033–1043. <https://doi.org/10.1175/2010jhm1224.1>.
- Vicente-Serrano, S.M., Quiring, S.M., Pena-Gallardo, M., Yuan, S., Dominguez-Castro, F., 2020. A review of environmental droughts: increased risk under global warming? *Earth Sci. Rev.* 201, 102953.
- Wei, L., Jiang, S., Ren, L., Wang, M., Zhang, L., Liu, Y., Yuan, F., Yang, X., 2021. Evaluation of seventeen satellite-, reanalysis-, and gauge-based precipitation products for drought monitoring across mainland China. *Atmos. Res.* 263, 105813. <https://doi.org/10.1016/j.atmosres.2021.105813>.
- Wilhite, D.A., 2000. Drought as a natural hazard: concepts and definitions.
- WMO, G., 2016. Handbook of drought indicators and indices (M. Svoboda and BA Fuchs). *Integrat. Drought Manag. Programme (IDMP), Integrat. Drought Manag. Tools Guidelines Ser.* 2.
- Won, J., Choi, J., Lee, O., Kim, S., 2020. Copula-based joint drought Index using SPI and EDDI and its application to climate change. *Sci. Total Environ.* 744, 140701. <https://doi.org/10.1016/j.scitotenv.2020.140701>.
- Xu, K., Yang, D., Yang, H., Li, Z., Qin, Y., Shen, Y., 2015. Spatio-temporal variation of drought in China during 1961–2012: a climatic perspective. *J. Hydrol. (Amst.)* 526, 253–264. <https://doi.org/10.1016/j.jhydrol.2014.09.047>.
- Zhang, L., Li, X., Cao, Y., Nan, Z., Wang, W., Ge, Y., Wang, P., Yu, W., 2020. Evaluation and integration of the top-down and bottom-up satellite precipitation products over mainland China. *J. Hydrol.* 581, 124456. <https://doi.org/10.1016/j.jhydrol.2019.124456>.
- Zhong, R., Chen, X., Lai, C., Wang, Z., Lian, Y., Yu, H., Wu, X., 2019. Drought monitoring utility of satellite-based precipitation products across mainland China. *J. Hydrol.* 568, 343–359. <https://doi.org/10.1016/j.jhydrol.2018.10.072>.

Warsaw, 26/03/2024

Mohammadreza Einikarimkandi
d003066@sggw.edu.pl

**Institute of Environmental Engineering,
Mining, and Energy, Discipline
Council**

**of the Warsaw University of Life
Sciences**

Co-authorship statement

I hereby represent that in the below publication “Eini, M. R., Ziveh, A. R., Salmani, H., Mujahid, S., Ghezelayagh, P., & Piniewski, M. (2023). Detecting drought events over a region in Central Europe using a regional and two satellite-based precipitation datasets. *Agricultural and Forest Meteorology*, 342, 109733. <https://doi.org/10.1016/j.agrformet.2023.109733>” my individual contribution in the development thereof involved, Conceptualization, methodology, software, validation, writing – original draft, writing – review & editing, visualization.


Signature
Mohammad Reza
Eini Karimkandi

Prague, 26/03/2024

Akbar Rahmati Ziveh
rahmati_ziveh@fzp.czu.cz

**Institute of Environmental Engineering,
Mining, and Energy, Discipline
Council
of the Warsaw University of Life
Sciences**

Co-authorship statement

I hereby represent that in the publication Eini, M. R., Ziveh, A. R., Salmani, H., Mujahid, S., Ghezelayagh, P., & Piniewski, M. (2023). Detecting drought events over a region in Central Europe using a regional and two satellite-based precipitation datasets. *Agricultural and Forest Meteorology*, 342, 109733. <https://doi.org/10.1016/j.agrformet.2023.109733> my individual contribution in the development thereof involved data assessments, reading and editing the manuscript and literature review.

A handwritten signature in dark ink, appearing to be 'A. Rahmati Ziveh', enclosed within a thin black rectangular border.

Signature

Madrid, 26/03/2024

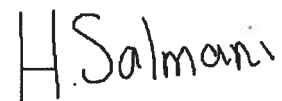
Haniyeh Salmani
haniyeh.salmani@usal.es

**Institute of Environmental Engineering,
Mining, and Energy, Discipline
Council
of the Warsaw University of Life
Sciences**

Co-authorship statement

I hereby represent that in the publication Eini, M. R., Ziveh, A. R., Salmani, H., Mujahid, S., Ghezelayagh, P., & Piniewski, M. (2023). Detecting drought events over a region in Central Europe using a regional and two satellite-based precipitation datasets. *Agricultural and Forest Meteorology*, 342, 109733. <https://doi.org/10.1016/j.agrformet.2023.109733>

my individual contribution in the development thereof involved software, reading and editing the manuscript and literature review.

A handwritten signature in black ink that reads "H. Salmani". The signature is written in a cursive, slightly slanted style.

Signature

Brescia, 26/03/2024

Seemab Mujahid

s.mujahid@studenti.unibs.it

**Institute of Environmental Engineering,
Mining, and Energy, Discipline
Council**

**of the Warsaw University of Life
Sciences**

Co-authorship statement

I hereby represent that in the below publications

Eini, M. R., Ziveh, A. R., Salmani, H., Mujahid, S., Ghezelayagh, P., & Piniewski, M. (2023).
Detecting drought events over a region in Central Europe using a regional and two satellite-
based precipitation datasets. *Agricultural and Forest Meteorology*, 342, 109733.
<https://doi.org/10.1016/j.agrformet.2023.109733>

my individual contribution in the development thereof involved literature review and reading and
editing the manuscript.



Signature

Warsaw, 26/03/2024

Pouya Ghezel Ayagh

pouya_ghezelayagh@sggw.edu.pl


**Institute of Environmental Engineering,
Mining, and Energy, Discipline
Council
of the Warsaw University of Life
Sciences**

Co-authorship statement

I hereby represent that in the below publications

Eini, M. R., Ziveh, A. R., Salmani, H., Mujahid, S., Ghezelayagh, P., & Piniewski, M. (2023). Detecting drought events over a region in Central Europe using a regional and two satellite-based precipitation datasets. *Agricultural and Forest Meteorology*, 342, 109733. <https://doi.org/10.1016/j.agrformet.2023.109733>

my individual contribution in the development thereof involved literature review and reading and editing the manuscript.

Signature

26.03.2024

Warsaw, 26/03/2024

Dr hab. Mikołaj Piniewski, prof. SGGW
Department of Hydrology, Meteorology and Water Management
Institute of Environmental Engineering
Warsaw University of Life Sciences
mikolaj_piniewski@sggw.edu.pl

**Institute of Environmental Engineering,
Mining, and Energy, Discipline
Council
of the Warsaw University of Life
Sciences**

Co-authorship statement

I hereby represent that in the below publication “Eini, M. R., Ziveh, A. R., Salmani, H., Mujahid, S., Ghezelayagh, P., & Piniewski, M. (2023). Detecting drought events over a region in Central Europe using a regional and two satellite-based precipitation datasets. *Agricultural and Forest Meteorology*, 342, 109733. <https://doi.org/10.1016/j.agrformet.2023.109733>” my individual contribution in the development thereof involved, conceptualization, methodology, writing – review & editing.



Signature

10. Publication 2

Eini, M. R., Rahmati, A., & Piniewski, M. (2022). Hydrological application and accuracy evaluation of PERSIANN satellite-based precipitation estimates over a humid continental climate catchment. *Journal of Hydrology: Regional Studies*, 41, 101109. <https://doi.org/10.1016/j.ejrh.2022.101109>

Impact factor: 4.7 – MeiN: 100



Hydrological application and accuracy evaluation of PERSIANN satellite-based precipitation estimates over a humid continental climate catchment

Mohammad Reza Eini^a, Akbar Rahmati^b, Mikołaj Piniewski^{a,*}

^a Department of Hydrology, Meteorology, and Water Management, Institute of Environmental Engineering, Warsaw University of Life Sciences, Warsaw, Poland

^b Department of Irrigation and Drainage Engineering, College of Abureyhan, University of Tehran, Iran

ARTICLE INFO

Keywords:

Satellite-derived rainfall
Real-time
Central Europe
High resolution
Gridded dataset

ABSTRACT

Study region: The Wełna catchment (52°30'–53°N and 16°35'–17°50'E) is a medium-sized, low-land catchment in the central part of Poland in Central Europe with a total catchment area of 2621 km².

Study focus: Research evaluating the performing of satellite-based precipitation datasets in Poland and Central Europe is scarce. This study assesses the accuracy and implements five satellite-based precipitation estimates in hydrological simulations. PERSIANN (a satellite-based precipitation dataset) family datasets (consisting of PERSIANN, PERSIANN-CDR, PERSIANN-CCS, PDIR-NOW, PERSIANN-CCS-CDR) was evaluated in daily steps and seasonal steps against a regional gridded dataset (G2DC-PL+) in the period 2003–2019. Soil and Water Assessment Tool+ (SWAT+), a relatively new eco-hydrological model, was employed to simulate runoff in daily time steps.

New hydrological insights for the region: Our results revealed that PERSIANN family products could accurately detect precipitation events according to POD, FAR, and CSI indicators. PERSIANN-CDR has a better correlation in the northern and central parts, and shows low accuracy in the southeastern catchment with a higher altitude. A similar pattern is observed in PDIR-NOW and PERSIANN-CCS for R². Moreover, the SWAT+ results demonstrate that G2DC-PL+ could be a reliable source alternative to gauge data in runoff simulations. PERSIANN-CDR performed slightly better in runoff simulations compared to other gridded datasets.

1. Introduction

Recent developments in global gridded datasets have facilitated worldwide simulations in hydrology, environment, crop yield, climate change, and Earth system processes in general. For example, several gridded climatic parameters, namely soil moisture, land use, cropping systems, living species, or even sea level fluctuation datasets have been developed and used over the recent decades. Moreover, several products and outputs of models at a global or regional scale have been released, and are publicly accessible (Althoff et al., 2020; Eini et al., 2021; Gregor and Gruber, 2021; Gueymard et al., 2021; Iizumi and Sakai, 2020; Lloyd et al., 2017; Ndhlovu and Woyessa, 2021; Reichler et al., 2003).

* Corresponding author.

E-mail address: mikolaj.piniewski@sggw.edu.pl (M. Piniewski).

<https://doi.org/10.1016/j.ejrh.2022.101109>

Received 22 February 2022; Received in revised form 27 April 2022; Accepted 11 May 2022

Available online 18 May 2022

2214-5818/© 2022 The Author(s). Published by Elsevier B.V. This is an open access article under the CC BY-NC-ND license (<http://creativecommons.org/licenses/by-nc-nd/4.0/>).

These datasets cover most of the land surface and atmosphere parameters, and each parameter has its own accuracy and characteristics. Precipitation is the most essential and primary input in several hydrological or ecohydrological models (Tan et al., 2021; Tan and Yang, 2020). The parameter plays the main role in the hydrological process. Its accuracy in gauge recorded or gridded datasets has a significant effect on model outputs. A minimum of 30 years of daily precipitation dataset is suggested to sufficiently capture long-term climate conditions such as drought and its effect on parameters within hydrological models (Qin et al., 2014; Tan et al., 2021). Moreover, in hydrological evaluation, a reliable rainfall database leads to a more precise simulation of runoff,

Table 1

Review of studies employing the SWAT model and global precipitation datasets with a focus on the PERSIANN family of satellite precipitation.

Study	Region	Datasets	Time period	Result
Bitew and Gebremichael (2011)	Ethiopian highlands	CMORPH, TMPA 3B42RT, TMPA 3B42, PERSIANN	2003–2007	PERSIANN has poor or no skills for runoff simulations.
Bitew et al. (2012)	A Mountainous Watershed in Ethiopia	CMORPH, TRMM, TMPA 3B42RT, TMPA 3B42, PERSIANN	2003–2008	The 3B42RT and CMORPH products perform better than the 3B42 and PERSIANN.
Vu et al. (2012)	Vietnam river basin	APHRODITE, TRMM, PERSIANN, GPCP, GHCN2, NCEP/NCAR	1996–2006	APHRODITE dataset performed very well on a daily scale simulation and PERSIANN did not show good performance.
Zhu et al. (2016)	A Humid regions in China	PERSIANN-CDR, TRMM 3B42V7, NCEP-CFSR	2004–2013	PERSIANN-CDR and 3B42V7 show encouraging potential for runoff simulation over the two humid regions.
Tan et al. (2017)	Malaysia	APHRODITE, PERSIANN-CDR, NCEP-CFSR	1983–2007	The results present that the APHRODITE performed better in precipitation estimation, followed by the PERSIANN-CDR and NCEP-CFSR.
Thom et al. (2017)	Vietnam	APHRODITE, CFSR, PERSIANN, TRMM	2000–2006	TRMM and APHRODITE show better match to rain gauges data in simulating the daily and monthly runoff.
Eini et al. (2018)	A semi dry basin, Iran	PERSIANN-CDR	1983–2013	PERSIANN-CDR has low accuracy in estimating precipitation and runoff simulation.
Gao et al. (2018)	Xiang River Basin, China	CMADS, NCEP-CFSR, TRMM, PERSIANN-CDR	2009–2014	CMADS and TMPA are better than PERSIANN-CDR and NCEP-CFSR in correlation with observed data and runoff simulation.
Ren et al. (2018)	Luanhe River Basin, China	TRMM 3B42RT, TRMM 3B42, PERSIANN	2001–2012	The TRMM 3B42 present a better hydrological performance, while PERSIANN shows unsatisfactory hydrological performance.
Vu et al. (2018)	Han River Basin in the Korean Peninsula	TRMM, PERSIANN, PERSIANN-CDR, CMADS	2008–2013	TRMM and CMADS can be used to simulate the streamflow of the Han River Basin with acceptable accuracy.
Ajaaj et al. (2019)	Tigris River Basin in Iraq	PERSIANN-CDR, MSWEP, APHRODITE, CPC	1983–1997 ^a	APHRODITE has better performance in monthly runoff simulations.
Ma et al. (2019)	Southwest China	TMPA 3B42V7, PERSIANN-CDR, NCEP-CFSR	2004–2008	TMPA 3B42V7 and PERSIANN-CDR present good capability for streamflow and sediment simulations on a monthly time step.
Musie et al. (2019)	Ethiopia	CFSR, CHIRPS, PERSIANN-CDR, TRMM	1985–2004	CHIRPS, PERSIANN-CDR, and TRMM performed well for monthly runoff simulations.
Tang et al. (2019)	Mekong River Basin, East Asia	AgMERRA, MSWEP, PERSANN-CDR, TMPA	2000–2007	MSWEP is better than other three products in term of both the model performance and parameter uncertainties.
Alnahit et al. (2020)	South Carolina, USA	TRMM 3B42, TRMM 3B42RT, PERSIANN-CDR, PERSIANN, GPCP, CFSR	2001–2014	TRMM 3B42 and PERSIANN-CDR had better performance whereas CFSR and PERSIANN relatively performed poorly for runoff and water quality simulations.
Jiang et al. (2020)	Upper Huaihe River Basin, China	CMADS, TRMM, CMORPH, CHRISP, PERSIANN-CDR	2008–2016	CMADS and CMORPH perform the best, followed by TMPA 3B42V7, CHIRPS, and PERSIANN-CDR.
Le et al. (2020)	Vietnam	TMPA ^b , GPM ^b , CHIRP ^b , PERSIANN, PERSIANN-CDR	2002–2017	GPM exhibited the best overall performances among other datasets in comparison with the rain gauges for the simulation of runoff.
Zhang et al. (2020)	Northeastern China	TMPA 3B42V7, PERSIANN-CDR	2002–2015	TMPA 3B42V7 and PERSIANN-CDR have satisfactory result in runoff simulation.
Jimeno-Saez et al. (2021)	El Salvador	CFSR, MSWEP, PERSIANN-CDR, CMORPH, CHIRPS	2005–2010	PERSIANN-CDR produced the best simulation results, including runoff simulation.
Li et al. (2021)	Tuojiang River Basin, China	CFSR, TRMM, PERSIANN-CDR	1980–2000	TRMM have the best performance among the other gridded datasets.
Talchabhadel et al. (2021)	Western Nepal	CHIRPS, PERSIANN-CDR, IMERG	1986–2015	IMERG proved to be superior among three datasets.
Wang et al. (2021)	A humid region of southern China	CHIRPS, TMPA, CMORPH, PERSIANN	2000–2014	TMPA provides the most accurate hydrological model simulation results.

^a Varies for different datasets.

^b Different products.

flood/drought, and management decisions (Auerbach et al., 2016; Tan et al., 2021). The analysis of the characteristics of global precipitation datasets is therefore a crucial stage in applying them in evaluations of water resources at a global or regional scale (Satge et al., 2020).

The precision of precipitation gridded data depends on the source of raw data, development method, and region (Eini et al., 2021; Sun et al., 2018; Tan et al., 2021). These datasets are generally categorised into gauge-corrected (relatively more accurate) or non-gauge-corrected (relatively less accurate). Another classification designates satellite-derived, gauge-interpolated, ground-based weather radar, and reanalysis products. Sun et al. (2018) provide a detailed review of 30 precipitation gridded datasets.

In recent years, satellite-derived gridded datasets presenting wider and higher spatial distribution and resolutions (up to global scale and 16 km² cell sizes) (Sadeghi et al., 2021) as well as higher temporal resolution (sub-hour to yearly time steps) (Wang et al., 2021) have been considered a reliable alternative to point-based network for areas with no suitable point-based network coverage in hydrological simulations (Beck et al., 2017; Pradhan and Indu, 2021; Tan et al., 2021; Wang et al., 2021).

Among different satellite-derived precipitation gridded datasets, PERSIANN family datasets are some of the most commonly used satellite-based gridded datasets in hydrological simulations (Ajaaj et al., 2019; Al-Falahi et al., 2020; Alnahit et al., 2020; Bitew and Gebremichael, 2011; Bitew et al., 2012; Eini et al., 2018; Gao et al., 2018; Jiang et al., 2020; Jimeno-Saez et al., 2021; Le et al., 2020; Li et al., 2021; Ma et al., 2019; Musie et al., 2019; Qin et al., 2014; Ren et al., 2018; Shawul and Chakma, 2020; Talchabhadel et al., 2021; Tan et al., 2017; Tang et al., 2019; Thom et al., 2017; Vu et al., 2012, 2018; Wang et al., 2021; Xuan et al., 2018; Zhang et al., 2020; Zhu et al., 2016). This family of precipitation datasets covers five different datasets, namely PERSIANN, PERSIANN-CDR (Climate Data Record), PERSIANN-CCS (Cloud Classification System), PDIR-NOW (Dynamic Infrared (IR) Rain Rate near real-time), and PERSIANN-CCS-CDR (Cloud Classification System-Climate Data Record) (Nguyen et al., 2020, 2019; Sadeghi et al., 2021).

The Soil and Water Assessment Tool (SWAT) model has been comprehensively employed worldwide to evaluate agro-hydrological processes (Delavar et al., 2022; Eini et al., 2020; Piniewski et al., 2017; Tan et al., 2020). In the SWAT model, point-based weather gauge observations are frequently used to drive the model. In data-scarce regions, transboundary basins, and large scale or worldwide studies, however, gridded datasets have still been employed to cover the lack of observed datasets, or instead of them (Eini et al., 2019; Hajihosseini et al., 2016; Tan et al., 2021). Table 1 presents a review of studies combining the SWAT model and gridded datasets by focusing on PERSIANN family products.

According to studies mentioned in Table 1, the accuracy of the PERSIANN products in runoff simulations is still unknown in most regions, and particularly in Europe. PDIR-NOW and PERSIANN-CCS-CDR are relatively new products that require assessment in hydrological simulations in different regions.

Research evaluating the performing of satellite-based precipitation datasets in Poland and Central Europe is scarce. This study addresses the gap. It has two main objectives, namely (a) comprehensive assessment of the accuracy of precipitation acquired from the PERSIANN family of satellite products, and (b) evaluation of the performance of these products in runoff simulations over a watershed in Poland using the SWAT+ model (Bieger et al., 2017).

Throughout the study, we benchmarked the PERSIANN family of satellite products with reference to a gauge-based precipitation dataset, namely G2DC-PL+ (Piniewski et al., 2021) in the context of hydrology and meteorology.

2. Methodology

2.1. Case study

The Weina catchment (52°30'–53°N and 16°35'–17°50'E) is a medium-sized and flat catchment in the central part of Poland. It was selected as the study area (Fig. 1). The Weina River and its tributaries are part of the natural Polish river network of the Wielkopolska Lowland. The long -term average (1990–2019) precipitation and temperature for the area reach 561 mm and 9 °C, respectively. The stream network with its huge valleys and narrow lakes was formed in the late Pleistocene and Holocene as a result of the retreat and melting of glaciers (Knoben, 2013; Siniecki, 2009; Wira, 2011). The total catchment size of the Weina River upstream from the flow measuring station is 2611 km². Weina flows into the Warta river, the largest tributary of the Odra river flowing into the Baltic Sea. The catchment is covered by forest and rainfed agricultural areas, with several scattered urban areas. Three discharge stations measure discharge in the catchment. The annual average flow is approximately 10 m³/s (Knoben, 2013; Siniecki, 2009; Wira, 2011).

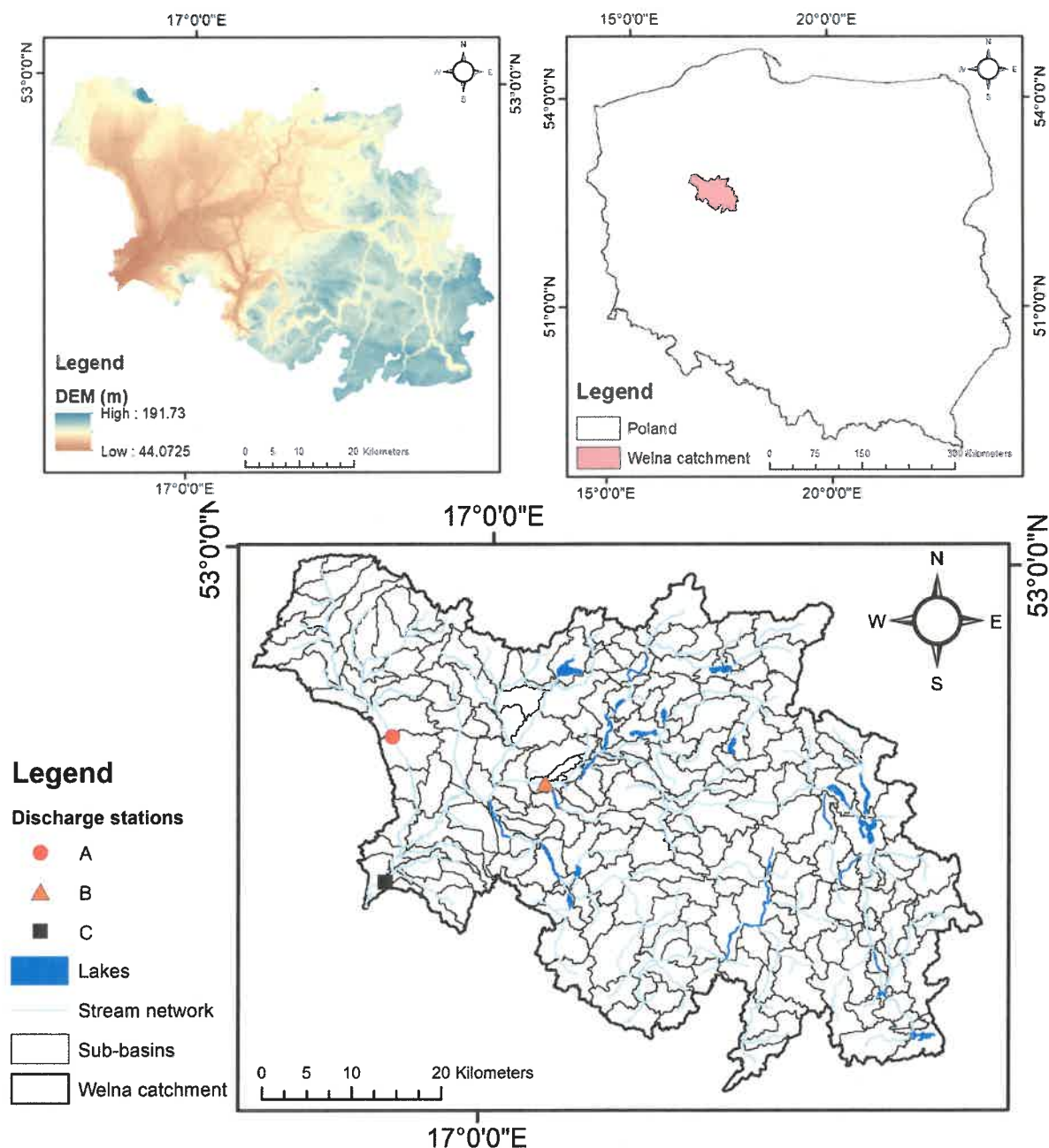


Fig. 1. Location of the Weina River catchment in Poland, lakes, stream network, subbasins, and DEM.

2.2. Precipitation datasets

2.2.1. PERSIANN products

PERSIANN satellite-based products are developed by the University of California, Irvine (UCI) (Sorooshian et al., 2000). An online website (<https://chrsdata.eng.uci.edu/>) is provided by developers to download all these datasets for different regions and basins, or globally (Nguyen et al., 2019). This family of precipitation datasets covers five different products: PERSIANN, PERSIANN-CDR, PERSIANN-CCS, PDIR-NOW, and PERSIANN-CCS-CDR, selected for the period 2003–2019 in this study (Table 2). The location of cell centers is presented in Fig. 2. In addition, the PERSIANN system is based on both Geostationary Earth Orbiting (GEO) satellites and Low Earth Orbiting (LEO) satellites (Nguyen et al., 2018).

Table 2
Characteristics of precipitation datasets used in the study.

Product	Time span	Spatial coverage	Temporal resolution	Spatial resolution	Link
G2DC-PL+	1951–2019	Polish territory and the Vistula and Odra basins	daily	2 km × 2 km	https://doi.org/10.4121/uuid:a3bed3b8-e22a-4b68-8d75-7b87109c9feb
PERSIANN	2000–Now	60°S to 60°N	hourly to yearly	0.25° × 0.25°	https://chrsdata.eng.uci.edu/
PERSIANN-CDR	1983–Now	60°S to 60°N	daily to yearly	0.25° × 0.25°	
PERSIANN-CCS	2003–Now	60°S to 60°N	hourly to yearly	0.04° × 0.04°	
PDIR-NOW	2000–Now	60°S to 60°N	hourly to yearly	0.04° × 0.04°	
PERSIANN-CCS-CDR	1983–Now	60°S to 60°N	3-hourly to yearly	0.04° × 0.04°	

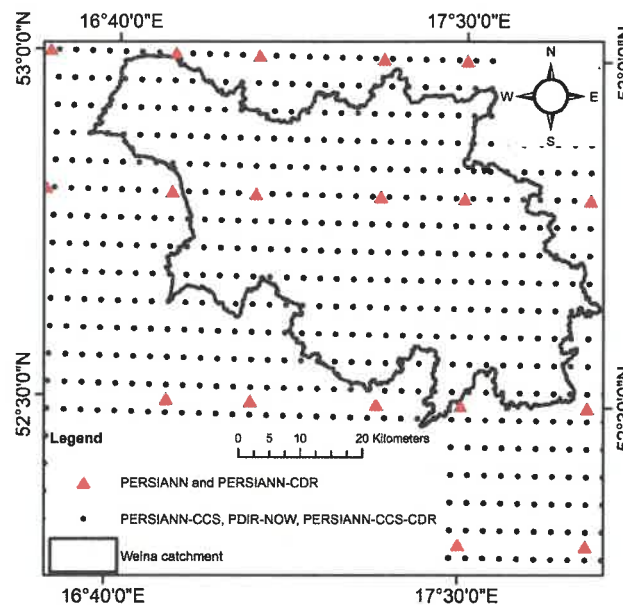


Fig. 2. Location of cell centers of each product over the study area.

2.2.1.1. PERSIANN. The current operational PERSIANN employs machine learning methods to determine an estimation of the precipitation ratio at each $0.25^\circ \times 0.25^\circ$ pixel of the IR brightness temperature image. The PERSIANN method was built on geostationary IR imagery, and later expanded to involve both IR and DVI (Hsu et al., 1997).

2.2.1.2. PERSIANN-CCS. PERSIANN-Cloud Classification System (PERSIANN-CCS) is a real-time high resolution ($0.04^\circ \times 0.04^\circ$) satellite-based precipitation dataset that enables the classification of cloud-patch features based on cloud height, areal extent, and variability of texture calculated from satellite imagery (Hong et al., 2004).

2.2.1.3. PERSIANN-CDR. PERSIANN-CDR provides daily precipitation values at 0.25° over 60N–60S. PERSIANN-CDR is designed to meet the need for a reliable, long-term, high-resolution, and global precipitation dataset for analysing variations and trends in daily precipitation, and particularly extreme precipitation events. PERSIANN-CDR is developed based on the PERSIANN method utilizing GridSat-B1 data, and adjusted by the GPCP product to provide the reliability of the two datasets at 2.5° (Ashouri et al., 2015).

2.2.1.4. PDIR-NOW. PDIR-NOW is a real-time global high resolution ($0.04^\circ \times 0.04^\circ$) satellite-based product relying on high frequency sampled IR imagery. The latency of PDIR-NOW from the time of precipitation event is very short. PDIR-NOW also accounts for the uncertainties and errors that arise from IR imagery by implementing a range of techniques most significant is the dynamic shifting of (Tb-R) curves using precipitation climatology. The short latency of PDIR-NOW renders the dataset well-fit for near-real-time hydrological applications such as flood predictions and developing flood maps (Nguyen et al., 2020).

2.2.1.5. PERSIANN-CCS-CDR. PERSIANN-CCS-CDR resolutions are $0.04^\circ \times 0.04^\circ$ and 3-hourly (1983–now) over the domain of 60°S to 60°N. PERSIANN-CCS-CDR is developed to provide rainfall with a finer resolution and a more extended period of data. PERSIANN-CCS-CDR combines the algorithms utilised in the development of PERSIANN-CCS and PERSIANN-CDR, and employs data from GEO satellites as input data. In this method, the PERSIANN-CCS method is employed to Gridded satellite (GridSat-B1) and CPC-4 km

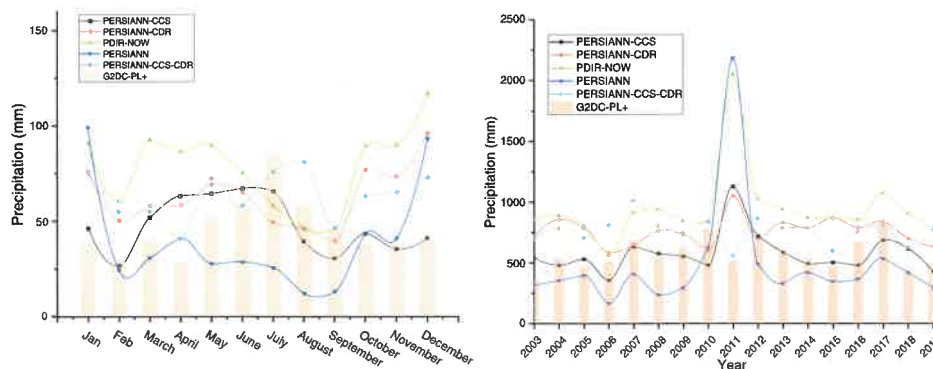


Fig. 3. Monthly and annual variability of precipitation in the study area.

merged IR datasets. The evaluations are then bias-corrected by applying the GPCP product to the entire period of the dataset (Sadeghi et al., 2021).

2.2.2. Reference dataset

This study employs a gridded daily climate dataset (G2DC-PL+). It is publicly available for the period 1951–2019 used as the reference dataset. The dataset stores daily data for precipitation, T_{min} , T_{max} , humidity, and wind speed. Geostatistical techniques (kriging) were applied to interpolate the studied climate variables in this dataset. The dataset was developed by Piniewski et al. (2021). Comprehensive details regarding the methods and accuracy are available in Berezowski et al. (2016) and Piniewski et al. (2021). A brief description of the dataset and the PERSIANN family is included in Table 2. Fig. 3 presents monthly and annual changes in precipitation in all the datasets. As shown in Fig. 3, PDIR-Now, PERSIANN-CDR, PERSIANN-CCS, and PERSIANN were not able to capture the precipitation behavior in 2011, and there is a systematic error in 2011 over this region in these products.

Each cell center from each satellite product and reference dataset was extracted based on each subbasin's centroid for the evaluation process. This method permits a robust comparison for hydrological simulation and precipitation evaluation, because each subbasin has precipitation precisely at the same points.

2.3. SWAT+ model

This study employed a new version of SWAT dubbed as SWAT+ (rev. 60.5.3) on a QGIS interface (QSWAT+ 2.0.6) and SWAT+ Editor (version 2.0.4) (Arnold et al., 2018; Chawanda et al., 2020). SWAT+ is an improved and widely revised version of the SWAT model. SWAT+ is an open-source, continuous-time, process-based, semi-distributed model developed by the USDA (Agricultural Research Service) for modeling hydrological cycle. It is efficient of continuous modeling over long and short periods (Bieger et al., 2017).

SWAT+ is relatively new and has several advantages, such as flexibility in defining the connection between different objects (lakes, aquifers, rivers, and other physical objects) in a basin decision table to simulate management. It is based on free software, and is more user-friendly (Senent-Aparicio et al., 2021; Sterl et al., 2021). A full description of SWAT and SWAT+ background, tools, and literature database is available at <https://swat.tamu.edu/>.

The Weina catchment was divided into 255 subbasins, 450 landscape units, and 1504 hydrologic response units (HRUs), including 25 natural lakes. Based on the consideration of three years of a warm-up period (2001–2003), three discharge stations were calibrated (2004–2011) and validated (2012–2019) at daily time steps. The Penman-Monteith method was selected as the potential evapotranspiration method. The source of discharge as well as radiation data was the Institute of Meteorology and Water Management, Warsaw, Poland). The map of the subbasins, stream network, and discharge stations is presented in Fig. 1.

The calibration process first involved the calibration and validation of the SWAT+ model with the G2DC-PL+ dataset. Then, based on similar parameters, SWAT+ was calibrated and validated using PERSIANN family products.

2.4. Performance evaluation indices and tools

The assessment of the accuracy of PERSIANN products and runoff simulation performance involved the application of the following statistics at daily time steps: R^2 (coefficient of determination), NSE (Nash-Sutcliffe Efficiency), KGE (Kling-Gupta Efficiency), RMSE (Root Mean Square Error, mm), and PBIAS (Percent bias indicator, %). Moreover, three categorical indices were employed (by considering a 2-mm threshold), namely Probability Of Detection (POD), False Alarm Ratio (FAR), and Critical Success Index (CSI). These performance indicators have been previously used for the evaluation of global datasets or models versus observed datasets in several studies such as Darand and Khandu (2020), and Eini et al. (2021). The calculation of these indices was based on “hydroGOF”, and “CDT” (<https://github.com/rjaf-iri/CDT>) in R. The details and equations of these statistics can be found at <https://cran.r-project.org/web/packages/hydroGOF/hydroGOF.pdf>.

3. Results and discussion

We first evaluated the accuracy of each dataset against G2DC-PL+ in overall and seasonal time frames, followed by the evaluation of hydrological modeling. Finally, the accuracy of PERSIANN products was investigated in runoff simulation.

3.1. Evaluation of PERSIANN products

The evaluation of the accuracy of PERSIANN products employed daily datasets over the Weina catchment. Our evaluation considered the weighted average method, where the distance from the given centroids gives the weight.

3.1.1. Overall evaluation of precipitation estimates

We extracted precipitation values for the centroids of each subbasin. According to Table 3, PERSIANN-CDR ($R^2 = 0.23$) and PDIR-NOW ($R^2 = 0.22$) show better correlations in comparison to other products. Lower PBIAS (%) is observed in PERSIANN-CCS (2.38%), followed by PERSIANN (−12.14%). RMSE (mm) shows that these products feature rather low similarities, and RMSE varies between 3.67 mm (PERSIANN-CCS) and 5.73 mm (PERSIANN). The NSE index, sensitive to outliers, shows negative values for all products, and the best value is −0.24 (PERSIANN-CCS).

According to Fig. 4, PERSIANN-CDR shows a better correlation in the northern and central part, and has low accuracy in the southeastern catchment with a higher altitude. A similar pattern is observed in the case of PDIR-NOW and PERSIANN-CCS for R^2 .

PERSIANN-CCS underestimated precipitation in the southeastern and central parts (−6.7% to −1.5%), and overestimated (14.8–5%) it northwest of the Weina catchment according to the PBIAS indicator. PERSIANN-CDR (28–42%), PDIR-NOW (59–81%), and PERSIANN-CCS-CDR (29–43%) overestimated precipitation values (Fig. 4).

RMSE (mm) indicator shows a lower error for PERSIANN-CCS in the northern and southwestern part of the catchment. PDIR-NOW shows no uniform or discernible pattern over the catchment. The difference between the maximum and the minimum RMSE for all

Table 3

Results of the comparison of PERSIANN family products against G2DC-PL+.

Name	PERSIANN	PERSIANN-CCS	PERSIANN-CDR	PDIR-NOW	PERSIANN-CCS-CDR
R^2	0.11	0.12	0.23	0.22	0.06
PBIAS (%)	−12.14	2.38	35.55	69.80	35.91
RMSE (mm)	5.73	3.67	3.76	4.45	4.77
NSE	−2.04	−0.24	−0.31	−0.83	−1.10
POD	0.56	0.69	0.81	0.93	0.61
FAR	0.24	0.26	0.29	0.34	0.34
CSI	0.48	0.55	0.61	0.63	0.47

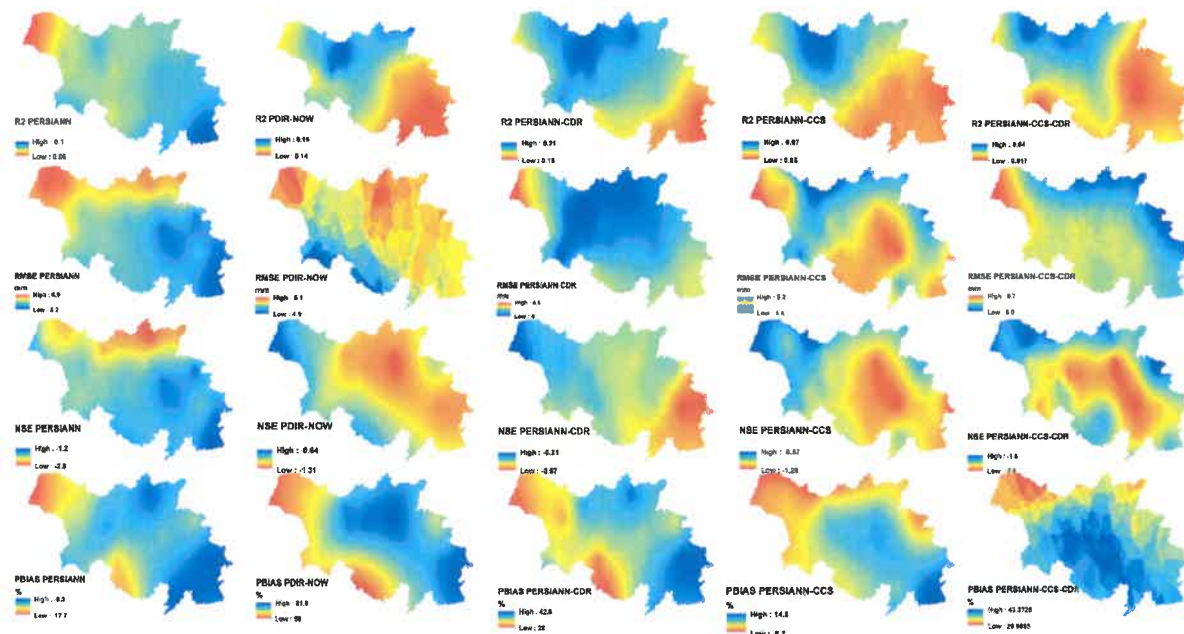


Fig. 4. Spatial pattern of R^2 , RMSE (mm), NSE, and PBIAS(%) for PERSIANN family datasets over the study area.

products is generally less than 2 mm, with no strong pattern. The error variations over the catchment are also low for the NSE indicator, with no distinguishable patterns (Fig. 4).

The POD and FAR statistics describe the core of the inaccuracies by gridded data. The detection skills are provided in Fig. 5 and Table 3. POD demonstrates superior performance of PDIR-NOW in detecting precipitation in the western parts (0.8–0.82), with a spatial average of 0.93, followed by PERSIANN-CDR (0.81). The POD range for other products is between 0.56 and 0.69. It could be considered an acceptable range for all products. According to FAR, PERSIANN has better accuracy (0.24), although all products provide good results (0.26–0.34), with no discernible patterns over the catchment area. CSI performance illustrates average accuracy for these products in events detection by the PERSIANN family (0.47–0.63). PDIR-NOW shows the highest performance compared to other datasets.

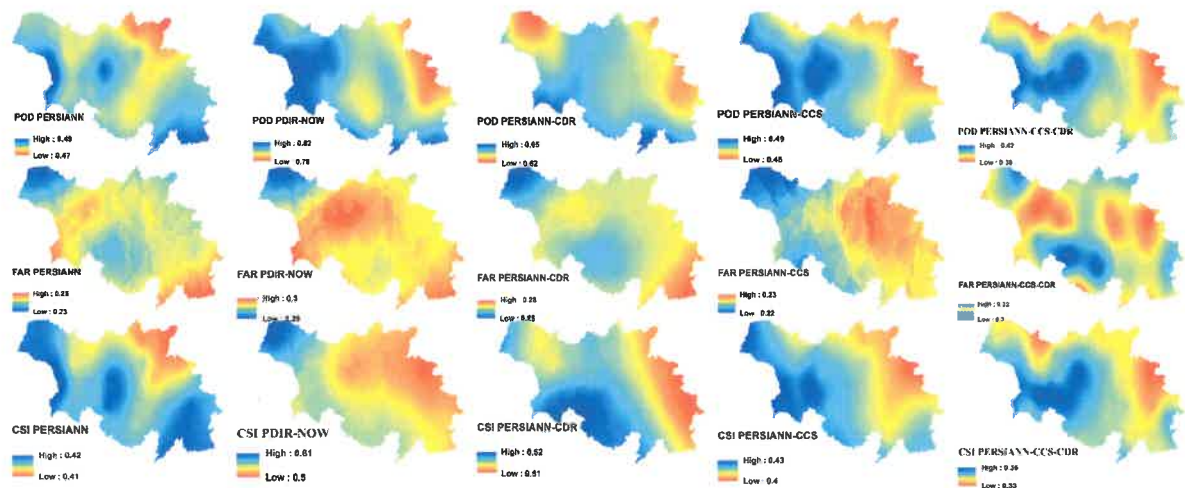


Fig. 5. Spatial pattern of categorical indicators for PERSIANN family products over the study area.

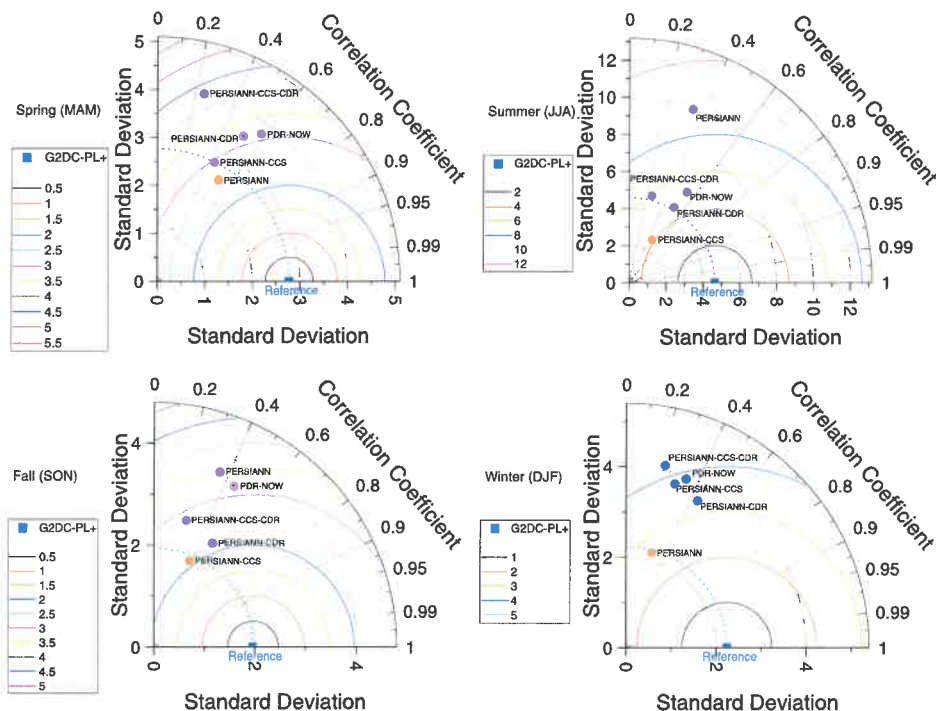


Fig. 6. Dataset comparisons based on the Taylor diagram at a seasonal scale.

Table 4

Seasonal comparison of performance indicators for PERSIANN family products over the study area.

Season	Name	PERSIANN	PERSIANN-CCS	PERSIANN-CDR	PDR-NOW	PERSIANN-CCS-CDR
Spring	R ²	0.27	0.19	0.26	0.34	0.06
	PBIAS (%)	-42.90	-0.37	34.17	50.70	40.26
	RMSE (mm)	2.66	2.95	3.21	3.20	4.34
	NSE	0.09	-0.13	-0.33	-0.32	-1.44
	POD	0.52	0.67	0.84	0.93	0.56
	FAR	0.23	0.28	0.33	0.38	0.40
	CSI	0.45	0.53	0.59	0.60	0.41
Summer	R ²	0.12	0.22	0.26	0.29	0.06
	PBIAS (%)	12.31	-41.21	18.57	43.08	5.19
	RMSE (mm)	9.45	4.23	4.68	5.22	5.82
	NSE	-3.14	0.17	-0.01	-0.26	-0.57
	POD	0.64	0.69	0.80	0.91	0.61
	FAR	0.21	0.22	0.24	0.28	0.31
	CSI	0.55	0.58	0.64	0.67	0.48
Fall	R ²	0.02	0.11	0.18	0.10	0.02
	PBIAS (%)	-13.74	22.05	45.69	109.06	49.42
	RMSE (mm)	4.70	3.37	3.30	4.80	4.45
	NSE	-2.10	-0.69	-0.53	-2.24	-1.78
	POD	0.54	0.64	0.79	0.91	0.57
	FAR	0.32	0.34	0.34	0.38	0.39
	CSI	0.43	0.48	0.56	0.59	0.42
Winter	R ²	0.05	0.08	0.07	0.11	0.19
	PBIAS (%)	80.62	69.20	-28.48	96.61	61.15
	RMSE (mm)	2.71	3.93	3.25	4.05	3.43
	NSE	-2.82	-2.08	-0.46	-2.27	-1.35
	POD	0.68	0.75	0.52	0.96	0.84
	FAR	0.28	0.23	0.25	0.33	0.26
	CSI	0.53	0.61	0.44	0.66	0.65

3.1.2. Seasonal evaluation precipitation estimates

The evaluation of seasonal accuracy employed the Taylor diagram. According to this diagram, in spring (MAM), PERSIANN shows the highest accuracy (RMSE = 2.66 mm), followed by PERSIANN-CCS (RMSE = 2.95 mm). According to Fig. 6 and Table 4, in MAM, PDR-NOW shows higher correlation ($R^2 = 0.34$), and PERSIANN-CCS-CDR has the weakest accuracy according to the correlation coefficient. Similarly, in summer (JJA), PERSIANN-CCS-CDR shows the lowest correlation. It also has the lowest PBIAS (5.19%). The highest correlation ($R^2 = 0.29$) and detection ability (POD = 0.91, and CSI = 0.67) in JJA is recorded for PDR-NOW. PERSIANN-CCS has the lowest RMSE (4.23 mm), but it is not far from PERSIANN-CDR (RMSE = 4.68 mm).

During Fall (SON), PERSIANN-CDR performed better according to RMSE = 3.30 mm, NSE = -0.53, and R^2 . Like MAM, JJA, in winter (DJF), PDR-NOW detected precipitation more accurately than other SON products. Finally, in DJF, PERSIANN-CDR performed relatively better than other products.

In the current case study, the catchment experiences high intensive precipitation during JJA; the following studies also have shown similar results in similar conditions (intense precipitation in summer). In this regard, Li et al. (2021) showed the smallest correlation for PERSIANN-CDR among four gridded precipitation products in a subtropical humid monsoon climate zone in China. Over a tropical zone, Tan et al. (2017) revealed that PERSIANN-CDR data resulted in a slight underestimation of the observed dataset in a catchment in the north of Malaysia, and an overestimation of precipitation in the southern parts of Malaysia. In Korea, over a humid monsoon climate zone, Vu et al. (2018) showed that TRMM and CMADS perform better than PERSIANN and PERSIANN-CDR when compared to rain gauge measurements which the major part of surface runoff and precipitation (70%) occur during the monsoon season (June–September). In a similar monsoon climate zone in the west of China, Jiang et al. (2020) tested five gridded datasets, and concluded that PERSIANN-CDR has the lowest correlation and detection ability, and the highest error compared to the observed dataset. In the Mekong River Basin, with diverse climate zones (temperate to tropical), PERSIANN-CDR also had the lowest rank and accuracy among four gridded datasets (Tang et al., 2019). Moreover, like our study, other studies also have shown the insufficient accuracy of PERSIANN products in hydrological simulations and against the observed dataset in different regions (Gao et al., 2018; Jimeno-Saez et al., 2021). In most of the aforementioned studies, the PERSIANN family has shown good detection ability regarding POD, FAR, and CSI indicators.

According to various studies, precipitation estimates during summer are less accurate due to convective precipitation (which exists in the current case study) and the difficulty of measuring these precipitations by radars (Emmanuel et al., 2012; Goudenhoofd and Delobbe, 2009; Jurczyk et al., 2020; Sokol et al., 2021).

3.2. Evaluation of hydrological modeling using G2DC-PL+

The calibration and validation results demonstrate sufficient accuracy of G2DC-PL+ in runoff simulations. According to the KGE performance indicator, the model at all three discharge stations showed acceptable performance. Table 5 presents the calibration and validation results. Fig. 7 shows the simulated and observed time series (station C). Table 6 provides selected parameters and the final range.

Table 5

Accuracy of the SWAT+ model with various precipitation datasets in the calibration and validation phases.

	Calibration		Validation	
	KGE	PBIAS%	KGE	PBIAS%
Station A				
G2DC-PL+	0.73	-1.6	0.67	-11.7
PERSIANN	-11	17.5	-9	19
PERSIANN-CCS	-0.69	-59.7	-1.5	-31
PERSIANN-CDR	-0.5	-43	-0.97	-51
PDIR-NOW	-1.29	66.6	-4.95	89
PERSIANN-CCS-CDR	-2.17	120	-2.59	174
Station B				
G2DC-PL+	0.74	1.6	0.62	-22.6
PERSIANN	-8	-26.2	-7	135
PERSIANN-CCS	0.14	36.6	0.09	55
PERSIANN-CDR	0.08	64.1	-1.2	73
PDIR-NOW	-0.6	-8.6	-3.98	136
PERSIANN-CCS-CDR	-0.14	-69	-1.25	-73
Station C				
G2DC-PL+	0.79	2.2	0.65	28.2
PERSIANN	-9.4	180	-8	125.9
PERSIANN-CCS	0.31	153.9	0.22	138.1
PERSIANN-CDR	0.34	153.3	0.13	197.1
PDIR-NOW	-0.33	408.4	-1.51	381.5
PERSIANN-CCS-CDR	0.07	222.2	-3.59	198.9

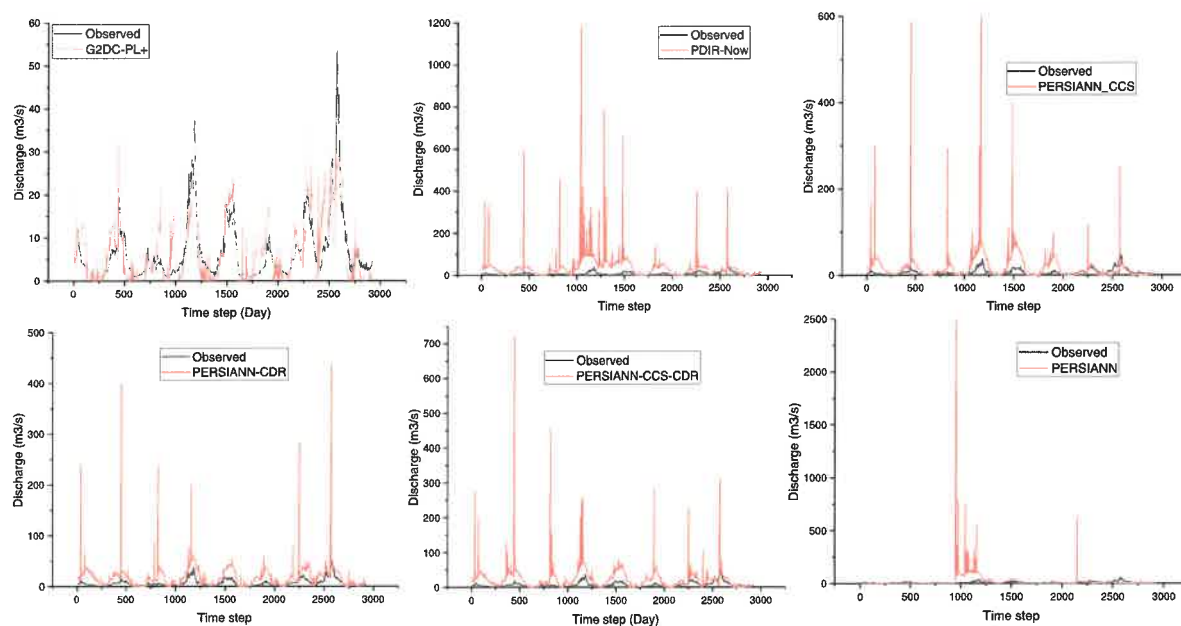


Fig. 7. Observed and simulated runoff (discharge station C) by SWAT+ for all precipitation products for the calibration period 2003–2019.

Table 6
Selected SWAT+ parameters in the calibration and validation process.

Parameter	Object	Minimum	Maximum
r*_k	sol	-0.21	-0.13
r_bd	sol	-0.20	-0.19
r_awc	sol	-0.26	-0.23
r_cn2	mgt	0.07	0.10
V*_ovn	hru	0.33	0.45
V_lat_time	hru	11.97	12.82
V_canmx	hru	2.84	3.30
V_esco	hru	0.99	0.99
V_epco	hru	0.11	0.14
V_perco	hru	0.90	0.91
V_surlag	hru	14.13	15.12
V_alpha	gw	0.02	0.02
V_bf_max	gw	0.86	0.89
V_deep_seep	gw	0.19	0.20
V_flo_min	gw	1.50	2.90
V_revap_co	gw	0.17	0.19
V_revap_min	gw	135.45	187.79
V_sp_yld	gw	0.12	0.13
V_chn	rte	0.03	0.03
V_chk	rte	1.72	1.83

r: relative change; V: replace value.

3.3. Evaluation of the accuracy of PERSIANN products in runoff simulation

After the calibration process for each product, the PERSIANN family showed no acceptable results in runoff simulations in our study (Table 5). The range of KGE for these products is from -11 to 0.34 , and PBIAS has shown high errors out of the acceptable range in the simulated runoff. Fig. 7 illustrates the observed and simulated runoff for Station C.

The hydrological model configuration and calibrated parameters, as well as the driving data are the three significant sources of uncertainty that can influence the performance of runoff modeling. Inaccuracies in rainfall input can produce substantial uncertainties in runoff simulations (Wang et al., 2021).

Similar to our results based on the SWAT model, Musie et al. (2019) concluded that the PERSIANN-CDR product performed poor and unsatisfactory runoff simulations at monthly and daily time steps in a catchment in Ethiopia. In this study, the CHIRPS performed the best among the satellite precipitation products in the statistical assessments and daily and monthly runoff simulations. Our results also confirm the assumption made by Musie et al. (2019) and Zhu et al. (2016) that BIAS of precipitation products affects the accuracy of runoff simulation in water resources models. Over a humid area in southern China, among the four satellite-based precipitation products, CMORPH and TMPA achieved runoff modeling outputs superior to those of PERSIANN and CHIRPS (Wang et al., 2021). In Vietnam, PERSIANN-CDR did not perform well compared to other gauge-corrected datasets in runoff simulations at a daily time step (Le et al., 2020).

Nonetheless, in another study from Vietnam, PERSIANN-CDR performed slightly better than CPC in streamflow modeling employing a hydrological model (Ilyas et al., 2021). Zhu et al. (2016) explored the role of PERSIANN-CDR, TMPA, and NCEP-CFSR in forcing runoff simulations employing SWAT in China. They discovered that both PERSIANN-CDR and TMPA 3B42V7 are datasets useful in runoff prediction at daily and monthly scales. Results of another study in China revealed that TMPA outperformed PERSIANN-CDR in estimating the precipitation and runoff simulations with SWAT (Le et al., 2020). In a semi-arid catchment in Iran, PERSIANN-CDR also showed low accuracy in runoff simulations at monthly time steps (Eini et al., 2018).

Several of the aforementioned studies compared satellite-based datasets against gauge interpolated datasets and reanalysis. Regarding the development methods of these different datasets, satellite-based datasets usually show the weakest performance in precipitation comparisons and runoff simulations. PERSIANN-CDR and PERSIANN-CCS-CDR, however, are gauge-corrected datasets, and they could show better accuracy than other PERSIANN family products. In the current study, PERSIANN-CDR performed better than others in runoff simulations, although the performance level is still unacceptable.

As mentioned in the seasonal evaluation of PERSIANN products, these products have shown less accuracy over regions that have high intensive precipitation during summer. During summer, this uncertainty in satellite-derived products (due to brightness temperatures in individual spectral channels and obtained rain rates is less deterministic compared to, for instance, radar reflectivity and rain intensity) leads to higher uncertainty of the precipitation estimates and, consequently, unrealistic results of hydrological simulation in small catchments (Sokol et al., 2021).

3.4. Limitations and further study

This study evaluated PERSIANN family products in a catchment in Poland in daily time steps for all the period and seasonal assessments. The datasets were extracted for centroids of each sub-basin. We therefore suggest that it could be valuable in further studies, if researchers compare these datasets at the center of each product. In addition, a further study for a larger catchment (or at the country

scale) is needed to capture more geographical complexity and grids in the study.

Moreover, the comparison is made against a regional gauge interpolated dataset (GD2DC-PL+). According to Eini et al. (2021), this type of comparison could increase the uncertainties of results. Further research should therefore evaluate these datasets against gauge stations.

Daily comparisons in both accuracy evaluation and runoff simulations in daily steps showed no acceptable accuracy. It is recommended that in future studies researchers evaluate these datasets in monthly comparisons, because some of the hydrological models can use both daily and monthly time series as the input. The results should be useful in water balance and long-term studies.

PERSIANN family products also have sub-daily datasets. The accuracy of these datasets is still unknown in this part of the world. Analysing these datasets in flood modeling and sub-daily precipitation evaluation would greatly benefit extreme analysis and disaster management assessments.

Finally, GD2DC-PL+ has one important limitation, it is available for a fixed period, with updates occurring every several years. In contrast, PERSIANN family products are real-time or near-real-time datasets which makes them an attractive data source for some specific hydrological applications. However, to keep integrity and reliability of results in global studies, we suggest applying a bias-correction method (Salmani-Dehaghi and Samani, 2021; Xiao et al., 2021) for the PERSIANN family products in daily time steps over Poland. This could be done by using G2DC-PL+ over the Odra River basin and Vistula River basin in central Europe, or at watershed and catchment levels in Poland.

4. Conclusion

This study assesses the performance of PERSIANN family satellite-based precipitation datasets against a regional gridded dataset over a catchment in Poland. It is the first time we used PERSIANN-CCS-CDR, PDIR-NOW in runoff simulations using a relatively new model SWAT+.

This study is composed of two parts: 1) the evaluation of PERSIANN family satellite-based precipitation products to G2DC-PL+ in the period 2003–2019, and 2) use of the hydrological SWAT+ model to simulate daily runoff. Our conclusions can be summarised as follows:

- a) PERSIANN family products could detect the precipitation events accurately according to POD, FAR, and CSI indicators.
- b) PERSIANN-CDR and PDIR-NOW show better correlations compared to other products.
- c) The SWAT+ results demonstrate that G2DC-PL+ could be used as a reliable source instead of gauge data in runoff simulations.
- d) PERSIANN-CDR performed slightly better in runoff simulations compared to other gridded datasets.
- e) PERSIANN family products are unreliable in daily precipitation estimates and runoff simulations.

CRedit authorship contribution statement

Mohammad Reza Eini: Conceptualization, Methodology, Software, Validation, Writing – original draft, Writing – review & editing, Visualization. **Akbar Rahmati:** Methodology, Software, Writing – review & editing, Visualization. **Mikołaj Piniewski:** Methodology, Writing – original draft, Writing – review & editing, Supervision, Funding acquisition.

Declaration of Competing Interest

The authors declare that they have no known competing financial interests or personal relationships that could have appeared to influence the work reported in this paper.

Acknowledgment

We would like to thank the editor and reviewers for their thoughtful comments and efforts towards improving our manuscript. MRE is funded by the National Science Centre (Narodowe Centrum Nauki), Warsaw, Poland (PRELUDIUM BIS-1 project, UMO-2019/35/O/ST10/04392). The Institute of Meteorology and Water Management (IMGW-PIB) is acknowledged for providing hydrometeorological data.

References

- Ajaaj, A.A., Mishra, A.K., Khan, A.A., 2019. Evaluation of satellite and gauge-based precipitation products through hydrologic simulation in Tigris river basin under data-scarce environment. *J. Hydrol. Eng.* 24, 18.
- Al-Palahi, A.H., Saddique, N., Spank, U., Gebrechorkos, S.H., Bernhofer, C., 2020. Evaluation the performance of several gridded precipitation products over the highland region of Yemen for water resources management. *Remote Sens.* 12, 23.
- Alnahit, A.O., Mishra, A.K., Khan, A.A., 2020. Evaluation of high-resolution satellite products for streamflow and water quality assessment in a Southeastern US watershed. *J. Hydrol.-Reg. Stud.* 27, 18.
- Althoff, D., Dias, S.H.B., Filgueiras, R., Rodrigues, L.N., 2020. ETo-Brazil: a daily gridded reference evapotranspiration data set for Brazil (2000–2018). *Water Resour. Res.*, vol. 56, e2020WR027562.
- Arnold, J.G., Bieger, K., White, M.J., Srinivasan, R., Dunbar, J.A., Allen, P.M., 2018. Use of decision tables to simulate management in SWAT+. *Water* 10, 713.
- Ashouri, H., Hsu, K.-L., Sorooshian, S., Braithwaite, D.K., Knapp, K.R., Cecil, L.D., Nelson, B.R., Prat, O.P., 2015. PERSIANN-CDR: daily precipitation climate data record from multisatellite observations for hydrological and climate studies. *Bull. Am. Meteorol. Soc.* 96, 69–83.

- Auerbach, D.A., Easton, Z.M., Walter, M.T., Flecker, A.S., Fuka, D.R., 2016. Evaluating weather observations and the climate forecast system reanalysis as inputs for hydrologic modelling in the tropics. *Hydrol. Process.* 30, 3466–3477.
- Beck, H.E., Vergopolan, N., Pan, M., Levizzani, V., van Dijk, A., Weedon, G.P., Brocca, L., Pappenberger, F., Huffman, G.J., Wood, E.F., 2017. Global-scale evaluation of 22 precipitation datasets using gauge observations and hydrological modeling. *Hydrol. Earth Syst. Sci.* 21, 6201–6217.
- Berezowski, T., Szcześniak, M., Kardel, I., Michalowski, R., Okruszko, T., Mezghani, A., Piniewski, M., 2016. CPLFD-GDPT5: high-resolution gridded daily precipitation and temperature data set for two largest Polish river basins. *Earth Syst. Sci. Data* 8, 127–139.
- Bieger, K., Arnold, J.G., Rathjens, H., White, M.J., Bosch, D.D., Allen, P.M., Volk, M., Srinivasan, R., 2017. Introduction to SWAT+, a completely restructured version of the soil and water assessment tool. *JAWRA J. Am. Water Resour. Assoc.* 53, 115–130.
- Bitew, M.M., Gebremichael, M., 2011. Assessment of satellite rainfall products for streamflow simulation in medium watersheds of the Ethiopian highlands. *Hydrol. Earth Syst. Sci.* 15, 1147–1155.
- Bitew, M.M., Gebremichael, M., Ghebremichael, L.T., Bayissa, Y.A., 2012. Evaluation of high-resolution satellite rainfall products through streamflow simulation in a hydrological modeling of a small mountainous watershed in Ethiopia. *J. Hydrometeorol.* 13, 338–350.
- Chawanda, C.J., George, C., Thiery, W., Van Griensven, A., Tech, J., Arnold, J., Srinivasan, R., 2020. User-friendly workflows for catchment modelling: towards reproducible SWAT+ model studies. *Environ. Model. Softw.* 134, 104812.
- Darand, M., Khandu, K., 2020. Statistical evaluation of gridded precipitation datasets using rain gauge observations over Iran. *J. Arid Environ.* 178, 104172.
- Delavar, M., Eini, M.R., Kuchak, V.S., Zaghiyan, M.R., Shahbazi, A., Nourmohammadi, F., Motamedi, A., 2022. Model-based water accounting for integrated assessment of water resources systems at the basin scale. *Sci. Total Environ.* 830, 154810.
- Eini, M.R., Javadi, S., Delavar, M., Darand, M., 2018. Accuracy of PERSIANN-CDR precipitation satellite database in simulation assessment of runoff in SWAT Model on Maharlou Basin. *Phys. Geogr. Res. Q.* 50, 563–576.
- Eini, M.R., Javadi, S., Delavar, M., Gassman, P.W., Jarihani, B., 2020. Development of alternative SWAT-based models for simulating water budget components and streamflow for a karstic-influenced watershed. *Catena* 195, 104801.
- Eini, M.R., Javadi, S., Delavar, M., Monteiro, J.A., Darand, M., 2019. High accuracy of precipitation reanalyses resulted in good river discharge simulations in a semi-arid basin. *Ecol. Eng.* 131, 107–119.
- Eini, M.R., Olyaei, M.A., Kamyab, T., Teymoori, J., Brocca, L., Piniewski, M., 2021. Evaluating three non-gauge-corrected satellite precipitation estimates by a regional gauge interpolated dataset over Iran. *J. Hydrol.: Reg. Stud.* 38, 100942.
- Emmanuel, I., Andrieu, H., Leblois, E., Flahaut, B., 2012. Temporal and spatial variability of rainfall at the urban hydrological scale. *J. Hydrol.* 430, 162–172.
- Gao, X.C., Zhu, Q., Yang, Z.Y., Wang, H., 2018. Evaluation and hydrological application of CMADS against TRMM 3B42V7, PERSIANN-CDR, NCEP-CPSR, and gauge-based datasets in Xiang river basin of China. *Water* 10, 24.
- Goudenhoofd, E., Delobbe, L., 2009. Evaluation of radar-gauge merging methods for quantitative precipitation estimates. *Hydrol. Earth Syst. Sci.* 13, 195–203.
- Gregor, L., Gruber, N., 2021. OceanSODA-ETHZ: a global gridded data set of the surface ocean carbonate system for seasonal to decadal studies of ocean acidification. *Earth Syst. Sci. Data* 13, 777–808.
- Gueymard, C.A., Lara-Fanego, V., Sengupta, M., Habte, A., 2021. Surface albedo spatial variability in North America: gridded data vs. local measurements. *Sol. Energy*.
- Hajihosseini, H., Hajihosseini, M., Morid, S., Delavar, M., Booi, M.J., 2016. Hydrological assessment of the 1973 Treaty on the Transboundary Helmand River, using the SWAT model and a global climate database. *Water Resour. Manag.* 30, 4681–4694.
- Hong, Y., Hsu, K.-L., Sorooshian, S., Gao, X., 2004. Precipitation estimation from remotely sensed imagery using an artificial neural network cloud classification system. *J. Appl. Meteorol.* 43, 1834–1853.
- Hsu, K.-L., Gao, X., Sorooshian, S., Gupta, H.V., 1997. Precipitation estimation from remotely sensed information using artificial neural networks. *J. Appl. Meteorol.* 36, 1176–1190.
- Iizumi, T., Sakai, T., 2020. The global dataset of historical yields for major crops 1981–2016. *Sci. Data* 7, 97.
- Ilyas, A.M., Pham, Q.B., Zhu, D.H., Elahi, E., Linh, N.T.T., Anh, D.T., Khedher, K.M., Ahmaddou, M., 2021. Multi sources hydrological assessment over Vu Gia Thu Bon Basin, Vietnam. *Hydrol. Sci. J.-J. Sci. Hydrol.* 66, 1383–1392.
- Jiang, S.H., Liu, R.L., Ren, L.L., Wang, M.H., Shi, J.C., Zhong, F., Duan, Z., 2020. Evaluation and hydrological application of CMADS reanalysis precipitation data against four satellite precipitation products in the Upper Huaihe River Basin, China. *J. Meteorol. Res.* 34, 1096–1113.
- Jimeno-Saez, P., Blanco-Gomez, P., Perez-Sanchez, J., Cecilia, J.M., Senent-Aparicio, J., 2021. Impact assessment of gridded precipitation products on streamflow simulations over a poorly gauged basin in El Salvador. *Water* 13, 21.
- Jurczyk, A., Szturc, J., Otop, I., Osórdka, K., Struzik, P., 2020. Quality-based combination of multi-source precipitation data. *Remote Sens.* 12, 1709.
- Knoben, W., 2013. Estimation of Non-stationary Hydrological Model Parameters for the Polish Welná Catchment. University of Twente.
- Le, M.H., Lakshmi, V., Bolten, J., Bui, D.D., 2020. Adequacy of satellite-derived precipitation estimate for hydrological modeling in Vietnam basins. *J. Hydrol.* 586, 19.
- Li, Y., Wang, W.S., Wang, G.Q., Yu, S.Y., 2021. Evaluation and hydrological application of a data fusing method of multi-source precipitation products—a case study over Tuojiang River basin. *Remote Sens.* 13, 28.
- Lloyd, C.T., Sorichetta, A., Tatem, A.J., 2017. High resolution global gridded data for use in population studies. *Sci. Data* 4, 1–17.
- Ma, D., Xu, Y.P., Gu, H.T., Zhu, Q., Sun, Z.L., Xuan, W.D., 2019. Role of satellite and reanalysis precipitation products in streamflow and sediment modeling over a typical alpine and gorge region in Southwest China. *Sci. Total Environ.* 685, 934–950.
- Musie, M., Sen, S., Srivastava, P., 2019. Comparison and evaluation of gridded precipitation datasets for streamflow simulation in data scarce watersheds of Ethiopia. *J. Hydrol.* 579, 17.
- Ndhlovu, G., Woyessa, Y., 2021. Use of gridded climate data for hydrological modelling in the Zambezi River Basin, Southern Africa. *J. Hydrol.* 602, 126749.
- Nguyen, P., Ombadi, M., Gorioh, V.A., Shearer, E.J., Sadeghi, M., Sorooshian, S., Hsu, K., Bolvin, D., Ralph, M.F., 2020. PERSIANN dynamic infrared-rain rate (PDIR-Now): a near-real-time, quasi-global satellite precipitation dataset. *J. Hydrometeorol.* 21, 2893–2906.
- Nguyen, P., Ombadi, M., Sorooshian, S., Hsu, K., AghaKouchak, A., Braithwaite, D., Ashouri, H., Thorstensen, A.R., 2018. The PERSIANN family of global satellite precipitation data: a review and evaluation of products. *Hydrol. Earth Syst. Sci.* 22, 5801–5816.
- Nguyen, P., Shearer, E.J., Tran, H., Ombadi, M., Hayatbini, N., Palacios, T., Huynh, P., Braithwaite, D., Updegraff, G., Hsu, K., 2019. The CHRS Data Portal, an easily accessible public repository for PERSIANN global satellite precipitation data. *Sci. Data* 6, 1–10.
- Piniewski, M., Szcześniak, M., Kardel, I., Berezowski, T., Okruszko, T., Srinivasan, R., Vikhamar-Schuler, D., Kundzewicz, Z.W., 2017. Hydrological modelling of the Vistula and Odra river basins using SWAT. *Hydrol. Sci. J.* 62, 1266–1289.
- Piniewski, M., Szcześniak, M., Kardel, I., Chattopadhyay, S., Berezowski, T., 2021. G2DC-PL+: a gridded 2 km daily climate dataset for the union of the Polish territory and the Vistula and Odra basins. *Earth Syst. Sci. Data* 13, 1273–1288.
- Pradhan, A., Indu, J., 2021. Assessment of SM2RAIN derived and IMERG based precipitation products for hydrological simulation. *J. Hydrol.* 127191.
- Qin, D., Plattner, G., Tignor, M., Allen, S., Boschung, J., Nauels, A., Xia, Y., Bex, V., Midgley, P., 2014. Climate change 2013: the physical science basis. In: Stocker, T. F., et al. (eds.), *Contribution of Working Group I to the Fifth Assessment Report of the Intergovernmental Panel on Climate Change*, pp. 5–14.
- Reichler, T., Dameris, M., Sausen, R., 2003. Determining the tropopause height from gridded data. *Geophys. Res. Lett.* 30.
- Ren, P.Z., Li, J.Z., Feng, P., Guo, Y.G., Ma, Q.S., 2018. Evaluation of multiple satellite precipitation products and their use in hydrological modelling over the Luanhe River basin, China. *Water* 10, 23.
- Sadeghi, M., Nguyen, P., Naeini, M.R., Hsu, K., Braithwaite, D., Sorooshian, S., 2021. PERSIANN-CCS-CDR, a 3-hourly 0.04° global precipitation climate data record for heavy precipitation studies. *Sci. Data* 8, 1–11.
- Salmani-Delaghi, N., Samani, N., 2021. Development of bias-correction PERSIANN-CDR models for the simulation and completion of precipitation time series. *Atmos. Environ.* 246, 117981.
- Satge, F., Hussain, Y., Molina-Carpio, J., Pillco, R., Laugner, C., Akhter, G., Bonnet, M.P., 2020. Reliability of SM2RAIN precipitation datasets in comparison to gauge observations and hydrological modelling over and regions. *Int. J. Climatol.* 20.

- Senent-Aparicio, J., George, C., Srinivasan, R., 2021. Introducing a new post-processing tool for the SWAT+ model to evaluate environmental flows. *Environ. Model. Softw.* 136, 104944.
- Shawul, A.A., Chakma, S., 2020. Suitability of global precipitation estimates for hydrologic prediction in the main watersheds of Upper Awash basin. *Environ. Earth Sci.* 79, 18.
- Siniecki, 2009. The role of small retention and water cooperatives in water management illustrated by the River Wena case study. *Ecol. Issues* 83.
- Sokol, Z., Szturc, J., Orellana-Alvear, J., Popová, J., Jurczyk, A., Céleri, R., 2021. The role of weather radar in rainfall estimation and its application in meteorological and hydrological modelling—a review. *Remote Sens.* 13, 351.
- Sorooshian, S., Hsu, K.-L., Gao, X., Gupta, H.V., Imam, B., Braithwaite, D., 2000. Evaluation of PERSIANN system satellite-based estimates of tropical rainfall. *Bull. Am. Meteorol. Soc.* 81, 2035–2046.
- Sterl, S., Fadly, D., Liersch, S., Koch, H., Thiery, W., 2021. Linking solar and wind power in eastern Africa with operation of the Grand Ethiopian Renaissance Dam. *Nat. Energy* 6, 407–418.
- Sun, Q., Miao, C., Duan, Q., Ashouri, H., Sorooshian, S., Hsu, K.L., 2018. A review of global precipitation data sets: data sources, estimation, and intercomparisons. *Rev. Geophys.* 56, 79–107.
- Talchabhadel, R., Aryal, A., Kawaike, K., Yamanoi, K., Nakagawa, H., Bhatta, B., Karki, S., Thapa, B.R., 2021. Evaluation of precipitation elasticity using precipitation data from ground and satellite-based estimates and watershed modeling in Western Nepal. *J. Hydrol.-Reg. Stud.* 33, 18.
- Tan, M.L., Gassman, P.W., Cracknell, A.P., 2017. Assessment of three long-term gridded climate products for hydro-climatic simulations in tropical river basins. *Water* 9, 24.
- Tan, M.L., Gassman, P.W., Liang, J., Haywood, J.M., 2021. A review of alternative climate products for SWAT modelling: sources, assessment and future directions. *Sci. Total Environ.* 795, 148915.
- Tan, M.L., Gassman, P.W., Yang, X., Haywood, J., 2020. A review of SWAT applications, performance and future needs for simulation of hydro-climatic extremes. *Adv. Water Resour.* 143, 103662.
- Tan, M.L., Yang, X., 2020. Effect of rainfall station density, distribution and missing values on SWAT outputs in tropical region. *J. Hydrol.* 584, 124660.
- Tang, X.P., Zhang, J.Y., Gao, C., Ruben, G.B., Wang, G.Q., 2019. Assessing the uncertainties of four precipitation products for swat modeling in Mekong River Basin. *Remote Sens.* 11, 24.
- Thom, V.T., Khoi, D.N., Linh, D.Q., 2017. Using gridded rainfall products in simulating streamflow in a tropical catchment – a case study of the Srepok River Catchment, Vietnam. *J. Hydrol. Hydromech.* 65, 18–25.
- Vu, M.T., Raghavan, S.V., Liong, S.Y., 2012. SWAT use of gridded observations for simulating runoff – a Vietnam river basin study. *Hydrol. Earth Syst. Sci.* 16, 2801–2811.
- Vu, T.T., Li, L., Jun, K.S., 2018. Evaluation of multi-satellite precipitation products for streamflow simulations: a case study for the Han River Basin in the Korean Peninsula, East Asia. *Water* 10, 23.
- Wang, Q., Xia, J., She, D.X., Zhang, X., Liu, J., Zhang, Y., 2021. Assessment of four latest long-term satellite-based precipitation products in capturing the extreme precipitation and streamflow across a humid region of southern China. *Atmos. Res.* 257, 13.
- Wira, 2011. Evaluation of impact of selected physical and biological indices upon quality of water in the Welna. *Sci. Pap. Civ. Eng. Shap. Environ.* 3.
- Xiao, S., Zou, L., Xia, J., Yang, Z., Yao, T., 2021. Bias correction framework for satellite precipitation products using a rain/no rain discriminative model. *Sci. Total Environ.*, 151679.
- Xuan, W.D., Fu, Q., Qin, G.H., Zhu, C., Pan, S.L., Xu, Y.P., 2018. Hydrological simulation and runoff component analysis over a Cold Mountainous River Basin in Southwest China. *Water* 10, 16.
- Zhang, L., Xin, Z.H., Zhou, H.C., 2020. Assessment of TMPA 3B42V7 and PERSIANN-CDR in driving hydrological modeling in a semi-humid watershed in Northeastern China. *Remote Sens.* 12, 20.
- Zhu, Q., Xuan, W.D., Liu, L., Xu, Y.P., 2016. Evaluation and hydrological application of precipitation estimates derived from PERSIANN-CDR, TRMM 3B42V7, and NCEP-CFSR over humid regions in China. *Hydrol. Process.* 30, 3061–3083.

Warsaw, 26/03/2024

Mohammadreza Einikarimkandi
d003066@sggw.edu.pl

**Institute of Environmental Engineering,
Mining, and Energy, Discipline
Council
of the Warsaw University of Life
Sciences**

Co-authorship statement

I hereby represent that in the below publication “Eini, M. R., Rahmati, A., & Piniewski, M. (2022). Hydrological application and accuracy evaluation of PERSIANN satellite-based precipitation estimates over a humid continental climate catchment. Journal of Hydrology: Regional Studies, 41, 101109. <https://doi.org/10.1016/j.ejrh.2022.101109>” my individual contribution in the development thereof involved, Conceptualization, methodology, software, validation, writing – original draft, writing – review & editing, visualization.


Signature
Mohammad Reza
Eini Karimkandi

Prague, 26/03/2024

Akbar Rahmati Ziveh
rahmati_ziveh@fzp.czu.cz

**Institute of Environmental Engineering,
Mining, and Energy, Discipline
Council
of the Warsaw University of Life
Sciences**

Co-authorship statement

I hereby represent that in the publication Eini, M. R., Rahmati, A., & Piniewski, M. (2022). Hydrological application and accuracy evaluation of PERSIANN satellite-based precipitation estimates over a humid continental climate catchment. Journal of Hydrology: Regional Studies, 41, 101109. <https://doi.org/10.1016/j.ejrh.2022.101109> my individual contribution in the development thereof involved data assessments, reading and editing the manuscript and literature review.

A handwritten signature in dark ink, appearing to be 'A. Rahmati', written over a light gray rectangular background.

Signature

Warsaw, 26/03/2024

Dr hab. Mikołaj Piniewski, prof. SGGW
Department of Hydrology, Meteorology and Water Management
Institute of Environmental Engineering
Warsaw University of Life Sciences
mikołaj_piniewski@sggw.edu.pl

**Institute of Environmental Engineering,
Mining, and Energy, Discipline
Council**

**of the Warsaw University of Life
Sciences**

Co-authorship statement

I hereby represent that in the below publication “Eini, M. R., Rahmati, A., & Piniewski, M. (2022). Hydrological application and accuracy evaluation of PERSIANN satellite-based precipitation estimates over a humid continental climate catchment. Journal of Hydrology: Regional Studies, 41, 101109. <https://doi.org/10.1016/j.ejrh.2022.101109>” my individual contribution in the development thereof involved, conceptualization, methodology, writing – review & editing.



Signature

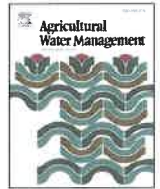
11. Publication 3

Eini, M. R., Salmani, H., & Piniewski, M. (2023). Comparison of process-based and statistical approaches for simulation and projections of rainfed crop yields.

Agricultural Water Management, 277, 108107.

<https://doi.org/10.1016/j.agwat.2022.108107>

Impact factor: 6.7 – MeiN: 140



Comparison of process-based and statistical approaches for simulation and projections of rainfed crop yields

Mohammad Reza Eini^a, Haniyeh Salmani^b, Mikołaj Piniewski^{a,*}

^a Department of Hydrology, Meteorology and Water Management, Institute of Environmental Engineering, Warsaw University of Life Sciences, Warsaw, Poland

^b Department of Civil Engineering, Ale Taha University, Tehran, Iran

ARTICLE INFO

Keywords:

Global warming
Oder River basin
Baltic Sea basin
Machine learning
Artificial Neural Network

ABSTRACT

Accurate and comprehensive modelling aimed at investigating the impact of climate change on rainfed crop yields is of great importance due to the interconnected issues of water scarcity and food security. Because the process-based and statistical approaches to simulating crop yields are different in nature, a comparison between them is needed. This study investigates the accuracy of crop yield simulations in the historical period as well as future projections using two modelling approaches: 1) a process-based approach employing the Soil and Water Assessment Tool+ (SWAT+) model, and 2) a statistical approach employing a data-driven model, Feed Forward Back Propagation Neural Network (FFBPNN) over a medium-sized catchment in north-western Poland. The application of two potential evapotranspiration methods (Penman-Monteith and Hargreaves) in SWAT+ permitted calibration (2004–2011) and validation (2012–2019) of runoff and yields of winter wheat and spring barley. Different combinations of climatic parameters with a drought index based on Joint Deficit Index were applied to simulate and project rainfed crop yields (winter wheat, barley, potato, rye, rapeseed, sugar beets, cereals, maize for grain, maize for green forage, pulses) with FFBPNN. The results reveal that adding the new drought index helped increase the FFBPNN performance. This approach showed that future yields of the studied crops would slightly increase under RCP8.5 by 2060. Winter wheat and spring barley projections from SWAT+ showed very small changes using both the Penman-Monteith and Hargreaves method. Policy-wise, the results should be of interest to climate change adaptation practitioners and food security experts. Future studies should aim at more thorough investigation of the role of the downscaling technique and extreme events, as well as the effect of elevated CO₂ on future crop yields.

1. Introduction

Due to an increase in anomalies in the atmosphere in recent years, such as climate change, several aspects of human life have been under threat. This has a significant effect on water, the most crucial material in the environment that all living things depend on (Zepeda, 2001; Salehnia et al., 2020). Global warming has been identified as a vital issue in the context of climate change during the current and future centuries (Zepeda, 2001; Pachauri et al., 2014; Tomczyk et al., 2022). Several studies have shown that lack of water is critical for life security, food security, and the economy (World-Bank, 2005). For example, Traore et al. (2013) revealed that an increase in maximum temperature in Mali leads to a reduction in cotton yield, affecting the economy. In northern Thailand, rainfed rice and corn production may be reduced under climate change conditions, influencing food security and the economy

(Amnuaylojaroen et al., 2021). All of these factors are interlinked. Evaluation of the future and prevention of acute situations requires availability of a simulation of the future for scientists and authorities (Pachauri et al., 2014).

The accuracy of estimations plays a significant role here. Obtaining a robust and reliable estimate of these conditions involved the development of several methods in different fields of science. General Circulation Models (GCMs) have been developed and used for climate change projections over the last three decades (Pachauri et al., 2014; Chen et al., 2021a). GCMs are numerical models capable of interpreting physical interactions of the atmosphere and ocean to simulate global climate response to rising greenhouse gas emissions. Different methods are developed in the realm of hydrology using different concepts, such as the process-based and statistical approaches (Gassman et al., 2007). Finally, like in hydrology, as a representative of food production, crop yield

* Corresponding author.

E-mail address: mikolaj.piniewski@sggw.edu.pl (M. Piniewski).

modelling could be based on different approaches and concepts (van Klompenburg et al., 2020; Dinh and Aires, 2021). Moreover, both hydrological and crop models are commonly forced by GCMs to project the future state of water resources and crop yields, respectively (Tao et al., 2020). Some complex hydrological models also have their crop growth modules and can serve both purposes.

Statistical approaches aim to find links between a set of meaningful and effective variables and crop yield (Chlingaryan et al., 2018; Leng and Hall, 2020; van Klompenburg et al., 2020). These approaches are based on data, and long-term datasets are needed for high estimation accuracy (Leng and Hall, 2020). The very nature of crop datasets is that they contain only one value per year for a given crop and spatial unit (Dinh and Aires, 2021). Different numerical methods have been applied to address this observation of data scarcity, with a robust model and projections. For example, Machine Learning (ML), a member of data-driven and Artificial Intelligence (AI) methods focusing on learning, is a useful method that can predict and simulate crop yields based on several features (Chlingaryan et al., 2018; van Klompenburg et al., 2020). ML can discover patterns and similarities between inputs and outputs. The models need to be trained using datasets. The results are interpreted based on prior information and knowledge (Chlingaryan et al., 2018; van Klompenburg et al., 2020). Moreover, several statistical/regression-based models, such as the Panel, ABSOLUT, and IRMA, are employed to simulate crop yields (Hsiao, 2014; Conradt et al., 2016; Gornott and Wechsung, 2016; Salehnia et al., 2020; Conradt, 2021).

Several studies have used AI methods to simulate crop yields in different regions and climatic conditions. For example, Ruß et al. (2008) applied Neural Networks to predict wheat yield using nitrogen fertilizer, red edge inflection point vegetation index, and soil electrical conductivity. Everingham et al. (2009) used Forward Stagewise Algorithm to forecast regional sugarcane crop production. In another study, Clustering methods, Random Forest, and Support Vector Machine were employed to obtain a robust model for wheat yield prediction (Ruß and Kruse, 2010). In the studies, weather parameters were directly applied as inputs in statistical models. However, a drought indicator based on precipitation or soil moisture data could also have substantial effects on the accuracy of statistical models (Peichl et al., 2018; Salehnia et al., 2020).

Artificial Neural Networks (ANNs) have been employed more frequently than other AI methods due to their higher flexibility in crop yield simulations (van Klompenburg et al., 2020). According to literature, different inputs such as satellite datasets, climatic variables, soil properties, and geographic information are included in ANNs to simulate crop yields (Ruß et al., 2008; Baral, Çakır et al., 2011, 2014; Matsumura et al., 2015; Gandhi et al., 2016; Cheng et al., 2017; Crane-Droesch, 2018). ANNs are a technique that identifies the underlying relationship between data by processing them. Neural network training aims to learn the process and provide an appropriate output for each input. ANNs can detect complex nonlinear relationships between input and output vectors (Khatibi et al., 2020; Snieder et al., 2020; Abhishek et al., 2021; Kundu and Sinha, 2021; Shinde et al., 2021).

In process-based approaches, crop simulation is based on physical or empirical equations (Gassman et al., 2007; Leng and Hall, 2020). In these models, inputs could be remarkably simple, or numerous datasets could be included in the modelling process (Williams et al., 1989; Gassman et al., 2007). An example of widely used process-based model with high input data requirements is the Soil and Water Assessment Tool (SWAT), recently extensively revised into the new version called SWAT+ (Bieger et al., 2017; Arnold et al., 2018; Nkwasa et al., 2022; Wagner et al., 2022). SWAT has been used to model various agronomic practices, assess the impact of climate change on hydrology and crop yields, and project nutrient loads in basins (Gassman et al., 2007; Piniewski et al., 2017; Eini et al., 2020; Tan et al., 2021). SWAT as an agro/eco-hydrological model has been widely used for crop yield simulations in regions with different climatic conditions worldwide

(Sabzadeh and Shourian, 2020; Chen et al., 2021b; Eini et al., 2021a; Jeyrani et al., 2021; Jiang et al., 2021; Liu et al., 2021; Delavar et al., 2022). In the aforementioned studies, however, only one of the potential evapotranspiration (PET) methods in the SWAT model was employed (SWAT covers three PET methods, including Hargreaves (temperature-based method), Priestley-Taylor (radiation-based method), and Penman-Monteith (temperature- and radiation-based method)). Actual evapotranspiration in SWAT is controlled by the PET method, and each of the aforementioned methods could provide different results under climate change scenarios. The necessity of the comparisons between these methods is well described in Lemaitre-Basset et al. (2021). A comparison of the Penman-Monteith and Hargreaves methods under humid conditions was presented in Trajkovic (2007).

In this field of research, different models have been shown to provide different results for the projections, which shows the high-level uncertainty in crop models (Tao et al., 2020). Major worldwide projects have attempted to assess and adjust crop simulators, and measure, control, or decrease uncertainties from the crop simulator method in projecting climate effects on crop yield. For example, two large-scale projects (AgMIP (Ruane et al., 2017) and MACSUR projects (Ewert et al., 2015)) focused on this objective (Tao et al., 2018; Tao et al., 2020).

This study's primary objective is to compare the statistical and process-based modelling approaches in the simulation and projection of crop yields in the Weina catchment located in the north-western part of Poland. The study is based on the following three hypotheses: (a) a high temperature increase projected under the RCP8.5 scenario would lead to a decline in crop yields projected by both types of models in north-western Poland; (b) crop yields projected by process-based models would depend on the selected PET method; and (c) drought-based indicators (i.e. SPI) have advantages over direct use of weather parameters in statistical simulations of crop yields.

2. Methodology

2.1. Case study

A humid continental climate catchment in central Europe was selected to simulate and project crop yields. The Weina catchment is a flat catchment located in Poland and part of the Oder River basin (Siniński, 2009; Wira, 2011; Knob, 2013; Eini et al., 2022b). The local agricultural activities are based on rainfed crops. The catchment has relatively homogeneous climatic conditions. More details on the catchment, such as the applied data and weather conditions, are available in Eini et al. (2022a). Fig. 1 presents the position of the Weina catchment, land use, stream network, discharge stations, and sub-basin configuration for process-based modelling. The dominant agricultural crops in the study area include winter wheat (30% of the area ~ 135,500 ha) and spring barley (14.8% of the area ~ 21,500 ha). The growing period of the majority of spring crops starts in the second half of March or first half of April. In this region of Poland, droughts are reported to happen most frequently and lead to largest crop losses in Poland (Oleksiak et al., 2022).

2.2. The Soil and Water Assessment Tool+ and crop simulation

The SWAT+ agro-hydrological model (an extensively modified version of the SWAT) is a relatively new model used in this study as the process-based model (more details available in Wagner et al., 2022; Nkwasa et al., 2022, and Bailey et al., 2022). SWAT+ simulates the plant growth process by employing a basic version of the EPIC's generic crop growth method (Williams et al., 1989). Crop maturity is based on accumulating either "days to maturity" (a new option in SWAT+) or "potential heat units." Once the total heat units required to reach crop maturity (or days to maturity) are exceeded, the crop growth ends. Daily biomass production is affected by static absorbed photosynthetically active radiation, radiation use efficiency of the crop, and LAI (Leaf Area

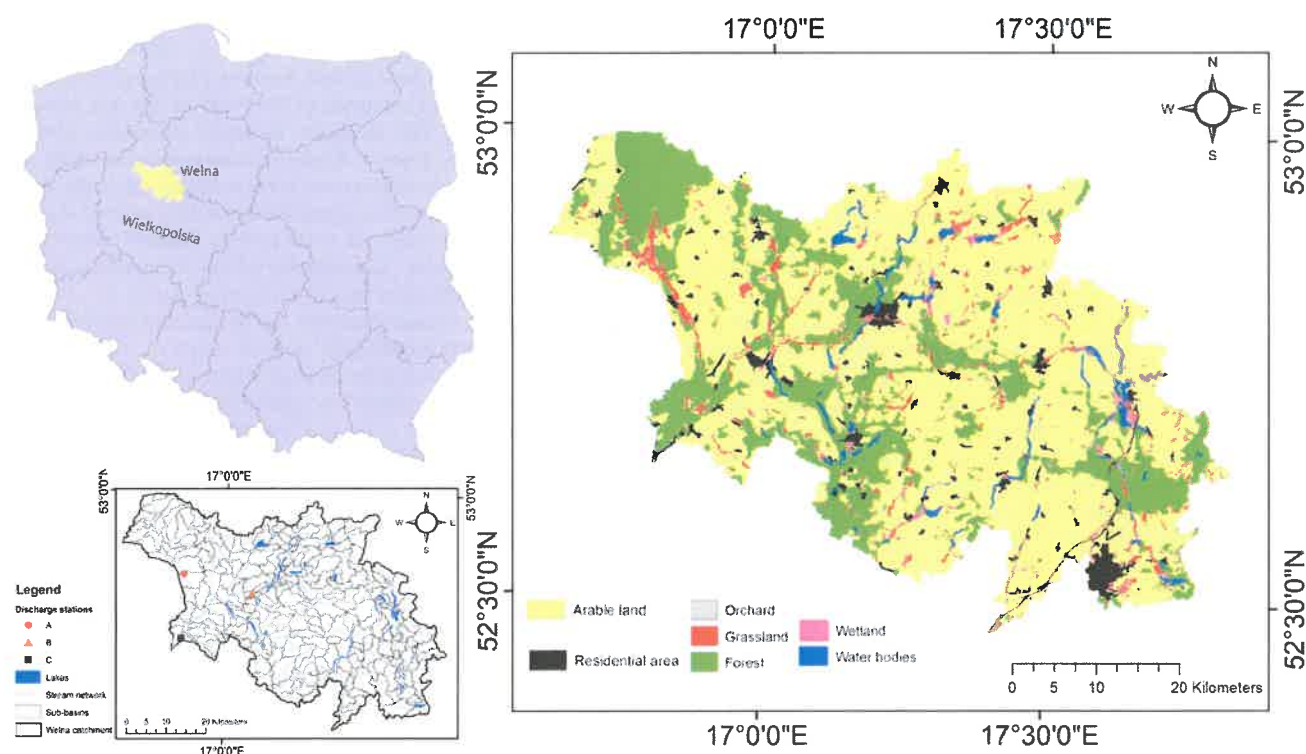


Fig. 1. Position of Wełna in Poland and the province, land use map, river network, discharge stations, and lakes.

Index) (Nair et al., 2011; Musyoka et al., 2021).

In SWAT+, evaporation and evapotranspiration are assessed by a preliminary computation of potential evaporation (PET), representing the evaporative demand of the atmosphere. The Penman-Monteith and Hargreaves methods were used to calculate PET for a better understanding of crop yields in the future, and to evaluate the influence of these methods on crop yields in the Wełna catchment (Hargreaves and Samani, 1985; Allen et al., 1998). The Penman-Monteith method uses net radiation, relative humidity, 2-m wind speed, and air temperature, but the Hargreaves method only uses air temperature.

Considering 2001–2003 as the warm-up period, the SWAT+ model was calibrated for the period 2004–2011, and validated for the years 2012–2019 for daily runoff and crop yields (winter wheat and spring barley). The calibration and validation steps employed 20 parameters, including soil parameters (k , bd , awc), hydrologic response unit parameters ($cn2$, ovn , lat_{time} , $canmx$, $esco$, $epco$, $perco$, $surlag$), groundwater parameters (α , bf_{max} , $deep_{seep}$, flo_{min} , $revap_{co}$, $revap_{min}$, sp_{yld}), and channel parameters (chn , chk). The ranges and optimal values of the calibrated parameters are available in the study by Eini et al. (2022a), where the hydrological component of SWAT+ was applied for the first time. To focus on crop yield simulations and reduce the duplication with the preceding study, runoff modelling and its details are excluded from the Results section. Readers can find more details

about the model setup and runoff results in Eini et al. (2022a).

An important feature of the SWAT+ setup from the point of view of crop yield calibration is a crop-specific land cover map and timing of key management operations for all crops. In this study we used the same land use map that was prepared for the Poland-wide SWAT model (Marcinkowski et al., 2021). Table 1 presents sowing and harvest dates for six crops included in the SWAT+ setup for the Wełna catchment, including two most dominant ones, namely winter wheat and spring barley, used in further assessments.

2.3. Artificial Neural Network structure

Due to the widespread use of ANNs as a simulation tool for Earth's processes, the Feed Forward Back Propagation Neural Network (FFBPNN) (complete theoretical background available in Shinde et al., 2021), widely examined in Earth-process modelling and predicting, was employed (Coulibaly et al., 2000; Samani et al., 2007; Zounemat-Kermani et al., 2019; Abhishek et al., 2021). FFBPNN consists of one input, one or more hidden layers (where data are processed to build a model), and the output layer (where outputs are generated). Moreover, FFBPNN can be categorised in Multilayer Perceptron (MLP) Neural Network Models.

Table 1

Sowing and harvest dates of crops implemented in SWAT+.

Crop	SWAT+ code	Sowing date	Harvest date	Area [ha]	Fraction [%]
Winter wheat*	WWHT	13-Oct	3-Jul	80,000	30.68%
Spring barley*	BARL	31-Mar	5-Aug	38,500	14.80%
Silage maize	CSIL	1-May	12-Aug	11,500	4.43%
Potato	POTA	16-Apr	10-Oct	3,500	1.35%
Maize	CORN	30-Apr	30-Sep	4,800	1.83%
Sugar beet	SGBT	7-Apr	9-Aug	3,600	1.38%

* These crops were used in further analyses with SWAT+.

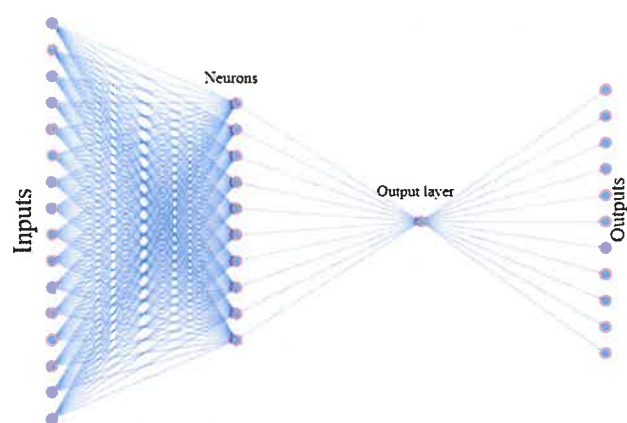


Fig. 2. Structure of employed FFBPNN with inputs and output.

2.3.1. Feed forward back propagation neural network architecture

Some initial parameters should be fixed to start simulating with FFBPNN models. The article provides brief information about these initialisations. First, by means of a trial-and-error process (using all the inputs and outputs), the Levenberg-Marquardt backpropagation (LMBP) algorithm was found to be the best algorithm for FFBPNN training (complete details of the LMBP algorithm are described by Lv et al., 2017). Moreover, LMBP has been used in several hydrological/Earth-process studies, and has been recognised as a reliable training algorithm with a more accurate curve fitting ability utilised in input-output data (Coulbaly et al., 2000; Samani et al., 2007; Zounemat-Kermani et al., 2019; Khatibi et al., 2020; Snieder et al., 2020; Abhishek et al., 2021; Kundu and Sinha, 2021). Additionally, the sigmoid and linear activation functions, commonly utilised for Earth-process modelling objectives, were employed in the hidden and output layers (Deo and Şahin, 2016; Zounemat-Kermani, 2017; Zounemat-Kermani et al., 2019). One hidden layer was chosen for FFBPNN topology based on several studies, due to its sufficient ability to simulate complex systems such as Earth or hydrological processes (Deo et al., 2019; Zounemat-Kermani et al., 2019; and Snieder et al., 2020). The ideal number of neurons (between 5 and 15) in the hidden layer was determined by means of the trial-and-error method in accordance with the MSE, and the value of 10 was selected. Fig. 2 displays the FFBPNN schematic in our study. In the current study, 70% of data were used for

train, 15% for validation, and 15% for test periods.

2.4. Meteorological drought index

This study employs the Joint Deficit Index (JDI) method for meteorological drought calculation. JDI is developed based on the Standardised Precipitation Index (SPI) and its structure (Kao and Govindaraju and Mirabbasi et al., 2010, 2013). In this study, we have applied Gamma distribution to determine SPI, and because using the JDI method is different from the standard SPI method, it is called “mod SPI.” A derived monthly drought index (mod SPI) based on JDI can simultaneously detect emerging and prolonged meteorological droughts (Mirabbasi et al., 2013). JDI represents the overall precipitation deficiency situation regarding the joint accumulative probability. JDI therefore presents a more sophisticated evaluation of the meteorological drought status.

Moreover, JDI can support monthly step meteorological drought evaluation. The amount needed for rainfall to attain normal situations in the following months can be concluded by JDI (Kao and Govindaraju, 2010; Mirabbasi et al., 2013). The classification scale of mod SPI is the same as SPI. The ranges and differences are described in Bazrafshan et al. (2015).

Because all crops in our case study are rainfed, employing a robust method for determining the meteorological drought is necessary, and could improve the trustworthiness and reliability of the results. Moreover, JDI is sensitive to previous months' droughts which is a good representer of drought (monthly and seasonal), and is effective in crop yield modelling. Crops such as winter wheat, rye, and winter barley are sensitive to precipitation during winter and spring. Other crops in our case study, such as potato and maize, are sensitive to the amount of precipitation during spring and summer (Piniewski et al., 2020). Yearly precipitation data are therefore inadequate and could increase statistical models' error and uncertainty for crop yield simulations. Furthermore, monthly precipitation indicates only the amount of precipitation in a particular month. In other words, it is independent of the previous month's precipitation. We used 30 years (1990–2019) of precipitation data to obtain a robust statistical index for drought to determine mod SPI.

2.5. Climate change scenarios

In this study, 19 GCMs under the Coupled Model Intercomparison Project – Phase 5 (CMIP5) were downscaled (Wilby and Wigley, 1997) to the RCP8.5 scenario (the concentration of carbon dioxide that delivers

Table 2

Details of climatic parameters in selected GCMs. * Moderate scenario for horizon 2021–2040 ** Moderate scenario for horizon 2041–2060. [±] Warm and dry scenario for both horizons [×] Warm and wet scenario for both horizons.

GCM	Model	2021–2040		2041–2060	
		TMP (absolute change)	PCP (relative change)	TMP (absolute change)	PCP (relative change)
GCM1	ACCESS1-3	1.20	0.11	2.92	0.03
GCM2	BCC-CSM1-1	0.90	0.01	2.20	0.01
GCM3	CanESM2	1.17	0.13	2.05	0.16
GCM4	CMCC-CM**	1.51	0.11	2.51	0.04
GCM5	CNRM-CM5	0.89	0.09	1.90	0.16
GCM6	CSIRO-MK36	1.13	0.04	2.19	0.06
GCM7	EC-EARTH	1.12	0.11	2.21	0.04
GCM8	GFDL-CM3 [×]	2.54	0.14	3.95	0.12
GCM9	GISS-E2-R-CC	1.46	0.04	2.21	0.05
GCM10	HadGEM2-ES [±]	2.19	0.00	3.23	-0.04
GCM11	INMCM4	1.10	0.08	1.20	-0.03
GCM12	IPSL-CM5A-MR	1.78	-0.02	2.80	-0.01
GCM13	MIROC5	1.98	-0.02	2.59	0.09
GCM14	MIROC-ESM	2.25	0.14	3.41	0.23
GCM15	MPI-ESM-MR	0.71	0.00	1.38	0.06
GCM16	MRI-CGCM3	0.84	0.07	1.58	0.06
GCM17	NCAR-CCSM4	1.07	-0.01	1.99	0.02
GCM18	NCAR-CESM1-CAM5*	1.46	0.05	2.77	0.09
GCM19	NorESM1-M	1.25	0.02	1.76	0.03

global warming at an average of 8.5 watts/m² by 2100) which is the worst projection according to Riahi et al. (2011), and two different time horizons (2021–2040 and 2041–2060) in the Weina catchment.

This study employed LARS-WG 6.0 built-in GCMs (Table 2). LARS-WG 6.0, containing 19 GCMs based on the IPCC Fifth Assessment Report, is a stochastic weather generator and downscaling tool for generating regional-scale climate scenarios (<https://sites.google.com/view/lars-wg/>). Precipitation, maximum and minimum temperature, and solar radiation are four weather parameters extracted from built-in GCMs in LARS-WG 6.0 (Chen et al., 2021a, <https://www.ipcc.ch/>).

The downscaling process (as well as input for statistical modelling) employed the LARS-WG 6.0 statistical downscaling model (Kolberg et al., 2019). The performance of LARS-WG 6.0 in generating historical time series was statistically acceptable (according to p-value > 0.05) for all the weather parameters. The authors wrote a script in Python to apply the climate change effect on the SWAT+ model inputs. The script reads SWAT+ input (*. PCP, *. TMP, *. SLR) and, by using the delta change method, applies the climatic changes to the input (<https://github.com/MR-Eini/SWAT-plus-climate-change-code>).

Table 2 shows all the considered climatic models and three climatic scenarios selected for further consideration based on average relative changes in precipitation (PCP) and average absolute temperature change (TMP). The first climatic scenario is the moderate scenario, the second one is the “warm and dry” scenario, and the third one is the “warm and wet” scenario. The precipitation and temperature changes of the middle GCM for each time horizon (average changes in precipitation and temperature relative to other GCMs) are selected as the moderate scenario. Considering the maximum increment in temperature and the maximum decrement in precipitation (simultaneously), the GCM of the warm and dry scenario was selected. Finally, a GCM for the warm and wet scenario was chosen based on the maximum temperature increment and precipitation increment.

Fig. 3 presents the condition of these scenarios compared to other scenarios. For the time horizon 2021–2040, NCAR-CESM1-CAM5 (moderate scenario), HadGEM2-ES (warm and dry scenario), and GFDL-CM3 (warm and wet scenario) were selected for climatic projections. Accordingly, for the time horizon 2041–2060, CMCC-CM

(moderate scenario), HadGEM2-ES (warm and dry scenario), and GFDL-CM3 (warm and wet scenario) were selected for climatic projections.

2.6. Data selection and statistical indices

This study employed Principal Component Analysis (PCA). A 2D diagram analysis approach of PCA was employed to (1) discover the relationship between weather inputs to ascertain how they correlated to or diverged from each other before starting using FFBPNN; (2) identify the similarity between crops – this step also helped select crops with higher divergencies from each other. These steps lead to a more robust and reliable statistical model, and avoid overtraining/fitting the model by decreasing the number of vectors on both sides of the model. The input and output vectors were normalised (between 0 and 1) before applying them to PCA so that all vectors have the same weight.

For evaluation and testing the accuracy of modelled datasets, NSE (Nash–Sutcliffe Efficiency), PBIAS (Percent bias), MSE (Mean Square Error), CC (coefficient of correlation), MAE (Mean Absolute Error), RMSE (Root Mean Square Error), and R-square (Coefficient of Determination) were applied. The indices are described in HydroGOF (R package). Moreover, some examples of applications, acceptable ranges, and optimum values can be found in several studies such as Eini et al. (2021b), Eini et al. (2019), Duan et al. (2016), Moriasi et al. (2015), and Ritter and Munoz-Carpena (2013).

2.7. Software, packages, and environments

The employed approaches are presented in Fig. 4 in addition to the flow chart with consecutive study steps. Moreover, the sources of the employed data, software, packages, and environments are included in Table 3. The crop yield data used for the calibration of the statistical model were extracted from the datasets mentioned in Table 3 at the Wielkopolska province level. The wet weight yield data were corrected to the dry matter yield before calibration in SWAT+.

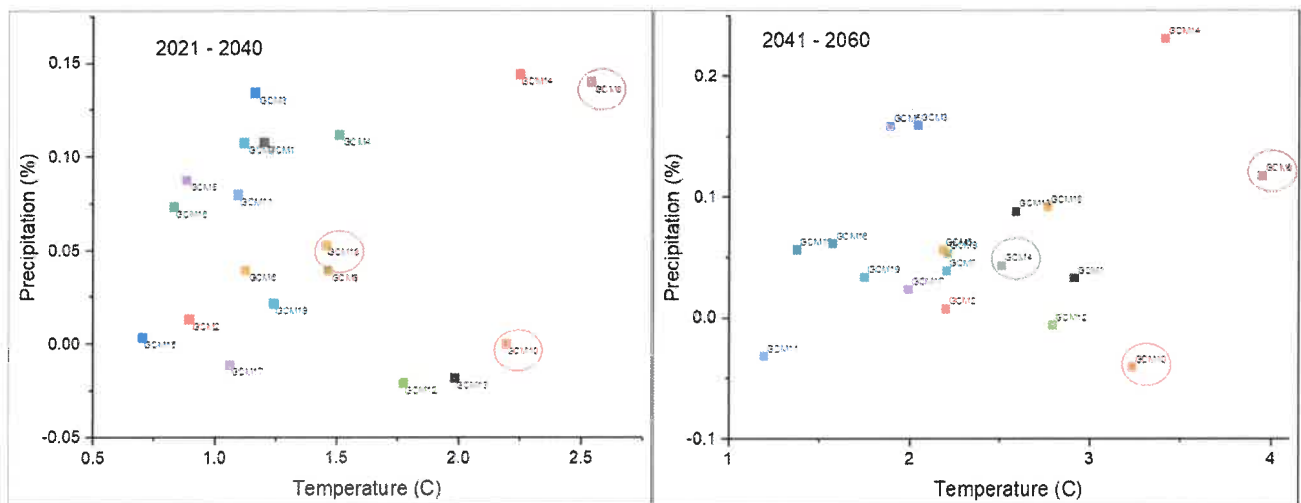


Fig. 3. Position of GCMs compared to each other for two time horizons (red circles point to the selected models).

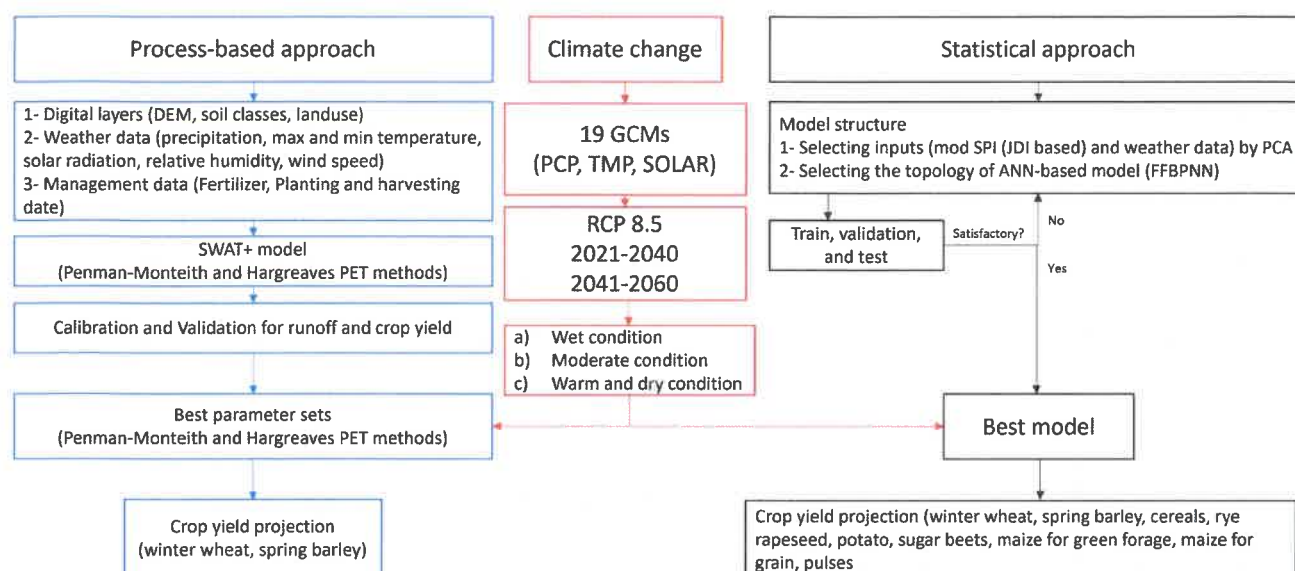


Fig. 4. Flowchart and steps of each approach and climate change investigation.

Table 3

List of employed software, packages, and environments that were used in this study.

Tool or data	Description	Source
QGIS (3.16.4)	Developing SWAT+ model, Visualization	https://www.qgis.org/en/site/
QSWAT+	Developing SWAT+ model	https://swat.tamu.edu/software/plus/
SWATplusEditor	Developing SWAT+ model	https://swat.tamu.edu/software/plus/
HydroGOF	Evaluation of statistics	https://cran.r-project.org/web/packages/hydroGOF/hydroGOF.pdf
factoextra	Extract and visualize the results of multivariate data analyses	https://cran.r-project.org/web/packages/factoextra/factoextra.pdf
ggplot2	Visualization	https://ggplot2.tidyverse.org/
SWAT+ Climate Change Code	Climate Change for SWAT+	https://github.com/MR-Eini/SWAT-plus-climate-change-code
LarsWG6	LARS-WG weather generator	https://sites.google.com/view/lars-wg/
neuralnet	Training of Neural Networks	https://cran.r-project.org/web/packages/neuralnet/neuralnet.pdf
G2DC-PL+	Climatic variables (PCP, TMP max, TMP min)	https://doi.org/10.4121/uuid:a3bed3b8-e22a-4b68-8d75-7b87109c9feb
Solar radiation	Institute of Meteorology and Water Management (IMGW-PIB)	https://danepubliczne.imgw.pl/
Crop yield records	Central Statistical Office of Poland (GUS)	https://stat.gov.pl/en/topics/agriculture-forestry/

3. Results

3.1. Data pre-processing

Time series datasets were normalised between 0 and 1, and PCA was used to identify differences and similarities between input and output data individually. The correlation coefficient matrices are shown in Table 4 for inputs (climatic parameters and mod SPI) and Table 5 for

crop yields. As presented in Table 4, a clear correlation between precipitation (mm) and mod SPI is observed. Maximum and minimum temperature (°C) and solar radiation (MJ/m²) had no strong correlation to each other, and had a negative correlation with precipitation and mod SPI. Hence, precipitation, maximum and minimum temperature, and solar radiation were included as the major variables for inputs. Using mod SPI vectors created a different structure for the FFBPNN model.

According to Table 5, 10 different crops were selected as output in

Table 4

Correlation matrix between inputs.

	PCP	Max. Temp	Min. Temp	Solar	SPI1	SPI2	SPI3	SPI4	SPI5	SPI6	SPI7	SPI8	SPI9	SPI10	SPI11	SPI12
PCP	1	-0.56	-0.14	-0.68	0.94	0.95	0.96	0.97	0.95	0.91	0.87	0.85	0.80	0.76	0.71	0.67
Max. Temp	-0.56	1	0.85	0.20	-0.52	-0.45	-0.45	-0.47	-0.46	-0.44	-0.42	-0.40	-0.38	-0.34	-0.31	-0.28
Min. Temp	-0.14	0.85	1	-0.22	-0.09	-0.03	-0.01	-0.03	-0.05	-0.05	-0.05	-0.05	-0.05	-0.03	-0.03	-0.02
Solar	-0.68	0.20	-0.22	1	-0.66	-0.71	-0.69	-0.66	-0.59	-0.51	-0.46	-0.42	-0.37	-0.32	-0.27	-0.22
SPI1	0.94	-0.52	-0.09	-0.66	1	0.98	0.96	0.95	0.91	0.87	0.83	0.80	0.76	0.71	0.66	0.60
SPI2	0.95	-0.45	-0.03	-0.71	0.98	1	0.99	0.96	0.92	0.87	0.83	0.80	0.75	0.71	0.65	0.60
SPI3	0.96	-0.45	-0.01	-0.69	0.96	0.99	1	0.99	0.96	0.92	0.88	0.86	0.82	0.77	0.72	0.67
SPI4	0.97	-0.47	-0.03	-0.66	0.95	0.96	0.99	1	0.99	0.96	0.93	0.91	0.87	0.83	0.79	0.75
SPI5	0.95	-0.46	-0.05	-0.59	0.91	0.92	0.96	0.99	1	0.99	0.97	0.95	0.93	0.90	0.86	0.82
SPI6	0.91	-0.44	-0.05	-0.51	0.87	0.87	0.92	0.96	0.99	1	0.99	0.98	0.97	0.94	0.92	0.88
SPI7	0.87	-0.42	-0.05	-0.46	0.83	0.83	0.88	0.93	0.97	0.99	1	0.99	0.98	0.97	0.95	0.92
SPI8	0.85	-0.40	-0.05	-0.42	0.80	0.80	0.86	0.91	0.95	0.98	0.99	1	0.99	0.98	0.97	0.94
SPI9	0.80	-0.38	-0.05	-0.37	0.76	0.75	0.82	0.87	0.93	0.97	0.98	0.99	1	0.99	0.99	0.97
SPI10	0.76	-0.34	-0.03	-0.32	0.71	0.71	0.77	0.83	0.90	0.94	0.97	0.98	0.99	1	0.99	0.99
SPI11	0.71	-0.31	-0.03	-0.27	0.66	0.65	0.72	0.79	0.86	0.92	0.95	0.97	0.99	0.99	1	0.99
SPI12	0.67	-0.28	-0.02	-0.22	0.60	0.60	0.67	0.75	0.82	0.88	0.92	0.94	0.97	0.99	0.99	1

Table 5
Correlation matrix between crop yields.

Crop	Winter wheat	Barley	Potato	Cereals	Basic and mixed cereals	Basic cereals	Rye	Oats	Triticale	Mixed cereals	Sugar beets	Rapeseed	Maize for grain	Maize for green forage	Pulses	Oil seed	Sunflower
A Winter wheat	1																
B Barley	0.92	1															
C Potato	0.58	0.58	1														
D Cereals	0.93	0.93	0.77	1													
E Basic and mixed cereals	0.97	0.97	0.65	0.97	1												
F Basic cereals	0.98	0.96	0.64	0.97	0.99	1											
G Rye	0.93	0.95	0.65	0.95	0.97	0.97	1										
H Oats	0.80	0.96	0.58	0.86	0.89	0.86	0.88	1									
I Triticale	0.96	0.97	0.58	0.93	0.98	0.97	0.95	0.90	1								
J Mixed cereals	0.78	0.94	0.57	0.85	0.88	0.83	0.84	0.98	0.87	1							
K Sugar beets	0.60	0.52	0.88	0.76	0.64	0.65	0.60	0.42	0.56	0.43	1						
L Rapeseed	0.71	0.62	0.15	0.56	0.64	0.67	0.58	0.45	0.69	0.42	0.30	1					
M Maize for grain	0.46	0.51	0.77	0.62	0.52	0.50	0.48	0.56	0.48	0.60	0.67	-0.01	1				
N Maize for green forage	0.54	0.58	0.77	0.68	0.60	0.57	0.56	0.62	0.53	0.65	0.68	0.04	0.97	1			
O Pulses	0.27	0.47	0.03	0.23	0.33	0.29	0.35	0.61	0.42	0.56	-0.22	0.24	0.22	0.22	1		
P Oil seed	0.39	0.39	-0.17	0.23	0.36	0.35	0.30	0.40	0.46	0.37	-0.16	0.63	-0.09	-0.08	0.54	1	
Q Sunflower	0.16	0.04	0.25	0.10	0.10	0.11	0.08	0.07	0.10	0.01	0.17	-0.07	0.18	0.12	0.18	0.03	1

FFBPNN. We have excluded basic and mixed cereals, basic cereals, oats, triticale, mixed cereals, oil seed, and sunflower due to high correlation with other crops and incomplete time series in some of the crops (i.e. sunflower). Winter wheat, barley, potato, rye, sugar beet, rapeseed, maize for grain, maize for green forage, and pulses show the most negligible correlation. These can be counted as the major crops relative to other crops in the study area (Fig. 5). The red and pink points in Fig. 5 depict the number of years (i.e. 1999 is 1, 2000 is 2, and so on). Fig. 5 also shows that crops are clustered into three major groups in the PCA plot: (1) cereals (2) root crops and maize; (3) rapeseed, oil seed and pulses. Sunflower is an outlier, possibly due to missing data. According to Table 5, almost all the crops have the least correlation with sunflower, pulses, and oil seed.

3.2. Process-based approach

Based on the SWAT+ model, next to runoff (details described in Eini et al., 2022a), crop yields of winter wheat and spring barley were calibrated by means of two different PET methods.

The outputs of the model and observed values are presented in Table 6. The violin plot in Fig. 6 depicts the variation of SWAT+ results, which is much higher than in the observed dataset. According to Fig. 7, Penman-Monteith method shows higher crop yields (i.e., winter wheat and spring barley) in the wet years (with very wet 2010 being an exception), while, for lower crop yields, both PET methods have rather close crop yields. Moreover, in dry 2006 characterized by low crop yields, both PET methods simulated considerably lower values than the observed ones. In addition, in 2015, a year with severe drought in Central Europe (Ionita et al., 2017; Laaha et al., 2017) observed crop yields did not experience a considerable decrement, but both PET methods had lower crop yields than the observed data. The reason may be that drought conditions developed in August, thus affecting mainly late harvest crops, whereas winter wheat and spring barley are harvested early and suffer mostly from spring droughts (Piniewski et al., 2020; Oleksiak et al., 2022).

3.3. Statistical approach

The study involved testing of 14 different combinations of inputs in FFBPNN. Table 7 presents the combination of inputs and the result of training, validation, and test steps for all combinations. In this approach, all types of crops were added into the one FFBPNN model. According to R^2 and RMSE in Table 7, increasing the number of inputs improves the performance FFBPNN. According to the results, "Scenario M" had comparatively superior performance to other scenarios, and was selected as the best scenario. Moreover, it can be seen that the drought indicator has significantly improved the result of the statistical approach in crop yield simulation.

We first compared all the generated crop yields in standardised values with the observed values for the final evaluation. Fig. 8 shows the beeswarm plot and notched box plot of standardised values. According to the beeswarm plot, the FFBPNN model did not accurately simulate the maximum and minimum values, but the density of points between - 0.5 and 0.5 are close. The notched box plot shows no considerable differences for the medians. Similarly, the median and average of the FFBPNN model have the same values, and the range between the first and third quartile of the box for FFBPNN is wider than the observed data.

The analysis of individual crops is presented in a half violin plot in Fig. 9. The half violin plot is useful for the assessment of the distribution of each dataset. For example for spring barley, both datasets (FFBPNN and observed) have a similar distribution, but the generated datasets for pulses or maize for green forage show different distribution (multimodal or more than one peak) than the observed data. Fig. 9 generally shows that the variation of the generated dataset and observed dataset are in the same range, and there are no significant differences between the observed and generated values for each crop.

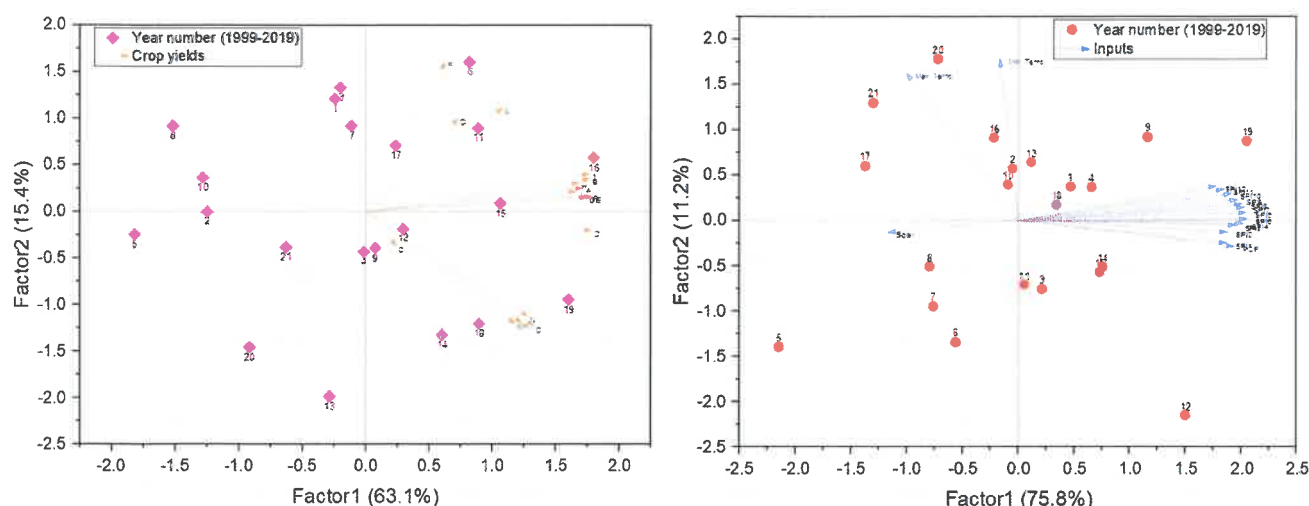


Fig. 5. PCA analysis results for inputs and outputs (see crop name codes A-Q in Table 5).

Table 6
Crop yield modelled by SWAT+ with two different PET methods.

Year	Winter Wheat			Spring Barley		
	Hargreaves	Penman-Monteith	Observed	Hargreaves	Penman-Monteith	Observed
1999	3.41	3.6	4.02	2.89	3.12	3.53
2000	4.76	5.11	3.46	4.37	4.9	2.81
2001	5.4	6.94	4.19	4.95	6.41	3.73
2002	2.46	3.13	4.18	2.42	2.62	3.55
2003	3.61	4.76	3.27	3.35	4.5	2.59
2004	3.6	3.06	4.85	2.49	2.99	4.06
2005	3.69	4.11	4.38	3.29	3.89	3.57
2006	1.96	1.95	3.46	1.54	1.87	2.87
2007	5.96	6.92	4.34	4.96	6.49	3.61
2008	3.27	2.92	3.9	2.02	2.62	2.76
2009	5.94	7.89	4.7	5.46	7.48	3.98
2010	3.53	2.92	4.58	2.49	2.52	3.72
2011	4.77	5.38	4.11	4.14	4.77	3.26
2012	5.93	6.86	4.07	5.92	6.53	3.86
2013	4.87	6.67	4.89	4.61	4.32	3.92
2014	3.56	3.11	5.21	2.26	2.6	4.36
2015	3.59	3.9	4.75	3.21	3.53	3.73
2016	5.13	5.27	4.63	4.32	4.79	3.8
2017	6.36	6.74	5.05	5.59	6.33	4.21
2018	2.21	2.29	3.86	1.95	1.98	2.84
2019	2.2	2.23	4.13	1.96	2	3.28

For a more detailed investigation, standard statistical indices are presented in Table 8. According to Table 8, FFBPNN has simulated crop yields with high accuracy for whole period. The average CC is 0.90, and MSE for sugar beets and maize for green forage is higher than the other crops due to crop yield differences. All NSE values are above 0.70, and the average of this index is 0.78, which is an acceptable result. Finally, MAE shows less than 1 ton/ha mean absolute error on average.

3.4. Effect of climate change on crop yield

This section assesses the effect of climate change on crop yields. First, we evaluated SWAT+ results using two PET methods and the statistical approach.

3.4.1. Effect of climate change on crop yields based on the process-based approach

The effect of climate change on crops is evaluated by implementing the climatic scenarios (changes in precipitation and temperature) on the calibrated model. Table 9 shows no significant decrease or increase in winter wheat and barley crop yields. On average, Penman-Monteith shows a slight decrease in crop yields in warm and dry situations. Results based on the Hargreaves method show lower variations than the Penman-Monteith method. It could be concluded that under the selected scenarios and two time horizons, crop yields are expected to not experience a notable change.

3.4.2. Effect of climate change on crop yield based on the statistical approach

According to the result for three scenarios in two different time horizons using FFBPNN, (a) the highest increases were observed in maize for green forage (9.5%) and cereals (8.1%); (b) this approach generally shows more increment in crop yield for the warm and dry scenario; (c) on average, an approximately 0.8 ton/ha increase in crop yield is expected; (d) pulses yield is estimated to decrease by approximately 2.5% in all scenarios. Table 10 presents the average changes in crop yield and percentage of change.

Results show that the FFBPNN method has estimated an increment in crop yields for all crops, excluding pulses. Only for the near period (2021–2040) under the moderate scenario, the process-based model using the Penman-Monteith method showed an increase in winter wheat yields (0.66%). In other scenarios, the yield of this crop is expected to decrease. The Hargreaves method, however, shows a positive trend for winter wheat yield under all the scenarios and periods, which is similar to FFBPNN results.

Under the warm and dry scenario (for both time horizons and PET methods), barley yields are expected to decrease (from $\sim -0.77\%$ to -4.88%). In other scenarios, a rise in barley yields is projected (0.73–5.64%). FFBPNN projects similar behaviour (increment).

4. Discussion

According to studies discussed in the introduction section, different behaviour in crop yield projections is expected using different modelling approaches under climate change conditions. In this regard, we simulated crop yields with the application of the machine learning method

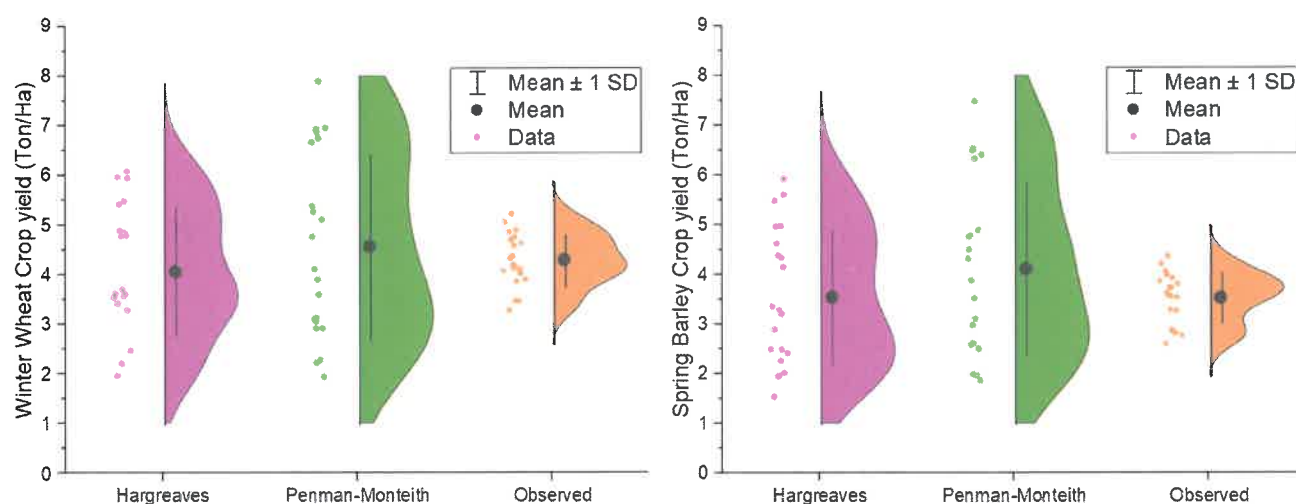


Fig. 6. Violin plot of crop yield of winter wheat and spring barley modelled by SWAT+ employing two PET methods.

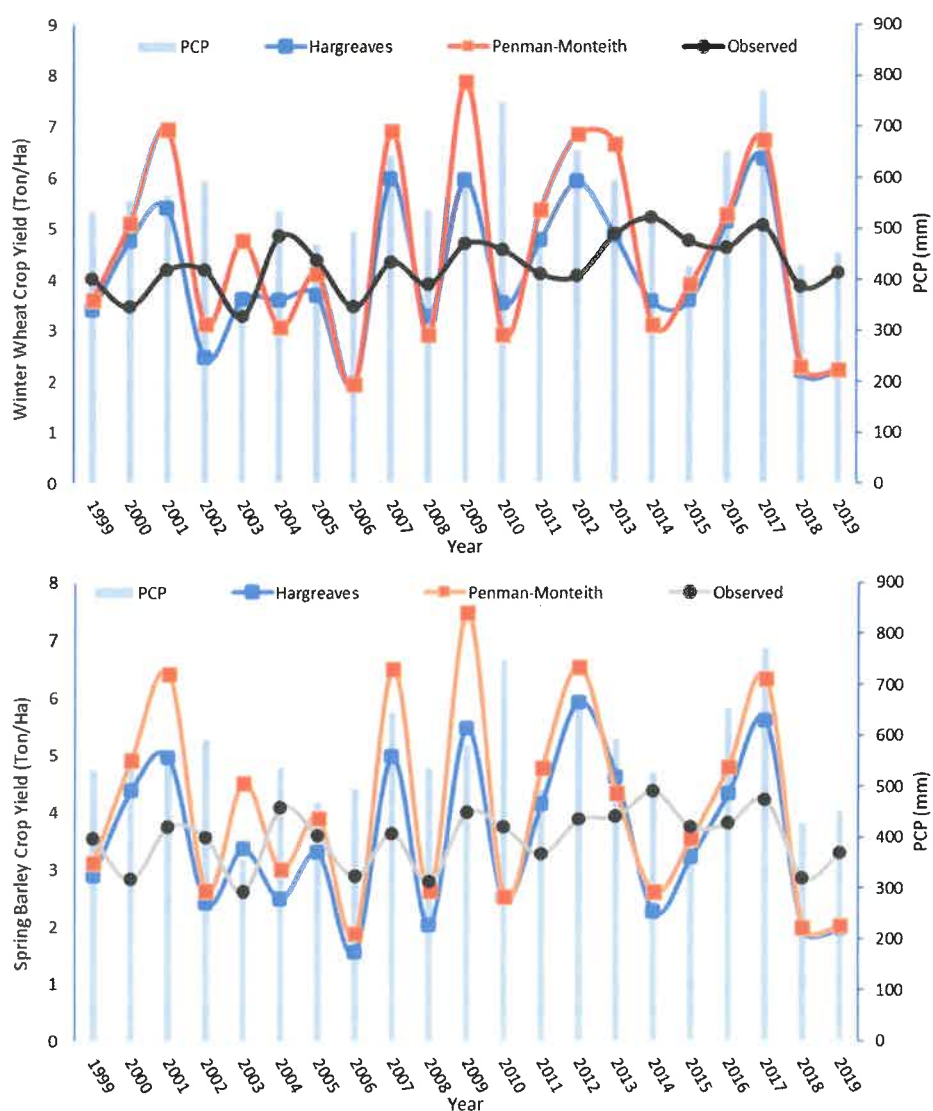


Fig. 7. Timeseries of crop yield of winter wheat and spring barley modelled by SWAT+ employing two PET methods.

Table 7

Model inputs and results of each scenario in training, validation, and test steps.

Inputs	Scenario	RMSE			R-square			
		Train	Validation	Test	Train	Validation	Test	All
PCP, TMP max, TMP min, Solar	A	0.25	0.27	0.49	0.81	0.58	0.34	0.72
PCP, TMP max, TMP min, Solar, mod SPI1	B	0.28	0.24	0.54	0.85	0.74	0.49	0.81
PCP, TMP max, TMP min, Solar, mod SPI1 to mod SPI2	C	0.29	0.45	0.50	0.64	0.71	0.21	0.72
PCP, TMP max, TMP min, Solar, mod SPI1 to mod SPI3	D	0.38	0.38	0.26	0.62	0.49	0.67	0.61
PCP, TMP max, TMP min, Solar, mod SPI1 to mod SPI4	E	0.31	0.29	0.40	0.72	0.83	0.72	0.72
PCP, TMP max, TMP min, Solar, mod SPI1 to mod SPI5	F	0.36	0.37	0.37	0.64	0.69	0.55	0.61
PCP, TMP max, TMP min, Solar, mod SPI1 to mod SPI6	G	0.36	0.30	0.55	0.55	0.69	0.34	0.53
PCP, TMP max, TMP min, Solar, mod SPI1 to mod SPI7	H	0.38	0.08	0.11	0.52	0.90	0.83	0.67
PCP, TMP max, TMP min, Solar, mod SPI1 to mod SPI8	I	0.23	0.35	0.23	0.79	0.90	0.79	0.77
PCP, TMP max, TMP min, Solar, mod SPI1 to mod SPI9	J	0.37	0.22	0.16	0.59	0.92	0.90	0.67
PCP, TMP max, TMP min, Solar, mod SPI1 to mod SPI10	K	0.38	0.28	0.14	0.56	0.64	0.92	0.66
PCP, TMP max, TMP min, Solar, mod SPI1 to mod SPI11	L	0.32	0.58	0.37	0.72	0.66	0.71	0.77
PCP, TMP max, TMP min, Solar, mod SPI1 to mod SPI12	M	0.35	0.03	0.07	0.76	0.98	0.98	0.81
PCP, TMP max, TMP min, Solar, mod SPI3, mod SPI6, mod SPI9, mod SPI12	N	0.37	0.09	0.10	0.58	0.94	0.98	0.76

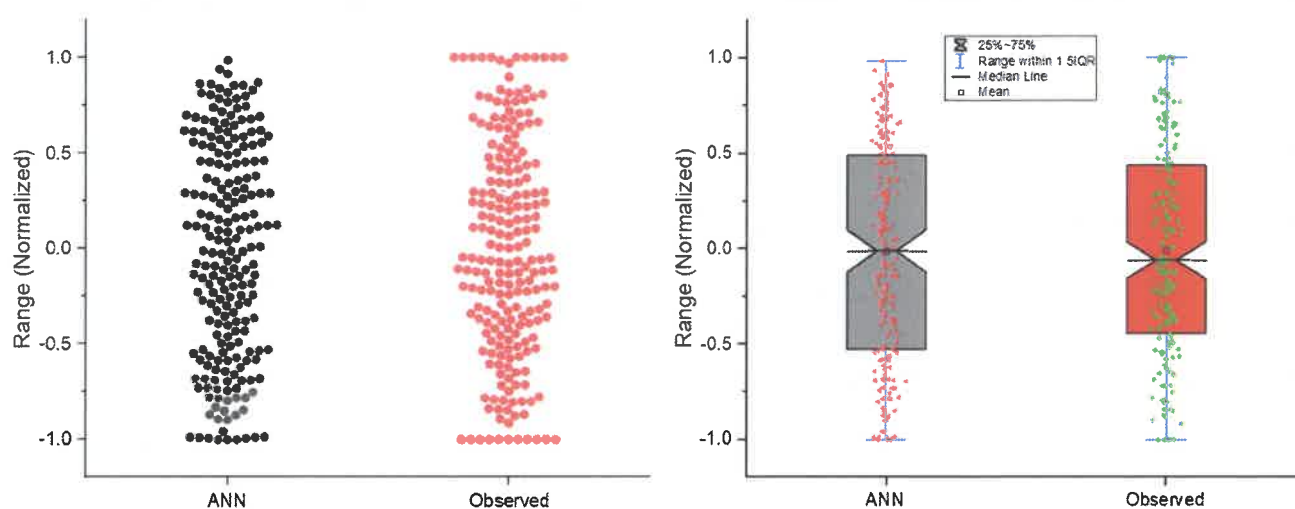
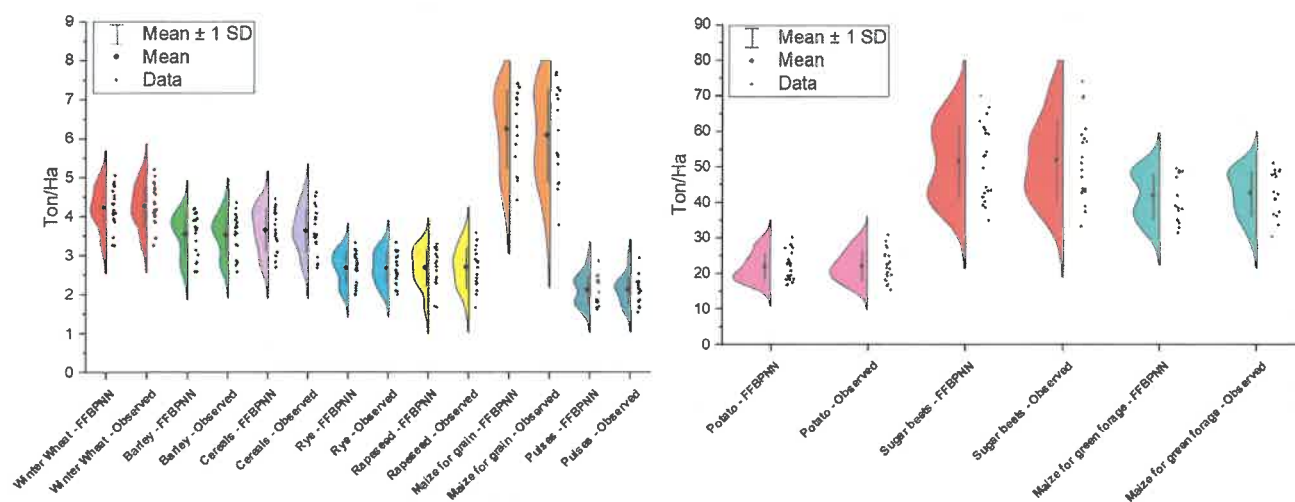
**Fig. 8.** The beeswarm plot and notched box plot of simulated crop yields and observed data.**Fig. 9.** Distribution of crop yields simulated using FFBPNN against observed values by a half violin plot for all crops.

Table 8

Accuracy of the selected FFBPNN-based model (Scenario M) for each crop.

Crop	NSE	PBIAS (%)	MSE (ton/ha)	CC	MAE (ton/ha)
Winter wheat	0.75	0.70	0.06	0.88	0.14
Spring barley	0.82	-1.00	0.05	0.91	0.15
Cereals	0.81	1.10	2.99	0.91	1.14
Rye	0.78	-0.40	0.06	0.89	0.17
Rapeseed	0.85	-0.10	0.02	0.93	0.09
Potato	0.81	-0.10	0.04	0.91	0.17
Sugar beets	0.78	0.50	23.34	0.90	3.66
Maize for green forage	0.74	1.90	10.26	0.88	2.03
Maize for grain	0.70	-2.60	0.29	0.90	0.39
Pulses	0.81	0.30	0.02	0.90	0.10

Table 9

Projection of crop yields based on SWAT+ model.

Yield (ton/ha)								
Crops	PET method	Historical	2021–2040			2041–2060		
			Moderate	Warm and dry	Warm and wet	Moderate	Warm and dry	Warm and wet
Winter Wheat	Penman-Monteith	4.56	4.59	4.39	4.47	4.54	4.31	4.44
	Hargreaves	4.11	4.19	4.17	4.21	4.14	4.12	4.17
Spring Barley	Penman-Monteith	4.1	4.13	3.91	4.17	4.15	3.9	4.14
	Hargreaves	3.9	4.1	3.87	4.11	4.12	3.78	4.12
Percentage of change								
Crops	PET method		2021–2040			2041–2060		
			Moderate	Warm and dry	Warm and wet	Moderate	Warm and dry	Warm and wet
Winter Wheat	Penman-Monteith		0.66	-3.73	-1.97	-0.44	-5.48	-2.63
	Hargreaves		1.95	1.46	2.43	0.73	0.24	1.46
Spring Barley	Penman-Monteith		0.73	-4.63	1.71	1.22	-4.88	0.98
	Hargreaves		5.13	-0.77	5.38	5.64	-3.08	5.64

Table 10

Projection of crop yields based on FFBPNN.

Yield (ton/ha)							
Crops	Historical	2021–2040			2041–2060		
		Moderate	Warm and dry	Warm and wet	Moderate	Warm and dry	Warm and wet
Winter Wheat	4.29	4.46	4.46	4.43	4.43	4.49	4.48
Barley	3.53	3.62	3.63	3.60	3.61	3.64	3.63
Potato	22.12	23.40	24.23	23.64	23.59	24.80	23.85
Rye	3.65	3.85	3.86	3.82	3.82	3.91	3.89
Rapeseed	2.70	2.77	2.78	2.75	2.76	2.80	2.77
Sugar beets	51.97	53.62	54.50	52.95	53.77	56.35	54.33
Cereals	2.70	2.82	2.81	2.79	2.81	2.82	2.82
Maize for grain	6.10	6.68	6.68	6.65	6.64	6.67	6.74
Maize for green forage	42.69	44.81	44.95	44.81	44.58	44.79	45.11
Pulses	2.13	2.07	2.08	2.06	2.08	2.09	2.06
Percentage of change							
Crops		2021–2040			2041–2060		
		Moderate	Warm and dry	Warm and wet	Moderate	Warm and dry	Warm and wet
Winter Wheat		3.94	4.01	3.39	3.37	4.63	4.52
Barley		2.78	2.85	2.21	2.33	3.20	3.05
Potato		5.76	9.52	6.83	6.62	12.08	7.81
Rye		5.45	5.71	4.73	4.74	6.96	6.55
Rapeseed		2.55	2.80	1.87	2.27	3.60	2.62
Sugar beets		3.18	4.87	1.89	3.47	8.44	4.54
Cereals		4.29	3.80	3.15	3.79	4.27	4.28
Maize for grain		9.55	9.57	9.17	8.99	9.42	10.61
Maize for green forage		4.96	5.29	4.97	4.43	4.92	5.66
Pulses		-2.60	-2.11	-3.02	-2.28	-1.77	-2.84

(FFBPN) and a process-based model (SWAT+). The machine learning method employed not only weather parameters, but also a modified SPI index. In several studies, however, soil information was critical in crop yield modelling based on a statistical approach, followed by nutrients and field management (Chlingaryan et al., 2018; Modanesi et al., 2020; Tao et al., 2020; van Klompenburg et al., 2020). These parameters, however, are still rare and largely inaccessible in many regions.

4.1. Improvements in statistical approach by drought indicators

Using climatic parameters such as precipitation, maximum and minimum temperature, and solar radiation, directly in statistical models is a common way of simulating crop yields (Conradt, 2022). In addition to these parameters, we employed SPI as a drought indicator. Our results show that employing a metrological drought index as an input can

increase the reliability of the statistical approach in crop yield modeling. Some studies in Germany and India revealed that soil moisture anomalies are a good predictor of silage maize yields, which supports our results (Peichl et al., 2018; Modanesi et al., 2020).

4.2. Accuracy of SWAT+ model and FFBPNN

We employed two different PET methods within the SWAT+ model for the process-based approach. This model proved to be a valuable tool for crop yield simulation and projections in several studies (Eini et al., 2021a; Jeyrani et al., 2021; Jiang et al., 2021; Liu et al., 2021; Delavar et al., 2022). Our result proved that SWAT+ and FFBPNN can simulate crop yield reasonably well, which is consistent with other studies (Eini et al., 2021a; Jeyrani et al., 2021; Jiang et al., 2021; Liu et al., 2021). It should be mentioned that SWAT+ simulates higher variability of crop yield compared to the observed data. This could be explained by the fact that the observed data is an average of farm-level data across an area (Wielkopolska province) larger than the catchment, making the spatially averaged yield statistics less variable. SWAT+ has a reasonable crop yield estimation in years with normal precipitation, but there are some opposite trends and correlations between observed data and models in some years.

4.3. Effect of climate change on crop yields

The effect of climate change on crop yields showed no substantial changes in winter wheat and spring barley yields based on SWAT+ . Other research, however, revealed that the average total wheat yields could increase during the future period (Salehnia et al., 2020). According to the results of three climatic projections, FFBPNN shows an increment in crop yields for warm and dry scenarios (approximately 0.8 tons/ha). Different studies show that using different models and climatic scenarios can lead to different results of crop yield projections, particularly based on machine learning methods, for both an increase and decrease under similar conditions (Çakır et al., 2014; Ewert et al., 2015; Matsumura et al., 2015; Gandhi et al., 2016; Cheng et al., 2017; Chlingaryan et al., 2018; Crane-Droesch, 2018; Tao et al., 2018; Kolberg et al., 2019; Leng and Hall, 2020; Tao et al., 2020; van Klompenburg et al., 2020; Chen et al., 2021b; Eini et al., 2021a). Studies on yield projections in Poland have been scarce to date, while there is a strong evidence on the effect of drought on decreasing yields in historical records (Łabędzki and Bak, 2017; Oleksiak et al., 2022). This study is one of the first that provides quantitative estimates of future yields.

4.4. Limitations and outlook

The aforementioned differences between these two approaches may result from the fact that FFBPNN is based on observed data and uses a statistical method to project crop yield. In contrast, SWAT+ , as a process-based model, uses empirical equations to project crop yield. Unseen situations for precipitation (mm), maximum and minimum temperature (°C), and solar radiation (MJ/m²) under climate change scenarios could be a source of uncertainty in FFBPNN results, and make the results inaccurate.

One of the hypotheses in this study was the negative effect of climate change on crop yields under RCP8.5. Our results reveal that in this region, the hypothesis could be rejected. It should be mentioned, however, that both approaches could have uncertainties due to unseen climatic situations in the calibration period, but this effect could be more critical in statistical modelling due to the fact that SWAT+ has been already implemented in areas with temperature higher than that in the current study area. The PET method also does not considerably affect crop yield projections in the study area in the process-based approach. However, we would like to recommend examining the process-based approach in more arid climatic zones where irrigation is applied. The last hypothesis was that adding a drought indicator could increase the accuracy of the

statistical model. The results of the employed statistical model show that adding SPI as an additional input parameter increases the models' accuracy, and could lead to more reliable projection results.

5. Conclusion

The study employed two different approaches to simulate and project rainfed crop yields in the Wełna catchment in Poland over the historical period 2001–2019 and two future periods (2021–2040 and 2041–2060). We found that adding a meteorological drought index as an additional input parameter improved the accuracy of our statistical approach. We also found that winter wheat and spring barley yields are projected to change very little under future climate based on SWAT+ . According to the results from FFBPNN, yields of various studied crops were projected to increase in most cases, and the highest increase was recorded for potato and grain maize.

In a wider context, there is a concern that Central Europe currently faces increased frequency and severity of droughts (Piniewski et al., 2022) strongly contributing to crop losses (Beillouin et al., 2020; Trnka et al., 2020; Brás et al., 2021). While future warming is certain, with its magnitude largely dependent on the emission scenario, future precipitation change in Central Europe is much less certain. Our results from two independent approaches show no major crop losses in north-western Poland, even under the “warm and dry” scenario. Although it is not in contrast with the existing research at the European level (see e.g. meta-analysis of Knox et al., 2016), this poses an interpretational challenge that future studies should address. Two issues are of particular interest: (1) the role of downscaling techniques; (2) the role of CO₂ effect. In the case of the former, the question is if future crop yield projections from process-based models driven by more sophisticated downscaling techniques (e.g. bias-corrected RCMs) show a different pattern than those obtained using a simple delta change method failing to take into account changes in climate variability and extreme events (Fowler et al., 2007). In the case of the latter, the globally projected increase in atmospheric CO₂ concentration adds another layer of complexity to the already complex problem, with impacts on transpiration, photosynthesis, and water use efficiency.

Declaration of Competing Interest

The authors declare that they have no known competing financial interests or personal relationships that could have appeared to influence the work reported in this paper.

Data availability

Data will be made available on request.

Acknowledgement

We would like to acknowledge the editors and four anonymous reviewers for providing insightful reviews of the manuscript, which improved the quality of the manuscript. This research was financially supported by the National Science Centre (Narodowe Centrum Nauki), Poland (PRELUDIUM BIS-1 project, UMO-2019/35/O/ST10/04392). The Institute of Meteorology and Water Management (IMGW-PIB) is acknowledged for providing hydrometeorological data.

References

- Abhishek, T., Kinouchi, Sayama, T., 2021. A comprehensive assessment of water storage dynamics and hydroclimatic extremes in the Chao Phraya River Basin during 2002–2020. *J. Hydrol.* 603, 126868.
- Allen, R.G., L.S. Pereira, D. Raes, and M. Smith, 1998, Crop evapotranspiration-Guidelines for computing crop water requirements-FAO Irrigation and drainage paper 56. Fao, Rome 300:D05109.

- Amnuaylojaroen, T., Chanvichit, P., Janta, R., Surapipith, V., 2021. Projection of rice and maize productions in northern thailand under climate change scenario RCP8.5. *Agric. -Basel* 11, 23.
- Arnold, J.G., Bieger, K., White, M.J., Srinivasan, R., Dunbar, J.A., Allen, P.M., 2018. Use of decision tables to simulate management in SWAT. *Water* 10, 713.
- Bailey, R.T., Bieger, K., Flores, L., Tomer, M., 2022. Evaluating the contribution of subsurface drainage to watershed water yield using SWAT+ with groundwater modeling. *Sci. Total Environ.* 802, 149962.
- Batal, S., A. Kumar Tripathy, and P. Bijayasingh. 2011. *Yield Prediction Using Artificial Neural Networks. Pages 315–317 in Computer Networks and Information Technologies. Springer Berlin Heidelberg, Berlin, Heidelberg.*
- Bazrafshan, J., Nadi, M., Ghorbani, K., 2015. Comparison of Empirical Copula-Based Joint Deficit Index (JDI) and Multivariate Standardized Precipitation Index (MSPJ) for Drought Monitoring in Iran. *Water Resour. Manag.* 29, 2027–2044.
- Beillouin, D., Schaubert, B., Bastos, A., Clais, P., Makowski, D., 2020. Impact of extreme weather conditions on European crop production in 2018. *Philos. Trans. R. Soc. Lond. B Biol. Sci.* 375, 20190510.
- Bieger, K., Arnold, J.G., Rathjens, H., White, M.J., Bosch, D.D., Allen, P.M., Volk, M., Srinivasan, R., 2017. Introduction to SWAT+, A Completely Restructured Version of the Soil and Water Assessment Tool. *JAWRA J. Am. Water Resour. Assoc.* 53, 115–130.
- Brás, T.A., Seixas, J., Carvalhais, N., Jägermeyr, J., 2021. Severity of drought and heatwave crop losses tripled over the last five decades in Europe. *Environ. Res. Lett.* 16, 065012.
- Çakır, Y., M. Kirci, and E.O. Güneş. 2014. *Yield prediction of wheat in south-east region of Turkey by using artificial neural networks. Pages 1–4 in 2014 The Third International Conference on Agro-Geoinformatics. IEEE.*
- Chen, C.A., Hsu, H.H., Liang, H.C., 2021a. Evaluation and comparison of CMIP6 and CMIP5 model performance in simulating the seasonal extreme precipitation in the Western North Pacific and East Asia. *Weather Clim. Extrem.* 31, 100303.
- Chen, Y., Marek, G.W., Marek, T.H., Porter, D.O., Brauer, D.K., Srinivasan, R., 2021b. Simulating the effects of agricultural production practices on water conservation and crop yields using an improved SWAT model in the Texas High Plains, USA. *Agric. Water Manag.* 244, 106574.
- Cheng, H., Damerow, L., Sun, Y.R., Blanke, M., 2017. Early yield prediction using image analysis of apple fruit and tree canopy features with neural networks. *J. Imaging* 3, 6.
- Chlingaryan, A., Sukkari, S., Whelan, B., 2018. Machine learning approaches for crop yield prediction and nitrogen status estimation in precision agriculture: A review. *Comput. Electron. Agric.* 151, 61–69.
- Conradt, T., 2021. The multiple linear regression modelling algorithm ABSOLUT v1.0 for weather-based crop yield prediction and its application to Germany at district level. *Geosci. Model Dev. Discuss.* 1–34.
- Conradt, T., 2022. Choosing multiple linear regressions for weather-based crop yield prediction with ABSOLUT v1.2 applied to the districts of Germany. *Int. J. Biometeorol.* 66 (2287–2300).
- Conradt, T., Gornott, C., Wechsung, F., 2016. Extending and improving regionalized winter wheat and silage maize yield regression models for Germany: Enhancing the predictive skill by panel definition through cluster analysis. *Agric. For. Meteorol.* 216, 68–81.
- Coulibaly, P., Ancil, F., Bobee, B., 2000. Daily reservoir inflow forecasting using artificial neural networks with stopped training approach. *J. Hydrol.* 230, 244–257.
- Crane-Droesch, A., 2018. Machine learning methods for crop yield prediction and climate change impact assessment in agriculture. *Environ. Res. Lett.* 13, 114003.
- Delavar, M., Eini, M.R., Kuchak, V.S., Zaghiyan, M.R., Shahbazi, A., Nourmohammadi, F., Motamedi, A., 2022. Model-based water accounting for integrated assessment of water resources systems at the basin scale. *Sci. Total Environ.* 830, 154810.
- Deo, R.C., Şahin, M., 2016. An extreme learning machine model for the simulation of monthly mean streamflow water level in eastern Queensland. *Environ. Monit. Assess.* 188, 90.
- Deo, R.C., Şahin, M., Adamowski, J.F., Mi, J.C., 2019. Universally deployable extreme learning machines integrated with remotely sensed MODIS satellite predictors over Australia to forecast global solar radiation: A new approach. *Renew. Sustain. Energy Rev.* 104, 235–261.
- Dinh, T.L.A., Aires, F., 2021. Using the leave-two-out method to determine the optimal statistical crop model. *Geosci. Model Dev. Discuss.* 2021, 1–23.
- Duan, Z., Liu, J., Tuo, Y., Chiogna, G., Disse, M., 2016. Evaluation of eight high spatial resolution gridded precipitation products in Adige Basin (Italy) at multiple temporal and spatial scales. *Sci. Total Environ.* 573, 1536–1553.
- Eini, M.R., Javadi, S., Delavar, M., Monteiro, J.A.F., Darand, M., 2019. High accuracy of precipitation reanalyses resulted in good river discharge simulations in a semi-arid basin. *Ecol. Eng.* 131, 107–119.
- Eini, M.R., Javadi, S., Delavar, M., Gassman, P.W., Jarihani, B., 2020. Development of alternative SWAT-based models for simulating water budget components and streamflow for a karstic-influenced watershed. *CATENA* 195, 104801.
- Eini, M.R., Javadi, S., Hashemy Shahdany, M., Kisi, O., 2021a. Comprehensive assessment and scenario simulation for the future of the hydrological processes in Dez river basin, Iran. *Water Supply* 21, 1157–1176.
- Eini, M.R., Olyaei, M.A., Kamyab, T., Teymoori, J., Brocca, L., Piniewski, M., 2021b. Evaluating three non-gauge-corrected satellite precipitation estimates by a regional gauge interpolated dataset over Iran. *J. Hydrol. -Reg. Stud.* 38, 100942.
- Eini, M.R., Rahmati, A., Piniewski, M., 2022a. Hydrological application and accuracy evaluation of PERSIANN satellite-based precipitation estimates over a humid continental climate catchment. *J. Hydrol. -Reg. Stud.* 41, 101109.
- Eini, M.R., Rahmati, A., Salmani, H., Brocca, L., Piniewski, M., 2022b. Detecting characteristics of extreme precipitation events using regional and satellite-based precipitation gridded datasets over a region in Central Europe. *Sci. Total Environ.* 852, 158497.
- Ewert, F., Rotter, R.P., Bindi, M., Webber, H., Trnka, M., Kersebaum, K.C., Olesen, J.E., van Ittersum, M.K., Janssen, S., Rivington, M., Semenov, M.A., Wallach, D., Porter, J. R., Stewart, D., Verhagen, J., Gaiser, T., Palosuo, T., Tao, F., Nendel, C., Roggero, P. P., Bartosova, L., Asseng, S., 2015. Crop modelling for integrated assessment of risk to food production from climate change. *Environ. Model. Softw.* 72, 287–303.
- Fowler, H.J., Blenkinsop, S., Tebaldi, C., 2007. Linking climate change modelling to impacts studies: recent advances in downscaling techniques for hydrological modelling. *Int. J. Climatol.* 27, 1547–1578.
- Gandhi, N., Armstrong, L.J., Petkar, O., Tripathy, A.K., 2016. Rice crop yield prediction in India using support vector machines. *Pages 1–5 2016 13th Int. Jt. Conf. Comput. Sci. Softw. Eng. (JCSSE). IEEE.*
- Gassman, P.W., Reyes, M.R., Green, C.H., Arnold, J.G., 2007. The soil and water assessment tool: Historical development, applications, and future research directions. *Trans. ASABE* 50, 1211–1250.
- Gornott, C., Wechsung, F., 2016. Statistical regression models for assessing climate impacts on crop yields: A validation study for winter wheat and silage maize in Germany. *Agric. For. Meteorol.* 217, 89–100.
- Hargreaves, G.H., Samani, Z.A., 1985. Reference crop evapotranspiration from temperature. *Appl. Eng. Agric.* 1, 96–99.
- Hsiao, C., 2014. *Analysis of Panel Data.* Cambridge University Press.
- Ionita, M., Tallaksen, L.M., Kingston, D.G., Stagge, J.H., Laaha, G., Van Lanen, H.A., Scholz, P., Chelcea, S.M., Haslinger, K., 2017. The European 2015 drought from a climatological perspective. *Hydrol. Earth Syst. Sci.* 21, 1397–1419.
- Jeyrani, F., Morid, S., Srinivasan, R., 2021. Assessing basin blue-green available water components under different management and climate scenarios using SWAT. *Agric. Water Manag.* 256, 107074.
- Jiang, F., Drohan, P.J., Gibin, R., Preisendanz, H.E., White, C.M., Veith, T.L., 2021. Reallocating crop rotation patterns improves water quality and maintains crop yield. *Agric. Syst.* 187, 103015.
- Kao, S.C., Govindaraju, R.S., 2010. A copula-based joint deficit index for droughts. *J. Hydrol.* 380, 121–134.
- Khatibi, R., Ghorbani, M.A., Naghshara, S., Aydin, H., Karimi, V., 2020. A framework for 'Inclusive Multiple Modelling' with critical views on modelling practices - Applications to modelling water levels of Caspian Sea and Lakes Urmia and Van. *J. Hydrol.* 587, 124923.
- Knoben, W., 2013. *Estimation of non-stationary hydrological model parameters for the Polish Welna catchment. University of Twente.*
- Knox, J., Daccache, A., Hess, T., Haro, D., 2016. Meta-analysis of climate impacts and uncertainty on crop yields in Europe. *Environ. Res. Lett.* 11, 113004.
- Kolberg, D., Persson, T., Mangerud, K., Riley, H., 2019. Impact of projected climate change on workability, attainable yield, profitability and farm mechanization in Norwegian spring cereals. *Soil Tillage Res.* 185, 122–138.
- Kundu, S., Sinha, R.R., 2021. Space fractional kinetic model for different types of suspension profiles in turbulent flows with a neural network-based estimation of fractional orders. *J. Hydrol.* 602, 126707.
- Laaha, G., Gauster, T., Tallaksen, L.M., Vidal, J.-P., Stahl, K., Prudhomme, C., Heudorfer, B., Vlas, R., Ionita, M., Van Lanen, H.A., 2017. The European 2015 drought from a hydrological perspective. *Hydrol. Earth Syst. Sci.* 21, 3001–3024.
- Łabędzki, L., Bąk, B., 2017. Impact of meteorological drought on crop water deficit and crop yield reduction in Polish agriculture. *J. Water Land Dev.* 34, 181–190.
- Lemaître-Basset, T., Oudin, L., Thirel, G., Collet, L., 2021. Unravelling the contribution of potential evaporation formulation to uncertainty under climate change. *Hydrol. Earth Syst. Sci. Discuss.* 2021, 1–18.
- Leng, G., Hall, J.W., 2020. Predicting spatial and temporal variability in crop yields: an inter-comparison of machine learning, regression and process-based models. *Environ. Res. Lett.* 15, 044027.
- Liu, D.T., Song, C.C., Fang, C., Xin, Z.H., Xi, J., Lu, Y.Z., 2021. A recommended nitrogen application strategy for high crop yield and low environmental pollution at a basin scale. *Sci. Total Environ.* 792, 148464.
- Lv, C., Xing, Y., Zhang, J., Na, X., Li, Y., Liu, T., Cao, D., Wang, F.-Y., 2017. Levenberg–Marquardt backpropagation training of multilayer neural networks for state estimation of a safety-critical cyber-physical system. *IEEE Trans. Ind. Inform.* 14, 3436–3446.
- Marcinkowski, P., Kardel, I., Placzkowska, E., Gielczewski, M., Osuch, P., Okruszko, T., Venegas-Cordero, N., Ignar, S., Piniewski, M., 2021. High-resolution simulated water balance and streamflow data set for 1951–2020 for the territory of Poland. *Geosci Data J.*
- Matsumura, K., Gaitan, C.F., Sugimoto, K., Cannon, A.J., Hsieh, W.W., 2015. Maize yield forecasting by linear regression and artificial neural networks in Jilin, China. *J. Agric. Sci.* 153, 399–410.
- Mirabbasi, R., Anagnostou, E.N., Fakheri-Fard, A., Dinpashoh, Y., Eslamian, S., 2013. Analysis of meteorological drought in northwest Iran using the Joint Deficit Index. *J. Hydrol.* 492, 35–48.
- Modanesi, S., Massari, C., Camici, S., Brocca, L., Amannath, G., 2020. Do Satellite Surface Soil Moisture Observations Better Retain Information About Crop-Yield Variability in Drought Conditions? *Water Resour. Res.* 56 e2019WR025855.
- Moriasi, D.N., Gitau, M.W., Pai, N., Dagupati, P., 2015. Hydrologic and Water Quality Models: Performance Measures and Evaluation Criteria. *Trans. ASABE* 58, 1763–1785.
- Musyoka, F.K., Strauss, P., Zhao, G.J., Srinivasan, R., Klik, A., 2021. Multi-Step Calibration Approach for SWAT Model Using Soil Moisture and Crop Yields in a Small Agricultural Catchment. *Water* 13, 2238.

- Nair, S.S., King, K.W., Witter, J.D., Sohngen, B.L., Fausey, N.R., 2011. Importance of crop yield in calibrating watershed water quality simulation tools 1. JAWRA J. Am. Water Resour. Assoc. 47, 1285–1297.
- Nkwasa, A., Chawanda, C.J., Jagermeyr, J., van Griensven, A., 2022. Improved representation of agricultural land use and crop management for large-scale hydrological impact simulation in Africa using SWAT. Hydrol. Earth Syst. Sci. 26, 71–89.
- Oleksiak, T., Spyroglou, I., Paoñ, D., Matysik, P., Pernisová, M., Rybka, K., 2022. Effect of drought on wheat production in Poland between 1961 and 2019. Crop Sci. 62, 728–743.
- Pachauri, R.K., M.R. Allen, V.R. Barros, J. Broome, W. Cramer, R. Christ, J.A. Church, L. Clarke, Q. Dahe, and P. Dasgupta. 2014. **Climate change 2014: synthesis report. Contribution of Working Groups I, II and III to the fifth assessment report of the Intergovernmental Panel on Climate Change. Ipcc.**
- Peichl, M., Thober, S., Meyer, V., Samaniego, L., 2018. The effect of soil moisture anomalies on maize yield in Germany. Nat. Hazards Earth Syst. Sci. 18, 889–906.
- Piniewski, M., Szczesniak, M., Kardel, I., Berezowski, T., Okruszko, T., Srinivasan, R., Schuler, D.V., Kundzewicz, Z.W., 2017. Hydrological modelling of the Vistula and Odra river basins using SWAT. Hydrol. Sci. J. -J. Des. Sci. Hydrol. 62, 1266–1289.
- Piniewski, M., Marcinkowski, P., O'Keeffe, J., Szczesniak, M., Nierobca, A., Kozyra, J., Kundzewicz, Z.W., Okruszko, T., 2020. Model-based reconstruction and projections of soil moisture anomalies and crop losses in Poland. Theor. Appl. Climatol. 140, 691–708.
- Piniewski, M., Eini, M.R., Chattopadhyay, S., Okruszko, T., Kundzewicz, Z.W., 2022. Is there a coherence in observed and projected changes in riverine low flow indices across Central Europe? Earth-Sci. Rev. 233, 104187.
- Riahi, K., Rao, S., Krey, V., Cho, C., Chirkov, V., Fischer, G., Kindermann, G., Nakicenovic, N., Rafaj, P., 2011. RCP 8.5—A scenario of comparatively high greenhouse gas emissions. Clim. Change 109, 33–57.
- Ritter, A., Munoz-Carpena, R., 2013. Performance evaluation of hydrological models: Statistical significance for reducing subjectivity in goodness-of-fit assessments. J. Hydrol. 480, 33–45.
- Ruane, A.C., Rosenzweig, C., Asseng, S., Boote, K.J., Elliott, J., Ewert, F., Jones, J.W., Martre, P., McDermid, S.P., Muller, C., Snyder, A., Thorburn, P.J., 2017. An AgMIP framework for improved agricultural representation in integrated assessment models. Environ. Res. Lett. 12, 125003.
- Ruß, G., Kruse, R., 2010. Regression Models for Spatial Data: An Example from Precision Agriculture. Pages 450–463 in *Advances in Data Mining. Applications and Theoretical Aspects*. Springer Berlin Heidelberg, Berlin, Heidelberg.
- Ruß, G., Kruse, R., Schneider, M., Wagner, P., 2008. Data mining with neural networks for wheat yield prediction. Pages 47–56 in *Industrial Conference on Data Mining*. Springer.
- Sabzadeh, I., Shourian, M., 2020. Maximizing crops yield net benefit in a groundwater-irrigated plain constrained to aquifer stable depletion using a coupled PSO-SWAT-MODFLOW hydro-agronomic model. J. Clean. Prod. 262, 121349.
- Salehnia, N., Salehnia, N., Torshizi, A.S., Kolsoumi, S., 2020. Rainfed wheat (*Triticum aestivum* L.) yield prediction using economical, meteorological, and drought indicators through pooled panel data and statistical downscaling. Ecol. Indic. 111, 105991.
- Samani, N., Gohari-Moghadam, M., Safavi, A.A., 2007. A simple neural network model for the determination of aquifer parameters. J. Hydrol. 340, 1–11.
- Shinde, S., Wadhwa, L., Bhalke, D., 2021. Feedforward Back Propagation Neural Network (FFBPNN) Based Approach for the Identification of Handwritten Math Equations. Springer International Publishing, Cham., pp. 757–775.
- Siniecki, 2009. The role of small retention and water cooperatives in water management illustrated by the River Wena case study. Ecol. Issues 83.
- Snieder, E., Shakir, R., Khan, U.T., 2020. A comprehensive comparison of four input variable selection methods for artificial neural network flow forecasting models. J. Hydrol. 583, 124299.
- Tan, M.L., Gassman, P.W., Liang, J., Haywood, J.M., 2021. A review of alternative climate products for SWAT modelling: Sources, assessment and future directions. Sci. Total Environ. 795, 148915.
- Tao, F., Rotter, R.P., Palosuo, T., Gregorio Hernandez Diaz-Ambrona, C., Minguez, M.I., Semenov, M.A., Kersebaum, K.C., Nendel, C., Specka, X., Hoffmann, H., Ewert, F., Dambreville, A., Martre, P., Rodriguez, L., Ruiz-Ramos, M., Gaiser, T., Hohn, J.G., Salo, T., Ferrise, R., Bindi, M., Cammarano, D., Schulman, A.H., 2018. Contribution of crop model structure, parameters and climate projections to uncertainty in climate change impact assessments. Glob. Chang. Biol. 24, 1291–1307.
- Tao, F., Palosuo, T., Rötter, R.P., Díaz-Ambrona, C.G.H., Inés Minguez, M., Semenov, M. A., Kersebaum, K.C., Cammarano, D., Specka, X., Nendel, C., Srivastava, A.K., Ewert, F., Padovan, G., Ferrise, R., Martre, P., Rodríguez, L., Ruiz-Ramos, M., Gaiser, T., Höhn, J.G., Salo, T., Dibari, C., Schulman, A.H., 2020. Why do crop models diverge substantially in climate impact projections? A comprehensive analysis based on eight barley crop models. Agric. For. Meteorol. 281, 107851.
- Tomczyk, A.M., Piniewski, M., Eini, M.R., Bednorz, E., 2022. Projections of changes in maximum air temperature and hot days in Poland. Int. J. Climatol. 42, 5242–5254.
- Trajkovic, S., 2007. Hargreaves versus Penman-Monteith under humid conditions. J. Irrig. Drain. Eng. 133, 38–42.
- Traore, B., Corbeels, M., van Wijk, M.T., Rufino, M.C., Giller, K.E., 2013. Effects of climate variability and climate change on crop production in southern Mali. Eur. J. Agron. 49, 115–125.
- Trnka, M., Hlavinka, P., Mozyr, M., Semerádova, D., Stepanek, P., Balek, J., Bartosova, L., Zahradnick, P., Blahova, M., Skalák, P., Farda, A., Hayes, M., Vyboda, M., Wagner, W., Eitzinger, J., Fischer, M., Zalud, Z., 2020. Czech Drought Monitor System for monitoring and forecasting agricultural drought and drought impacts. Int. J. Climatol. 40, 5941–5958.
- van Klompenburg, T., Kassahun, A., Catal, C., 2020. Crop yield prediction using machine learning: A systematic literature review. Comput. Electron. Agric. 177, 105709.
- Wagner, P.D., Bieger, K., Arnold, J.G., Fohrer, N., 2022. Representation of hydrological processes in a rural lowland catchment in Northern Germany using SWAT and SWAT. Hydrol. Process. 36, e14589.
- Wilby, R.L., Wigley, T.M., 1997. Downscaling general circulation model output: a review of methods and limitations. Prog. Phys. Geogr. 21, 530–548.
- Williams, J.R., Jones, C.A., Kiniry, J.R., Spaniel, D.A., 1989. The epic crop growth-model. Trans. ASAE 32, 497–511.
- Wira, 2011. Evaluation of impact of selected physical and biological indices upon quality of water in the Welna. Sci. Pap. Civ. Eng. Shap. Environ. 3.
- World-Bank, 2005. Agricultural growth for the poor: an agenda for development. World Bank.
- Zepeda, L., 2001. Agricultural investment and productivity in developing countries. Food Agric. Org.
- Zounemat-Kermani, M., 2017. Assessment of several nonlinear methods in forecasting suspended sediment concentration in streams. Hydrol. Res. 48, 1240–1252.
- Zounemat-Kermani, M., Seo, Y., Kim, S., Ghorbani, M.A., Samadianfard, S., Naghsara, S., Kim, N.W., Singh, V.P., 2019. Can Decomposition Approaches Always Enhance Soft Computing Models? Predicting the Dissolved Oxygen Concentration in the St. Johns River, Florida. Appl. Sci. 9, 2534.

Warsaw, 26/03/2024

Mohammadreza Einikarimkandi
d003066@sggw.edu.pl

**Institute of Environmental Engineering,
Mining, and Energy, Discipline
Council
of the Warsaw University of Life
Sciences**

Co-authorship statement

I hereby represent that in the below publication “Eini, M. R., Salmani, H., & Piniewski, M. (2023). Comparison of process-based and statistical approaches for simulation and projections of rainfed crop yields. *Agricultural Water Management*, 277, 108107. <https://doi.org/10.1016/j.agwat.2022.108107>” my individual contribution in the development thereof involved, Conceptualization, methodology, software, validation, writing – original draft, writing – review & editing, visualization.


Signature
Mohammad Reza
Eini Karimkandi

Madrid, 26/03/2024

Haniyeh Salmani
haniyeh.salmani@usal.es

**Institute of Environmental Engineering,
Mining, and Energy, Discipline
Council
of the Warsaw University of Life
Sciences**

Co-authorship statement

I hereby represent that in the publication Eini, M. R., Salmani, H., & Piniewski, M. (2023). Comparison of process-based and statistical approaches for simulation and projections of rainfed crop yields. Agricultural Water Management, 277, 108107. <https://doi.org/10.1016/j.agwat.2022.108107>

my individual contribution in the development thereof involved software, reading and editing the manuscript and literature review.

H. Salmani
Signature

Warsaw, 26/03/2024

Dr hab. Mikołaj Piniewski, prof. SGGW
Department of Hydrology, Meteorology and Water Management
Institute of Environmental Engineering
Warsaw University of Life Sciences
mikolaj_piniewski@sggw.edu.pl

**Institute of Environmental Engineering,
Mining, and Energy, Discipline
Council**

**of the Warsaw University of Life
Sciences**

Co-authorship statement

I hereby represent that in the below publication “Eini, M. R., Salmani, H., & Piniewski, M. (2023). Comparison of process-based and statistical approaches for simulation and projections of rainfed crop yields. Agricultural Water Management, 277, 108107. <https://doi.org/10.1016/j.agwat.2022.108107>” my individual contribution in the development thereof involved, conceptualization, methodology, writing – review & editing.



Signature

12. Publication 4

Eini, M. R., Massari, C., & Piniewski, M. (2023). Satellite-based soil moisture enhances the reliability of agro-hydrological modeling in large transboundary river basins. *Science of the Total Environment*, 873, 162396.
<https://doi.org/10.1016/j.scitotenv.2023.162396>

Impact factor: 9.8 – MeiN: 200



Satellite-based soil moisture enhances the reliability of agro-hydrological modeling in large transboundary river basins

Mohammad Reza Eini^{a,*}, Christian Massari^b, Mikołaj Piniewski^a

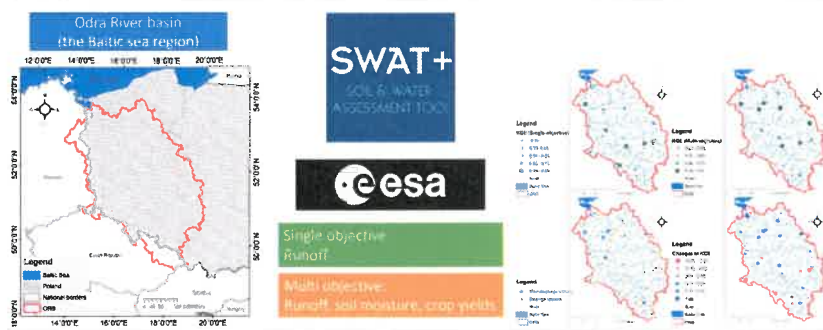
^a Department of Hydrology, Meteorology, and Water Management, Institute of Environmental Engineering, Warsaw University of Life Sciences, Warsaw, Poland

^b Research Institute for Geo-Hydrological Protection, National Research Council, Perugia, Italy

HIGHLIGHTS

- Satellite-based soil moisture (CCI) was used to calibrate the SWAT+ model.
- Single- and multi-objective strategies were employed in runoff of crop yield simulations.
- Model-based soil moisture was calibrated for two layers via employing the SWI index.
- CCI could improve the reliability of the SWAT+ model in transboundary river basins.

GRAPHICAL ABSTRACT



ARTICLE INFO

Editor: Fernando A.L. Pacheco

Keywords:
Hydrology
Gridded datasets
Flood
Drought
Remote sensing

ABSTRACT

Satellite-based observations of soil moisture, leaf area index, precipitation, and evapotranspiration facilitate agro-hydrological modeling thanks to the spatially distributed information. In this study, the Climate Change Initiative Soil Moisture dataset (CCI SM, a product of the European Space Agency (ESA)) adjusted based on Soil Water Index (SWI) was used as an additional (in relation to discharge) observed dataset in agro-hydrological modeling over a large-scale transboundary river basin (Odra River Basin) in the Baltic Sea region. This basin is located in Central Europe within Poland, Czech Republic, and Germany and drains into the Baltic Sea. The Soil and Water Assessment Tool+ (SWAT+) model was selected for agro-hydrological modeling, and measured data from 26 river discharge stations and soil moisture from CCI SM (for topsoil and entire soil profile) over 1476 sub-basins were used in model calibration for the period 1997–2019. Kling–Gupta efficiency (KGE) and SPATIAL EFFICIENCY (SPAEP) indices were chosen as objective functions for runoff and soil moisture calibration, respectively. Two calibration strategies were compared: one involving only river discharge data (single-objective - SO), and the second one involving river discharge and satellite-based soil moisture (multi-objective - MO). In the SO approach, the average KGE for discharge was above 0.60, whereas in the MO approach, it increased to 0.67. The SPAEP values showed that SWAT+ has acceptable accuracy in soil moisture simulations. Moreover, crop yield assessments showed that MO calibration also increases the crop yield simulation accuracy. The results show that in this transboundary river basin, adding satellite-based soil moisture into the calibration process could improve the accuracy and consistency of agro-hydrological modeling.

* Corresponding author.

E-mail addresses: mohammad_eini@sggw.edu.pl (M.R. Eini), christian.massari@irpi.cnr.it (C. Massari), mikolaj_piniewski@sggw.edu.pl (M. Piniewski).

1. Introduction

Several complex processes, such as interactions between groundwater and surface water, river flows, crop-related processes, nutrient transport, and anthropogenic effects occur simultaneously in river basins (Fernandez-Palomino et al., 2021; Koohi et al., 2022; Ma et al., 2019). Though understanding these processes on small scales, such as laboratory or controlled farms, seems straightforward, but in the real world, with numerous unpredictable effects on these processes, analyzing and finding precise relations between them is almost unattainable (Fernandez-Palomino et al., 2021; Guse et al., 2016; McDonnell et al., 2007; Sivapalan et al., 2012; Triana et al., 2019). Due to the high variability in the real world, similar farms in the same region by employing the same farm management plan could have different crop yields, or similar water-saving plans in different regions could have totally different outputs (Feng et al., 2006; Fohrer et al., 2001; Gupta et al., 2006; Montanari and Koutsoyiannis, 2012).

In this regard, several types of hydrological models as managerial tools are developed to simulate and project the consequence of different possible scenarios (Devia et al., 2015; Sood and Smakhtin, 2015). In the realm of hydrology, distributed hydrological models are widely used to comprehensively simulate the effects of human-caused activities such as land use changes, and natural-caused effects such as heatwaves and extreme precipitation events on water quantity, quality and crops (Alfieri et al., 2022; Delavar et al., 2022; Eini et al., 2020; Eini et al., 2022a; Ilampooranan et al., 2021; Ma et al., 2019). In several studies, distributed hydrological models have been calibrated only by considering runoff. However, other elements of the hydrological process, such as the share of evapotranspiration in water balance or infiltration rate, can be misrepresented by models; for example, assessing the effect of climate change on the water balance in an intensively irrigated area is not solid when a hydrological model is calibrated only by focusing on runoff (Gupta et al., 2006; Montanari and Koutsoyiannis, 2012; Pokhrel et al., 2012). It is reported that selecting different parameter sets can lead to similarly good results for simulated discharge, which is referred to as equifinality (Abbaspour, 2022; Beven, 2006). One of the possible ways to avoid equifinality is multi-objective calibration, i.e. employing in calibration additional temporal and spatial variables, such as crop yields, soil moisture, base flow, potential and actual evapotranspiration, leaf area index (LAI), infiltration, biomass index, and tile flow can be included in calibration processes (Alfieri et al., 2022; Azimi et al., 2020; Brocca et al., 2017; Brocca et al., 2020; Ciabatta et al., 2016; De Santis et al., 2021; Fernandez-Palomino et al., 2021; Pfannerstill et al., 2017; Pokhrel et al., 2012). For example, Ilampooranan et al. (2021) have used crops as a sensor to increase the reliability of the hydrological model in an agricultural watershed in Iowa. In their research, crop yield calibration reduced the model's parameter uncertainty and predictive ability. Distributed variables such as crop yield, Soil Moisture (SM), and LAI are helpful variables in the calibration step to increase the runoff accuracy and the accuracy of ET or general water balance components (Ilampooranan et al., 2021).

Achieving accurate results by employing hydrological models could be a particular challenge for hydrologists in trans-boundary basins, when adequate measured data is not available freely or the available datasets have different accuracy or resolutions (Aslam et al., 2020; De Lannoy et al., 2022; Hirbo Gelebo et al., 2022; Liersch et al., 2017; Mianabadi et al., 2020; Rougé et al., 2018). The importance of hydrological assessments in transboundary basins is not only related to the comprehensive evaluation of water balance but has an impact on the issues related to international conflict management strategies and sustainable basin-wide management, particularly in the era of climate change (Hajihosseini et al., 2020; Hirbo Gelebo et al., 2022; Khan et al., 2017; Liersch et al., 2017; Mianabadi et al., 2020; Rougé et al., 2018).

Global gridded datasets have been employed to deal with gaps in the datasets, inadequately measured datasets, or entirely unavailable datasets (Beck et al., 2017; Eini et al., 2019; Eini et al., 2021b; Koohi et al., 2021). Generally, these global (or regional) datasets can be categorized into three groups: purely ground-based, satellite-based, and the combined first

two datasets (Brocca et al., 2019; Eini et al., 2019; Eini et al., 2021b; Piniewski et al., 2021). In recent years, remotely sensed datasets have been widely applied in hydrology for calibration and validation steps of models and as ancillary datasets, such as meteorological data, in the set-up step (Alfieri et al., 2022; Eini et al., 2022a). It is highlighted that satellite products can improve the consistency of distributed hydrological models by providing spatially distributed data (Ilampooranan et al., 2021; Ren et al., 2018). Finally, in several studies, the accuracy of results is enhanced by adding new processes or modifying default empirical equations in process-based models (Delavar et al., 2022; Delavar et al., 2020; Eini et al., 2020). All of the mentioned approaches eventually could enhance the model's results for the water balance simulations at the basin scale.

Soil moisture (SM) is one of the most important variables linking energy and water cycle and its knowledge is strategic both for runoff formation and crop development (Azimi et al., 2020; Brocca et al., 2017). This variable, which covers the basin area, influences runoff, land-atmosphere carbon fluxes, vegetation, and evapotranspiration processes (Azimi et al., 2020; Brocca et al., 2020; De Santis et al., 2021; Lal, 2004; Or et al., 2013). In the real world, SM varies not only temporally and in two spatial dimensions but also vertically. Since meteorological parameters, soil texture, land cover and land use, groundwater water table level, and topography are effective on SM, thus, ground-based measuring of this variable requires a large network of spots. Moreover, the model uses parameterization of soil and land cover and climate forcing, which is not always accurate. So having spatially distributed information on soil moisture is paramount to improving their skills and building a robust system (Massari et al., 2014; Ochsner et al., 2013). Gravimetric sampling or Time Domain Reflectometry (TDR) can be considered as the most feasible measurement techniques for determining SM. Simple mechanisms and the capability to determine SM at various depths are the advantages, while being costly and time-consuming are the disadvantages of this method (Azimi et al., 2020; Huisman et al., 2001).

To overcome this issue, SM satellite-based products could be an alternative of in-situ measurements. According to the literature, several SM products from different satellites are available and usable in hydrological simulations. Three satellite missions have been particularly launched for the SM measurements (in 2006, The Advanced Scatterometer (ASCAT), in 2010, the Soil Moisture Ocean Salinity- (SMOS) and, in 2015, the Soil Moisture Active and Passive mission SMAP) (Entekhabi et al., 2010; Kerr et al., 2010; Wagner et al., 2013). One of the largest projects belongs to European Space Agency (ESA), namely, the Soil Moisture CCI project (<https://esa-soilmoisture-cci.org/>) which uses several active and passive sensors on 13 satellites to provide a globally gridded SM dataset (Brocca et al., 2011; Dorigo et al., 2017). The global SM satellite-based datasets have successfully been applied in flood and runoff modeling in different regions. However, the small infiltration depth (less than 50 mm) and the large spatial resolution (more than 25 km) of the SM products cause critical challenges in hydrological modeling (Azimi et al., 2020; Brocca et al., 2017; Brocca et al., 2011; De Santis et al., 2021; Modanesi et al., 2020). Moreover, Modanesi et al. (2020) stressed the importance of satellite surface soil moisture datasets to provide the highest level of information about the impacts of dry and drought conditions on crop yields in India.

As an agro-hydrological model, the Soil and Water Assessment Tool (SWAT) has been globally employed in simulating agro-hydrological processes, such as surface runoff, evapotranspiration, crop growth, vegetation dynamics, and snow melt (Akoko et al., 2021; Eini et al., 2023; Gassman et al., 2014; Piniewski et al., 2017; Tan et al., 2019; van Griensven et al., 2012; Wang et al., 2019). This model by providing a wide range of tools, such as farm management modules (e.g., irrigation, fertilizer, tillage, grazing, and pesticide), daily and sub-daily runoff modules, land use changes module, water quality module, crop growth module, and options for implementing man-made structures, facilitates users to have comprehensive and reliable assessments of the hydrological cycle within a catchment (Arnold et al., 2012; Gassman et al., 2007). In addition, this model is freely available, and users can modify the core of the model for different purposes (Delavar et al., 2022; Eini et al., 2020). An enhanced version of this model, entitled SWAT+, was recently released (Bieger et al., 2019;

Bieger et al., 2017; Wagner et al., 2022). The new version is extensively changed and provides decision tables in the modeling process to improve the realism of farm management and reservoir operation (Arnold et al., 2018; Wu et al., 2020). In addition, in the SWAT+ model, the new “gwflow” module is included for entirely connected interactions between surface and groundwater simulations (Bailey et al., 2022; Bailey et al., 2020). Several studies have forced SWAT to run or calibrate with remotely sensed datasets. Satellite-based products, such as SM, leaf area index, precipitation, temperature, evapotranspiration, and land use maps, are used in both SWAT configuration and calibration steps (Azimi et al., 2020; Eini et al., 2019; Eini et al., 2022a; Ma et al., 2019; Pfannerstill et al., 2017). The key highlight of these studies is calibration SWAT with satellite-based products enhances model performance. Moreover, multi objective calibration helps to reduce uncertainty range and equifinality of SWAT, especially by employing remotely sensed datasets (Kundu et al., 2017; Rajib and Merwade, 2016; Rajib et al., 2016). Still, according to the literature, application of satellite-based SM in the calibration of the SWAT model in transboundary river basins and different depth of soil is assessed in few studies; in addition, in this study, a new performance indicator (SPAtial Efficiency (SPAEF), Demirel et al. (2018)) is used to evaluate the accuracy of SM as a spatial variable. This indicator is developed particularly for spatially distributed variables, and the advantages of employing this indicator is discussed in Demirel et al. (2018).

In this study, a modified version of the SWAT+ model for the first time was calibrated by employing a multi-objective modeling approach that involved not only discharge stations, but also the CCI-SM product (remotely sensed dataset). Two calibration scenarios were tested: the first, conventional one, employing discharge data; and the second one, employing both discharge and satellite-based SM data. The effect of multi objective scenario and single objective scenario on crop yields also was assessed. The Odra (Oder) River Basin (ORB), a large-scale transboundary river basin in Central Europe that drains water from areas in the Czech Republic, Poland, and Germany to the Baltic Sea, is selected as the study area (Eini et al., 2022b; Piniewski et al., 2017).

2. Methodology

2.1. Study area

The Odra River Basin (ORB) is located in Central Europe and is among the largest river basins in European Union (the fifth largest river basin). The mean annual runoff of this transboundary basin is 154 mm (567 m³/s), and the long-term annual average of precipitation is approximately 650 mm. ORB covers 119,041 km², of which 89 % is located in Poland, 4.9 % in Germany, and 6.1 % in the Czech Republic. of the river is approximately 840 km long, with sources in the Sudetes Mountains in the Czech Republic and the estuary to the Szczecin Lagoon connected to the Baltic Sea in its southern part. The great majority of the drainage area spans the Central European Plain, with only southern-most parts being mountainous (Fig. 1). More details are available in Piniewski et al. (2021), Piniewski et al. (2017), and Marcinkowski et al. (2022). The location of ORB and its hydrologic objects are presented in Fig. 1.

The historical crop yield data for major crops (winter wheat, spring barley, rapeseed, and corn) were extracted from Central Statistical Office of Poland (GUS, <https://stat.gov.pl/en/topics/agriculture-forestry/>) database at province level. The average of crop yields in Wielkopolskie, Zachodniopomorskie, Lubuskie, Dolnośląskie, Śląskie, Łódzkie, and Opolskie provinces were included in this study.

2.2. Configuration of agro-hydrological model

The new version of SWAT, namely, SWAT+, was used in this study. This study uses a modified version of SWAT+. In the modified version, minor and major errors in some subroutines in standard SWAT+, such as misnamed variables related to groundwater module, water quality module, wrong initialized constant values for surface processes, evapotranspiration module, tillage operations, crop simulation module, and lateral flow

module, were fixed and some improvements in wetland condition were made. These modifications and codes are available on <https://github.com/andrejstnh/SWATplus>. The model was set up in the QGIS interface, which is also an open-access software, using the QSWAT+ plugin (SWAT+ installer v.2.1.4, <https://swat.tamu.edu/software/plus/>).

The ORB was divided into 1476 subbasins and 20,000 hydrologic response units (HRUs). The pre-defined watershed delineation option was chosen in the setup process and the subbasins and channels from the Poland SWAT model setup of Marcinkowski et al. (2022) were used. The ORB model contains 176 lakes (natural lakes and reservoirs), the management schedules of 11 major crops (including winter wheat, spring barley, corn, silage corn, sugar beet, potato, rapeseed, cabbage, apple, and fescue, which are all rainfed), and the tile drainage system. Weather data (precipitation, maximum and minimum temperature, humidity, wind speed) were extracted for each of the subbasins from a 2 km regional dataset (Piniewski et al., 2021), and solar radiation was extracted from Copernicus ERA5 global dataset (<https://cds.climate.copernicus.eu/>). The Penman-Monteith method was chosen for calculating potential evapotranspiration. Daily runoff (26 discharge stations, source: The Institute of Meteorology and Water Management (IMGW-PIB), Warsaw, Poland) and satellite-based SM were calibrated for the period 1997–2019 (1997–1999 warm-up period, 2000–2010 calibration, and 2011–2019 validation). Details of used digital layers, including the 50 m resolution digital elevation model, land use map, and soil map, are described in Marcinkowski et al. (2022).

The management schedules of mentioned crops is based on potential heat unit (PHU), and essential operations such as fertilizer, planting, tillage, harvest or harvest and kill were included in the model. In the modified version of used SWAT+ model, crops module is based on number of days to maturity and potential heat units.

2.3. Satellite-based SM dataset

This study employed ESA (European Space Agency) CCI (Climate Change Initiative) SM version 07.1. This product spans more than 40 years (1978–2021), and different active and passive sensors are used to generate this dataset. This product has three active, passive, and combined products; data are freely available at <https://esa-soilmoisture-cci.org/>. The resolution of this product is 0.25° and has daily time step. We have employed the combined dataset, which increases the chance of taking at least one sensed SM for a particular day and pixel, thus decreasing the number of data gaps. Additionally, combined satellite-based datasets generally perform better than individual sensor datasets (Modanesi et al., 2020). This product has been used in several studies with different purposes in different regions with diverse climates and has shown relatively good accuracy (Almendra-Martín et al., 2021; Dorigo et al., 2017; Kovačević et al., 2020; Ma et al., 2017; McNally et al., 2016; Modanesi et al., 2020; Zhang et al., 2019; Zhang et al., 2021). This dataset was extracted over the 20,000 HRUs, and average-weighted time series were calculated for each subbasin (1476 subbasins).

According to the literature, satellite-based SM datasets should be corrected due to the large-scale resolution and irregular time intervals on surface and depth (Albergel et al., 2008; Wagner et al., 1999). In this regard, Soil Water Index (SWI) is proposed. This method corrects the anomalies of satellite-based SM and is based on an exponential filter equation. In this study, SWI is employed to match the depth of simulated SM and satellite-based SM. Moreover, SWI is used in several studies with different proposes, and the effectiveness of this method for adjusting the SM time series is highlighted (Brocca et al., 2010; Dorigo et al., 2015; Dorigo et al., 2011; Liu et al., 2011). A comprehensive explanation and different applications of this index are presented in Massari et al. (2014) and additional features of this index can be found in Wagner et al. (1999), and Ceballos et al. (2005).

2.4. Objective functions

Finding an appropriate objective function for multi-objective calibration and validation is controversial, especially when one or more datasets are satellite-based products and spatially distributed over the study area.

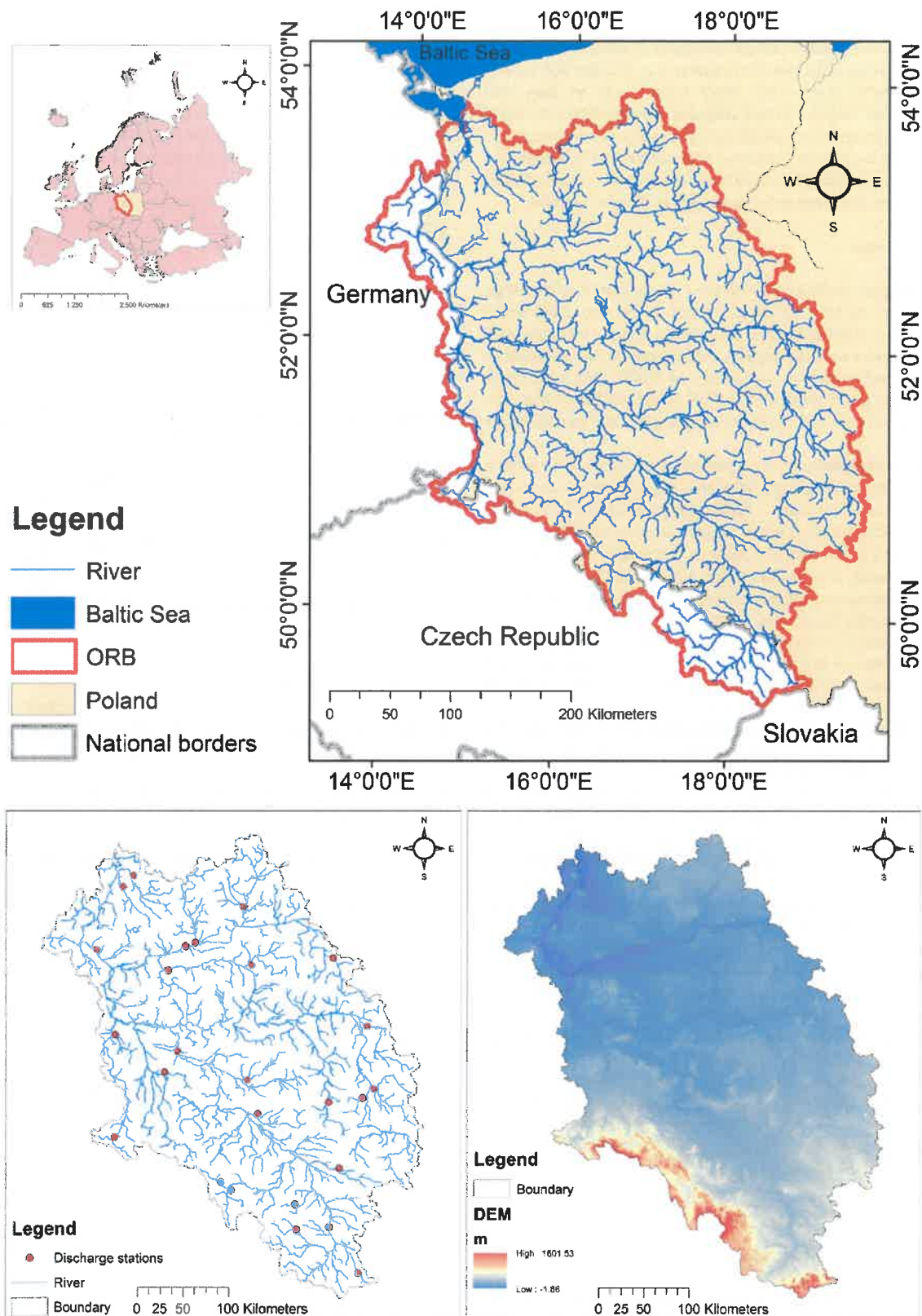


Fig. 1. The location of ORB in Europe, rivers, discharge stations, and topography.

Two objective functions were employed for discharge and SM values in this study. The first is a ground- and point-based dataset and the second is a satellite-based dataset distributed over ORB. According to the literature,

the Kling–Gupta efficiency (KGE) (Kling and Gupta, 2009) is widely used for discharge calibration (Knoben et al., 2019), and in this study, it also is selected for the discharge accuracy evaluation. For the distributed variable,

a relatively new metric, *SPAtial Efficiency* (SPAEF), is used (Demirel et al., 2018; Koch et al., 2018). SPAEF reflects correlation, coefficient of variation, and histogram overlap of the observed datasets (i.e., CCI-SM) and model's output (i.e., SWAT+) (Koch et al., 2018). In this study, we have used SPAEF based on time variation in each subbasin. Monthly SMs are assumed that are map pixels, and then, SPAEF for each subbasin was calculated. These two metrics are proposed to evaluate the accuracy of distributed hydrological models, particularly if one or more variables are spatially distributed over the study area, such as SM or evapotranspiration variables.

2.5. Calibration strategy

In the first step which is a single-objective (SO) calibration of discharge, KGE indicator was selected as an objective function. The second step which is a multi-objective (MO) calibration of discharge and soil moisture, KGE and SPAEF indicators were employed in calibration process. It should be mentioned that before starting to calibrate the model, crop yields were assessed and crop parameters, such as PHU (Potential Heat Unit), biomass/energy ratio, base and optimum temperature, and harvest index were fixed.

For discharge simulations at 26 discharge stations (2000–2010 calibration, and 2011–2019 validation), SWATplus-CUP (<https://www.2w2e.com/home/SwatPlusCup>) SUFI-2 (SPE) algorithm (Abbaspour et al., 2015) was used with 500 simulations in each iteration. For calibration of SM and calculating SPAEF indicator, a script in R programming language was used. The monthly river discharge was calibrated in discharge stations and SM was calibrated over subbasins at monthly time steps. In the SO step, the weight of objective function (maximizing KGE) for each discharge station was chosen based on long-term average of observed runoff. In the MO step, the objective function was maximizing KGE (for discharge) and SPAEF (for SM) indicators at the same time and both of these parameters had the same weight in the final multi-objective function. It should be mentioned that in the MO step, the same list of parameters, which were used in SO step, was also recalibrated with the similar initial ranges.

In the SWAT+ model, the SM output is the plant available water content in the soil. Its values can vary between the wilting point (0 mm of H₂O) and saturated conditions (value depending on the soil bulk density). SWAT+ provides SM at daily, monthly, and yearly time steps for the entire soil profile and 300 mm of topsoil for each HRU. In this regard, firstly, by employing the SWI index, the CCI-SM dataset was matched according to the depth (topsoil and entire soil profile) of the model's SM output, then the adjusted SM was employed for calibration. In the MO step, the constant value of the wilting point of each soil type was firstly added to the SWAT+ SM outputs at HRU level, and was then used in calibration process.

The calibration step includes sensitive parameters of the SWAT+ model in the study area. The parameter selection was done based on the authors' experience, sensitivity analyses in SWATplus-CUP software (comprehensive description of sensitivity analyses and uncertainty analysis in the SWAT model are available in Abbaspour et al. (2015), Yang et al. (2008) and Abbaspour et al. (2007)), and suggested parameters in the literature (Abbaspour et al., 2018). Moreover, discharge stations were classified into six groups according to the subbasins' land use and soil type for spatial calibration of influential parameters.

3. Results

3.1. Single-objective calibration approach

As mentioned before, in the SO step, discharge stations were calibrated without considering the SM spatial distribution. Sixteen parameters for each discharge station groups were calibrated. In the SWAT+ model, one of the newly introduced parameters is PERCO (percolation coefficient, which varies between 0 and 1). This parameter regulates percolation from the base soil layer and can be employed to control percolation if an impervious layer or high water table exists (Wagner et al., 2022). According to the analyses, this parameter was the most influential parameter on

discharge in the current study. In the first step, this parameter was calibrated and fixed to a value of 0.96, which in general results in relatively high percolation; then, other parameters were calibrated (Table 1). The model generally shows good accuracy in runoff simulations (according to Knoben et al. (2019)), and average KGE for all discharge stations is ~0.60 and ~0.63 in the calibration and validation periods, respectively. The results for the main discharge stations are presented in Table 2, and Fig. 2 presents the KGE index in all the discharge stations. However, in the north of the basin, there is a discharge station with the lowest KGE (−0.39, average runoff = 2.17 m³/s). Fig. 2 shows that the model in the south of the basin (mostly mountainous) has the lowest accuracy in runoff simulations.

3.2. Multi-objective calibration approach

3.2.1. Adjusting the SWI index

Based on the SWI index, the satellite-based SM dataset was adjusted. In Fig. 3, the effect of the SWI method on CCI SM at basin level is presented, and SWAT+ model SM in three different conditions, including, before calibration, the calibrated model only with runoff, and calibrated model with runoff and SM at daily steps, are shown (for the period 2000–2019). As it is visible, the soil water content in the SWAT+ model is underestimated. In this regard, SM was added to the calibration process. As mentioned, these variables were calibrated for two levels, including 300 mm of topsoil and the average available water content in the entire soil profile. Calibration and validation were done on the subbasin level, meaning 1476 SM times-series were extracted from CCI SM, then were adjusted using SWI and employed in calibration and validation periods.

3.2.2. SM and runoff calibration

The objective of MO strategy was to maximize the SPAEF index for SM and KGE for runoff. In MO strategy, the same set of parameters for each of the discharge station groups, which was previously used in the SO strategy (Table 1), was now used also in the MO calibration strategy. The soil available water content (AWC) was the most sensitive parameter in SM calibration, according to sensitivity analyses in SWATplus-CUP (Table 1). The accuracy of runoff simulations for discharge stations significantly increased (average of KGE in all discharge stations is ~0.67 in the calibration and ~0.69 in the validation periods) compared to the SO approach. It should be mentioned that for 16 discharge stations improvements in KGE were achieved, and for 10 discharge stations (mainly close to mountains), the

Table 1
Final values of calibrated parameters for both calibration strategies (average values across calibration groups) and initial parameter ranges.

Change method	Parameter	Initial range of parameters		Final value	
		Lower band	Upper band	Single-objective	Multi-objective
Absolute value	alpha.gw	0.01	0.1	0.06	0.04
	bf_max.gw	0.01	1	0.29	0.61
	chn.rte	0.05	0.2	0.18	0.08
	deep_seep.gw	0.001	0.2	0.05	0.14
	epco.hru	0	0.3	0.07	0.05
	esco.hru	0.5	1	0.94	0.95
	flo_min.gw	1	5	3.31	3.27
	lat_time.hru	0.5	2	1.04	0.93
	perco.hru	0.85	0.99	0.96	0.96
	revap_co.gw	0.02	0.1	0.023	0.04
	revap_min.gw	4	10	7.05	5.76
	sp_yld.gw	0	0.2	0.09	0.04
	awc.sol	−0.2	0.2	−0.155	0.14
	bd.sol	−0.3	0.3	0.29	0.02
	cn2.hru	−0.2	0.2	−0.02	0.11
	cn3_swf.hru	−0.5	0.5	−0.29	−0.35
Relative value	k.sol	−0.2	0.2	−0.195	−0.02

Table 2
The accuracy of the model in runoff simulations in the main discharge stations.

River and discharge station name	Observed Q (m ³ /s)	KGE			
		Single objective		Multi objective	
		Calibration	Validation	Calibration	Validation
Odra at Gozdowice	474.1	0.77	0.78	0.81	0.83
Odra at Cigacice	188.1	0.86	0.81	0.75	0.79
Warta at Skwierzyna	117.36	0.73	0.78	0.84	0.85
Noteć at Nowe Drezdenko	66.32	0.56	0.63	0.81	0.88
Odra at Racibórz-Miedonia	63.28	0.45	0.53	0.67	0.65

KGE values were decreased. The accuracy of the runoff simulations is presented in Fig. 4 and Table 2.

Fig. 5 shows the SPAEF distribution for SM accuracy over sub-basins. As it is visible, SPAEF (average = 0.37 topsoil and 0.31 entire soil profile) shows that the model has relatively better accuracy in SM simulations. According to Fig. 5, there is no visible pattern in the spatial distribution of the model's accuracy in SM simulations. Moreover, SPAEF determines that the

model has better accuracy in topsoil SM simulations. This could be expected to the nature of the CCI SM dataset, which is reliable for the 5 cm of topsoil.

3.3. Effect of different approaches on crop yields

In order to have a robust comparison between the SO and MO strategies, crop yields were also assessed. In this regard, the yields of major crops in the ORB, including winter wheat, spring barley, rapeseed, and corn, were extracted from the SWAT + model for both strategies and were compared with observed data, which is the annual average of mentioned provinces in Section 2.1. It should be mentioned that the SWAT + model provides the dry weight of crop yields, and for assessments, the observed values were converted from fresh weight to dry weight yields, assuming that humidity equals 15 % and 20 % for winter wheat/spring barley and corn/rapeseed, respectively.

As it is visible in Fig. 6, crops have wider ranges of yields in MO approach, which is closer to observed data (excluding winter wheat). The positive effect of MO approach is most visible in rapeseed yields. Both approaches have a wider estimates of winter wheat and mainly over estimated winter wheat yields.

According to Fig. 7, for barley and wheat the SO approach produced mostly overestimated crop yields compared to the MO approach. The

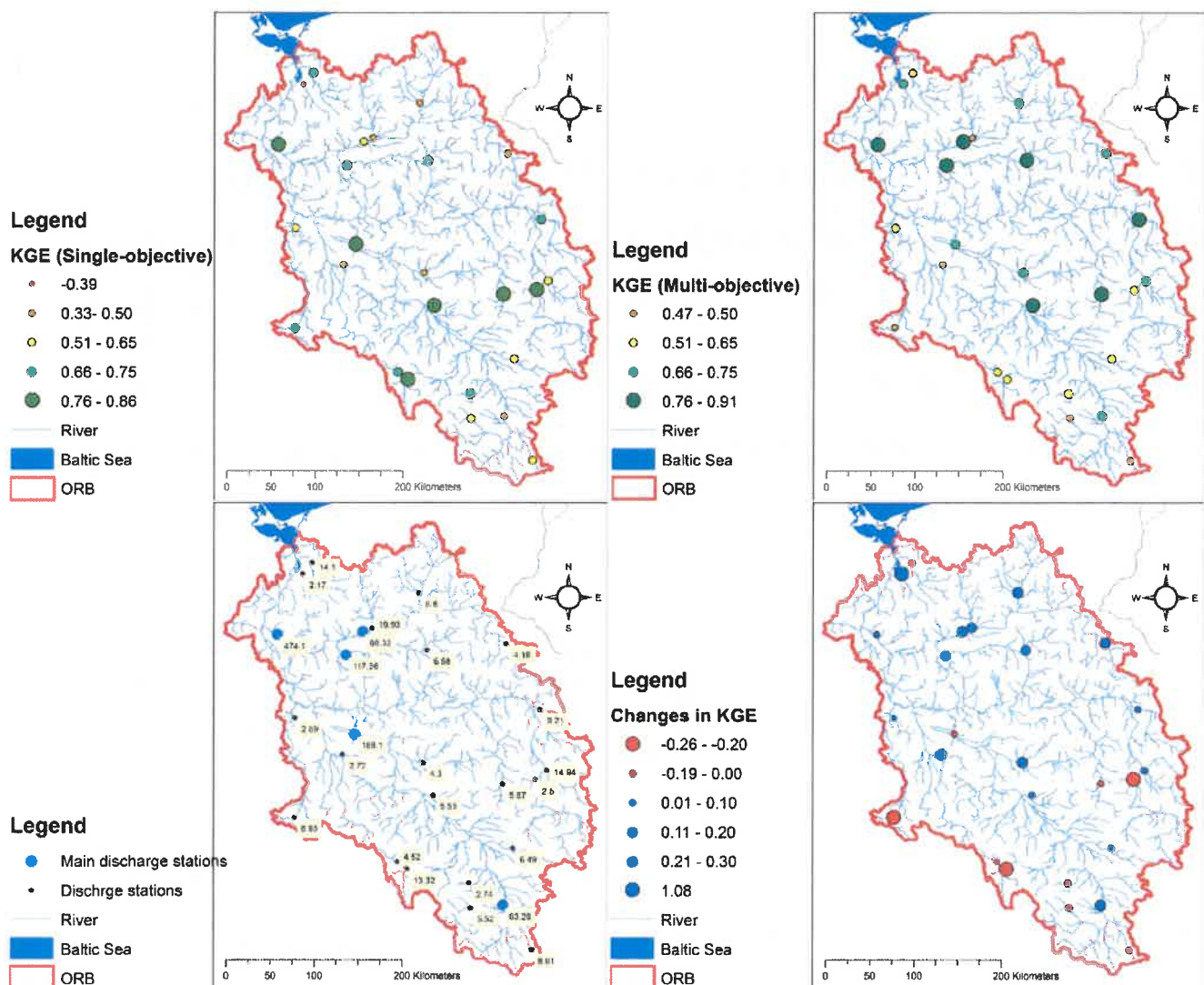


Fig. 2. The spatial distribution of the KGE indicator for both strategies, average of river discharge (down left, m³/s), and changes in KGE (improvements or reductions for a multi-objective strategy relative to a single-objective strategy).

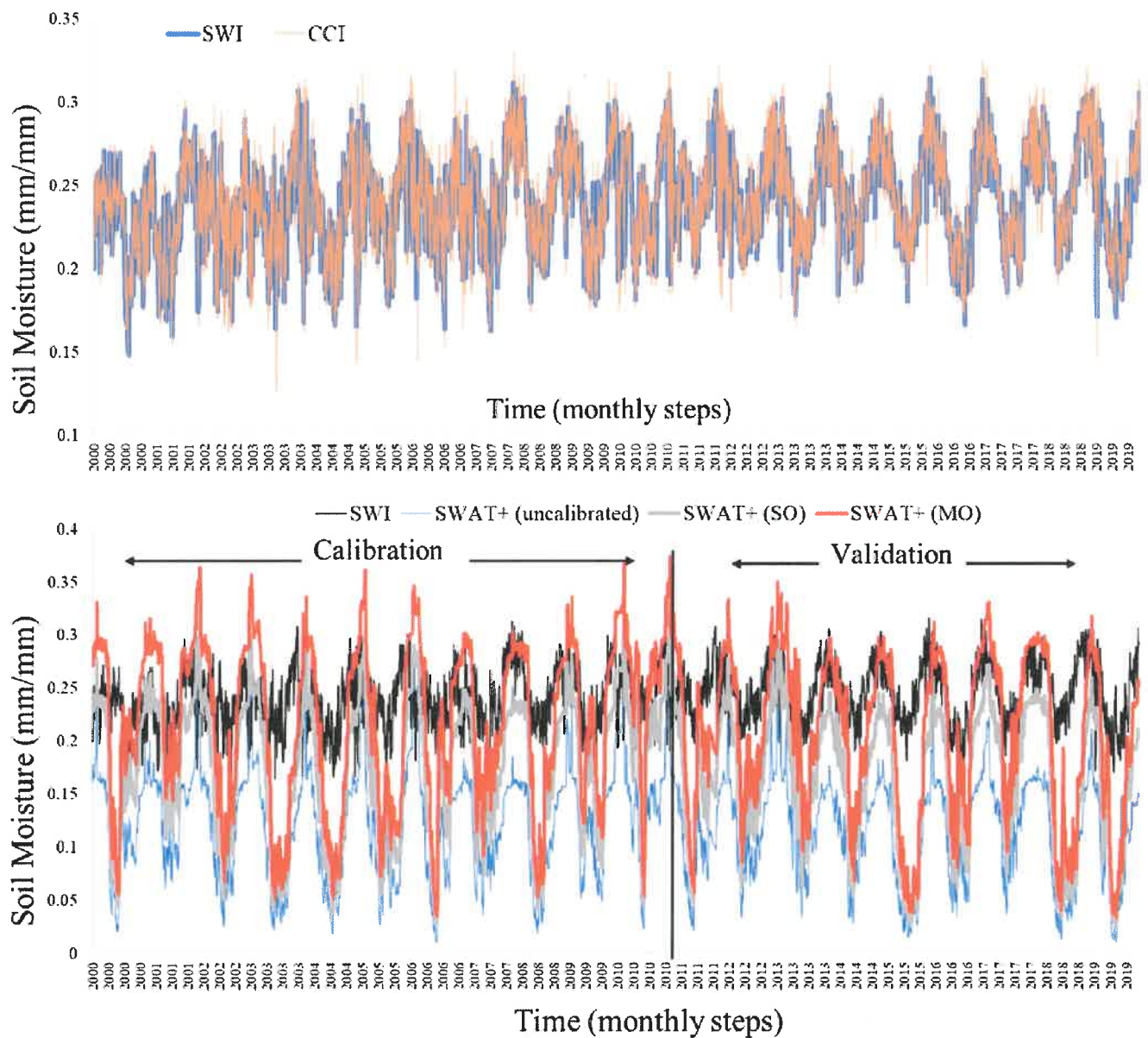


Fig. 3. Basin-averaged changes in SM in the entire soil profile (mm/mm): CCI SM, adjusted SM based on SWI, SWAT +, and the effect of calibration on SM for the period 2000–2019.

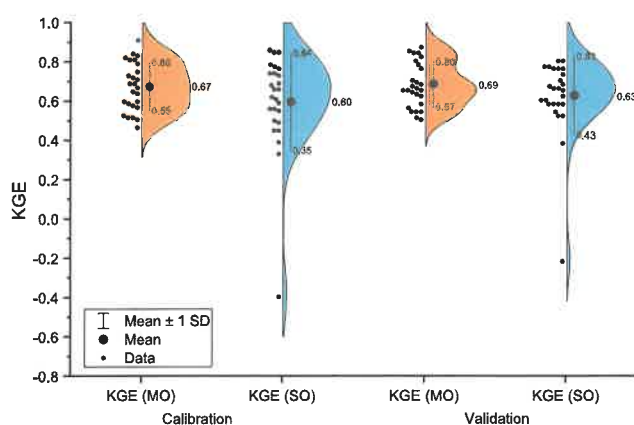


Fig. 4. Distribution of KGE for river discharge in SO and MO approaches.

opposite effect (underestimated yields in SO approach) is visible for rapeseed. For corn, the difference between yield dynamics in SO and MO approaches is very low. The correlation between simulated and observed yields is generally low, mainly due to the fact that numerous anthropogenic factors, not accounted for in SWAT +, can affect crop yields. Moreover, in 2015 Central Europe had experienced a severe drought (Jonita et al., 2017). In this particular year, according to the observed datasets barley, wheat, and rapeseed yields did not change substantially, but corn yields were more sensitive to drought. This is understandable, because drought developed in August–September, mostly after harvest of cereals and rapeseed, whereas corn which is harvested in late summer was more strongly affected. This drop in corn yields is reflected in both SO and MO approaches, however in the MO approach the response is more in line with observations.

The model performance in crop yield simulation is presented in Table 3. To evaluate the performance of SWAT + in both approaches, mean error (tons/ha), coefficient of determination (R^2) and percentage bias (PBIAS %) were employed. According to the mean error and PBIAS, MO approach performed better than SO approach being close to zero which is the optimum

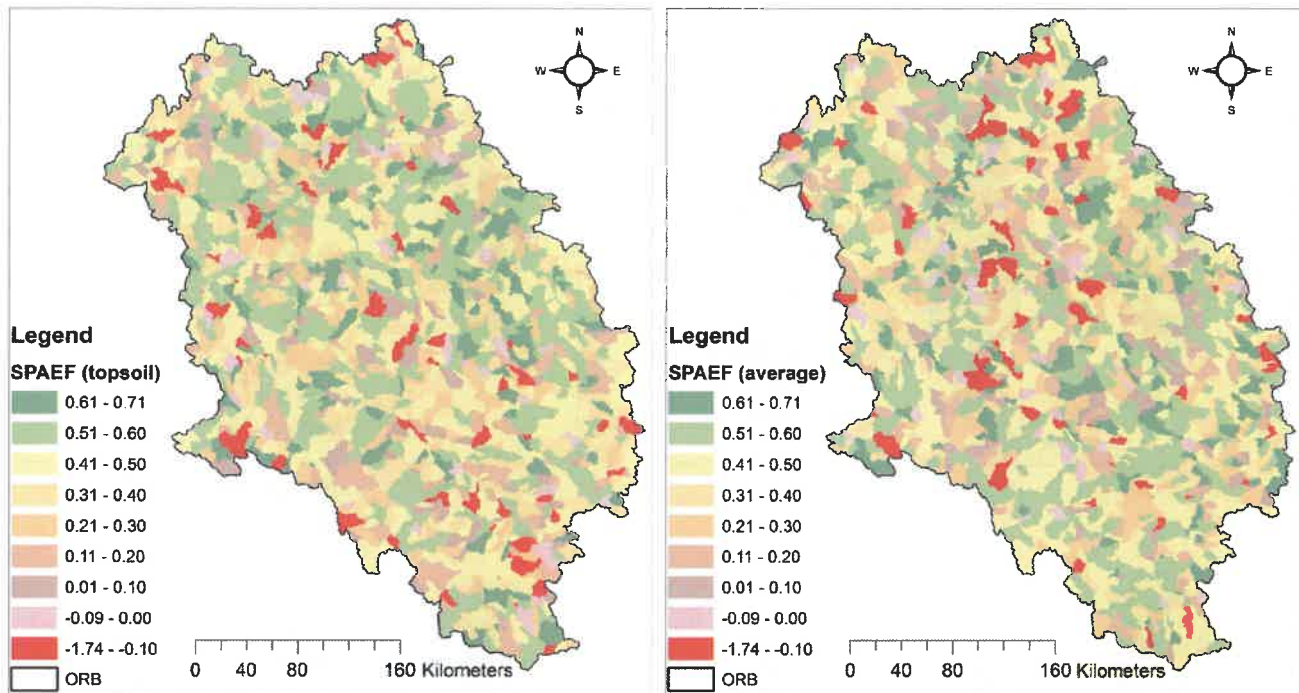


Fig. 5. Accuracy distribution of SM (topsoil and average SM) according to SPAEF.

value for these statistics. As it was already mentioned, correlation between simulated crop yields and observed data is not acceptable.

4. Discussion

In this study the multi-objective calibration enhanced the SWAT+ model's accuracy in river discharge and crop yields simulations. Improving the river discharge simulations and water balance components via multi-objective calibration in the SWAT model was reported before in several studies. For example, Eini et al. (2020), Eini et al. (2021a), and Delavar et al. (2022) have employed runoff, aquifer water table, infiltration rate, crop yields, and ET to increase the model consistency. By providing different distributed outputs, SWAT facilitates multi-objective calibration and robust results for scenario simulations (Delavar et al., 2022). Moreover, Ma et al. (2019) show that MODIS-based LAI significantly enhanced the model flexibility and spatial distribution of vegetation cover in sub-tropical regions.

Rajib and Merwade (2016) employed a time-dependent Soil Moisture Accounting method in the SWAT model calibration and evaluated SM in different layers in two watersheds in Indiana. They concluded that adding SM into the calibration process leads to higher fitness of simulations and observed datasets and improved efficiency metrics; the same result is observed in our study. In addition, it is mentioned that SM calibration based on in-situ root zone SM provides considerable improvement in SWAT performance (Rajib et al., 2016). The SM, based on Advanced Microwave Scanning Radiometer-Earth Observing System (AMSR-EOS) for 1 cm of topsoil, was used in their study for HRU and sub-basin level, and it improved the model's outputs in terms of root zone SM and runoff with corresponding measured datasets (Rajib et al., 2016). Azimi et al. (2020) showed that satellite-based SM assimilated from SMAP and Sentinel-1 could improve the accuracy of river discharge simulations in the SWAT model.

In the SWAT model, the ET processes start from the HRU level at daily steps, and each HRU has different land use, soil type, and slope (Arnold et al., 2012; Gassman et al., 2007; Gassman et al., 2014). In this regard, calibrating the SWAT model at the HRU level, particularly for distributed variables, could lead to more consistent results (Ma et al., 2019). In the current study, calibration was done at the subbasin level due to a large number of

HRUs, large variability of hydroclimatic parameters, which affect the SM values, and the resolution of CCI SM product. Thus, a similar approach could be done in the smaller watershed and evaluate the SM accuracy of the SWAT+ model at the HRU level. Pfannerstill et al. (2017) proposed that expert knowledge could help accomplish hydrologically reliable model results regarding the simulation of runoff and water balance components. Multi-objective calibrated models can be used for water balance and water accounting assessments; in addition, in transboundary basins, these models are helpful for (inter-) national studies (De Lannoy et al., 2022). Moreover, we would like to mention that capturing the dynamic of crop yields in this large basin with a wide range of recorded crop yields was one of our limits. In future works, this limit can be addressed by employing satellite-based datasets such as LAI or canopy height estimations.

The calibration process using SM can change the water balance of the basin and increase the uncertainty of the output; thus it should be mentioned that the water balance of the basin should be checked via available parameters such as ET, crop yields, groundwater recharge, and river discharge (De Lannoy et al., 2022; Delavar et al., 2022; Eini et al., 2020; Koohi et al., 2022). Moreover, it could be recommended to evaluate the effect of root zone soil moisture datasets (such as the dataset which is provided by Grillakis et al. (2021) or Copernicus Global Land service) in improving the accuracy of the SWAT+ model. Furthermore, it could be stated that satellite-based soil moisture data can be validated by in-situ observations and then added into the calibration step this approach can decrease the uncertainty of hydrological modeling; however, in large river basins it could be expected that only short time series of in-situ soil moisture are available. Effect of multi-objective calibration on crop yield, ET, and infiltration rate can be assessed, and this could decrease the uncertainty of comprehensive hydrological modeling.

5. Conclusion

In this study, a transboundary basin in the Baltic Sea region (Odra river basin) was selected to investigate the accuracy of the SWAT+ agro-hydrological model in river discharge, crop yields and soil moisture simulations. A satellite-based soil moisture dataset (CCI SM) was chosen as the observed soil moisture dataset. In the single-objective calibration (only

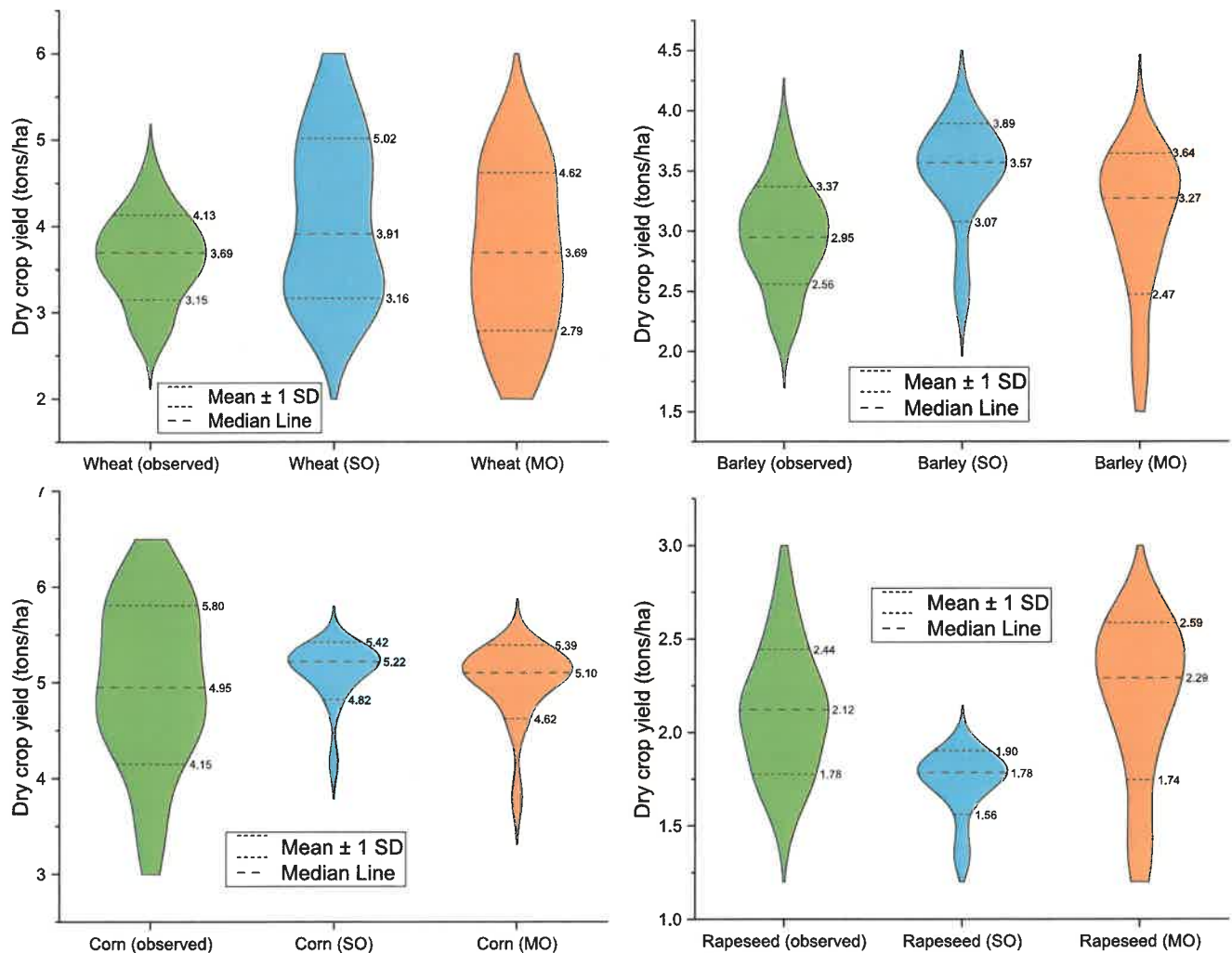


Fig. 6. Distribution of major crop yields in SO and MO strategies with the observed data (for period 1999–2019 for winter wheat, barley, and rapeseed; for period 2004–2019 for corn).

discharge) approach, the SWAT+ model showed good accuracy in runoff simulations, and the average KGE was above 0.60 and 0.63 in the calibration and validation periods, respectively. Satellite-based soil moisture was adjusted with SWI index and was added to the calibration step as the second variable in the multi-objective approach. In the multi-objective approach (discharge and soil moisture), the accuracy of simulations in river discharge stations substantially increased ($KGE = 0.67$ in the calibration and 0.69 in the validation periods) compared to the single-objective approach. The SPAEF index indicated that adding soil moisture in the calibration process (as we did using MO approach in this study) could improve the model's reliability. Moreover, assessing crop yields shows that multi-objective calibration also could improve the accuracy of model in estimating crop yields. The current results and presented approach can be used in transboundary river basins and regions that lack observed data, and it is important for climate change studies since this method delivers a robust model. It will also be a useful approach for model-based water accounting studies. Moreover, we recommend comparing different soil moisture products (especially high-resolution products) in future studies and trying to capturing dynamic of crop yields.

CRedit authorship contribution statement

Mohammad Reza Eini: Conceptualization, Methodology, Software, Writing – review & editing. **Christian Massari:** Conceptualization,

Methodology, Writing – review & editing. **Mikołaj Piniewski:** Conceptualization, Methodology, Writing – review & editing.

Data availability

Data will be made available on request.

Declaration of competing interest

The authors declare that they have no known competing financial interests or personal relationships that could have appeared to influence the work reported in this paper.

Acknowledgement

We would like to express our gratitude to the editor and reviewers for their valuable feedback and diligent efforts in enhancing the quality of our manuscript. This research was made possible by the support of the National Science Centre (Narodowe Centrum Nauki), Warsaw, Poland (PRELUDIUM BIS-1 project, UMO-2019/35/O/ST10/04392). We would also like to extend our appreciation to the Hydrology group at the Institute of Geo-Hydrological Protection, National Research Council (IRPI-CNR) in Perugia, Italy for hosting MRE during an internship that led to this research (supported by Warsaw University of Life Sciences, SGGW's Own

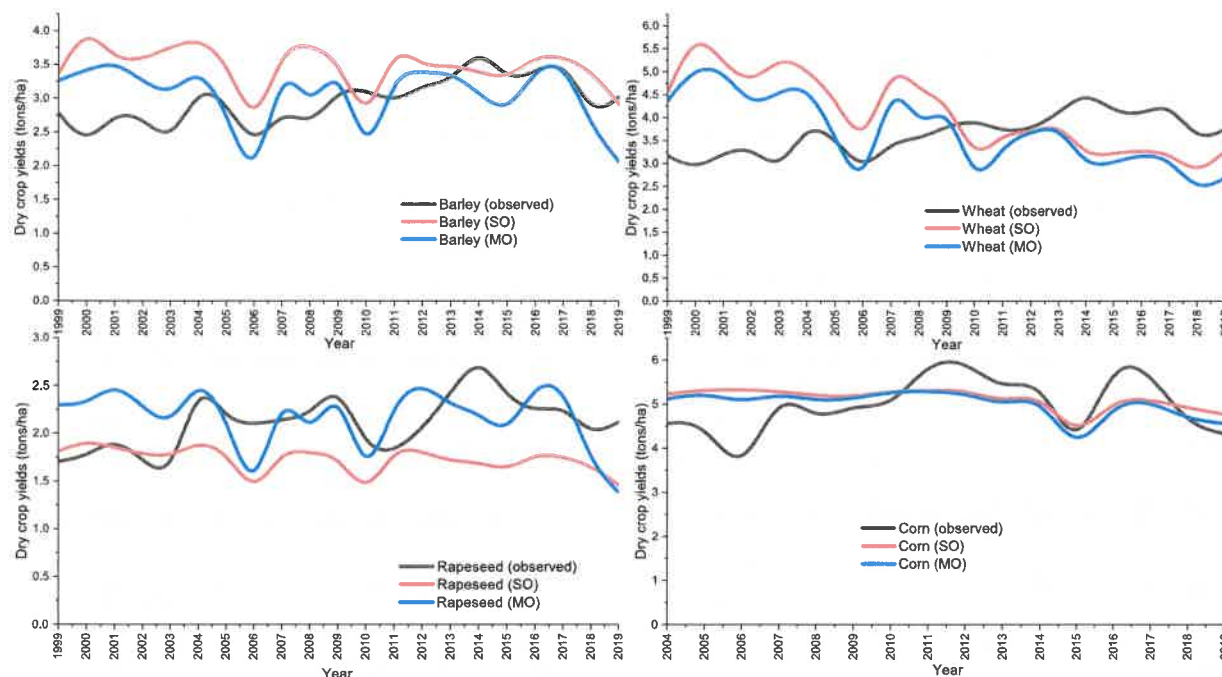


Fig. 7. Temporal variation of basin-averaged simulated (SO and MO) and observed crop yields in the ORB.

Table 3

Performance of SWAT+ in crop yields simulations for both approaches.

	Winter wheat		Barley		Rapeseed		Corn	
	SO	MO	SO	MO	SO	MO	SO	MO
Mean error (tons/ha)	0.45	0.06	0.52	0.09	-0.38	0.06	0.14	0.03
R ²	0.32	0.14	0	0.08	0	0.05	0.18	0.31
PBIAS %	12	1.7	17	3.2	-18	2	2.9	0.6

Scholarship Fund for outstanding PhD Students and Employees, BWM/51/2022). The Institute of Meteorology and Water Management - National Research Institute (IMGW-PIB) is acknowledged for providing river flow data.

References

- Abbaspour, K.C., 2022. The fallacy in the use of the “best-fit” solution in hydrologic modeling. *Sci. Total Environ.* 802, 149713. <https://doi.org/10.1016/j.scitotenv.2021.149713>.
- Abbaspour, K.C., Rouholahnejad, E., Vaghefi, S., Srinivasan, R., Yang, H., Klove, B., 2015. A continental-scale hydrology and water quality model for Europe: calibration and uncertainty of a high-resolution large-scale SWAT model. *J. Hydrol.* 524, 733–752. <https://doi.org/10.1016/j.jhydrol.2015.03.027>.
- Abbaspour, K.C., Vaghefi, S.A., Srinivasan, R., 2018. A guideline for successful calibration and uncertainty analysis for soil and water assessment: a review of papers from the 2016 international SWAT conference. *Water* 10, 6. <https://doi.org/10.3390/w10010006>.
- Abbaspour, K.C., Yang, J., Maximov, I., Siber, R., Bogner, K., Mieleitner, J., Zobrist, J., Srinivasan, R., 2007. Modelling hydrology and water quality in the pre-alpine/alpine thur watershed using SWAT. *J. Hydrol.* 333, 413–430. <https://doi.org/10.1016/j.jhydrol.2006.09.014>.
- Akoko, G., Le, T.H., Gomi, T., Kato, T., 2021. A review of SWAT model application in Africa. *Water* 13, 1313. <https://doi.org/10.3390/w13091313>.
- Albergel, C., Rudiger, C., Pellarin, T., Calvet, J.C., Fritz, N., Froissard, F., Suquia, D., Petitpa, A., Piguet, B., Martin, E., 2008. From near-surface to root-zone soil moisture using an exponential filter: an assessment of the method based on in-situ observations and model simulations. *Hydrol. Earth Syst. Sci.* 12, 1323–1337. <https://doi.org/10.5194/hess-12-1323-2008>.
- Alfieri, L., Avanzi, F., Delogo, F., Gabellani, S., Bruno, G., Campo, L., Libertino, A., Massari, C., Tarpanelli, A., Rains, D., Miralles, D.G., Quast, R., Vreugdenhil, M., Wu, H., Brocca, L., 2022. High-resolution satellite products improve hydrological modeling in northern Italy. *Hydrol. Earth Syst. Sci.* 26, 3921–3939. <https://doi.org/10.5194/hess-26-3921-2022>.
- Almendra-Martín, L., Martínez-Fernández, J., Piles, M., González-Zamora, Á., 2021. Comparison of gap-filling techniques applied to the CCI soil moisture database in southern

- Europe. *Remote Sens. Environ.* 258, 112377. <https://doi.org/10.1016/j.rse.2021.112377>.
- Arnold, J.G., Bieger, K., White, M.J., Srinivasan, R., Dunbar, J.A., Allen, P.M., 2018. Use of decision tables to simulate management in SWAT. *Water* 10, 713. <https://doi.org/10.3390/w10060713>.
- Arnold, J.G., Moriasi, D.N., Gassman, P.W., Abbaspour, K.C., White, M.J., Srinivasan, R., Santhi, C., Harmel, R.D., van Griensven, A., Van Liew, M.W., Kannan, N., Jha, M.K., 2012. Swat: model use, calibration, and validation. *Trans. ASABE* 55, 1491–1508. <https://doi.org/10.13031/2013.42256>.
- Aslam, R.A., Shrestha, S., Pala, I., Ninsawat, S., Shanmugam, M.S., Anwar, S., 2020. Projections of climatic extremes in a data poor transboundary river basin of India and Pakistan. *Int. J. Climatol.* 40, 4992–5010. <https://doi.org/10.1002/joc.6501>.
- Azimi, S., Dariane, A.B., Modanesi, S., Bauer-Marschallinger, B., Bindlish, R., Wagner, W., Massari, C., 2020. Assimilation of sentinel 1 and SMAP - based satellite soil moisture retrievals into SWAT hydrological model: the impact of satellite revisit time and product spatial resolution on flood simulations in small basins. *J. Hydrol. (Amst)* 581, 124367. <https://doi.org/10.1016/j.jhydrol.2019.124367>.
- Bailey, R.T., Bieger, K., Flores, L., Tomer, M., 2022. Evaluating the contribution of subsurface drainage to watershed water yield using SWAT+ with groundwater modeling. *Sci. Total Environ.* 802, 149962. <https://doi.org/10.1016/j.scitotenv.2021.149962>.
- Bailey, R.T., Park, S., Bieger, K., Arnold, J.G., Allen, P.M., 2020. Enhancing SWAT plus simulation of groundwater flow and groundwater-surface water interactions using MODFLOW routines. *Environ. Model. Softw.* 126, 104660. <https://doi.org/10.1016/j.envsoft.2020.104660>.
- Beck, H.E., Vergopolan, N., Pan, M., Levizzani, V., van Dijk, A.I.J.M., Weedon, G.P., Brocca, L., Pappenberger, F., Huffman, G.J., Wood, E.F., 2017. Global-scale evaluation of 22 precipitation datasets using gauge observations and hydrological modeling. *Hydrol. Earth Syst. Sci.* 21, 6201–6217. <https://doi.org/10.5194/hess-21-6201-2017>.
- Beven, K., 2006. A manifesto for the equifinality thesis. *J. Hydrol.* 320, 18–36. <https://doi.org/10.1016/j.jhydrol.2005.07.007>.
- Bieger, K., Arnold, J.G., Rathjens, H., White, M.J., Bosch, D.D., Allen, P.M., 2019. Representing the connectivity of upland areas to floodplains and streams in SWAT+. *J. Am. Water Resour. Assoc.* 55, 578–590. <https://doi.org/10.1111/1752-1688.12728>.
- Bieger, K., Arnold, J.G., Rathjens, H., White, M.J., Bosch, D.D., Allen, P.M., Volk, M., Srinivasan, R., 2017. Introduction to SWAT plus, a completely restructured version of the soil and water assessment tool. *J. Am. Water Resour. Assoc.* 53, 115–130. <https://doi.org/10.1111/1752-1688.12482>.
- Brocca, L., Ciabatta, L., Massari, C., Camici, S., Tarpanelli, A., 2017. Soil moisture for hydrological applications: open questions and new opportunities. *Water* 9, 140. <https://doi.org/10.3390/w9020140>.
- Brocca, L., Filippucci, P., Hahn, S., Ciabatta, L., Massari, C., Camici, S., Schuller, L., Bojkov, B., Wagner, W., 2019. SM2RAIN-ASCAT (2007–2018): global daily satellite rainfall data from ASCAT soil moisture observations. *Earth Syst. Sci. Data* 11, 1583–1601. <https://doi.org/10.5194/essd-11-1583-2019>.
- Brocca, L., Hasenauer, S., Lacava, T., Melone, F., Moramarco, T., Wagner, W., Dorigo, W., Matgen, P., Martínez-Fernández, J., Llorens, P., Latron, J., Martin, C., Bittelli, M., 2011. Soil moisture estimation through ASCAT and AMSR-E sensors: an intercomparison and validation study across Europe. *Remote Sens. Environ.* 115, 3390–3408. <https://doi.org/10.1016/j.rse.2011.08.003>.

- Brocca, L., Massari, C., Pellarin, T., Filippucci, P., Ciabatta, L., Camici, S., Kerr, Y.H., Fernandez-Prieto, D., 2020. River flow prediction in data scarce regions: soil moisture integrated satellite rainfall products outperform rain gauge observations in West Africa. *Sci. Rep.* 10, 12517. <https://doi.org/10.1038/s41598-020-69343-x>.
- Brocca, L., Melone, F., Moramarco, T., Wagner, W., Hasenauer, S., 2010. ASCAT soil wetness index validation through in situ and modeled soil moisture data in Central Italy. *Remote Sens. Environ.* 114, 2745–2755. <https://doi.org/10.1016/j.rse.2010.06.009>.
- Ceballos, A., Scipal, K., Wagner, W., Martinez-Fernandez, J., 2005. Validation of ERS scatterometer-derived soil moisture data in the central part of the Duero Basin, Spain. *Hydrol. Process.* 19, 1549–1566. <https://doi.org/10.1002/hyp.5585>.
- Ciabatta, L., Brocca, L., Massari, C., Moramarco, T., Gabellani, S., Puca, S., Wagner, W., 2016. Rainfall-runoff modelling by using SM2RAIN-derived and state-of-the-art satellite rainfall products over Italy. *Int. J. Appl. Earth Obs. Geoinf.* 48, 163–173. <https://doi.org/10.1016/j.jag.2015.10.004>.
- De Lannoy, G.J.M., Bechtold, M., Albergel, C., Brocca, L., Calvet, J.-C., Carrarsi, A., Crow, W.T., de Rosnay, P., Durand, M., Forman, G., Geppert, G., Grotto, M., Hendricks Franssen, H.-J., Jonas, T., Kumar, S., Lievens, H., Lu, Y., Massari, C., Pauwels, V.R.N., Reichle, R.H., Steele-Dunne, S., 2022. Perspective on satellite-based land data assimilation to estimate water cycle components in an era of advanced data availability and model sophistication. *Front. Water* 4. <https://doi.org/10.3389/frwa.2022.981745>.
- De Santis, D., Biondi, D., Crow, W., Camici, S., Modanesi, S., Brocca, L., Massari, C., 2021. Assimilation of satellite soil moisture products for river flow prediction: an extensive experiment in over 700 catchments throughout Europe. *Water Resour. Res.* 57, e2021WR029643. <https://doi.org/10.1029/2021WR029643>.
- Delavar, M., Eini, M.R., Kuchak, V.S., Zaghiyan, M.R., Shahbazi, A., Nourmohammadi, F., Motamedi, A., 2022. Model-based water accounting for integrated assessment of water resources systems at the basin scale. *Sci. Total Environ.* 830, 154810. <https://doi.org/10.1016/j.scitotenv.2022.154810>.
- Delavar, M., Morid, S., Morid, R., Farokhnia, A., Babaeian, F., Srinivasan, R., Karimi, P., 2020. Basin-wide water accounting based on modified SWAT model and WA plus framework for better policy making. *J. Hydrol.* 585, 124762. <https://doi.org/10.1016/j.jhydrol.2020.124762>.
- Demirel, M.C., Mai, J., Mendiguren, G., Koch, J., Samaniego, L., Stisen, S., 2018. Combining satellite data and appropriate objective functions for improved spatial pattern performance of a distributed hydrologic model. *Hydrol. Earth Syst. Sci.* 22, 1299–1315. <https://doi.org/10.5194/hess-22-1299-2018>.
- Devia, G.K., Ganatri, B.P., Dwarakish, G.S., 2015. A review on hydrological models. *Aquat. Procedia* 4, 1001–1007. <https://doi.org/10.1016/j.aqpro.2015.02.126>.
- Dorigo, W., Wagner, W., Albergel, C., Albrecht, F., Balsamo, G., Brocca, L., Chung, D., Ertl, M., Forkel, M., Gruber, A., Haas, E., Hamer, P.D., Hirsch, M., Ikonen, J., de Jeu, R., Kidd, R., Lahoz, W., Liu, Y.Y., Miralles, D., Mielstebauer, T., Nicolai-Shaw, N., Parinussa, R., Pratola, C., Reimer, C., van der Schalie, R., Seneviratne, S.I., Smolander, T., Lecomte, P., 2017. ESA CCI soil moisture for improved earth system understanding: state-of-the-art and future directions. *Remote Sens. Environ.* 203, 185–215. <https://doi.org/10.1016/j.rse.2017.07.001>.
- Dorigo, W.A., Gruber, A., De Jeu, R.A.M., Wagner, W., Stacke, T., Loew, A., Albergel, C., Brocca, L., Chung, D., Parinussa, R.M., Kidd, R., 2015. Evaluation of the ESA CCI soil moisture product using ground-based observations. *Remote Sens. Environ.* 162, 380–395. <https://doi.org/10.1016/j.rse.2014.07.023>.
- Dorigo, W.A., Wagner, W., Hohensinn, R., Hahn, S., Paulik, C., Xaver, A., Gruber, A., Drusch, M., Mecklenburg, S., van Oevelen, P., Robock, A., Jackson, T., 2011. The international soil moisture network: a data hosting facility for global in situ soil moisture measurements. *Hydrol. Earth Syst. Sci.* 15, 1675–1698. <https://doi.org/10.5194/hess-15-1675-2011>.
- Eini, M.R., Javadi, S., Delavar, M., Gassman, P.W., Jarihani, B., 2020. Development of alternative SWAT-based models for simulating water budget components and streamflow for a karstic-influenced watershed. *Catena* 195, 104801. <https://doi.org/10.1016/j.catena.2020.104801>.
- Eini, M.R., Javadi, S., Delavar, M., Monteiro, J.A.F., Darand, M., 2019. High accuracy of precipitation reanalyses resulted in good river discharge simulations in a semi-arid basin. *Ecol. Eng.* 131, 107–119. <https://doi.org/10.1016/j.ecoleng.2019.03.005>.
- Eini, M.R., Javadi, S., Hashemy Shahdany, M., Kisi, O., 2021a. Comprehensive assessment and scenario simulation for the future of the hydrological processes in dez river basin. *Water Supply* 21, 1157–1176. <https://doi.org/10.2166/ws.2020.363>.
- Eini, M.R., Olyaei, M.A., Kamyab, T., Teymoori, J., Brocca, L., Piniewski, M., 2021b. Evaluating three non-gauge-corrected satellite precipitation estimates by a regional gauge interpolated dataset over Iran. *J. Hydrol. Reg. Stud.* 38, 100942. <https://doi.org/10.1016/j.ejrh.2021.100942>.
- Eini, M.R., Rahmati, A., Piniewski, M., 2022a. Hydrological application and accuracy evaluation of PERSIANN satellite-based precipitation estimates over a humid continental climate catchment. *J. Hydrol. Reg. Stud.* 41, 101109. <https://doi.org/10.1016/j.ejrh.2022.101109>.
- Eini, M.R., Rahmati, A., Salmani, H., Brocca, L., Piniewski, M., 2022b. Detecting characteristics of extreme precipitation events using regional and satellite-based precipitation gridded datasets over a region in Central Europe. *Sci. Total Environ.* 852, 158497. <https://doi.org/10.1016/j.scitotenv.2022.158497>.
- Eini, M.R., Salmani, H., Piniewski, M., 2023. Comparison of process-based and statistical approaches for simulation and projections of rainfed crop yields. *Agric. Water Manag.* 277, 108107. <https://doi.org/10.1016/j.agwat.2022.108107>.
- Entekhabi, D., Njoku, E.G., O'Neill, P.E., Kellogg, K.H., Crow, W.T., Edelstein, W.N., Entin, J.K., Goodman, S.D., Jackson, T.J., Johnson, J., 2010. The soil moisture active passive (SMAP) mission. *Proc. IEEE* 98, 704–716. <https://doi.org/10.1109/JPROC.2010.2043918>.
- Feng, H.L., Kurkhalova, L.A., Kling, C.L., Gassman, P.W., 2006. Environmental conservation in agriculture: land retirement vs. Changing practices on working land. *J. Environ. Econ. Manag.* 52, 600–614. <https://doi.org/10.1016/j.jeem.2006.03.004>.
- Fernandez-Palomino, C.A., Hattermann, F.F., Krysanova, V., Vega-Jacome, F., Bronstert, A., 2021. Towards a more consistent eco-hydrological modelling through multi-objective calibration: a case study in the andean Vilcanota River basin, Peru. *Hydrol. Sci. J.* 66, 59–74. <https://doi.org/10.1080/02626667.2020.1846740>.
- Fohrer, N., Haverkamp, S., Eckhardt, K., Frede, H.G., 2001. Hydrologic response to land use changes on the catchment scale. *Phys. Chem. Earth Part B* 26, 577–582. [https://doi.org/10.1016/S1464-1909\(01\)00052-1](https://doi.org/10.1016/S1464-1909(01)00052-1).
- Gassman, P.W., Reyes, M.R., Green, C.H., Arnold, J.G., 2007. The soil and water assessment tool: historical development, applications, and future research directions. *Trans. ASABE* 50, 1211–1250. <https://doi.org/10.13031/2013.23637>.
- Gassman, P.W., Sadeghi, A.M., Srinivasan, R., 2014. Applications of the SWAT model special section: overview and insights. *J. Environ. Qual.* 43, 1–8. <https://doi.org/10.2134/jeq2013.11.0466>.
- Grillakis, M.G., Koutoulis, A.G., Alexakis, D.D., Polykretis, C., Daliakopoulos, I.N., 2021. Regionalizing root-zone soil moisture estimates from ESA CCI soil water index using machine learning and information on soil, vegetation, and climate. *Water Resour. Res.* 57, e2020WR029249. <https://doi.org/10.1029/2020WR029249>.
- Gupta, H.V., Beven, K.J., Wagener, T., 2006. Model calibration and uncertainty estimation. *Encycl. Hydrol. Sci.* <https://doi.org/10.1002/0470848944.hsa138>.
- Guse, B., Pfannerstall, M., Gafurov, A., Fohrer, N., Gupta, H., 2016. Demasking the integrated information of discharge: advancing sensitivity analysis to consider different hydrological components and their rates of change. *Water Resour. Res.* 52, 8724–8743. <https://doi.org/10.1002/2016wr018894>.
- Hajihosseini, M., Hajihosseini, H., Morid, S., Delavar, M., Booi, M.J., 2020. Impacts of land use changes and climate variability on transboundary Hiran River using SWAT. *J. Water Clim. Chang.* 11, 1695–1711. <https://doi.org/10.2166/wcc.2019.100>.
- Hirbo Gelebo, A., Kasviswanathan, K.S., Khare, D., Pingale, S.M., 2022. Assessment of spatial and temporal distribution of surface water balance in a data-scarce african transboundary river basin. *Hydrol. Sci. J.* 67, 1561–1581. <https://doi.org/10.1080/02626667.2022.2094268>.
- Huisman, J.A., Sperl, C., Bouten, W., Verstraten, J.M., 2001. Soil water content measurements at different scales: accuracy of time domain reflectometry and ground-penetrating radar. *J. Hydrol.* 245, 48–58. [https://doi.org/10.1016/S0022-1694\(01\)00336-5](https://doi.org/10.1016/S0022-1694(01)00336-5).
- Ilampooranan, I., Schnoor, J.L., Basu, N.B., 2021. Crops as sensors: using crop yield data to increase the robustness of hydrologic and biogeochemical models. *J. Hydrol.* 592, 125599. <https://doi.org/10.1016/j.jhydrol.2020.125599>.
- Ionita, M., Tallaksen, L.M., Kingston, D.G., Stagge, J.H., Laaha, G., Van Lanen, H.A.J., Scholz, P., Chelcea, S.M., Haslinger, K., 2017. The European 2015 drought from a climatological perspective. *Hydrol. Earth Syst. Sci.* 21, 1397–1419. <https://doi.org/10.5194/hess-21-1397-2017>.
- Kerr, Y.H., Waldeufel, P., Wigneron, J.-P., Delwart, S., Cabot, F., Boutin, J., Escorihuela, M.-J., Font, J., Reul, N., Gruhier, C., 2010. The SMOS mission: new tool for monitoring key elements of the global water cycle. *Proc. IEEE* 98, 666–687. <https://doi.org/10.1109/JPROC.2010.2043032>.
- Khan, H.F., Yang, Y.C.E., Xie, H., Ringler, C., 2017. A coupled modeling framework for sustainable watershed management in transboundary river basins. *Hydrol. Earth Syst. Sci.* 21, 6275–6288. <https://doi.org/10.5194/hess-21-6275-2017>.
- Kling, H., Gupta, H., 2009. On the development of regionalization relationships for lumped watershed models: the impact of ignoring sub-basin scale variability. *J. Hydrol.* 373, 337–351. <https://doi.org/10.1016/j.jhydrol.2009.04.031>.
- Knoben, W.J.M., Freer, J.E., Woods, R.A., 2019. Technical note: inherent benchmark or not? Comparing Nash-sutcliffe and kling-gupta efficiency scores. *Hydrol. Earth Syst. Sci.* 23, 4323–4331. <https://doi.org/10.5194/hess-23-4323-2019>.
- Koch, J., Demirel, M.C., Stisen, S., 2018. The SPAtial Efficiency metric (SPAEEF): multiple-component evaluation of spatial patterns for optimization of hydrological models. *Geosci. Model Dev.* 11, 1873–1886. <https://doi.org/10.5194/gmd-11-1873-2018>.
- Koohi, S., Azizian, A., Brocca, L., 2021. Spatiotemporal drought monitoring using bottom-up precipitation dataset (SM2RAIN-ASCAT) over different regions of Iran. *Sci. Total Environ.* 779, 146535. <https://doi.org/10.1016/j.scitotenv.2021.146535>.
- Koohi, S., Azizian, A., Brocca, L., 2022. Calibration of a distributed hydrological model (VIC-3L) based on global water resources reanalysis datasets. *Water Resour. Manag.* 36, 1287–1306. <https://doi.org/10.1007/s11269-022-03081-9>.
- Kovačević, J., Cvijetović, Ž., Stanić, N., Brodić, N., Mihajlović, D., 2020. New downscaling approach using ESA CCI SM products for obtaining high resolution surface soil moisture. *Remote Sens.* 12, 1119. <https://doi.org/10.3390/rs12071119>.
- Kundu, D., Vervoort, R.W., van Ogtrop, F.F., 2017. The value of remotely sensed surface soil moisture for model calibration using SWAT. *Hydrol. Process.* 31, 2764–2780. <https://doi.org/10.1002/hyp.11219>.
- Lal, R., 2004. Soil carbon sequestration to mitigate climate change. *Geoderma* 123, 1–22. <https://doi.org/10.1016/j.geoderma.2004.01.032>.
- Liersch, S., Koch, H., Hattermann, F.F., 2017. Management scenarios of the grand Ethiopian renaissance dam and their impacts under recent and future climates. *Water* 9, 728. <https://doi.org/10.3390/w9100728>.
- Liu, Y.Y., Parinussa, R.M., Dorigo, W.A., De Jeu, R.A.M., Wagner, W., van Dijk, A.I.J.M., McCabe, M.F., Evans, J.P., 2011. Developing an improved soil moisture dataset by blending passive and active microwave satellite-based retrievals. *Hydrol. Earth Syst. Sci.* 15, 425–436. <https://doi.org/10.5194/hess-15-425-2011>.
- Ma, S.Y., Wu, Q.X., Wang, J., Zhang, S.Q., 2017. Temporal evolution of regional drought detected from GRACE TWSA and CCI SM in Yunnan Province, China. *Remote Sensing* 9, 1124. <https://doi.org/10.3390/rs9111124>.
- Ma, T.X., Duan, Z., Li, R.K., Song, X.F., 2019. Enhancing SWAT with remotely sensed LAI for improved modelling of ecohydrological process in subtropics. *J. Hydrol.* 570, 802–815. <https://doi.org/10.1016/j.jhydrol.2019.01.024>.
- Marcinkowski, P., Kardel, I., Placzkowska, E., Gielczewski, M., Osuch, P., Okruszko, T., Venegas-Cordero, N., Ignar, S., Piniewski, M., 2022. High-resolution simulated water balance and streamflow data set for 1951–2020 for the territory of Poland. *Geosci. Data J. n/a* <https://doi.org/10.1002/gdj3.152>.

- Massari, C., Brocca, L., Barbetta, S., Papathanasiou, C., Mimikou, M., Moramarco, T., 2014. Using globally available soil moisture indicators for flood modelling in Mediterranean catchments. *Hydrol. Earth Syst. Sci.* 18, 839–853. <https://doi.org/10.5194/hess-18-839-2014>.
- McDonnell, J.J., Sivapalan, M., Vache, K., Dunn, S., Grant, G., Haggerty, R., Hinz, C., Hooper, R., Kirchner, J., Roderick, M.L., Selker, J., Weiler, M., 2007. Moving beyond heterogeneity and process complexity: a new vision for watershed hydrology. *Water Resour. Res.* 43. <https://doi.org/10.1029/2006wr005467>.
- McNally, A., Shukla, S., Arsenault, K.R., Wang, S., Peters-Lidard, C.D., Verdin, J.P., 2016. Evaluating ESA CCI soil moisture in East Africa. *Int. J. Appl. Earth Obs. Geoinf.* 48, 96–109. <https://doi.org/10.1016/j.jag.2016.01.001>.
- Mianabadi, A., Davary, K., Mianabadi, H., Karimi, P., 2020. International environmental conflict Management in Transboundary River Basins. *Water Resour. Manag.* 34, 3445–3464. <https://doi.org/10.1007/s11269-020-02576-7>.
- Modanesi, S., Massari, C., Camici, S., Brocca, L., Amarnath, G., 2020. Do satellite surface soil moisture observations better retain information about crop-yield variability in drought conditions? *Water Resour. Res.* 56, e2019WR025855. <https://doi.org/10.1029/2019WR025855>.
- Montanari, A., Koutsogiannis, D., 2012. A blueprint for process-based modeling of uncertain hydrological systems. *Water Resour. Res.* 48. <https://doi.org/10.1029/2011wr011412>.
- Ochsner, T.E., Cosh, M.H., Cuenca, R.H., Dorigo, W.A., Draper, C.S., Hagimoto, Y., Kerr, Y.H., Larson, K.M., Njoku, E.G., Small, E.E., Zreda, M., 2013. State of the art in large-scale soil moisture monitoring. *Soil Sci. Soc. Am. J.* 77, 1888–1919. <https://doi.org/10.2136/sssaj2013.03.0093>.
- Or, D., Lehmann, P., Shahraeeni, E., Shokri, N., 2013. Advances in soil evaporation physics—a review. *Vadose Zone J.* 12, 1–16. <https://doi.org/10.2136/vzj2012.0163>.
- Pfannerstill, M., Bieger, K., Guse, B., Bosch, D.D., Fohrer, N., Arnold, J.G., 2017. How to constrain multi-objective calibrations of the Swat model using water balance components. *J. Am. Water Resour. Assoc.* 53, 532–546. <https://doi.org/10.1111/1752-1688.12524>.
- Piniewski, M., Szczesniak, M., Kardel, I., Berezowski, T., Okruszko, T., Srinivasan, R., Schuler, D.V., Kundzewicz, Z.W., 2017. Hydrological modelling of the Vistula and Odra river basins using SWAT. *Hydrol. Sci. J.* 62, 1266–1289. <https://doi.org/10.1080/02626667.2017.1321842>.
- Piniewski, M., Szczesniak, M., Kardel, I., Chattopadhyay, S., Berezowski, T., 2021. G2DC-PL+: a gridded 2 km daily climate dataset for the union of the Polish territory and the Vistula and Odra basins. *Earth Syst. Sci. Data* 13, 1273–1288. <https://doi.org/10.5194/essd-13-1273-2021>.
- Pokhrel, P., Yilmaz, K.K., Gupta, H.V., 2012. Multiple-criteria calibration of a distributed watershed model using spatial regularization and response signatures. *J. Hydrol.* 418, 49–60. <https://doi.org/10.1016/j.jhydrol.2008.12.004>.
- Rajib, M.A., Merwade, V., 2016. Improving soil moisture accounting and streamflow prediction in SWAT by incorporating a modified time-dependent curve number method. *Hydrol. Process.* 30, 603–624. <https://doi.org/10.1002/hyp.10639>.
- Rajib, M.A., Merwade, V., Yu, Z., 2016. Multi-objective calibration of a hydrologic model using spatially distributed remotely sensed/in-situ soil moisture. *J. Hydrol.* 536, 192–207. <https://doi.org/10.1016/j.jhydrol.2016.02.037>.
- Ren, P.Z., Li, J.Z., Feng, P., Guo, Y.G., Ma, Q.S., 2018. Evaluation of multiple satellite precipitation products and their use in hydrological modelling over the Luanhe River Basin, China. *Water* 10, 677. <https://doi.org/10.3390/w10060677>.
- Rougé, C., Tilmant, A., Zaitchik, B., Dezfuli, A., Salman, M., 2018. Identifying key water resource vulnerabilities in data-scarce Transboundary River basins. *Water Resour. Res.* 54, 5264–5281. <https://doi.org/10.1029/2017wr021489>.
- Sivapalan, M., Savenije, H.H.G., Blöschl, G., 2012. Socio-hydrology: a new science of people and water. *Hydrol. Process.* 26, 1270–1276. <https://doi.org/10.1002/hyp.8426>.
- Sood, A., Smakhtin, V., 2015. Global hydrological models: a review. *Hydrol. Sci. J.* 60, 549–565. <https://doi.org/10.1080/02626667.2014.950580>.
- Tan, M.L., Gassman, P.W., Srinivasan, R., Arnold, J.G., Yang, X.Y., 2019. A review of SWAT studies in Southeast Asia: applications, challenges and future directions. *Water* 11, 914. <https://doi.org/10.3390/w11050914>.
- Triana, J.S.A., Chu, M.L., Guzman, J.A., Moriasi, D.N., Steiner, J.L., 2019. Beyond model metrics: the perils of calibrating hydrologic models. *J. Hydrol.* 578, 124032. <https://doi.org/10.1016/j.jhydrol.2019.124032>.
- van Griensven, A., Ndomba, P., Yalaw, S., Kilonzo, F., 2012. Critical review of SWAT applications in the upper Nile basin countries. *Hydrol. Earth Syst. Sci.* 16, 3371–3381. <https://doi.org/10.5194/hess-16-3371-2012>.
- Wagner, P.D., Bieger, K., Arnold, J.G., Fohrer, N., 2022. Representation of hydrological processes in a rural lowland catchment in northern Germany using SWAT and SWAT. *Hydrol. Process.* 36, e14589. <https://doi.org/10.1002/hyp.14589>.
- Wagner, W., Hahn, S., Kidd, R., Melzer, T., Bartalis, Z., Hasenauer, S., Figa, J., De Rosnay, P., Jann, A., Schneider, S., 2013. The ASCAT soil moisture product: a review of its. *Meteorol. Z.* 22, 1–29. <https://doi.org/10.1127/0941-2948/2013/0399>.
- Wagner, W., Lemoine, G., Rott, H., 1999. A method for estimating soil moisture from ERS scatterometer and soil data. *Remote Sens. Environ.* 70, 191–207. [https://doi.org/10.1016/S0034-4257\(99\)00036-X](https://doi.org/10.1016/S0034-4257(99)00036-X).
- Wang, Y.P., Jiang, R.G., Xie, J.C., Zhao, Y., Yan, D.F., Yang, S.Y., 2019. Soil and water assessment tool (SWAT) model: a systemic review. *J. Coast. Res.* 93, 22–30. <https://doi.org/10.2112/SI93-004.1>.
- Wu, J.W., Yen, H., Arnold, J.G., Yang, Y.C.E., Cai, X.M., White, M.J., Santhi, C., Miao, C.Y., Srinivasan, R., 2020. Development of reservoir operation functions in SWAT plus for national environmental assessments. *J. Hydrol.* 583, 124556. <https://doi.org/10.1016/j.jhydrol.2020.124556>.
- Yang, J., Reichert, P., Abbaspour, K.C., Xia, J., Yang, H., 2008. Comparing uncertainty analysis techniques for a SWAT application to the Chaohe Basin in China. *J. Hydrol.* 358, 1–23. <https://doi.org/10.1016/j.jhydrol.2008.05.012>.
- Zhang, L.Q., Liu, Y., Ren, L.L., Jiang, S.H., Yang, X.L., Yuan, F., Wang, M.H., Wei, L.Y., 2019. Drought monitoring and evaluation by ESA CCI soil moisture products over the Yellow River Basin. *IEEE J. Sel. Top. Appl. Earth Observ. Remote Sens.* 12, 3376–3386. <https://doi.org/10.1109/Jstars.2019.2934732>.
- Zhang, L.Q., Liu, Y., Ren, L.L., Teuling, A.J., Zhang, X.X., Jiang, S.H., Yang, X.L., Wei, L.Y., Zhong, F., Zheng, L.H., 2021. Reconstruction of ESA CCI satellite-derived soil moisture using an artificial neural network technology. *Sci. Total Environ.* 782, 146602. <https://doi.org/10.1016/j.scitotenv.2021.146602>.

Warsaw, 26/03/2024

Mohammadreza Einikarimkandi
d003066@sggw.edu.pl

**Institute of Environmental Engineering,
Mining, and Energy, Discipline
Council
of the Warsaw University of Life
Sciences**

Co-authorship statement

I hereby represent that in the below publication “Eini, M. R., Massari, C., & Piniewski, M. (2023). Satellite-based soil moisture enhances the reliability of agro-hydrological modeling in large transboundary river basins. Science of the Total Environment, 873, 162396. <https://doi.org/10.1016/j.scitotenv.2023.162396>” my individual contribution in the development thereof involved, Conceptualization, methodology, software, validation, writing – original draft, writing – review & editing, visualization.


Signature
Mohammad Reza
Eini Karimkandi

Perugia, 26/03/2024

Christian Massari

christian.massari@.cnr.it

**Institute of Environmental Engineering,
Mining, and Energy, Discipline
Council
of the Warsaw University of Life
Sciences**

Co-authorship statement

I hereby represent that in the publication Eini, M. R., Massari, C., & Piniewski, M. (2023). Satellite-based soil moisture enhances the reliability of agro-hydrological modeling in large transboundary river basins. Science of the Total Environment, 873, 162396. <https://doi.org/10.1016/j.scitotenv.2023.162396> my individual contribution in the development thereof involved conceptualization, methodology, review and editing the manuscript.

Signature

A handwritten signature in black ink that reads "Christian Massari". The script is cursive and fluid, with the first name and last name clearly distinguishable.

Warsaw, 26/03/2024

Dr hab. Mikołaj Piniewski, prof. SGGW
Department of Hydrology, Meteorology and Water Management
Institute of Environmental Engineering
Warsaw University of Life Sciences
mikolaj_piniewski@sggw.edu.pl

**Institute of Environmental Engineering,
Mining, and Energy, Discipline
Council
of the Warsaw University of Life
Sciences**

Co-authorship statement

I hereby represent that in the below publication "Eini, M. R., Massari, C., & Piniewski, M. (2023). Satellite-based soil moisture enhances the reliability of agro-hydrological modeling in large transboundary river basins. Science of the Total Environment, 873, 162396. <https://doi.org/10.1016/j.scitotenv.2023.162396>" my individual contribution in the development thereof involved, conceptualization, methodology, writing – review & editing.



Signature

13. Publication 5

Eini, M. R., Najminejad, F., & Piniewski, M. (2023). Direct and indirect simulating and projecting hydrological drought using a supervised machine learning method. *Science of The Total Environment*, 898, 165523.

<https://doi.org/10.1016/j.scitotenv.2023.165523>

Impact factor: 9.8 – MeiN: 200



Direct and indirect simulating and projecting hydrological drought using a supervised machine learning method

Mohammad Reza Eini^{a,b,*}, Farzaneh Najminejad^c, Mikołaj Piniewski^a

^a Department of Hydrology, Meteorology and Water Management, Institute of Environmental Engineering, Warsaw University of Life Sciences, Warsaw, Poland

^b Potsdam Institute for Climate Impact Research (PIK), Member of the Leibniz Association, Telegraphenberg A 31, 14473 Potsdam, Germany

^c College of Agriculture & Natural Resources, University of Tehran, Karaj, Iran

ARTICLE INFO

Editor: Fernando A.L. Pacheco

Keywords:

Climate change

Hydrological drought

Standardized drought index

Data-driven models

ABSTRACT

There is a trend in using Artificial Intelligence methods as simulation tools in different aspects of hydrology, including river discharge simulations, drought predictions, and crop yield simulations. The motivation of this work was to assess two various concepts in applying these methods in simulations and projections of hydrological drought. In this study, Standardized Runoff Index (SRI) was simulated and projected using Artificial Neural Networks (ANNs). Maximum and minimum temperature, precipitation, and meteorological drought indicators (the Standardized Precipitation Index (SPI)) were selected as predictors. A direct approach (directly simulating and projecting SRI) and an indirect approach (simulating and projecting river discharge, then calculating SRI) were assessed. Our results show that the indirect approach performs better than the direct approach in simulations of SRI in four discharge stations in the Odra River Basin (a transboundary river basin in Central Europe) from 2000 to 2019. Moreover, a considerable difference between these two approaches was detected in projections of hydrological drought under the RCP8.5 emission scenario for two horizons (near future: 2021–2040, and far future: 2041–2060). Based on the run theory, both approaches show somewhat similar drought conditions for future projections.

1. Introduction

Drought is an indicator of the below-normal availability of water in the environment (Piri et al., 2022; Prodhan et al., 2022). In various regions of the world, drought events have been increasing in recent years, and their consequences have been more harmful owing to increased water needs and climatic changes (Shamshirband et al., 2020; Wang et al., 2022). Thus, drought has drawn consideration, and studying the attributes of this natural hazard from various points of view has been a topic of high priority for researchers (Prodhan et al., 2022). Drought begins with a substantial lack of precipitation and continues to agricultural drought (lack of water in the soil), and then causes hydrological drought (declining in river discharges) (Lin et al., 2023; Ma et al., 2023; Zhang et al., 2022). Hydrological and agricultural droughts threaten the food security of society, farmers' financial situations, and water accessibility for people and the ecosystem (Mishra, 2020; Teutschbein et al., 2023). Moreover, it is reported that drought events correlate with inland and international conflicts in some parts of the world (Gleick, 2014). In

this regard, assessing the projections of drought events could be an emergency practice, especially in transboundary river basins (Adaawen et al., 2019).

Drought can be divided into different types, such as meteorological drought, hydrological drought, and agricultural drought (Teutschbein et al., 2023). In this regard, several drought indicators have been developed, such as SPEI (Standardized Precipitation Evapotranspiration Index) (Vicente-Serrano et al., 2010), SPI (Standardized Precipitation Index) (McKee et al., 1993), and SRI (Standardized Runoff Index) (Shukla and Wood, 2008). By employing statistical methods, these indicators convert physical variables, such as precipitation, runoff, soil moisture, and evaporation, to categorized values and make it easier to interpret and analyze the lack of available water in a basin over a long period (Prodhan et al., 2022).

Precipitation and river discharge amounts can be used for determining meteorological droughts and hydrological droughts, respectively. These variables are available for historical periods (measured data) and can be estimated for future horizons using modeling

* Corresponding author at: Department of Hydrology, Meteorology and Water Management, Institute of Environmental Engineering, Warsaw University of Life Sciences, Warsaw, Poland.

E-mail address: mohammad_eini@sggw.edu.pl (M.R. Eini).

<https://doi.org/10.1016/j.scitotenv.2023.165523>

Received 28 March 2023; Received in revised form 11 July 2023; Accepted 11 July 2023

Available online 14 July 2023

0048-9697/© 2023 Elsevier B.V. All rights reserved.

approaches. According to the concept of climate change, future projections could be expected in various scenarios (Chen et al., 2021; Eini et al., 2023b). These scenarios range from optimistic scenarios to pessimistic scenarios. Employing General Circulation Models (GCMs) (Chen et al., 2021; Pachauri and Meyer, 2014) under defined scenarios for different horizons is the most common way of projecting precipitation and other climatic parameters; then projecting meteorological drought can be estimated (Eini et al., 2023b).

Several modeling approaches for projecting river discharge can be used, such as process-based and data-driven approaches (Eini et al., 2020b; Moghadam et al., 2022; Pektaş and Kerem Cigizoglu, 2013). In general, process-based hydrological modeling is time-consuming and requires extensive data, such as land use land cover maps, soil properties, climatic variables, and management schedules (Eini et al., 2020a). On the opposite, data-driven approaches can model river discharge by employing the minimum variables, such as climatic variables (Moghadam et al., 2022; Prodhon et al., 2022). Then, projections of river discharge (accordingly, hydrological drought) can be estimated by combining GCMs (as inputs), hydrological models, and data-driven approaches.

Artificial intelligence (AI) has recently attracted consideration from hydrologists to simulate and project various phenomena (Eini et al., 2023b; Moghadam et al., 2022; Prodhon et al., 2022). AI-based approaches are based on statistical and mathematical methods and try to find a pattern between input data and outputs. These approaches have shown high accuracy in simulating a broad range of processes in the realm of hydrology, agriculture, and meteorology, such as simulations and projections of soil moisture, crop yield, wind speed, solar radiation, river discharge, drought, and sedimentation (Deo et al., 2018; Pektaş and Kerem Cigizoglu, 2013; Piri et al., 2022; Prodhon et al., 2022; Wang et al., 2022). According to the literature, AI-based models, such as machine learning and deep learning, have considerably impacted drought management and have been used as alternative methods for process-based hydrological models (Eini et al., 2023b; Moghadam et al., 2022). Since drought is characteristically known as an attribute of nonlinearity and instability, AI-based models have the capacity of self-organizing and self-adaptive procedures with the nonlinear characteristic capable of simulating and projecting hydrological and meteorological data for drought detections (Prodhon et al., 2022). A long list of AI-based models has been tested in drought simulations. These models can generally be grouped into unsupervised and supervised learning methods. Supervised learning requires labelled data during training to enable the model to make predictions based on known outputs. The model learns the relationship between input and output variables by optimizing its parameters using the labelled examples. In contrast, unsupervised learning deals with unlabeled data to discover patterns and structures without predefined outputs. The model explores the data to identify similarities, differences, or clusters, revealing underlying relationships. Unsupervised learning is often used for clustering, anomaly detection, and dimensionality reduction tasks (Alloghani et al., 2020).

Supervised methods, such as artificial neural network (ANN), support vector machine (SVM), random forest (RF), and classification and regression tree (CART), are more considered in drought simulations and have shown reliable results in different studies (Prodhon et al., 2022).

Selecting predictors (as inputs) plays a vital role in the AI-based modeling approach. Various variables in different studies have been imported as predictors, such as river discharge, climatic parameters, meteorological drought indicators, soil moisture, precipitation anomalies, humidity, and evaporation, to simulate hydrological drought through AI-based methods (Eini et al., 2023b; Prodhon et al., 2022). These inputs have been extracted from different sources, such as measured databases and remotely sensed datasets. In some studies, it is noted that adding drought indicators in the simulation process of data-driven models could enhance modeling results and leads to a more reliable model (Eini et al., 2023b). Moreover, drought indicators can increase the number of predictors; in their nature, these indicators have

a memory of past conditions. As mentioned, a hydrological drought is a consequence of a meteorological drought and could happen several months after a meteorological drought. Consequently, meteorological drought indicators have a significant impact on hydrological drought simulations when utilizing AI-based models. The first approach is the direct simulation of drought indicators. In this approach, drought indicators are calculated directly from inputs. The second approach is the indirect approach, in which drought indicators are calculated based on simulated runoff by AI-based models (Prodhon et al., 2022). Both approaches have their advantages and limitations. Indirect simulation using AI-based models can provide a more accurate prediction of drought based on physical processes, but it may be more computationally intensive and require more data to train the models. In comparison, direct simulation relies on the assumption that past drought events can be used to predict future events, which may not always be the case, but can be less computationally intensive and require fewer data. A direct approach in simulating and projecting hydrological droughts was used in Yang et al. (2015), whereas stream flow simulations and drought projections using ANN by an indirect approach was done in Gao et al. (2010), Zeng et al. (2012), and Su et al. (2015).

The similarities and differences between direct and indirect approaches are open questions and motivated us to analyze both approaches for the first time in a large transboundary river basin (Odra/Oder River Basin) in Central Europe. Drought in the Odra River Basin is typically caused by a combination of factors, including low precipitation, high temperatures, and strong winds (Hao et al., 2022; Liu et al., 2022). This region, as well as other river basins in Central Europe, has experienced severe droughts in recent years, which resulted in water shortages, changes in low riverine flow, crop losses, and forest fires (Ionita et al., 2017; Jaagus et al., 2022; Laaha et al., 2017; Leuzinger et al., 2005; Piniewski et al., 2022). According to Meier et al. (2022), alterations in the hydrological cycle over the Baltic Sea basins are projected to become noticeable in the following decades. At the same time, Jaagus et al. (2022) concluded that the meteorological drought situations in central and eastern Europe remained unchanged over the 1949–2018 period. Hence, assessments of historical and drought projections in this region are extremely important as a growth in the severity of different types of droughts in the coming decades is expected (Hari et al., 2020; Jaagus et al., 2022).

The objectives of this study are simulations and projections of hydrological drought by employing ANN through direct and indirect approaches and then assessing the similarities and differences between projections. In this regard, the RCP8.5 climate change scenario (the concentration of carbon dioxide that delivers global warming at an average of 8.5 watts/m² by 2100 (Riahi et al., 2011)) based on GCMs for two horizons is selected, and then by employing a supervised method (ANN), droughts are projected. In this study, four hypotheses are considered: (1) ANN has a high accuracy in runoff and drought simulations; (2) meteorological drought indicator (i.e., SPI) can be used as a predictor of runoff and hydrological drought; (3) with the same predictors, direct and indirect approaches do not have considerable differences in estimating hydrological drought indicators; (4) under the condition of the worst scenario for far future droughts are expected to become more frequent and more severe than for the historical period.

2. Materials and method

2.1. Study area

The Odra (Oder) River Basin (ORB) is located in the Baltic Sea region (placed in Poland (89 %), Germany (4.9 %), and the Czech Republic (6.1 %)) and is listed as the fifth largest river basin in European Union. This transboundary basin's mean annual river discharge is 154 mm (567 m³/s), and the long-term yearly average of precipitation is around 650 mm. ORB covers 119,041 km², and the river is approximately 854 km long (the second longest river in Poland), with sources in the Sudetes

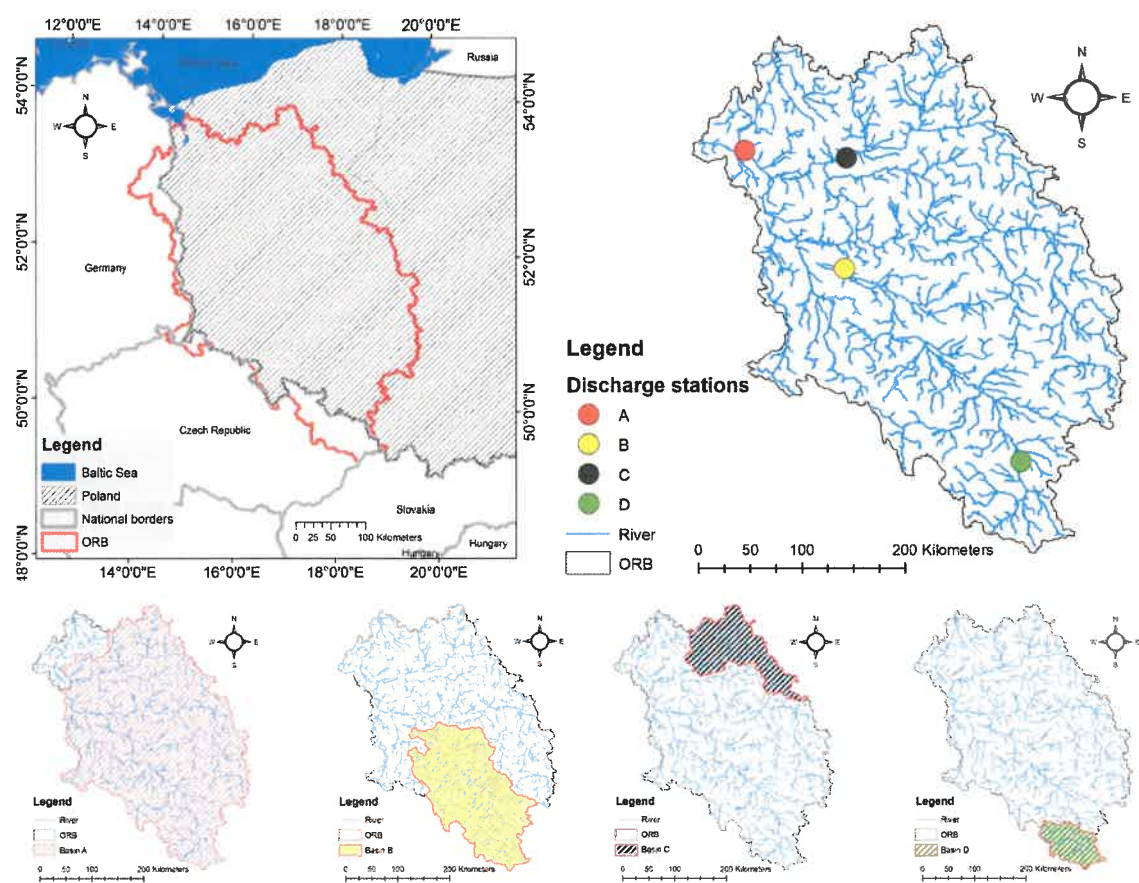


Fig. 1. The location of the Odra River Basin in Central Europe and selected discharge stations and their drainage areas, and river network.

Table 1
Statistical parameters of selected river discharge stations (2000–2019).

River and discharge station	Odra at Gozdowice	Odra at Cigacice	Noteć at Nowe Drezdenko	Odra at Racibórz-Miedonia
ID	A	B	C	D
Drainage area (km ²)	110,000	37,200	16,500	6700
Mean river discharge (m ³ /s)	472	182	68	61
Absolute Minimum river discharge (m ³ /s)	144	53	27	11
Absolute Maximum river discharge (m ³ /s)	1412	680	188	413
Standard deviation (m ³ /s)	235	107	27	45

Mountains in the Czech Republic and the estuary to the Szczecin Lagoon connected to the Baltic Sea in its southern part. The great majority of the drainage area spans the Central European Plain, with only the southernmost regions being mountainous (Fig. 1) (Eini et al., 2023a; Marcinkowski et al., 2022; Piniewski et al., 2017b; Piniewski et al., 2017c). This river is a narrow and mountainous river in its upper section (upstream from the Kędzierzyn-Koźle city). Then, on its lower section (outlet of Warta River), the river is roughly flat, and which slope changes between 0.05 m/km and 0.001 m/km (Halicki et al., 2023). The study area and Central Europe experienced severe drought during the summer of 2015 (Ionita et al., 2017; Laaha et al., 2017). In this study, four discharge stations from the Institute of Meteorology and Water Management – National Research Institute (IMGW-PIB) in this basin are selected. In Fig. 1 and Table 1, the location and details of these discharge stations are presented.

2.2. Hydrometeorological data

A regional gridded weather dataset (G2DC-PL+: a gridded 2 km daily

climate dataset for the union of the Polish territory and the Vistula and Odra basins) was selected to extract precipitation and maximum and minimum temperature over this region. The time span of this dataset is 1951–2019, and daily precipitation, maximum and minimum temperature, wind speed, and relative humidity are included in G2DC-PL+ (Berezowski et al., 2016; Piniewski et al., 2021). This dataset is employed in several studies, especially in agro-hydrological modeling, and has shown acceptable accuracy (Eini et al., 2022a; Eini et al., 2022b; Marcinkowski et al., 2022). River discharge data were obtained from the Institute of Meteorology and Water Management (IMGW-PIB: <https://danepubliczne.imgw.pl/>). In this study, four river discharge stations were selected. The selections are based on the annual river discharge, and these river discharge stations can be considered as the main river discharge stations. The annual average of the river discharges varies between 61 m³/s (Odra at Racibórz-Miedonia) and 472 m³/s (Odra at Gozdowice). The properties of the selected river discharge time-series are presented in Table 1.

This study employs the monthly average of the maximum and minimum temperature, river discharge, and monthly precipitation for

2000–2019. It should be mentioned that the precipitation and temperature variables were calculated for each drainage area separately (four drainage areas based on river discharge stations).

2.3. Standardized drought indicators

SPI and SRI were selected as meteorological and hydrological drought indicators, respectively. SPI and SRI as drought indicators can be calculated by precipitation and river discharge data, respectively. These indicators can show the drought in different time scales. The SPI was designed to compute precipitation scarcity for various time scales (Kao and Govindaraju, 2010). These time scales reflect the impact of drought on the availability of different water resources. McKee et al. (1993) originally determined the SPI for 3- (short-term drought), 6- (mid-term drought), and 12-, 24-, and 48-month (long-term drought) time scales. SPI or SRI can be grouped into different classes, including above 0 as the wet condition, below 0 as the dry conditions, and less than -1 as the severe drought. Nevertheless, these classifications could vary in different studies and regions (e.g., less than -1.5 can be chosen as severe drought in dry areas (Piri et al., 2022)). The concept and calculation methods of SPI (the same as SRI) are presented in several studies, such as McKee et al. (1993), Mirabbasi et al. (2013), and Jain et al. (2015). We employed long-term precipitation data (30 years, 1990–2019) to increase the accuracy of SPI estimation, but 20 years (2000–2019) of river discharge data were employed to calculate SRI.

This study used gamma distribution to calculate SPI and SRI indicators. SPI and SRI can be calculated for different monthly scales. According to Shukla and Wood (2008), in determining the hydrological drought, the gamma distribution performs better for low runoff values compared to the log-normal distribution; also McKee et al. (1993) suggested that the gamma distribution can be applied to other drought-related variables such as river discharge. Our research has chosen SPI-1 to SPI-12 as inputs to the data-driven model. For hydrological drought analyses, SRI-3 (short-term drought), SRI-6 (mid-term drought), SRI-9 (mid-term drought), and SRI-12 (long-term drought) were assessed.

In calculating drought indicators for the future, in the first step, the gamma distribution was fitted using the historical time series (reference periods were 1990–2019 and 2000–2019 for SPI and SRI, respectively). Then, the fitted distribution was employed for the projections.

To evaluate the hydrological drought properties, the run theory is employed (Mesbahzadeh et al., 2020; Yevjevich, 1967). Based on this theory, drought severity, duration, and frequency are equivalent to the accumulation of the SRI values below the threshold level (here -1 is assumed as the threshold level), the number of months in which the SRI value is continuously below the threshold level, and the number of drought events when the SRI is below the threshold, respectively (Guo

et al., 2022; Mesbahzadeh et al., 2020). Fig. 2 illustrates the run theory assumptions (-1 is assumed as the threshold level).

According to the objectives of this study, SPI was chosen as the influential input parameter for hydrological drought simulations by data-driven models, as well as precipitation and temperature. Moreover, it is employed in other studies as an influential predictor of different types of droughts and crop yield simulations (Eini et al., 2023b; Prodhon et al., 2022; Wang et al., 2022). Additionally, it is crucial to have more rational inputs in data-driven models to have a robust model. Monthly precipitation indicates the amount of precipitation in a given month, but river discharge and hydrological drought, especially in large basins and cold climates, also rely on precipitation in previous months. Hence, SPI, as an indicator of short-term to long-term meteorological droughts, could increase the reliability of data-driven models to simulate river discharge and hydrological drought. Another purpose of selecting SPI as a predictor of SRI is that this variable can be obtained from precipitation for both historical and projection periods. While estimating other climatic variables, such as solar radiation, wind speed, and humidity, for the projection period is not simply feasible.

2.4. Artificial neural network design

ANNs, as supervised machine learning models, are extensively employed in Earth's process simulations and projections (Lugato et al., 2020; Prodhon et al., 2022). Among the wide list of algorithms that can be used for the learning process in ANN-based models, Feed Forward Back Propagation Neural Network (FFBPNN) has been employed widely and has shown a robust algorithm for classification, regression, and pattern encoding between inputs and outputs (Abhishek, 2021; Eini et al., 2023b). In this algorithm, one layer belongs to inputs and one layer to outputs, and the algorithm can have one or more hidden layers for data processing and model building. In this study, Levenberg-Marquardt backpropagation was selected to train the FFBPNN (based on the trial-and-error process and suggestions in other studies in agro-hydrological simulations). Several studies have shown that one hidden layer has sufficient ability to process the data and find the pattern between inputs and outputs (Abhishek, 2021; Eini et al., 2023b; Zounemat-Kermani et al., 2019); hence, in this study, one hidden layer was employed, and the sigmoid and linear activation functions were used in to transfer data from inputs to the hidden layer and from hidden layer to output layer, respectively. Different settings were tested to select the number of neurons in the hidden layer, and 12 neurons were employed. After coordinating the input and output data between -1 and 1 , data were randomly divided into three blocks (training, test, and validation, respectively 70 %, 15 %, and 15 % of data).

We used monthly minimum and maximum temperature, monthly precipitation, and SPI-1 to SPI-12 as predictors of runoff (indirect approach) and SRI (direct approach). The details of inputs and outputs are described in Table 1. In the direct approach, SRI is simulated and projected directly from mentioned predictors; in the indirect approach, river discharge is the output of ANN, and accordingly, SRI is calculated. Then, by passing the training, validation, and test steps, two ANN models will be ready for estimating runoff (indirect approach) and SRI (direct approach) projections.

2.5. Climate change scenarios

In this study, four GCMs out of 19 GCMs (based on Coupled Model Intercomparison Project – Phase 5 (CMIP5), built in GCMs in Lars-WG 6.0 software, <https://sites.google.com/view/lars-wg/>) were chosen, and changes in precipitation and temperature were extracted from these models for RCP 8.5 emission scenario for two horizons (2021–2040 as the near future, and 2041–2060 as the far future). The method of selecting the GCMs has been described in our previous study in Eini et al. (2023b), which is freely available, and to reduce the duplicates, we have included a brief of this part in Table 2.

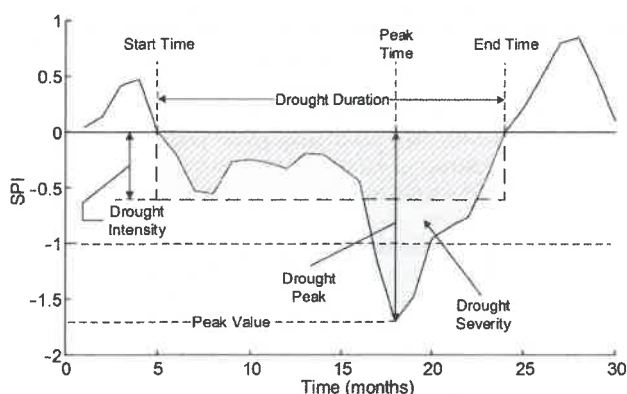


Fig. 2. Drought properties (SRI or SPI) based on run theory assumptions (in the current study, the threshold level is -1); adopted from Guo et al. (2022).

Table 2

Features of climatic parameters in selected GCMs under RCP8.5 in the current study, 1990–2019 was selected as baseline (more details can be found in Eini et al. (2023)).

Scenario	Model	Near Future (2021–2040)		Far Future (2041–2060)	
		Temperature (absolute change)	Precipitation (relative change)	Temperature (absolute change)	Precipitation (relative change)
Moderate	CMCC-CM	–	–	2.51	0.04
Warm and wet	GFDL-CM3	2.54	0.14	3.95	0.12
Warm and dry	HadGEM2-ES	2.19	0.00	3.23	–0.04
Moderate	NCAR-CESM1-CAM5	1.46	0.05	–	–

Table 3

Details of employed performance indicators and optimum values (O: observed data; M: simulated data; N: number of data; i: month indicator; avg.: average).

Index	Unit	Equation	Range of index	Optimum Value
R ²	–	$\left[\frac{\sum_1^N (O_i - O_{avg})(M_i - M_{avg})}{\sqrt{\sum_1^N (O_i - O_{avg})^2 + \sum_1^N (M_i - M_{avg})^2}} \right]^2$	[0, 1]	1
RMSE	–	$\sqrt{\frac{\sum_1^N (M_i - O_i)^2}{N}}$	[0, +∞)	0
PBIAS	%	$100 \times \frac{\sum_1^N (M_i - O_i)}{\sum_1^N O_i}$	(–∞, +∞)	0
KGE	–	$1 - \sqrt{(r-1)^2 + (\beta-1)^2 + (\gamma-1)^2}$ r : Pearson correlation coefficient $\beta = \frac{\mu_M}{\mu_O}, \gamma = \left(\frac{\sigma_M \times \mu_O}{\sigma_O \times \mu_M} \right)$	(–∞, 1)	1

Table 4

List of software, data, computational packages, and environments used in this study.

Tool or data	Description	Source
HydroGOF (R package)	Evaluating the performance indicators	https://cran.r-project.org/web/packages/hydroGOF/hydroGOF.pdf
Climate Data Tools (CDT, R package)	SPI and SRI calculations	https://github.com/rijaf-iri/CDT
LarsWG6	LARS-WG weather generator	https://sites.google.com/view/lars-wg/
G2DC-PL+	Time series of climatic variables	https://doi.org/10.4121/uuid:a3bed3b8-e22a-4b68-8d75-7b87109c9feb
River discharge	Time series of discharge data from the Institute of Meteorology and Water Management (IMGW-PIB)	https://danepubliczne.imgw.pl/

In the process of selecting GCMs and determining future climatic scenarios, we evaluated the annual average changes in temperature and precipitation for each GCM. The climatic scenarios are categorized into three: the moderate scenario, the warm and dry scenario, and the warm and wet scenario. For the moderate scenario, the GCM with the average of changes in precipitation and temperature compared to other GCMs was selected. The GCM for the warm and dry scenario was chosen based on the maximum temperature increment and maximum precipitation decrement. Similarly, the GCM for the warm and wet scenario is selected based on the maximum temperature increment and precipitation increment. The models and average changes in temperature and precipitation are shown in Table 2. It should be mentioned that these scenarios are the average scenarios for ORB. The daily precipitation and temperature data were downscaled using Lars-WG6 software by considering 1990–2019 as the baseline period.

2.6. Performance indicators, tools, and workflow

For assessing the accuracy of simulated datasets, KGE (Kling-Gupta Efficiency, Gupta et al. (2009)), RMSE (Root Mean Square Error), PBIAS (Percent bias), and R-square (R², Coefficient of Determination) were applied (Table 3). It should be pointed out that there are no guidelines for selecting these performance indicators, and these indicators can be chosen based on the user's experience and the type of simulated data. The sources of data, software, and computational packages are described in Table 4. The workflow of this study is presented in Fig. 3.

3. Results

3.1. Indirect simulation of hydrological drought

In the indirect simulation approach, by employing data and methods mentioned in Section 2, in the first step (monthly) river discharge for four discharge stations was simulated, and in the second step SRI-3, SRI-6, SRI-9, and SRI-12 were calculated.

3.1.1. River discharge simulations

ANN has shown high accuracy in river discharge simulations, according to the presented results in Table 5. In this regard, KGE varies between 0.83 and 0.95, PBIAS varies between –9.4 % and 1.1 %, and R² varies between 0.75 and 0.92. According to the criteria of performance indicators in runoff simulations (i.e., Moriasi and Gitau (2015) and Harmel et al. (2018)), ANN has a “very good” performance in runoff simulations. In addition, model performance in training (KGE = 0.89, PBIAS = –1.5 %, R² = 0.87), validation (KGE = 0.94, PBIAS = –2.1 %, R² = 0.9), and test (KGE = 0.91, PBIAS = 2.2 %, R² = 0.91) steps were also very good. Fig. 4 shows simulated time series against observed datasets. A visual inspection suggests that the discharge simulation by the ANN in the lowland catchment (gauge C) is excellent, especially for low flows. In contrast, simulations are much worse in the mountainous (gauge D) and semi-mountainous (gauge B) catchments, in which low flows are strongly underestimated and the model simulates zero flows for some months. Predictions for the entire basin (gauge A) are better than for mountainous catchments, but not as good as for a lowland

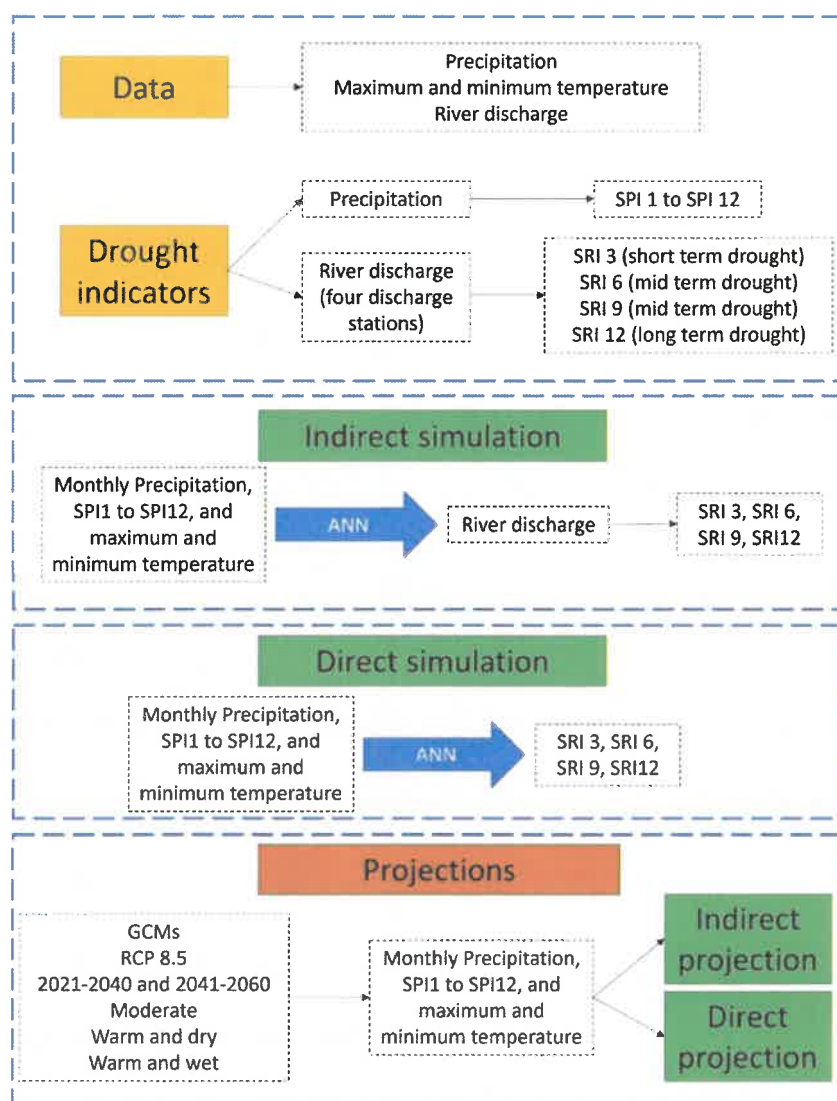


Fig. 3. Graphical diagram of the implemented methodology.

Table 5
Model performance in river discharge simulations (2000–2019).

Discharge station	Mean river discharge (m ³ /s)	KGE	PBIAS%	R ²
A	472	0.91	−2.8	0.84
B	182	0.86	−4.2	0.77
C	68	0.95	1.1	0.92
D	61	0.83	−9.4	0.75

catchment. Low flows in gauge A are usually underestimated.

3.1.2. Accuracy of indirect calculation of hydrological drought

Simulated river discharges were used in SRI calculations. According to the presented results in Table 6, calculated SRI based on simulated river discharge performs well in most cases. Table 6 shows that long-term hydrological drought indicators (i.e., SRI-9 and SRI-12) are more accurate than short-term indicators. A low accuracy can be seen in discharge station D, which results from poor simulations presented in Fig. 4. Accuracy of calculated SRI based on simulated runoff against calculated SRI based on observed data, in terms of KGE (0.28 to 0.95), RMSE (0.15 to 0.64 m³/s), and R² (0.6 to 0.97), is high. Fig. 5 presents calculated SRI values against simulated SRI values for all discharge

stations. In Fig. 6 distribution of calculated SRI values based on observed data, indirect approach, and direct approach are illustrated by a violin plot. The distribution of SRI values is well captured for both direct and indirect methods.

3.2. Direct simulations of hydrological drought indicators

Direct simulation refers to simulating SRI directly from predictors. According to Table 7, ANN could not show high performance in simulating SRI directly from predictors. While correlation (R²) of simulated and calculated SRI are acceptable, in terms of KGE, ANN could not show acceptable accuracy. In Fig. 5 and Fig. 6, the time series of SRI and the distribution of these indicators in all conditions are presented.

3.3. Hydrological drought characteristics

Historical hydrological drought characteristics based on run theory are presented in Table 8. According to the results, the outlet of the basin (station A) has experienced 34 months of severe short-term drought (SRI-3 ≤ −1), and the harshest drought was indicated as −1.56. The severity (see Fig. 2) of short-term drought in this discharge station,

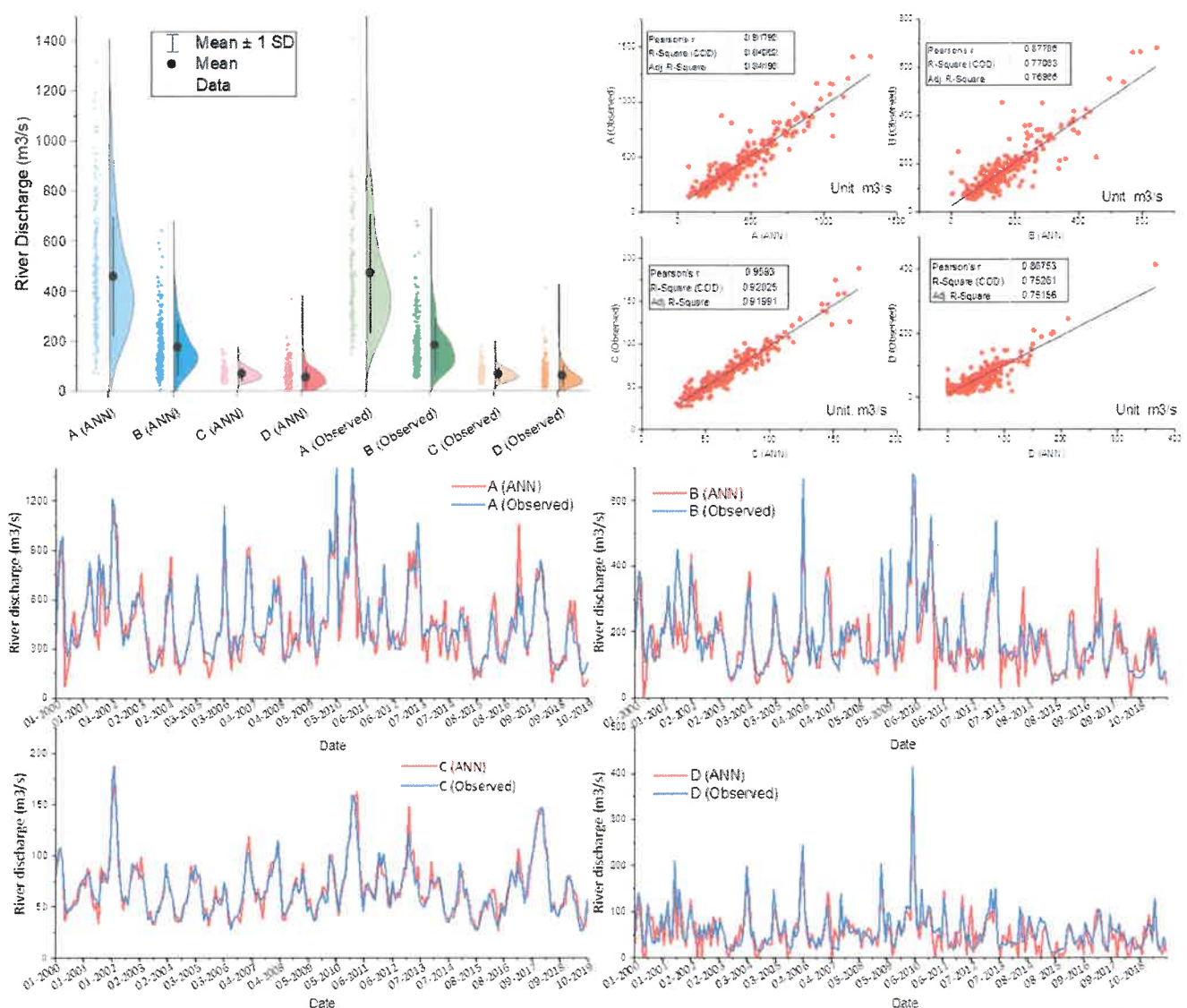


Fig. 4. Simulated river discharge time series against the observed data (2000–2019) – A, B, C, and D refer to discharge stations.

Table 6
Accuracy of calculated SRI based on simulated river discharge (indirect approach) against calculated SRI based on observed data (2000–2019).

Drought indicator	Discharge station	KGE	RMSE	R ²
SRI-3	A	0.69	0.39	0.83
	B	0.5	0.46	0.76
	C	0.84	0.27	0.91
	D	0.28	0.64	0.6
SRI-6	A	0.86	0.29	0.9
	B	0.63	0.38	0.84
	C	0.88	0.2	0.95
	D	0.57	0.53	0.71
SRI-9	A	0.94	0.26	0.92
	B	0.75	0.33	0.87
	C	0.91	0.17	0.96
	D	0.42	0.5	0.75
SRI-12	A	0.89	0.24	0.93
	B	0.86	0.29	0.9
	C	0.95	0.15	0.97
	D	0.37	0.47	0.77

which represents the total river discharge of the basin, is -42.32 , and the intensity is -1.24 . Estimations based on the indirect approach show that in this discharge station, 33 months in the studied period (2000–2019) have recorded severe droughts which is close to the calculated SRI-3 based on observed data. However, the peak value (-2.23) and severity (-46.44) are higher. Simulated SRI-3 based on the direct approach has determined less severe droughts (25 months) and severity (-32.71). In mid-term drought simulations (SRI-6 and SRI-9), the direct approach in discharge station A has shown a lower number of severe droughts (23 and 22 months) and lower severity (-30.61 and -29.45) against the calculated SRI based on the indirect approach and observed data. In long-term drought simulations in this discharge station, the indirect approach has a close peak (-1.73) and the same number of severe drought events (27 months) as the direct approach.

In discharge station B, the direct approach has determined a lower number of severe drought events against the direct approach and calculated SRI, while better estimations in the peak value (the most severe drought) can be seen in the direct approach against the indirect approach. Based on observed data, the number of months with severe droughts in this discharge station varies between 24 (SRI-3) to 33 (SRI-6), and intensity is close to -1.36 on average.

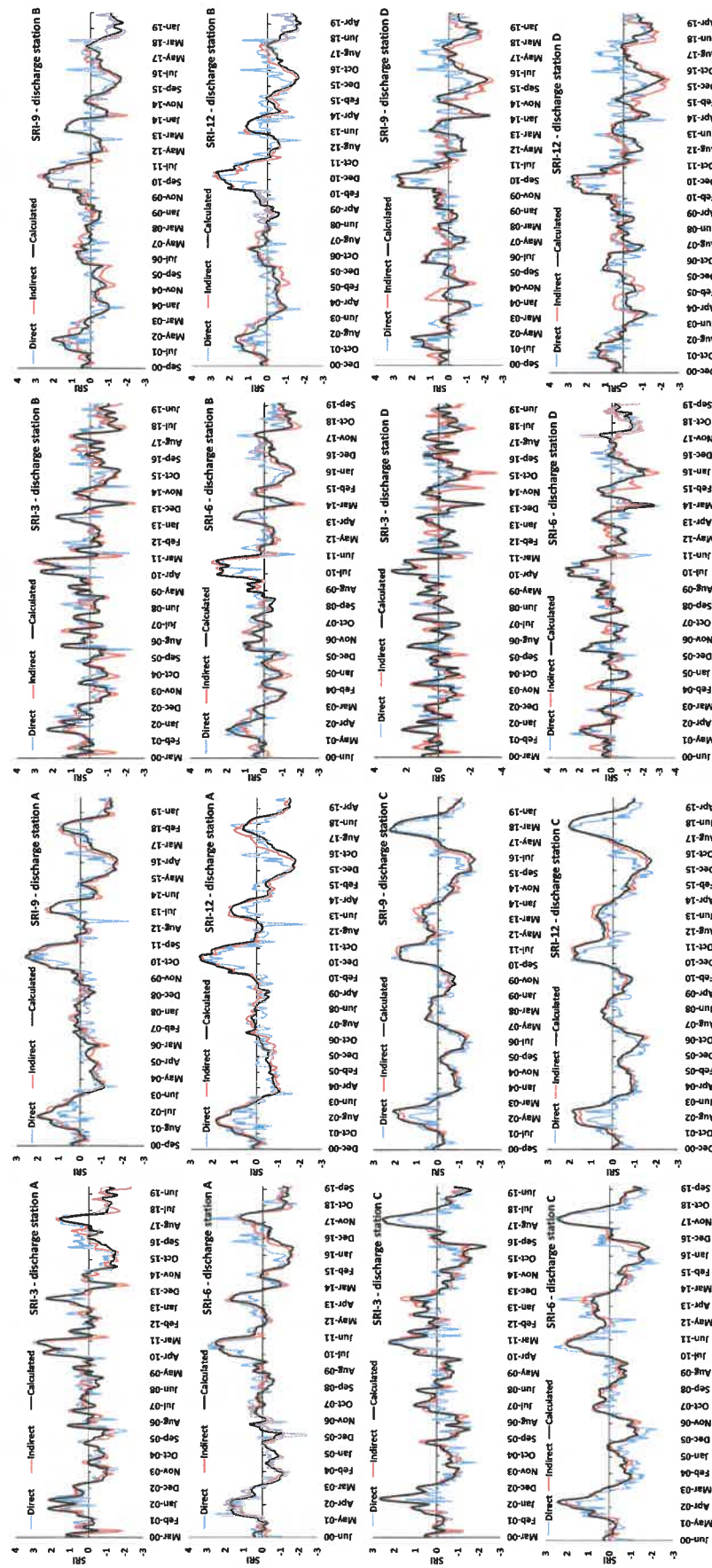


Fig. 5. Simulated (indirect approach) and calculated SRI values for all discharge stations.

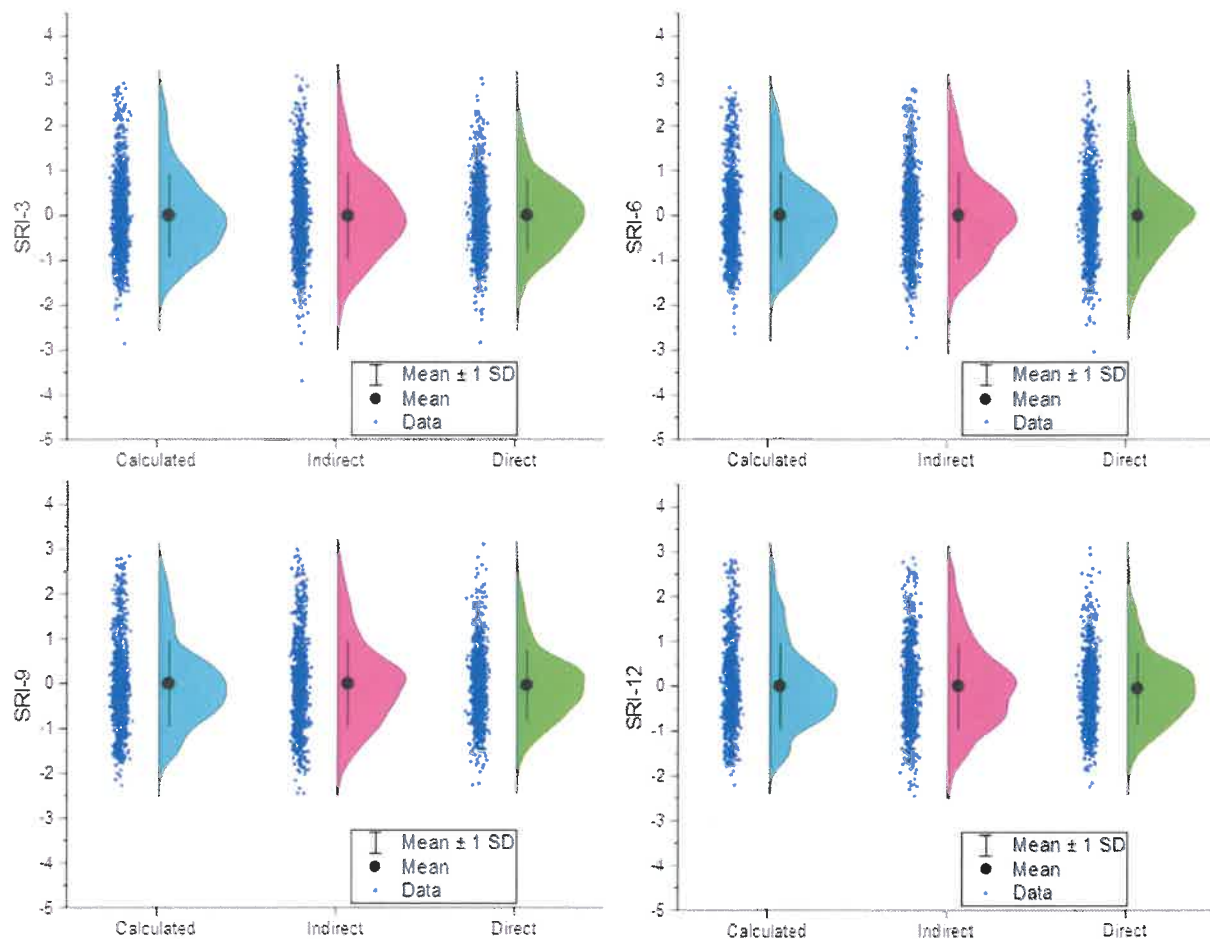


Fig. 6. Distribution of calculated and simulated (indirect and direct approach) SRI values in all discharge stations.

In discharge station C (lowland catchment located in the northeast of the basin), the direct approach has a higher estimated number of months with severe droughts (30 to 49 months) and higher severities (-37.08 to -70.29). On average, the number of months with severe drought based on calculated SRI from observed data is around 27 months, and the indirect approach estimated 30 months. The average of the most severe events is -1.91 , based on observed data in this discharge station.

Discharge station D, located in the foothills of the mountainous area,

has experienced more severities (-39.03 to -46.99) related to other discharge stations and higher peak values (-2.19 to -2.85). Results based on the indirect approach have higher values based on run theory indicators, which can be explained by underestimation of low flows reported above. In general, larger drainage areas have experienced lower numbers of drought events and lower intensities. More details are presented in Table 8.

3.4. River discharge and hydrological drought projections

Since SRI calculation based on the indirect approach needs to be determined from river discharge, in the following steps, discharge projections for each scenario are first provided, then hydrological drought projections based on run theory are discussed.

3.4.1. River discharge projections

River discharge was projected by forcing the trained ANN in the indirect approach with projections of climatic parameters. Fig. 7 provides changes in river discharge against the historical period (2000–2019). These results reveal that in the outlet of ORB (discharge station A) in the first quarter of the year (JFM), a substantial decrease in river discharge is expected, and in May and June, a reduction in river discharge could be expected. In all discharge stations, it can be seen that the moderate scenario for the near future (NF: 2021–2040) has projected the lowest river discharge, while the moderate scenario for the far future (FF: 2041–2060) in most of the months has projected the highest river discharge. The annual average of river discharge in the outlet could vary

Table 7

Accuracy of direct simulations of SRI against calculated SRI based on observed data (2000–2019).

Drought indicator	Discharge stations	KGE	RMSE	R ²
SRI-3	A	-3.5	0.59	0.61
	B	-9.1	0.7	0.47
	C	-36.7	0.66	0.59
	D	-2.4	0.74	0.41
SRI-6	A	-11	0.6	0.62
	B	-8.6	0.61	0.58
	C	-21	0.6	0.68
	D	-11	0.7	0.51
SRI-9	A	-14	0.57	0.65
	B	-0.36	0.61	0.57
	C	-14	0.48	0.75
	D	-11	0.65	0.55
SRI-12	A	-19	0.58	0.64
	B	-5.2	0.64	0.55
	C	-27	0.6	0.65
	D	-15	0.74	0.45

between 484 m³/s (moderate FF) and 440 m³/s (moderate NF). More details can be found in Fig. 7.

3.4.2. Indirect projections of hydrological drought

Similar to historical analyses, the run theory was employed to analyze the projected hydrological droughts. Fig. 8 presents the projected hydrological drought indicators via the indirect approach. In general, it can be seen that the most severe events of projected drought indicators are more intense than in the historical period. The number of severe droughts (months) does not show considerable changes (excluding discharge station D) compared to the historical period.

Regarding the severity indicator (sum of $SRI \leq -1$), in all scenarios, more severity is estimated. Accordingly, the intensity of drought in all projections is increased.

3.4.3. Direct projections of hydrological drought

According to the projected drought indicators via the direct approach, short term drought indicators based on the run theory have significantly higher values. Fig. 9 shows higher severity, duration, and intensity via the direct approach in scenarios compared to the historical period and the indirect approach for SRI-3 and SRI-6. There is no visible pattern in the results for different scenarios. Drier and warmer climate

Table 8

Severe hydrological drought ($SRI \leq -1$) characteristics based on run theory for 2000–2019 estimated for four discharge stations using three approaches (direct, indirect and calculated).

Discharge station	Run theory indicators	SRI-3			SRI-6			SRI-9			SRI-12		
		Direct	Indirect	Calculated	Direct	Indirect	Calculated	Direct	Indirect	Calculated	Direct	Indirect	Calculated
A	Peak value (most severe drought)	-2.08	-2.23	-1.56	-2.38	-1.61	-1.64	-2.20	-1.74	-1.72	-2.23	-1.73	-1.75
	Number of severe droughts (months)	25	33	34	23	40	34	22	33	31	24	27	27
	Severity (sum if $SRI \leq -1$)	-32.71	-46.44	-42.32	-30.61	-51.27	-44.12	-29.45	-43.87	-42.99	-32.08	-37.65	-39.35
	Intensity (Severity/Duration)	-1.31	-1.41	-1.24	-1.33	-1.28	-1.30	-1.34	-1.33	-1.39	-1.34	-1.39	-1.46
	Peak value (most severe drought)	-2.32	-2.45	-2.00	-1.75	-2.18	-1.73	-1.85	-1.97	-1.76	-1.86	-1.81	-1.76
B	Number of severe droughts (months)	10	35	24	16	34	33	18	35	30	18	33	26
	Severity (sum if $SRI \leq -1$)	-15.45	-49.95	-32.42	-19.07	-46.26	-42.79	-23.18	-46.09	-40.50	-23.06	-43.30	-37.44
	Intensity (Severity/Duration)	-1.54	-1.43	-1.35	-1.19	-1.36	-1.30	-1.29	-1.32	-1.35	-1.28	-1.31	-1.44
	Peak value (most severe drought)	-1.92	-1.58	-2.32	-2.30	-1.56	-1.86	-1.79	-1.52	-1.73	-1.81	-1.62	-1.76
	Number of severe droughts (months)	40	34	28	49	34	30	30	27	29	36	26	24
C	Severity (sum if $SRI \leq -1$)	-51.02	-41.76	-38.45	-70.29	-41.96	-40.15	-37.08	-34.67	-38.37	-44.94	-33.72	-33.10
	Intensity (Severity/Duration)	-1.28	-1.23	-1.37	-1.43	-1.23	-1.34	-1.24	-1.28	-1.32	-1.25	-1.30	-1.38
	Peak value (most severe drought)	-2.82	-3.67	-2.85	-3.02	-2.94	-2.61	-2.23	-2.44	-2.27	-2.15	-2.44	-2.19
	Number of severe droughts (months)	17	33	28	31	37	34	21	32	32	18	33	28
	Severity (sum if $SRI \leq -1$)	-24.64	-55.19	-40.14	-48.60	-55.32	-46.99	-28.39	-52.92	-45.61	-24.26	-53.93	-39.03
D	Intensity (Severity/Duration)	-1.45	-1.67	-1.43	-1.57	-1.50	-1.38	-1.35	-1.65	-1.43	-1.35	-1.63	-1.39

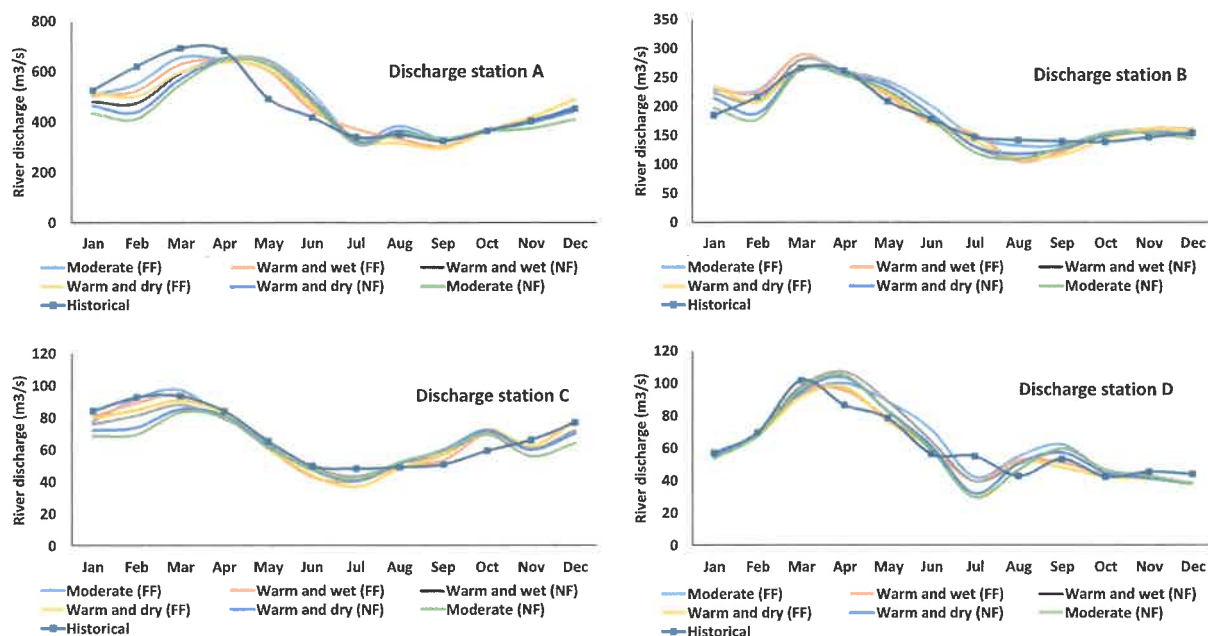


Fig. 7. Projected river discharge against historical data (FF: Far Future, NF: Near Future).

change scenarios do not necessarily show severe conditions in the future.

4. Discussion

4.1. River discharge simulations

The data-driven methods in river discharge simulations in other studies also have shown high accuracy. By employing five different data-driven methods, Ikram et al. (2022) tried to simulate monthly river discharge in mountainous areas of Pakistan and reported that these methods have high accuracy in runoff simulations. However, in another study in Iran, ANN, compared to SWAT and IHACRES, did not perform well in runoff simulations (Moghadam et al., 2022). Similar to our results, Kisi et al. (2013), in a study area in Turkey, approved that data-driven methods (i.e., ANN, ANFIS, and GEP) are valuable and accurate tools in runoff simulations. However, it should be mentioned that these methods suffer from the disability of capturing anthropogenic changes in a basin, and it could be expected that these methods perform better in natural basins (without agricultural activities or hydraulic structures). Conversely, we cannot rely on these methods in complex and managed basins. Our study showed that ANN had superior performance in discharge simulation in a lowland catchment compared to a mountainous catchment. This finding adds a new dimension to the existing knowledge on the effectiveness of ANN in hydrological modeling and highlights the influence of catchment characteristics on model performance. The current results prove our hypothesis that ANN has acceptable accuracy in runoff simulations.

4.2. Hydrological drought simulations

The utilization of data-driven methods in hydrological drought simulations has demonstrated satisfactory levels of accuracy. Shamshirband et al. (2020) simulated different drought indicators with the direct approach using three data-driven methods (SVR, GEP, and MT) in a basin in Iran. The current study has similar results to their research regarding correlation and RMSE performance indicators. Nabipour et al. (2020) attempted to forecast hydrological drought directly in a basin in

Iran by employing ANN. In their study, similar to the current study, SPI was used as a predictor of the Standardized Hydrological Drought Index (SHDI) in different time scales, and ANN showed similar results to our study. In other studies, which are described in Prodhon et al. (2022), the data-driven methods have very close results, in terms of performance indicators, to the current research. However, the direct approach has been used in all of the mentioned studies. Moreover, the first and second hypotheses of the current study can be accepted based on the results.

According to our results, indirect simulations of hydrological drought have a higher accuracy than the direct approach. It should be mentioned that since the accuracy of the indirect approach in hydrological drought simulations is based on runoff simulations, the higher runoff simulation accuracy leads to higher accuracy in hydrological drought simulations. Using the same predictors (precipitation, temperature, and SPI) in both approaches did not deliver a similar accuracy in hydrological drought simulations, and the indirect approach performed better. Thus, our third hypothesis is rejected.

4.3. Hydrological drought projections

Based on the projected hydrological droughts, two different results again reject our third hypothesis. Based on the projected indicators, all of the considered climate change scenarios indicate a slightly worsened outcome compared to the historical period when using the indirect approach. In contrast, the direct approach shows significant changes in hydrological drought projections compared to the historical period. The indirect approach rejects our fourth hypothesis, but the direct approach suggests that under the RCP8.5 climate change scenario, more severe droughts and more extended periods of hydrological drought, based on the run theory, can be expected. The accuracy of drought indicator simulations based on the direct approach are in agreement with Yang et al. (2015); however, in their study, hybrid drought index (HDI) was employed to assess the effect of climate change on hydrological drought using ANN.

In the projected results, it can be seen that the results are inconsistent with the scenarios. According to common expectations, more severe droughts can be expected in dry and warm conditions. However, among the projected drought indicators, there is no huge difference or visible

Scenario	SRI-3				SRI-6			
	Minimum (most severe drought)	Number of severe droughts (months)	Severity (sum if SRI ≤ -1)	Intensity (Severity /Duration)	Minimum (most severe drought)	Number of severe droughts (months)	Severity (sum if SRI ≤ -1)	Intensity (Severity /Duration)
Discharge station A								
Historical	-1.56	34	-42.32	-1.24	-1.64	34	-44.12	-1.3
Moderate (NF)	-2.99	36	-61.33	-1.7	2.94	36	-44.63	-1.22
Warm and dry (NF)	-3.03	32	-56.94	-1.78	2.9	37	-45.87	-1.2
Warm and wet (NF)	-2.97	32	-56.52	-1.77	-2.98	31	-50.33	-1.62
Moderate (FF)	-2.39	36	-59.17	-1.65	2.98	31	-50.34	-1.62
Warm and dry (FF)	-2.94	32	-56.92	-1.78	-3.11	31	-51.56	-1.61
Warm and wet (FF)	-2.28	31	-54.87	-1.77	3.07	32	-50.2	-1.57
Discharge station B								
Historical	-2	24	-32.42	-1.35	-1.73	33	-42.79	-1.3
Moderate (NF)	-3.73	29	-51.02	-1.7	2.26	32	-46.4	-1.46
Warm and dry (NF)	-3.69	31	-58.12	-1.76	-2.2	35	-49.7	-1.42
Warm and wet (NF)	-3.5	32	-52.11	-1.63	2.22	36	-50.46	-1.4
Moderate (FF)	-2.68	29	-49.51	-1.65	2.21	35	-49.64	-1.42
Warm and dry (FF)	-3.4	34	-61.93	-1.82	2.25	35	-51.54	-1.47
Warm and wet (FF)	-3.65	32	-50.96	-1.59	2.06	35	-49.72	-1.42
Discharge station C								
Historical	-2.32	28	-38.45	-1.37	-1.86	30	-40.15	-1.34
Moderate (NF)	-3.73	31	-49.12	-1.58	2.54	38	-50.32	-1.32
Warm and dry (NF)	-3.77	32	-50.36	-1.57	2.79	36	-48.57	-1.35
Warm and wet (NF)	-3.94	30	-48.32	-1.6	2.42	38	-48.37	-1.27
Moderate (FF)	-3.68	29	-47.33	-1.63	2.41	33	-44.97	-1.34
Warm and dry (FF)	-4.13	33	-52.34	-1.59	2.3	35	-48.36	-1.38
Warm and wet (FF)	-4.6	32	-53.28	-1.68	2.53	34	-46.05	-1.35
Discharge station D								
Historical	-2.85	28	-40.14	-1.43	-2.61	34	-46.99	-1.38
Moderate (NF)	-3.74	33	-47.99	-1.58	-2.52	33	-43.97	-1.36
Warm and dry (NF)	-3.69	41	-66.71	-1.63	2.37	38	-57.43	-1.51
Warm and wet (NF)	-3.64	41	-66.08	-1.61	2.9	36	-53.84	-1.55
Moderate (FF)	-2.97	30	-61.35	-1.59	2.63	39	-58.86	-1.51
Warm and dry (FF)	-2.96	42	-65.94	-1.57	2.43	41	-61.13	-1.49
Warm and wet (FF)	-4.33	41	-68.13	-1.68	2.83	34	-57.89	-1.56
SRI-9					SRI-12			
Scenario	Minimum (most severe drought)	Number of severe droughts (months)	Severity (sum if SRI ≤ -1)	Intensity (Severity /Duration)	Minimum (most severe drought)	Number of severe droughts (months)	Severity (sum if SRI ≤ -1)	Intensity (Severity /Duration)
Discharge station A								
Historical	-1.72	31	-42.99	-1.39	-1.75	27	-39.35	-1.46
Moderate (NF)	-2.76	28	-33.37	-1.2	-2.33	23	-38.22	-1.66
Warm and dry (NF)	-2.8	29	-46.46	-1.6	2.39	34	-39.85	-1.66
Warm and wet (NF)	-2.73	28	-45.82	-1.64	2.34	26	-42.1	-1.62
Moderate (FF)	-2.74	28	-46.11	-1.63	2.35	28	-44.42	-1.59
Warm and dry (FF)	-2.65	31	-50.17	-1.62	-2.3	27	-43.8	-1.61
Warm and wet (FF)	-2.44	30	-48.2	-1.61	2.25	26	-42.14	-1.62
Discharge station B								
Historical	-1.76	30	-40.5	-1.35	-1.76	26	-37.44	-1.44
Moderate (NF)	-2.16	34	-45.22	-1.33	1.84	23	-41.83	-1.86
Warm and dry (NF)	-2.17	34	-46.13	-1.36	1.77	37	-47	-1.27
Warm and wet (NF)	-2.08	39	-52.41	-1.34	1.89	38	-49.37	-1.3
Moderate (FF)	-2.07	41	-53.86	-1.36	1.91	41	-56.14	-1.34
Warm and dry (FF)	-2.14	41	-56.42	-1.38	1.89	41	-55.05	-1.33
Warm and wet (FF)	-2	38	-52.85	-1.42	1.84	38	-52.52	-1.38
Discharge station C								
Historical	-1.73	29	-38.37	-1.32	-1.76	24	-33.1	-1.38
Moderate (NF)	-1.93	48	-62.34	-1.3	-1.98	38	-46.63	-1.33
Warm and dry (NF)	-1.88	45	-56.54	-1.3	1.93	46	-61.48	-1.34
Warm and wet (NF)	-1.95	46	-59.41	-1.3	-1.98	47	-62.45	-1.33
Moderate (FF)	-1.96	41	-52.18	-1.27	1.99	46	-58.95	-1.28
Warm and dry (FF)	-1.91	37	-50.34	-1.36	1.96	46	-60.52	-1.52
Warm and wet (FF)	-2.01	38	-53.68	-1.41	2.02	38	-52.71	-1.34
Discharge station D								
Historical	-2.27	32	-45.61	-1.43	-2.19	28	-39.03	-1.39
Moderate (NF)	-2.12	42	-60.74	-1.45	2.03	43	-43.83	-1.48
Warm and dry (NF)	-2.18	39	-58.17	-1.49	2.04	42	-63.39	-1.51
Warm and wet (NF)	-2.09	38	-50	-1.47	2.08	40	-59.82	-1.49
Moderate (FF)	-2.21	39	-58.51	-1.5	2.23	42	-61.6	-1.47
Warm and dry (FF)	-2.24	41	-60.99	-1.49	-2.22	42	-64.67	-1.54
Warm and wet (FF)	-2.1	37	-53.62	-1.41	-2.22	38	-56.29	-1.53

Fig. 8. Projected SRI assessments based on the run theory using the indirect approach (FF: far future, NF: near future) – green, yellow, and red color scales show minimum value to highest value in projections.

pattern between the three different climate change scenarios, in both approaches. However, differences in river discharge simulations are visible, and a time shift in peak river discharge occurrence is estimated. Though, Piniewski et al. (2017a), in the same basin and using the SWAT model (a process-based model), have shown that under the climate change scenarios peaks in runoff can be expected to happen earlier (snowmelt peaks occur earlier). In our study, in two discharge stations (stations A and C) runoff peaks happen later relative to the historical period.

4.4. Limitations and suggestions

Based on the current results, we would like to recommend more investigations between indirect and direct approaches in various climatic regions. In the previous studies, according to our best knowledge, only

the direct approach was used; however, data-driven methods were extensively used in runoff simulations, but calculating hydrological drought indicators as an indirect result is not considered. The importance of this comparison is visible in projections of hydrological drought indicators.

One of the limitations of this study is the selection of a relatively short 20-year period for the analysis of river discharge data and the simulation of hydrological drought indicators. This limitation arose due to data management issues. However, in order to assess this limitation, the calculations were repeated using a longer period of 30 years for discharge station A, which represents the basin's outlet. Both approaches produced very similar results to the current findings in terms of both simulations and projections. Nonetheless, it is worth noting that the literature suggests that utilizing longer periods would likely lead to more robust results (Prodhan et al., 2022), and employing artificial neural

Scenario	SRI-3				SRI-6			
	Minimum (most severe drought)	Number of severe droughts (months)	Severity (sum if SRI ≤ -1)	Intensity (Severity /Duration)	Minimum (most severe drought)	Number of severe droughts (months)	Severity (sum if SRI ≤ -1)	Intensity (Severity /Duration)
Discharge station A								
Historical	-1.56	34	-52.22	-1.24	-1.64	34	-44.12	-1.3
Moderate (NF)	-2.03	77	-82.32	-1.06	-1.81	48	-87.36	-1.27
Warm and dry (NF)	-2	61	-77.23	-1.27	-1.81	43	-54.22	-1.26
Warm and wet (NF)	-1.93	63	-79.77	-1.27	-1.86	43	-54.74	-1.27
Moderate (FF)	-1.74	46	-40.18	-1.2	-1.72	37	-45.85	-1.24
Warm and dry (FF)	-1.92	54	-68.21	-1.26	-1.8	42	-53.07	-1.26
Warm and wet (FF)	-1.89	49	-62.32	-1.24	-1.82	41	-52.61	-1.28
Discharge station B								
Historical	-2	24	-32.42	-1.35	-1.73	33	-42.79	-1.3
Moderate (NF)	-1.66	38	-45.88	-1.2	-1.65	26	-31.24	-1.2
Warm and dry (NF)	-1.62	32	-38.29	-1.2	-1.58	25	-29.5	-1.18
Warm and wet (NF)	-1.75	35	-43.08	-1.24	-1.71	27	-33.83	-1.21
Moderate (FF)	-1.66	34	-39.28	-1.22	-1.55	23	-26.5	-1.17
Warm and dry (FF)	-1.58	29	-33.9	-1.17	-1.54	25	-29.71	-1.19
Warm and wet (FF)	-1.63	34	-40.45	-1.19	-1.59	27	-32.88	-1.22
Discharge station C								
Historical	-2.32	28	-38.45	-1.37	-1.86	30	-40.15	-1.34
Moderate (NF)	-2.01	46	-58.43	-1.27	-1.97	56	-70.38	-1.26
Warm and dry (NF)	-1.93	42	-52.59	-1.25	-1.88	54	-67.22	-1.24
Warm and wet (NF)	-1.94	46	-58.82	-1.28	-1.86	50	-63.84	-1.27
Moderate (FF)	-1.89	38	-48.47	-1.28	-1.83	51	-62.36	-1.25
Warm and dry (FF)	-1.97	39	-48.58	-1.28	-1.91	53	-67.13	-1.27
Warm and wet (FF)	-1.95	40	-51.59	-1.29	-1.91	53	-67.4	-1.27
Discharge station D								
Historical	-2.85	28	-40.14	-1.43	-2.61	34	-46.99	-1.38
Moderate (NF)	-2.36	33	-44.74	-1.36	-2.61	39	-48.48	-1.24
Warm and dry (NF)	-2.89	31	-42.41	-1.37	-2.6	34	-41.83	-1.26
Warm and wet (NF)	-2.77	32	-44.19	-1.38	-2.56	36	-46.34	-1.22
Moderate (FF)	-2.7	26	-39.26	-1.44	-2.54	33	-43.34	-1.31
Warm and dry (FF)	-2.75	29	-39.89	-1.38	-2.63	38	-46.44	-1.22
Warm and wet (FF)	-2.79	30	-41.73	-1.39	-2.61	38	-48.85	-1.33
SRI-9					SRI-12			
Scenario	Minimum (most severe drought)	Number of severe droughts (months)	Severity (sum if SRI ≤ -1)	Intensity (Severity /Duration)	Minimum (most severe drought)	Number of severe droughts (months)	Severity (sum if SRI ≤ -1)	Intensity (Severity /Duration)
Discharge Station A								
Historical	-1.72	31	-42.99	-1.39	-1.78	27	-39.35	-1.46
Moderate (NF)	-1.71	35	-44.01	-1.28	-1.85	32	-42.78	-1.34
Warm and dry (NF)	-1.88	35	-43.15	-1.23	-1.7	32	-44.74	-1.4
Warm and wet (NF)	-1.7	37	-45.8	-1.24	-1.88	34	-43.17	-1.27
Moderate (FF)	-1.69	33	-37.89	-1.22	-1.66	31	-41.54	-1.33
Warm and dry (FF)	-1.65	32	-39.49	-1.23	-1.83	33	-44.71	-1.35
Warm and wet (FF)	-1.73	34	-42.3	-1.24	-1.82	32	-44.99	-1.41
Discharge station B								
Historical	-1.76	30	-40.5	-1.35	-1.76	26	-37.44	-1.44
Moderate (NF)	-1.81	42	-51.22	-1.22	-1.77	35	-44.03	-1.26
Warm and dry (NF)	-1.78	36	-44.05	-1.22	-1.95	34	-45.51	-1.34
Warm and wet (NF)	-1.84	43	-52.78	-1.23	-1.87	38	-48.74	-1.28
Moderate (FF)	-1.7	31	-38.45	-1.24	-1.71	31	-42.51	-1.37
Warm and dry (FF)	-1.85	33	-40.38	-1.22	-1.77	36	-43.82	-1.23
Warm and wet (FF)	-1.87	33	-47.3	-1.23	-1.84	37	-48.36	-1.32
Discharge station C								
Historical	-1.73	29	-38.37	-1.32	-1.76	24	-33.1	-1.38
Moderate (NF)	-1.83	37	-45.27	-1.22	-1.8	34	-42.7	-1.61
Warm and dry (NF)	-1.89	37	-44.86	-1.21	-1.97	35	-42.14	-1.69
Warm and wet (NF)	-1.79	33	-43.04	-1.23	-1.99	33	-44.98	-1.66
Moderate (FF)	-1.88	37	-44.09	-1.19	-1.79	30	-44.25	-1.64
Warm and dry (FF)	-1.89	38	-47.39	-1.23	-1.82	32	-42.69	-1.62
Warm and wet (FF)	-1.95	38	-48.63	-1.23	-1.82	31	-43.82	-1.63
Discharge station D								
Historical	-2.27	32	-45.61	-1.43	-2.19	28	-39.03	-1.39
Moderate (NF)	-1.89	37	-43.09	-1.16	-2.5	33	-40.84	-1.34
Warm and dry (NF)	-1.81	31	-36.17	-1.17	-2.42	34	-43.11	-1.27
Warm and wet (NF)	-1.84	36	-42.31	-1.18	-2.95	32	-43.96	-1.37
Moderate (FF)	-1.82	25	-28.98	-1.16	-2.16	36	-48.34	-1.37
Warm and dry (FF)	-1.83	23	-26.09	-1.16	-2.53	34	-48	-1.32
Warm and wet (FF)	-1.78	29	-33.73	-1.16	-2.54	35	-46.43	-1.33

Fig. 9. Projected SRI assessments based on the run theory using the direct approach (FF: far future, NF: near future) – green, yellow, and red color scales show minimum value to highest value in projections.

networks (ANN) may offer better detection of patterns in river discharge and hydrological drought.

The ORB is located in a cold and humid temperate region, in which agricultural activities are based on rainfed farming; consequently, water withdrawals from rivers for irrigation are close to zero, and flow conditions in rivers are only slightly modified, mainly due to existing reservoirs. We believe that applying these approaches in other regions can improve our understanding of the application of data-driven methods in hydrological drought simulations and projections. In addition, a comparison between different data-driven methods could be interesting for further analyses.

One of the limitations of our study is that we have used only maximum and minimum temperature and precipitation as climatic

predictors since these parameters are most easily accessible from GCMs for climate change scenarios. We would like to suggest employing climatic parameters (such as solar radiation, humidity, and wind speed), remotely-sensed drought factors and potential evapotranspiration (PET) as predictors to have a more robust model (Ali et al., 2018; Feng et al., 2019). Moreover, other drought indicators such as SPEI also could be used instead of SPI in future studies.

The objective of this study was to show that ANN can be used to project droughts in this region as an alternative to other techniques, instead of studying the projected changes (e.g. derived using a process-based models) in ORB. Thus to have a more robust results, using Regional Climate Models (RCMs) for projecting climatic variables can be suggested instead of GCMs. In addition, applying new GCMs based on

CMIP6 can present different climatic scenarios and, consequently, different projections of hydrological drought. Using full climate model ensembles instead of selecting representative GCMs could also be recommended to increase the robustness of climate change impact assessment.

Comparing these approaches with a process-based approach (such as process-based hydrological models) could deliver a broader vision to understanding hydrological drought assessments and projections, especially in detecting differences between climatic scenarios (in hydrological process-based models, more complicated and nonlinear relations between objects are available (Eini et al., 2023b)).

5. Conclusion

The study investigated the efficiency and application of ANN in simulations and projections of river discharge and hydrological drought (SRI) in the Odra River Basin in Central Europe. Four river discharge stations were selected within the basin, and SRI-3 as a short-term drought indicator, SRI-6 and SRI-9 as mid-term drought indicators, and SRI-12 as a long-term indicator were simulated and projected. Two different approaches (the direct approach and the indirect approach) were employed. The direct approach simulated hydrological drought and projected directly from precipitation, maximum and minimum temperature, and SPI-1 to SPI-12 (meteorological drought indicators). In the indirect approach, we first simulated and projected river discharge, and then hydrological drought was calculated. To achieve projected precipitation and temperature for the near future (2021–2040) and the far future (2041–2060) under the worst scenario (RCP8.5), four GCMs (based on CMIP5) grouped into three scenarios (moderate, warm and dry, and warm and wet). Our results can be concluded as the following points:

- ANN has high performance in simulations of hydrological drought and river discharge in terms of KGE, RMSE, PBIAS, and R^2 .
- ANN performance in discharge and hydrological drought simulation is significantly higher in a lowland than in a mountainous catchment.
- The indirect approach performed better in hydrological drought simulations since it performed well in river discharge simulations.
- Projections of hydrological drought have major differences in two approaches.
- There are no detectable patterns in hydrological drought projections based on climate change scenarios. This means that ANN results are not linear in terms of lower precipitation or higher temperature leading to more severe and long periods of drought, and thus, they behave differently than process-based models.

CRedit authorship contribution statement

Mohammad Reza Eini: Conceptualization, Methodology, Software, Writing – review & editing. **Farzaneh Najminejad:** Software, Visualization, Methodology, Writing – review & editing. **Mikolaj Piniewski:** Conceptualization, Methodology, Writing – review & editing.

Declaration of competing interest

The authors declare that they have no known competing financial interests or personal relationships that could have appeared to influence the work reported in this paper.

Data availability

Data will be made available on request.

Acknowledgment

National Science Centre (Narodowe Centrum Nauki – NCN,

PRELUDIUM BIS-1 project, Poland), and Polish National Agency for Academic Exchange (NAWA), financially supported this research. We would also like to extend our appreciation to the Potsdam Institute for Climate Impact Research (PIK), in Potsdam, Germany for hosting MRE during an internship that led to this research (supported by NAWA). River discharge data was provided by the Institute of Meteorology and Water Management (IMGW-PIB), Warsaw, Poland.

References

- Abhishek, Kinouchi, T., Sayama, T., 2021. A comprehensive assessment of water storage dynamics and hydroclimatic extremes in the Chao Phraya River basin during 2002–2020. *J. Hydrol.* 603, 126868 <https://doi.org/10.1016/j.jhydrol.2021.126868>.
- Adaawen, S., Rademacher-Schulz, C., Schraven, B., Segadlo, N., 2019. Chapter 2- drought, migration, and conflict in sub-Saharan Africa: what are the links and policy options? *Current Directions in Water Scarcity Research* 2, 15–31. <https://doi.org/10.1016/B978-0-12-814820-4.00002-X>.
- Ali, M., Deo, R.C., Downs, N.J., Maraseni, T., 2018. Multi-stage committee based extreme learning machine model incorporating the influence of climate parameters and seasonality on drought forecasting. *Comput. Electron. Agric.* 152, 149–165. <https://doi.org/10.1016/j.compag.2018.07.013>.
- Alloghani, M., Al-Jumeily, D., Mustafina, J., Hussain, A., Aljaaf, A.J., 2020. A systematic review on supervised and unsupervised machine learning algorithms for data science. In: Berry, M.W., Mohamed, A., Yap, B.W. (Eds.), *Supervised and Unsupervised Learning for Data Science*. Springer International Publishing, Cham, pp. 3–21. https://doi.org/10.1007/978-3-030-22475-2_1.
- Berezowski, T., Szcześniak, M., Kardel, I., Michałowski, R., Okruszko, T., Mezghani, A., Piniewski, M., 2016. CPLFD-GDPT5: high-resolution gridded daily precipitation and temperature data set for two largest polish river basins. *Earth Syst. Sci. Data* 8, 127–139. <https://doi.org/10.5194/essd-8-127-2016>.
- Chen, C.-A., Hsu, H.-H., Liang, H.-C., 2021. Evaluation and comparison of CMIP6 and CMIP5 model performance in simulating the seasonal extreme precipitation in the Western North Pacific and East Asia. *Weather and Climate Extremes* 31, 100303. <https://doi.org/10.1016/j.wace.2021.100303>.
- Deo, R.C., Ghorbani, M.A., Samadianfard, S., Maraseni, T., Bilgili, M., Biazar, M., 2018. Multi-layer perceptron hybrid model integrated with the firefly optimizer algorithm for windspeed prediction of target site using a limited set of neighboring reference station data. *Renew. Energy* 116, 309–323. <https://doi.org/10.1016/j.renene.2017.09.078>.
- Eini, M.R., Javadi, S., Delavar, M., Gassman, P.W., Jarihani, B., 2020a. Development of alternative SWAT-based models for simulating water budget components and streamflow for a karstic-influenced watershed. *CATENA* 195, 104801. <https://doi.org/10.1016/j.catena.2020.104801>.
- Eini, M.R., Javadi, S., Hashemy Shahdany, M., Kisi, O., 2020b. Comprehensive assessment and scenario simulation for the future of the hydrological processes in Dez river basin, Iran. *Water Supply* 21, 1157–1176. <https://doi.org/10.2166/ws.2020.363>.
- Eini, M.R., Rahmati, A., Piniewski, M., 2022a. Hydrological application and accuracy evaluation of PERSIANN satellite-based precipitation estimates over a humid continental climate catchment. *Journal of Hydrology: Regional Studies* 41, 101109. <https://doi.org/10.1016/j.ejrh.2022.101109>.
- Eini, M.R., Rahmati, A., Salmani, H., Brocca, L., Piniewski, M., 2022b. Detecting characteristics of extreme precipitation events using regional and satellite-based precipitation gridded datasets over a region in Central Europe. *Sci. Total Environ.* 852, 158497. <https://doi.org/10.1016/j.scitotenv.2022.158497>.
- Eini, M.R., Massari, C., Piniewski, M., 2023a. Satellite-based soil moisture enhances the reliability of agro-hydrological modeling in large transboundary river basins. *Sci. Total Environ.* 873, 162396. <https://doi.org/10.1016/j.scitotenv.2023.162396>.
- Eini, M.R., Salmani, H., Piniewski, M., 2023b. Comparison of process-based and statistical approaches for simulation and projections of rainfed crop yields. *Agric. Water Manag.* 277, 108107. <https://doi.org/10.1016/j.agwat.2022.108107>.
- Feng, P., Wang, B., Liu, D.L., Yu, Q., 2019. Machine learning-based integration of remotely-sensed drought factors can improve the estimation of agricultural drought in south-eastern Australia. *Agric. Syst.* 173, 303–316. <https://doi.org/10.1016/j.agry.2019.03.015>.
- Gao, C., Gemmer, M., Zeng, X., Liu, B., Su, B., Wen, Y., 2010. Projected streamflow in the Huaihe River basin (2010–2100) using artificial neural network. *Stoch. Env. Res. Risk A.* 24, 685–697. <https://doi.org/10.1007/s00477-009-0355-6>.
- Gleick, P.H., 2014. Water, drought, climate change, and conflict in Syria. *Weather, Climate, and Society* 6, 331–340. <https://doi.org/10.1175/WCAS-D-13-00059.1>.
- Guo, H., Li, M., Nzabarinda, V., Bao, A., Meng, X., Zhu, L., De Maeyer, P., 2022. Assessment of three long-term satellite-based precipitation estimates against ground observations for drought characterization in northwestern China. *Remote Sens.* 14, 828. <https://doi.org/10.3390/rs14040828>.
- Gupta, H.V., Kling, H., Yilmaz, K.K., Martinez, G.F., 2009. Decomposition of the mean squared error and NSE performance criteria: implications for improving hydrological modelling. *J. Hydrol.* 377, 80–91. <https://doi.org/10.1016/j.jhydrol.2009.08.003>.
- Halicki, M., Schwatke, C., Niedzielski, T., 2023. The impact of the satellite ground track shift on the accuracy of altimetric measurements on rivers: a case study of the Sentinel-3 altimetry on the Odra/Oder River. *J. Hydrol.* 617, 128761. <https://doi.org/10.1016/j.jhydrol.2022.128761>.

- Hao, Z., Hao, F., Xia, Y., Feng, S., Sun, C., Zhang, X., Fu, Y., Hao, Y., Zhang, Y., Meng, Y., 2022. Compound droughts and hot extremes: characteristics, drivers, changes, and impacts. *Earth Sci. Rev.* 235, 104241 <https://doi.org/10.1016/j.earscirev.2022.104241>.
- Hari, V., Rakovec, O., Markonis, Y., Hanel, M., Kumar, R., 2020. Increased future occurrences of the exceptional 2018–2019 central European drought under global warming. *Sci. Rep.* 10, 12207. <https://doi.org/10.1038/s41598-020-68872-9>.
- Harmel, R.D., Baffaut, C., Douglas-Mankin, K., 2018. Review and development of ASABE engineering practice 621: “guidelines for calibrating, validating, and evaluating hydrologic and water quality models”. *Trans. ASABE* 61, 1393–1401. <https://doi.org/10.13031/trans.12806>.
- Ikram, R.M.A., Hazarika, B.B., Gupta, D., Heddiam, S., Kisi, O., 2022. Streamflow prediction in mountainous region using new machine learning and data preprocessing methods: a case study. *Neural Comput. & Applic.* <https://doi.org/10.1007/s00521-022-08163-8>.
- Ionita, M., Tallaksen, L.M., Kingston, D.G., Stagge, J.H., Laaha, G., Van Lanen, H.A.J., Scholz, P., Chelcea, S.M., Haslinger, K., 2017. The European 2015 drought from a climatological perspective. *Hydrol. Earth Syst. Sci.* 21, 1397–1419. <https://doi.org/10.5194/hess-21-1397-2017>.
- Jaagus, J., Aasa, A., Aniskevich, S., Boincean, B., Bojari, R., Briede, A., Danilovich, I., Castro, F.D., Dumitrescu, A., Labuda, M., Labudová, L., Lohmus, K., Melnik, I., Möisja, K., Pongracz, R., Potopová, V., Režničková, L., Rimkus, E., Semenova, L., Stonevičius, E., Štěpánek, P., Trnka, M., Vicente-Serrano, S.M., Wibig, J., Zahradníček, P., 2022. Long-term changes in drought indices in eastern and Central Europe. *Int. J. Climatol.* 42, 225–249. <https://doi.org/10.1002/joc.7241>.
- Jain, V.K., Pandey, R.P., Jain, M.K., Byun, H.-K., 2015. Comparison of drought indices for appraisal of drought characteristics in the Ken River basin. *Weather and Climate Extremes* 8, 1–11. <https://doi.org/10.1016/j.wace.2015.05.002>.
- Kao, S.-C., Govindaraju, R.S., 2010. A copula-based joint deficit index for droughts. *J. Hydrol.* 380, 121–134. <https://doi.org/10.1016/j.jhydrol.2009.10.029>.
- Kisi, O., Shiri, J., Tombul, M., 2013. Modeling rainfall-runoff process using soft computing techniques. *Comput. Geosci.* 51, 108–117. <https://doi.org/10.1016/j.cageo.2012.07.001>.
- Laaha, G., Gauster, T., Tallaksen, L.M., Vidal, J.P., Stahl, K., Prudhomme, C., Heudorfer, B., Vlnas, R., Ionita, M., Van Lanen, H.A.J., Adler, M.J., Caillouet, L., Delus, C., Fendekova, M., Gailliez, S., Hannaford, J., Kingston, D., Van Loon, A.F., Mediero, L., Osuch, M., Romanowicz, R., Sauquet, E., Stagge, J.H., Wong, W.K., 2017. The European 2015 drought from a hydrological perspective. *Hydrol. Earth Syst. Sci.* 21, 3001–3024. <https://doi.org/10.5194/hess-21-3001-2017>.
- Leuzinger, S., Zotz, G., Ashhoff, R., Körner, C., 2005. Responses of deciduous forest trees to severe drought in Central Europe. *Tree Physiol.* 25, 641–650. <https://doi.org/10.1093/treephys/25.6.641>.
- Lin, Q., Wu, Z., Zhang, Y., Peng, T., Chang, W., Guo, J., 2023. Propagation from meteorological to hydrological drought and its application to drought prediction in the Xijiang River basin, South China. *J. Hydrol.* 617, 128889 <https://doi.org/10.1016/j.jhydrol.2022.128889>.
- Liu, Y., Liu, Y., Wang, W., Fan, X., Cui, W., 2022. Soil moisture droughts in East Africa: spatiotemporal patterns and climate drivers. *Journal of Hydrology: Regional Studies* 40, 101013. <https://doi.org/10.1016/j.jhrs.2022.101013>.
- Lugato, E., Cescatti, A., Jones, A., Ceccherini, G., Duveiller, G., 2020. Maximising climate mitigation potential by carbon and radiative agricultural land management with cover crops. *Environ. Res. Lett.* 15, 094075 <https://doi.org/10.1088/1748-9326/ab1b7d>.
- Ma, Q., Li, Y., Liu, F., Feng, H., Biswas, A., Zhang, Q., 2023. SPEI and multi-threshold run theory based drought analysis using multi-source products in China. *J. Hydrol.* 616, 128737 <https://doi.org/10.1016/j.jhydrol.2022.128737>.
- Marcinkowski, P., Kardel, I., Placzkowska, E., Gielczewski, M., Osuch, P., Okruszko, T., Venegas-Cordero, N., Ignar, S., Piniewski, M., 2022. High-resolution simulated water balance and streamflow data set for 1951–2020 for the territory of Poland. *Geoscience Data Journal* n/a. <https://doi.org/10.1002/gdj3.152>.
- McKee, T.B., Doesken, N.J., Kleist, J., 1993. The Relationship of Drought Frequency and Duration to Time Scales. MA, USA, Boston.
- Meier, H.E.M., Kniesbusch, M., Dieterich, C., Gröger, M., Zorita, E., Elmgren, R., Myrberg, K., Ahola, M.P., Bartosova, A., Bonsdorff, E., Börgel, F., Capell, R., Carlen, I., Carlund, T., Carstensen, J., Christensen, O.B., Dierschke, V., Frauen, C., Frederiksen, M., Galet, E., Galatius, A., Haapala, J.J., Halkka, A., Hugelius, G., Hünicke, B., Jaagus, J., Jüssi, M., Käyhkö, J., Kirchner, N., Kjellström, E., Kulinski, K., Lehmann, A., Lindström, G., May, W., Miller, P.A., Mohrholz, V., Müller-Karulis, B., Pavón-Jordán, D., Quante, M., Reckermann, M., Rutgersson, A., Savchuk, O.P., Stendel, M., Tuomi, L., Viitasalo, M., Weisse, R., Zhang, W., 2022. Climate change in the Baltic Sea region: a summary. *Earth Syst. Dynam.* 13, 457–593. <https://doi.org/10.5194/esd-13-457-2022>.
- Mesbahzadeh, T., Mirakbari, M., Mohseni Saravi, M., Soleimani Sardoo, F., Miglietta, M., 2020. Meteorological drought analysis using copula theory and drought indicators under climate change scenarios (RCP). *Meteorol. Appl.* 27, e1856 <https://doi.org/10.1002/met.1856>.
- Mirabbasi, R., Anagnostou, E.N., Fakheri-Fard, A., Dinpashov, Y., Eslamian, S., 2013. Analysis of meteorological drought in Northwest Iran using the joint deficit index. *J. Hydrol.* 492, 35–48. <https://doi.org/10.1016/j.jhydrol.2013.04.019>.
- Mishra, V., 2020. Long-term (1870–2018) drought reconstruction in context of surface water security in India. *J. Hydrol.* 580, 124228 <https://doi.org/10.1016/j.jhydrol.2019.124228>.
- Moghadam, S.H., Ashofteh, P.-S., Loaiciga, H.A., 2022. Investigating the performance of data mining, lumped, and distributed models in runoff projected under climate change. *J. Hydrol.* 128992 <https://doi.org/10.1016/j.jhydrol.2022.128992>.
- Moriasi, D., Gitau, M., Pai, N., Daggupati, P., 2015. Hydrologic and water quality models: performance measures and evaluation criteria. *Trans. ASABE* 58, 1763–1785. <https://doi.org/10.13031/trans.58.10715>.
- Nabipour, N., Dehghani, M., Mosavi, A., Shamshirband, S., 2020. Short-term hydrological drought forecasting based on different nature-inspired optimization algorithms hybridized with artificial neural networks. *IEEE Access* 8, 15210–15222. <https://doi.org/10.1109/ACCESS.2020.2964584>.
- Pachauri, R., Meyer, L., 2014. Climate change 2014: Synthesis report. In: Contribution of Working Groups I, II and III to the Fifth Assessment Report of the Intergovernmental Panel on Climate Change, II and. https://epic.awi.de/id/eprint/37530/1/IPCC_AR5_SYR_Final.pdf.
- Pektaş, A.O., Kerem Cigizoglu, H., 2013. ANN hybrid model versus ARIMA and ARIMAX models of runoff coefficient. *J. Hydrol.* 500, 21–36. <https://doi.org/10.1016/j.jhydrol.2013.07.020>.
- Piniewski, M., Szczesniak, M., Huang, S., Kundzewicz, Z.W., 2017a. Projections of runoff in the Vistula and the Odra river basins with the help of the SWAT model. *Hydrol. Res.* 49, 303–317. <https://doi.org/10.2166/nh.2017.280>.
- Piniewski, M., Szczesniak, M., Kardel, I., Berezowski, T., Okruszko, T., Srinivasan, R., Vikhamar Schuler, D., Kundzewicz, Z.W., 2017b. Hydrological modelling of the Vistula and Odra river basins using SWAT. *Hydrol. Sci. J.* 62, 1266–1289. <https://doi.org/10.1080/02626667.2017.1321842>.
- Piniewski, M., Szczesniak, M., Kundzewicz, Z.W., Mezghani, A., Hov, Ø., 2017c. Changes in low and high flows in the Vistula and the Odra basins: model projections in the European-scale context. *Hydrol. Process.* 31, 2210–2225. <https://doi.org/10.1002/hyp.11176>.
- Piniewski, M., Szczesniak, M., Kardel, I., Chattopadhyay, S., Berezowski, T., 2021. G2DC-PL+: a gridded 2 km daily climate dataset for the union of the polish territory and the Vistula and Odra basins. *Earth Syst. Sci. Data* 13, 1273–1288. <https://doi.org/10.5194/essd-13-1273-2021>.
- Piniewski, M., Eini, M.R., Chattopadhyay, S., Okruszko, T., Kundzewicz, Z.W., 2022. Is there a coherence in observed and projected changes in riverine low flow indices across Central Europe? *Earth Sci. Rev.* 233, 104187 <https://doi.org/10.1016/j.earscirev.2022.104187>.
- Piri, J., Abdollahipour, M., Keshtegar, B., 2022. Advanced machine learning model for prediction of drought indices using hybrid SVR-RSM. *Water Resour. Manag.* 1–30 <https://doi.org/10.1007/s11269-022-03395-8>.
- Prodhan, A.A., Zhang, J., Hasan, S.S., Pangali Sharma, T.P., Mohana, H.P., 2022. A review of machine learning methods for drought hazard monitoring and forecasting: current research trends, challenges, and future research directions. *Environ. Model. Softw.* 149, 105327 <https://doi.org/10.1016/j.envsoft.2022.105327>.
- Riahi, K., Rao, S., Krey, V., Cho, C., Chirkov, V., Fischer, G., Kindermann, G., Nakicenovic, N., Rafaj, P., 2011. RCP 8.5—a scenario of comparatively high greenhouse gas emissions. *Clim. Chang.* 109, 33. <https://doi.org/10.1007/s10584-011-0149-y>.
- Shamshirband, S., Hashemi, S., Salimi, H., Samadianfard, S., Asadi, E., Shadkani, S., Kargar, K., Mosavi, A., Nabipour, N., Chau, K.-W., 2020. Predicting standardized streamflow index for hydrological drought using machine learning models. *Engineering Applications of Computational Fluid Mechanics* 14, 339–350. <https://doi.org/10.1080/19942060.2020.1715844>.
- Shukla, S., Wood, A.W., 2008. Use of a standardized runoff index for characterizing hydrologic drought. *Geophys. Res. Lett.* 35 <https://doi.org/10.1029/2007GL032487>.
- Su, B., Zeng, X., Zhai, J., Wang, Y., Li, X., 2015. Projected precipitation and streamflow under SRES and RCP emission scenarios in the Songhuajiang River basin, China. *Quat. Int.* 380–381, 95–105. <https://doi.org/10.1016/j.quaint.2014.03.049>.
- Teutschbein, C., Jonsson, E., Todorović, A., Tootoonchi, F., Stenfors, E., Grabs, T., 2023. Future drought propagation through the water-energy-food-ecosystem nexus – a Nordic perspective. *J. Hydrol.* 617, 128963 <https://doi.org/10.1016/j.jhydrol.2022.128963>.
- Vicente-Serrano, S.M., Beguería, S., López-Moreno, J.I., 2010. A multiscalar drought index sensitive to global warming: the standardized precipitation evapotranspiration index. *J. Clim.* 23, 1696–1718. <https://doi.org/10.1175/2009JCLI2909.1>.
- Wang, G.C., Zhang, Q., Band, S.S., Dehghani, M., Chau, K.W., Tho, Q.T., Zhu, S., Samadianfard, S., Mosavi, A., 2022. Monthly and seasonal hydrological drought forecasting using multiple extreme learning machine models. *Engineering Applications of Computational Fluid Mechanics* 16, 1364–1381. <https://doi.org/10.1080/19942060.2022.2089732>.
- Yang, T., Zhou, X., Yu, Z., Krysanova, V., Wang, B., 2015. Drought projection based on a hybrid drought index using artificial neural networks. *Hydrol. Process.* 29, 2635–2648. <https://doi.org/10.1002/hyp.10394>.
- Yevjevich, V.M., 1967. Objective Approach to Definitions and Investigations of Continental Hydrologic Droughts. An. Colorado State University, Libraries.
- Zeng, X., Kundzewicz, Z.W., Zhou, J., Su, B., 2012. Discharge projection in the Yangtze River basin under different emission scenarios based on the artificial neural networks. *Quat. Int.* 282, 113–121. <https://doi.org/10.1016/j.quaint.2011.06.009>.
- Zhang, X., Hao, Z., Singh, V.P., Zhang, Y., Feng, S., Xu, Y., Hao, F., 2022. Drought propagation under global warming: characteristics, approaches, processes, and controlling factors. *Sci. Total Environ.* 838, 156021 <https://doi.org/10.1016/j.scitotenv.2022.156021>.
- Zounemat-Kermani, M., Seo, Y., Kim, S., Ghorbani, M.A., Samadianfard, S., Naghshara, S., Kim, N.W., Singh, V.P., 2019. Can decomposition approaches always enhance soft computing models? Predicting the dissolved oxygen concentration in the St. Johns River, Florida. *Appl. Sci.* 9, 2534. <https://doi.org/10.3390/app9122534>.

Warsaw, 26/03/2024

Mohammadreza Einikarimkandi
d003066@sggw.edu.pl

**Institute of Environmental Engineering,
Mining, and Energy, Discipline
Council
of the Warsaw University of Life
Sciences**

Co-authorship statement

I hereby represent that in the below publication “Eini, M. R., Najminejad, F., & Piniewski, M. (2023). Direct and indirect simulating and projecting hydrological drought using a supervised machine learning method. Science of The Total Environment, 898, 165523. <https://doi.org/10.1016/j.scitotenv.2023.165523>” my individual contribution in the development thereof involved, Conceptualization, methodology, software, validation, writing – original draft, writing – review & editing, visualization.

 Signature
Mohammad Reza
Eini Karimkandi

Warsaw, 26/03/2024

Farzaneh Najminezhad
feri.najmi.ut@gmail.com

**Institute of Environmental Engineering,
Mining, and Energy, Discipline
Council
of the Warsaw University of Life
Sciences**

Co-authorship statement

I hereby represent that in the below publication Eini, M. R., Najminejad, F., & Piniewski, M. (2023). Direct and indirect simulating and projecting hydrological drought using a supervised machine learning method. Science of The Total Environment, 898, 165523. <https://doi.org/10.1016/j.scitotenv.2023.165523> my individual contribution in the development thereof involved literature review and editing the manuscript.

Farzaneh Najmi

Signature

Warsaw, 26/03/2024

Dr hab. Mikołaj Piniewski, prof. SGGW
Department of Hydrology, Meteorology and Water Management
Institute of Environmental Engineering
Warsaw University of Life Sciences
mikolaj_piniewski@sggw.edu.pl

**Institute of Environmental Engineering,
Mining, and Energy, Discipline
Council
of the Warsaw University of Life
Sciences**

Co-authorship statement

I hereby represent that in the below publication “Eini, M. R., Najminejad, F., & Piniewski, M. (2023). Direct and indirect simulating and projecting hydrological drought using a supervised machine learning method. Science of The Total Environment, 898, 165523. <https://doi.org/10.1016/j.scitotenv.2023.165523>” my individual contribution in the development thereof involved, conceptualization, methodology, writing – review & editing.



Signature

